Global analysis of host cell factors involved in the growth of *Salmonella* Typhimurium inside human epithelial cells

DISSERTATION

zur Erlangung des akademischen Grades

doctor rerum naturalium

(Dr. rer. nat.)

im Fach Biologie

eingereicht an der

Mathematisch-Naturwissenschaftlichen Fakultät I

der Humboldt-Universität zu Berlin

von

Dipl.-Biol. Oliver Riede
(geb. 28.07.1977 in Berlin)

Präsident der Humboldt-Universität zu Berlin
Prof. Dr. Dr. h.c. Christoph Markschies

Dekan der Mathematisch-Naturwissenschaftlichen Fakultät I
Prof. Dr. Lutz-Helmut Schön

Gutachter/innen:
1. Prof. Dr. Thomas F. Meyer
2. Prof. Dr. Norbert Suttorp
3. Prof. Dr. Thomas Rudel

Tag der mündlichen Prüfung: 10.12.2009

ZUSAMMENFASSUNG

Die molekularbiologische Untersuchung der Wechselwirkungen zwischen Pathogenen und ihren Wirtszellen ist ein wertvoller Ansatz zur Erschließung bakterieller Pathogenitätsmechnismen und trägt darüber hinaus dazu bei, unser ständig wachsendes Wissen über fundamentale Prozesse in eukaryotischen Zellen zu erweitern. Das Gram-negative, fakultativ intrazelluläre Bakterium *Salmonella* Typhimurium ist ein gängiger Modellorganismus, um den intrazellulären Lebensstil bakterieller Pathogene und deren Einfluss auf Wirtszellprozesse zu erforschen. In der vorliegenden Arbeit wurde ein Durchflusszytometrie-basierter Hochdurchsatz RNA Interferenz (RNAi) Screen einer humanen Kinase-Bibliothek etabliert und durchgeführt, um die Wirtszellfaktoren zu entschlüsseln, welche in die intrazelluläre Replikation von *Salmonella* Typhimurium involviert sind. Ein Salmonellen-Stamm, der zwei fluoreszierende Reporterproteine exprimiert, wurde konstruiert, um die bakterielle Replikation und die metabolische Aktivität in infizierten Wirtstzellen zu detektieren. Dies ermöglichte es, die Auswirkungen fehlender Wirtszellfaktoren auf das intrazelluläre Wachstum von Salmonellen zu untersuchen. In Vorversuchen wurde die humane Epithelzelllinie HeLa als adäquate Zelllinie für die Durchführung der Hochdurchsatzexperimente (Screen) bestimmt sowie geeignete Infektionsbedingungen festgelegt. Als inhibitorische Kontrolle für den Screen diente die Depletierung der GTPase Rab7A, welche einen essentiellen Faktor während der Salmonelleninfektion darstellt. Nachdem die technische Stabilität der Untersuchungsmethode und die Genauigkeit der ermittelten Daten überprüft wurden, konnte die Anwendbarkeit des Systems im Hochdurchsatz anhand ausgewählter chemischer Inhibitoren sowie einer innerhalb der Abteilung zusammengestellten siRNA-Bibliothek gezeigt werden. Der Einsatz der humanen Kinase-Bibliothek lieferte 48 potentielle Kandidatengene, von denen 15 in einer anschließenden Validierung als die Infektion beeinflussende Faktoren identifiziert werden konnten. Die Mitogen-aktivierte Protein Kinase (MAPK) MKK7, deren Herrunterregulation eine verminderte bakterielle Replikation zur Folge hatte, wurde für eine weitergehende funktionelle Charakterisierung ausgewählt. Es konnte gezeigt werden, dass reduzierte MKK7 Proteinmengen eine Verringerung des Proteins zytosolische Phospholipase A2 (cPLA2) zur Folge hatten. Dieser Einfluss auf die Menge von cPLA2 beruhte nicht auf einer direkten Interaktion der beiden Proteine, sondern auf der transkriptionellen Regulation von cPLA2 durch MKK7, wie die Herunterregulation der mRNA nach MKK7 Depletion zeigte. Die Bedeutung von cPLA2 für die bakterielle Infektion wurde durch die Salmonellen-induzierte, dauerhafte Phosphorylierung des Faktors deutlich und konnte darüber hinaus durch Replikationsvergleiche in cPLA2-depletierten und nicht-depletierten Zellen bestätigt werden. Weitergehende mikroskopische Experimente deuteten darauf hin, dass die Phospholipase A2 für den fehlerfreien Aufbau von Salmonellen-induzierten Filamenten notwendig ist, welche unerlässlich für die Salmonellenreplikation in Epithelzellen sind.

ABSTRACT

The study of pathogen-host cell interactions on the molecular level is a valuable tool to reveal bacterial pathogenicity mechanisms and, moreover, contributes to our increasing knowledge of fundamental cellular processes of eukaryotic cells. The Gram negative, facultative intracellular bacterium *Salmonella* Typhimurium is a well established model organism to investigate the intracellular lifestyle of bacterial pathogens and their modulation of host cell processes. In this work, a flow cytometry (FACS) based high-throughput RNA interference (RNAi) human kinome screen was established and performed in order to elucidate host cell factors involved in the intracellular replication of *Salmonella* Typhimurium. An elaborate *Salmonella* strain expressing two fluorescent reporter constructs was generated which allowed for monitoring the bacterial replication and metabolic activity within infected cells. This made it possible to robustly assess the impact of host cell gene knock down on *Salmonella* intracellular growth. The human epithelial cell line HeLa was evaluated as the suitable cell line for the screening experiments and proper infection conditions were determined. The knock down of the host cell small GTPase Rab7A was selected as the inhibitory control for the screen due to the essential role of this factor during the infection process of the pathogen. The technical stability of the FACS assay and the accuracy of the acquired data were verified before successfully testing the applicability of the system with a small screen employing chemical inhibitors and with an in-house RNAi library, serving as a proof-of-principle. The human kinome-wide siRNA library was screened and 48 candidates were chosen for further validation. Among these, 15 host cell genes were identified to influence *Salmonella* intracellular replication. The mitogen activated protein kinase (MAPK) MKK7, whose depletion caused a decrease in bacterial replication, was selected for a more profound functional characterization to reveal its role during *Salmonella* infection. It could be demonstrated that the knock down of MKK7 caused a decrease in phospholipase A2 (cPLA2) protein levels. This control of cPLA2 levels through MKK7 did not occur via a direct interaction but rather by a transcriptional regulation of cPLA2 which was demonstrated by reduced cPLA2 mRNA levels upon knock down of MKK7. A role for cPLA2 during bacterial intracellular lifestyle was implicated by the finding that *Salmonella* induced a permanent phosphorylation of the phospholipase. The necessity of cPLA2 was confirmed with replication assays in cPLA2 depleted cells using siRNA and shRNA mediated knock down strategies. Microscopic experiments indicated that the phospholipase A2 is involved in the accurate generation of *Salmonella*-induced filaments, structures that were reported to be indispensable for replication.

TABLE OF CONTENTS

ABBREVIATIONS

A	ampere
AA	arachidonic acid
Ab	antibody
ATP	adenosine triphosphate
bp	base pair
BSA	bovine serum albumin
cAMP	cyclic adenosine monophosphate
cfu	colony forming units
cm	centimetre
cPLA2	cytosolic phospholipase A2
ddH_2O	distilled water, millipore
DNA	deoxyribonucleic acid
dsRNA	double stranded RNA
e.g.	*exempli gratia*
EEA-1	early endosome antigen 1
ERK	extracellular signal-regulated kinase
F	Farad
FACS	fluorescence activated cell sorting
FCS	fetal calf serum
g	gram
g	relative centrifugal force
GEF	guanine nucleotide exchange factor
GFP	green fluorescent protein
h	hour
HRP	horseradish peroxidase
HTS	high-throughput sampler
i.e.	*id est*
IL	interleukin
JNK	c-Jun N-terminal kinase
kb	kilo base pairs
kDa	kilo Dalton
L	litre
LAMP-1	lysosomal-associated membrane protein 1
LB	lysogeny broth, also Luria-Bertani
LPS	lipopolysaccharide
M	molar; mol/L
MAPK	mitogen activated protein kinase
min	minute
miRNA	micro RNA
MOI	multiplicity of infection
mRNA	messenger RNA
NFκB	nuclear factor kappa B
Nº	number
nt	nucleotide(s)
$OD_{(xxx)}$	optical density (of xxx nm wavelength)

p.i.	*post infectionem*, post infection
PBS	phosphate buffered saline
PCN	minimal phosphate, carbon, nitrogen medium
PCR	polymerase chain reaction
PFA	paraformaldehyde
PIP	phosphatidyl-inositol phosphate
PMA	phorbol 12-myristate 13-acetate
rcf	relative centrifugal force
RNA	ribonucleic acid
RNAi	RNA interference
rpm	rounds per minute
RT	room temperature
S2 cell	*Drosophila melanogaster* Schneider 2 (S2) cells
SCV	*Salmonella* containing vacuole
SD	standard deviation
sec	second
shRNA	small hairpin RNA
Sif	*Salmonella* induced filament
siRNA	small interfering RNA
SPI-1	*Salmonella* pathogenicity island 1
SPI-2	*Salmonella* pathogenicity island 2
Stm	*Salmonella enterica* subsp. *enterica* serovar Typhimurium
subsp.	subspecies
T3SS	type three secretion system
TfR	transferrin receptor
TNF-α	tumour necrosis factor alpha
V	volt
v/v	volume per volume
w/v	weight per volume
wt	wild type

I Introduction

I.1 RNA interference

I.1.1 A short chronology

RNA interference (RNAi) describes a molecular pathway in which different RNA species are involved in the silencing of target genes either by inducing the cleavage of target mRNA (dsRNA and siRNA) or by inhibiting the translation of the mRNA (microRNA). During the last years a major research focus has been put on regulatory RNAs unravelling an increasing number of complex regulation mechanisms.
The first unintended indication for a mechanism of RNAi, also termed posttranscriptional gene silencing (PTGS), came from a study in plants performed by Napoli et al. (1990). The group introduced a chalcone synthase (*chsA*) transgene, responsible for the purple colour of the leaves, into petunia flowers. Unexpectedly, some of the transgenic plants produced pure white or variegated colours. Moreover, the level of *chsA* mRNA in these plants was decreased which was not due to lower transcription activity as could be shown later with transcription tests in isolated nuclei (van Blokland et al., 1994). The observation was named "co-supression" but the underlying mechanism remained unknown. In 1997, Metzlaff and colleagues pointed to a role of double-stranded RNA in the initiation of PTGS as they found that the expression of the *chsA* transgene resulted in the formation of double-stranded RNA which initiates PTGS (Metzlaff *et al.*, 1997). Although the first observations were made in plants, the phenomenon of PTGS is not limited to this evolutionary group. Shortly after the discovery in petunia plants, reversible gene silencing in the fungal species *Neurospora crassa* was demonstrated and termed "quelling". It was achieved by introducing plasmids containing different constructs of the albino-3 gene (*al-3*) or the *al-1* gene which are involved in the biosynthesis of carotenoids and subsequent screening for an albino phenotype (Romano *et al.*, 1992). When cultivating the resulting primary transformants for longer times a phenotypic reversion could be observed indicating that the gene silencing was only transient and not heritable in this model.
Although the biochemical nature of PTGS inducers was assumed to be double-stranded RNA, it was the group of Craig Mello and Andrew Fire who finally proofed this. In 1998, they injected different RNA molecules targeting the non-essential *unc* gene into *Caenorhabditis elegans* and examined the resulting phenotypes (Fire *et al.*, 1998). It could be shown conclusively that double-stranded RNA rather than single-stranded RNA (either sense or anti-sense strand) is a potent inducer of RNAi. This effect was evident in both the injected animals and their progeny arguing for a heritable mechanism in *C. elegans*. Moreover, they demonstrated that even a few molecules of dsRNA were enough to evoke the RNAi phenotype, thereby disproving the model of stochiometric gene silencing and indicating an amplification mechanism within the worms. This amplification of RNAi leading to systemic silencing was also detected in plants. When grafting a scion of a non-silenced tobacco plant on a beheaded stock plant which was silenced in the *nia2* gene causing chlorosis of the plant, the grafted scion also developed chlorosis (Palauqui *et al.*, 1997). With this experiment, a systemic spreading of the PTGS signals could be shown. Systemic RNAi was also shown for other organisms but not for flies or mammals and it involves a RNA-

dependent RNA polymerase (RdRP) and most likely membrane transport proteins to facilitate whole organism spread (Himber *et al.*, 2003).
First attempts to specifically silence genes in vertebrates and mammalian cell lines using dsRNAs failed (Oates *et al.*, 2000). This was mainly due to the fact that long dsRNA, consisting of more than 30 base pairs activates the mammalian protein kinase PKR (Manche *et al.*, 1992) which leads to a non-specific translation inhibition and eventually to apoptotic cell death (Gil *et al.*, 2000). In a cell-free system of *Drosophila* embryo lysates (Tuschl *et al.*, 1999) it could be demonstrated that long dsRNA is cleaved by an ATP dependent mechanism to RNA fragments of 21-23 nt which act as guiding strands for mRNA cleavage (Zamore *et al.*, 2000). Using the same *Drosphila in-vitro* system, the group of Thomas Tuschl could show that chemically synthesized small inhibitory RNA (siRNA) duplexes targeting specific mRNA sequences are potent inducers of RNAi in these lysates (Elbashir *et al.*, 2001b). This finding highlighted that long dsRNA was not necessarily required for gene silencing. The same group was then able to show that synthesized siRNA molecules of 21 nt length are competent to mediate RNAi in different mammalian cell lines without eliciting non-specific cellular responses as detected with longer dsRNA molecules (Elbashir *et al.*, 2001a). This observation made possible the employment of RNAi in virtually all commonly used laboratory cell lines. Since then significant improvement with respect to delivery of siRNAs, sequence specificity, and large-scale applications of RNAi has been made to answer important scientific questions.

I.1.2 The molecular mechanism of RNAi

Evolutionary, the RNAi pathway induced by dsRNA can be seen as a protective mechanism against viral attacks and to maintain genome integrity, possibly threatened by transposon elements. Indeed, the minimum components necessary for cleavage of long dsRNA into siRNA fragments and subsequent degradation of target RNAs are present in essentially all eukaryotic groups, suggesting a development that took place very early in the evolution of eukaryotic species (for overview see (Shabalina *et al.*, 2008).
The RNAi pathway can be divided into two stages: the initiation and the effector stage. During the initiation phase small interfering siRNAs are generated from long dsRNA molecules mediated by the enzyme Dicer. In a next step, these siRNA molecules are introduced into the RNA induced silencing complex (RISC), a high molecular weight protein complex, where the dsRNA fragments are unwound and subsequently bind to their target mRNA in a sequence specific manner to finally facilitate the degradation of the mRNA.
Dicer was identified as a dsRNA-specific RNase-III-type endonuclease with two RNaseIII domains and a dsRNA binding motif (Bernstein *et al.*, 2001). It is conserved structurally and functionally among eukaryotic species. Whereas humans possess only one Dicer protein (Provost *et al.*, 2002), the fruit fly *Drosophila melanogaster* encodes two paralogues, DCR-1 and DCR-2, which are involved in processing miRNAs and dsRNAs, respectively (Lee *et al.*, 2004). For the plant *Arabidopsis thaliana* as much as four Dicer-like proteins (DCL) have been identified so far, with each of them fulfilling different RNA-processing functions (Xie *et al.*, 2004). Dicer produces siRNA fragments of about 21 nt length with 5’ phosphates and 2-nucleotide 3’ overhangs, a process shown to be ATP-dependent for DCR-2 of *D. melanogaster* (Nykanen *et al.*, 2001), but not for human Dicer (Zhang *et al.*, 2002).
Several proteins have been reported to interact with Dicer at different stages of RNAi. One major group of proteins is the family of PPD (PAZ Piwi domain) proteins. These are highly conserved proteins that can be found in diverse organisms ranging from archae to humans. They possess two characteristic protein domains: a central PAZ domain (named after three

members of this group: Piwi, Ago, and Zwille) and a C-terminal PIWI domain (Cerutti *et al.*, 2000). The PAZ domain was reported to bind to the 2 nt 3' overhangs of the siRNA molecule, thereby enabling the introduction of the guide siRNA into the RISC (Song *et al.*, 2003, Ma *et al.*, 2004), whereas the PIWI domain is responsible for binding of the PPD proteins to Dicer (Tahbaz *et al.*, 2004). Most research has been performed on the group of PPD proteins named Ago. Ago1 and Ago2 of humans (Martinez *et al.*, 2002) and Ago2 of *Drosophila* (Hammond *et al.*, 2001) were among the first protein components of RISC to be identified during experiments to isolate the ribonucleoprotein structures. The crystal structure of an Ago protein from the archae *Pyrococcus furiosus* was resolved in 2004 and showed similarities to members of the RNase H family (Song *et al.*, 2004). Since RNase H enzymes are responsible for cleaving RNA in a RNA/DNA duplex it was proposed that Ago proteins are responsible for cleaving the target mRNA in the RISC during the stage of guide siRNA/target mRNA duplex formation. The proposed enzymatic activity was named Slicer and in humans this is performed by Ago2 (Meister *et al.*, 2004).
Several other non-PDD proteins were identified to be part of the RISC, many of them with so far unknown functions and the list is still expanding. The role of the *Drosophila* protein R2D2 in RNAi initiation and effector stage has been examined in more detail. It was identified as a dsRNA-binding protein co-fractionating in S2 cell extracts that displayed dsRNA-processing activity (Liu *et al.*, 2003). R2D2 forms a stable complex with Dcr2 and this complex is needed for efficient RISC stimulation. Furthermore, the Dcr2-R2D2 association is fundamental for binding and transfer of siRNA single strands to Ago2 in RISC (Liu *et al.*, 2003). The decision which single strand enters RISC is dependent on thermodynamic differences between the two siRNA strands, with the one whose 5' end is less tightly bound serving as guide strand which is transferred to Ago2 (Schwarz *et al.*, 2003). From this data and accumulating other observations a stepwise model was proposed for long dsRNA-mediated post transcriptional gene silencing in *Drosophila* which is probably also relevant for other species and their respective homologous RNAi proteins (see figure I.1).

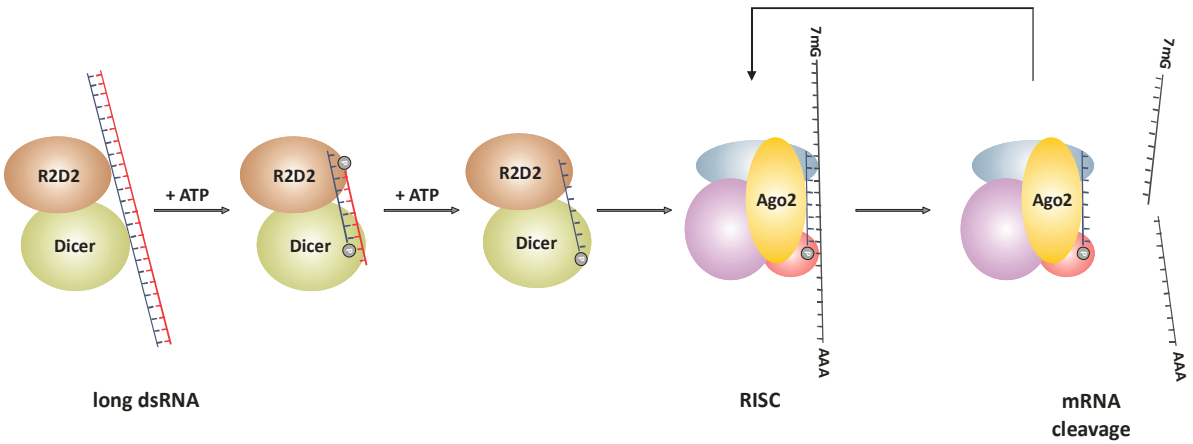

Figure I.1: Schematic overview of the RNAi pathway in *Drosophila melanogaster*.
This model has been proposed based on several experimental observations. See text for details.

In a first step, Dcr2 forms a complex with R2D2 and maybe additional proteins to bind to long dsRNA. Dicer then cleaves the molecule into siRNA fragments of about 21 nt with characteristic 2 nt 3' overhangs. Both the 3' end of the guide siRNA strand which enters RISC

as well as the 5' end of the non-incorporated strand bind to R2D2. In an ATP-dependent enzymatic step the double-stranded siRNA is unwound by helicase activity and the guide siRNA single strand is transferred from the Dcr2-R2D2 complex to Ago2 to facilitate target mRNA cleavage after complementary base pairing. This cleavage takes place between nt 10 and 11 relative to the 5' end of the guide siRNA (Elbashir *et al.*, 2001b). The cleaved mRNA is then targeted and degraded by cellular nucleases (Orban *et al.*, 2005) resulting in the silencing of gene expression. Subsequently, the RISC can undergo a new enzymatic RNAi cycle (Hutvagner *et al.*, 2002).

I.1.3 Applications of siRNA mediated gene knock down

I.1.3.1 RNAi screens

Although the precise molecular mechanisms of siRNA-mediated gene silencing as well as other post-transcriptional gene silencing pathways are still matter of intensive research, soon after the first discoveries the enormous potential of specifically knocking down gene expression was recognized. Especially the large scale application of RNAi developed very rapidly and enabled scientists to examine biological events and underlying genetic traits in high-throughput experiments, ending up finally with genome-wide siRNA screens.
Since the beginning of large-scale screening approaches respective scientific publications have been expanded in number and cover virtually every aspect of cellular biology. For example, a genome-wide screen for *Drosophila* cell morphology was performed by Kiger et al. (2003). The group constructed a library of long dsRNAs targeting about 1,000 different genes from various functional backgrounds to screen in a 384 well plate format. Using automated microscopy and differential staining they could identify several genes that altered the morphology of either round-shaped $S2R^+$ cells or flat-shaped Kc_{167} cells or both cell types with respect to actin organisation, cell size, and other features (Kiger *et al.*, 2003).
A screen conducted by Kamath et al. (2003) aimed to functionally analyse the genome of *Caenorhabditis elegans*. Since it is possible to induce RNAi in *C. elegans* by feeding the worms with bacteria expressing long dsRNA molecules (Timmons *et al.*, 1998), they constructed a respective library targeting about 87% of the predicted genome. Gene knock down mediated phenotypes such as sterility or larval lethality were assigned and the responsible genes were grouped to functionally cluster the assayed *C. elegans* genes (Kamath *et al.*, 2003).
To identify genes that are involved in cell division of the human cancer cell line HeLa, a plate-reader based screen was performed (Kittler *et al.*, 2007). The scientists used esiRNAs targeting about 18,000 genes and following knock down cellular DNA content was measured by propidium iodide staining using an Acumen plate reader device. EsiRNAs are enzymatically generated pools of siRNA-like molecules which mediate efficient gene knock down (Yang *et al.*, 2002). Hundreds of genes were identified to influence HeLa cell division although these results have to be judged carefully since HeLa cells, as nearly all laboratory tissue culture cell lines, are already transformed. Thus, it is very likely that genes important for non-transformed cells were not identified within this work.
Also in the field of infection biology large scale RNAi screens have been applied to examine pathogen-host cell interactions by studying the impact of host cell gene knock down on the infection process. One of the first of such screens was a genome-wide RNAi screen performed in *Drosophila* cells to elucidate host cell factors required for *Listeria*

monocytogenes intracellular replication (Agaisse *et al.*, 2005). Using automated microscopy and distinct bacterial intracellular phenotypes as read-out, about 200 targets that influenced *Listeria* replication were identified. In a comparable screen, Philips et al. (2005) identified CD36 family members as being involved in mycobacterial infection of *Drosophila* cells. Several screens have been published dealing with viral entry and/or intracellular replication, e.g. for hepatitis C virus (Randall *et al.*, 2007), West Nile virus (Krishnan *et al.*, 2008) or Influenza virus (Hao *et al.*, 2008).
In 2007, a kinome siRNA screen for intracellular growth of *Salmonella* Typhimurium was published in which the serine/threonine kinase PKB/Akt1 was reported to be essential for bacterial replication (Kuijl *et al.*, 2007). The screen was performed in MCF-7 cancer cells and analyzed using automated microscopy in 384 well format. The basic idea was to identify host cell targets that could be chemically inhibited to prevent intracellular bacterial replication and the group could show that H-89, a well-known protein kinase A (PKA) inhibitor, was able to decrease *Salmonella* replication. The group claimed that PKA is not the real target of H-89 and in order to identify it they performed a kinase library screen. Although the published primary data did not necessarily point to Akt1 as being a fundamental host cell factor for *Salmonella* infection, it was chosen for further analysis. In subsequent experiments, the Akt1 substrate AS160 was identified to be involved in *Salmonella* growth by repressing the activity of Rab 14 resulting in phagosomal fusion with lysosomes. When AS160 gets inactivated by Akt1 mediated phosphorylation this fusion is inhibited by the activity of Rab 14.
Interestingly, during the screen peformed in this work neither Akt1 nor any other kinase or kinase-related protein reported by this group could be identified as affecting *Salmonella* intracellular growth. This will be discussed in detail in the discussion section.

I.1.3.2 Therapeutic applications

The possibility to specifically degrade RNA by the means of siRNA molecules encouraged scientists to develop therapeutic applications, especially anti-viral and anti-cancer approaches. By using synthetic siRNAs targeting the human immunodeficiency virus (HIV) envelope gene *env*, Park and colleagues (2003) could inhibit viral replication in tissue culture cell lines as well as in activated peripheral blood mononuclear cells (PBMC). Also, inhibition of hepatitis B virus using small hairpin (sh) RNA constructs that targeted different viral components was successful in cell culture and in immunocompetent and –compromised mice (McCaffrey *et al.*, 2003). ShRNAs are retrovirally encoded RNAs that form a siRNA-like duplex by hairpin formation. These shRNAs are then recognized by the RNAi apparatus, thereby inducing target mRNA degradation. Since the retroviral construct is normally integrated into the host genome, a permanent inhibition of a specific gene expression can be achieved.
Several other reports on viral inhibition using RNAi were published, indicating a potential therapeutic strategy (Zhou *et al.*, 2008, Vigne *et al.*, 2009). Nevertheless, the rapid viral mutation rate limits these approaches since strict sequence complementarities are a prerequisite for efficient siRNA mediated gene silencing.
Another potential field of applied RNAi is the therapeutic treatment of cancer diseases. Since it is known that the overexpression of specific genes (oncogenes) favors the development of different forms of cancer, and indeed may serve as tumour markers, it was proposed to use RNAi as a gene therapeutic tool by inhibiting the expression of such oncogenes. It could, for example, be demonstrated that the stable gene silencing of the oncogenic allele K-RasV12 leads to a loss of tumorigenic properties of a mammalian cell line (Brummelkamp *et al.*,

2002). It is thus tempting to hope for the development of cancer-type specific gene therapies based on RNAi.

I.1.4 Summary

Since the first experimental discoveries of the siRNA mediated gene silencing strong effort has been made in order to elucidate the molecular mechanism and to develop suitable applications to use RNAi as a cell biological tool. Although the advances in this field are strikingly and have been achieved in comparatively short time, major drawbacks still exist and might remain. These are for example: off-target effects, i.e. the down-regulation of other transcripts than the targeted one, cell toxicity due to transfection reagents, non-specific cellular responses following transfection treatment, and hard-to-transfect cell lines such as immune cells. Nevertheless, the siRNA mediated gene silencing displays a precious tool to study gene function, possibly to combat diseases, and surely to examine host-pathogen interactions from the host cell side.

I.2 The biology of *Salmonella*

I.2.1 Overview

Salmonella are Gram negative, rod-shaped, facultative anaerob bacteria belonging to the genus Enterobacteriacea. They are mostly motile with peritricheous flagella and express different types of adhesins. *Salmonella* are very relevant pathogens of humans and livestock. Especially in under-developed countries with poor sanitary conditions infections with *Salmonella* display a significant health problem. The genus consists of only two species: *Salmonella* bongori and *Salmonella* enterica, the former one being a pathogen of cold-blooded animals such as reptiles. The latter one can be further divided into a large number of different sub-species and serovars as defined by the antigenic composition of their somatic and flagella antigens (see table I.1) (Tindall *et al.*, 2005).

Table I.1

Salmonella species	Subspecies	Important serovars
Salmonella enterica	*S. enterica* subsp. *enterica*	Typhi, Typhimurium
	S. enterica subsp. *salamae*	
	S. enterica subsp. *arizonae*	
	S. enterica subsp. *diarizonae*	
	S. enterica subsp. *houtenae*	
	S. enterica subsp. *indica*	
Salmonella bongori	none	

Nearly all reported cases of Salmonellosis in humans and livestock are caused by isolates from the *S. enterica* subsp. *enterica* subgroup. In humans, members of this subgroup are the causative agent of different diseases that range from mild, self-limiting gastro-intestinal disorders to severe systemic diseases with significant fatality. Although the systemic, life-

threatening typhoid fever, caused by the *S. enterica* subsp. *enterica* serovars Typhi and Paratyphi, does not play a significant role in industrialized countries, gastro-intestinal Salmonellosis infections are among the most frequently reported infectious diseases in many developed countries. In Germany, non-typhoid Salmonellosis showed an incidence of 67 cases per 100,000 inhabitants in 2007 and was therefore the second most prevalent bacterial infection (RKI: Epidemiologisches Bulletin 2008/16). *Salmonella* infections also constitute a major problem in animal husbandry, mainly by transmitting bacteria with contaminated food or water, while normally the animals are clinically silent.

I.2.2 *Salmonella* Typhimurium

Salmonella Typhimurium is the causative agent of mild to severe gastro-intestinal disorders and one of the major causes of food-poisoning. In contrats to humans, where *Salmonella* Typhimurium mainly remains extracellular in the gut's lumen, in mice it is capable of breaching the intestinal barrier and eliciting a systemic disease where it primarily targets macrophages. Owing to the strict human specificity of *Salmonella* Typhi, the causative agent of typhoid fever, *Salmonella* Typhimurium serves as a model organism to elucidate general mechanisms of pathogen-host interactions. Utilized in infection models with tissue culture cell lines and in mouse experiments, *Salmonella* Typhimurium is a very important tool for studying the intracellular lifestyle of a pathogen.

I.2.2.1 Attachment and invasion

The initial attachment of *Salmonella* Typhimurium (Stm) to host cells is mediated by a number of different fimbrial adhesins, especially type I fimbriae which have been shown to be important for binding to epithelial cell lines (Boddicker *et al.*, 2002, Althouse *et al.*, 2003). In contrast to *S.* Typhi, where the cystic fibrosis transmembrane conductance regulator (CFTR) was identified to be responsible for binding (Pier *et al.*, 1998), no specific host cell receptor has been determined for Stm yet. It was suggested that cellular membrane components sensitive to trypsin and neuraminidase are involved in bacterial invasion (Finlay *et al.*, 1989), thus arguing for a receptor-like structure. In another report the cholesterol-dependency of invasion was described, indicating that cholesterol-enriched membrane domains, such as lipid rafts, might be necessary for bacterial invasion, probably by serving as a docking station for the translocon component of the bacterial translocation system (Hayward *et al.*, 2005). This would explain the rather unspecific ability of Stm to infect a wide range of different cell lines and host species.
The expression of genes important for the invasion process is mainly regulated by the hyper-invasive-locus A (*hilA*), a transcriptional regulator encoded on a cluster of virulence genes named *Salmonella* pathogenicity island 1 (SPI-1) (Lee *et al.*, 1992, Bajaj *et al.*, 1995). HilA expression itself is controlled by environmental signals such as oxygen levels, osmolarity, bacterial growth phase or pH (Bajaj *et al.*, 1996). HilA activates the transcription of two important genes, *invF* and *sicA*, which then initiate the expression of several other invasion genes located inside and outside of SPI-1. Therefore, HilA constitutes a central regulator in bacterial invasion. As a response to environmental stimuli and controlled by HilA a specialized secretion apparatus encoded on SPI-1, the SPI-1 type-III secretion system (SPI-1 T3SS), is formed (Kubori *et al.*, 1998). This T3SS induces the uptake into non-phagocytic cells through the delivery of different effector proteins. It consists of more than 20 proteins and is

evolutionary related to the flagellar export system (see figure I.2). One set of proteins forms a supramolecular structure, referred to as the needle complex, consisting of two rings embedded into the inner and the outer membrane of the bacterium, a rod-like structure connecting the two rings and a filamentous needle connected to the outer ring (Marlovits *et al.*, 2004). At the tip of the needle a translocon complex is formed by the proteins SipB, SipC and SipD which is integrated into the host cell membrane to facilitate the translocation of bacterial proteins (Collazo *et al.*, 1997, Scherer *et al.*, 2000). In the absence of any of these components, effector proteins are unable to cross the host cell membrane and, instead, are

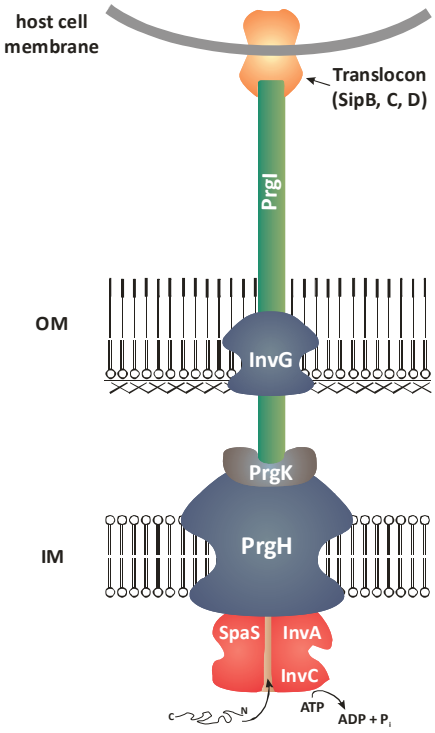

Figure I.2: Schematic illustration of the SPI-1 T3SS.
For clarity reasons only the main components are depicted. See text for details. IM: inner bacterial membrane, OM: outer bacterial membrane.
Adopted from Kimbrough and Miller, 2002

secreted into the medium. The secretion of effector proteins is mediated by a consensus sequence within the N-terminus of these proteins (Miao *et al.*, 2000). Most of these effectors are stabilized by chaperones which direct them to the secretion apparatus (Bronstein *et al.*, 2000, Tucker *et al.*, 2000). InvC, an ATPase located at the base of the needle complex, then drives the chaperone release and transport of proteins through the T3SS (Eichelberg *et al.*, 1994, Akeda *et al.*, 2005). Ten different effector proteins have been identified so far to be delivered via the SPI-1 encoded T3SS. Several of them (SipA, SipC, SopB, SopE, SopE2, and SptP) are either directly or indirectly involved in the sophisticated manipulation of the host cell actin cytoskeleton to facilitate entry into the cell. SopE and the highly similar SopE2, for instance, are guanine nucleotide exchange factors (GEF) for Rac1, Cdc42, and RhoG, thus activating these proteins which are critical for actin physiology (Hardt *et al.*, 1998, Stender *et al.*, 2000, Patel *et al.*, 2006). The precise function of SopB, a versatile protein with phosphatase activity on different phosphatidyl-inositol phosphate (PIP) species, is not yet understood in every detail but it contributes to *Salmonella* invasion by altering the $PIP(4,5)_2$ levels at the plasma membrane (Terebiznik *et al.*, 2002) and by indirectly activating RhoG through the stimulation of the exchange factor SGEF (Patel *et al.*, 2006). The activation of the host's small GTPases leads to the recruitment of the Arp2/3 complex via the WAVE and the WASP signaling pathways resulting in the induction of membrane ruffles (Criss *et al.*, 2003, Shi *et al.*, 2005). Although the recruitment of the Arp2/3 complex seems to be

essential for *Salmonella* invasion, its role in actin assembly during invasion is contradictory (Unsworth *et al.*, 2004).
Two other SPI-1 T3SS translocated effector proteins contribute to the induction of actin rearrangements, namely SipA and SipC. SipA directly binds to actin, induces its polymerisation and subsequently stabilizes actin filaments (Zhou *et al.*, 1999, Lilic *et al.*, 2003). SipC has been demonstrated to bundle actin *in-vitro* which was also confirmed in cell culture experiments with microinjected purified SipC (Hayward *et al.*, 1999). However, since it possesses a central hydrophobic region it was speculated that SipC acts from host cell membranes rather than from the cytosol. Additionally, it was shown that SipC also interacts with host cell keratins, components of the intermediate filament structure (Carlson *et al.*, 2002). Thus, SipC probably connects membrane-located keratins with actin filaments to promote the stability of the induced membrane protrusions. In another report it was described that SipA can enhance the activity of SipC, which indicates a cooperative action between these two proteins (McGhie *et al.*, 2001). The induced actin rearrangements leading to engulfment and uptake of adhesive *Salmonella* are counteracted by the effector protein SptP to ensure recovery of the cytoskeleton after invasion. SptP was shown to be able to reverse the GEF function of SopE on Rac1 and Cdc42 by preferentially binding to Rac1-GTP and Cdc42-GTP and exerting a GTPase activity, which downmodulates Rac1 and Cdc42 (Fu *et al.*, 1999). In a subsequent study, the fine-tuning between SopE and SptP activities was shown to be dependent on the different half-life of these proteins. Although both proteins are translocated in equal amounts, SopE is rapidly degraded by the host cell proteasome whereas SptP remains inside the cytosol for longer times. This enables SptP to reverse the SopE induced actin rearrangements (Kubori *et al.*, 2003).

I.2.2.2 Phagosome formation and intracellular replication

Once *Salmonella* entered the host cell it resides in a phagosome-like compartment called the *Salmonella*-containing vacuole (SCV), that was first described by Finlay and Falkow (1988), where the bacteria start to replicate after a lag period of about 3-4 hours (see figure I.3). The formation of the SCV and its subsequent development along the phagosome-maturation pathway has been the object of intensive studies, yet with partially conflicting data. This often attributed to the different pathogen-cell culture models used. It has been shown that the SCV transiently interacts with the early endocytic and the recycling pathway and rapidly acquires and loses respective markers such as early endosome antigen-1 (EEA1) and the transferrin receptor (TfR) (Steele-Mortimer *et al.*, 1999) or Rab11 (Smith *et al.*, 2005), respectively. Scott et al. (2002) could show that the recruitment of EEA1 is dependent on PI3P at the vacuole, and probably EEA1 is involved in the homotypic fusion of early SCVs to generate larger vacuoles (Mills *et al.*, 1998). Shortly after invasion, early endosomal markers are replaced by those of late endosomes like Rab7 and lysosomes such as LAMP-1 and vATPase (Steele-Mortimer *et al.*, 1999). The GTPase Rab7 replaces Rab5 to promote early to late endosome transition along the endocytic traffic of phagosomes (Rink *et al.*, 2005) and initiates the fusion with lysosomal compartments by recruiting the effector protein RILP. RILP interacts with the dynein-dynactin motor complex to facilitate transport of endosomes towards the minus-end of microtubules to lysosomes (Cantalupo *et al.*, 2001, Jordens *et al.*, 2001). It has been reported that the recruitment of Rab7 to SCV membranes is essential for a proper maturation of the SCV (Meresse *et al.*, 1999) and, indeed, in this work further evidence is presented on the essential role of Rab7 on *Salmonella* intracellular growth. There is contradictory data whether or not the SCV fuses with lysosomes. Although some

lysosomal markers are acquired during the maturation of the SCV, such as LAMP-1 (Garcia-del Portillo *et al.*, 1995) and the vacuolar ATPase (Steele-Mortimer *et al.*, 1999), others such as cathepsin D and mannose-6-phosphate-receptors could not be detected (Hashim *et al.*, 2000). *Salmonella* senses the intracellular milieu by different two-component systems with the PhoP/Q system being the best studied one. The SCV is poor in ions like Fe^{2+} and Mg^{2+} and slightly acidic as determined by respective reporter constructs and microarray studies (Garcia-del Portillo *et al.*, 1992, Rathman *et al.*, 1996, Martin-Orozco *et al.*, 2006, Hautefort *et al.*, 2008). The low magnesium concentration and probably also the low pH is sensed by

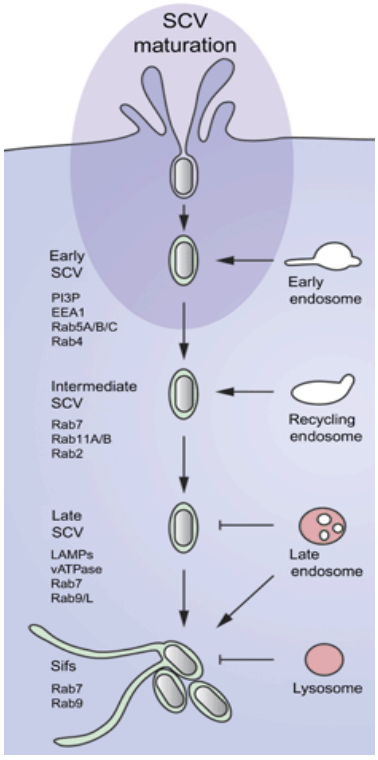

Figure I.3: Maturation of the *Salmonella*-containing vacuole (SCV). Following entry into the host cell, the newly formed SCV interacts with the endocytic pathway and acquires certain specific endosomal markers whereas others, especially lysosomal proteins, are avoided from the vacuole. This suggests an inhibition of lysosomal fusion with the SCV, controlled by the bacterium. See text for further details. Taken and modified from Bakowski et al. (2008).

the global regulator system PhoP/Q (Groisman, 2001, Garcia Vescovi *et al.*, 1996, Chamnongpol *et al.*, 2003) which then activates the transcription regulator PhoP. PhoP is responsible for the expression of a large number of virulence genes to promote intracellular survival and respective *Salmonella* mutants are strongly impaired in their virulence (Galan *et al.*, 1989, Miller *et al.*, 1989). Under the control of the PhoP/Q regulon and another transcriptional activator, OmpR, genes are expressed encoding a second T3SS located on SPI-2 which translocates effector proteins across the vacuolar membrane into the host cell cytosol (Shea *et al.*, 1996). The SPI-2 T3SS has been shown to be essential for virulence and the secreted effector proteins contribute to the intracellular survival of *Salmonella* by altering host cell processes. So far, about twenty different proteins have been described as being delivered by the SPI-2 T3SS, although the precise function and possible host cell targets are largely unknown (see figure I.4). Additionally, it is not clear whether all of these proteins play an essential role in survival since single gene knock out mutations do not impair growth *in-vivo* to the same extent as when deleting the entire SPI-2 T3SS, thus arguing for non-essential proteins and/or a functional redundancy among effector proteins. One of the best characterized SPI-2 effector is SifA, a protein that gets modified at the C-terminus by host cell enzymes after translocation to facilitate SCV membrane anchorage (Reinicke *et al.*, 2005, Boucrot *et al.*, 2003). SifA has been identified as being responsible for

the generation of filamentous, LAMP-1 enriched membrane structures that protrude from the SCV along microtubules and were termed *Salmonella* induced filaments (Sif) (Garcia-del Portillo *et al.*, 1993, Stein *et al.*, 1996, Brumell *et al.*, 2002). *SifA* mutants are impaired in replication inside macrophages due to the disruption of the vacuolar membrane and release of bacteria into the cytosol, indicating that SifA ensures the integrity of the SCV membrane (Beuzon *et al.*, 2000, Brumell *et al.*, 2001a). Using a yeast-two-hybrid approach Boucrot et al. (2005) could identify a human protein of unknown function as an interacting partner which was named SKIP (SifA and kinesin-interacting protein) due to the fact that SifA controls the

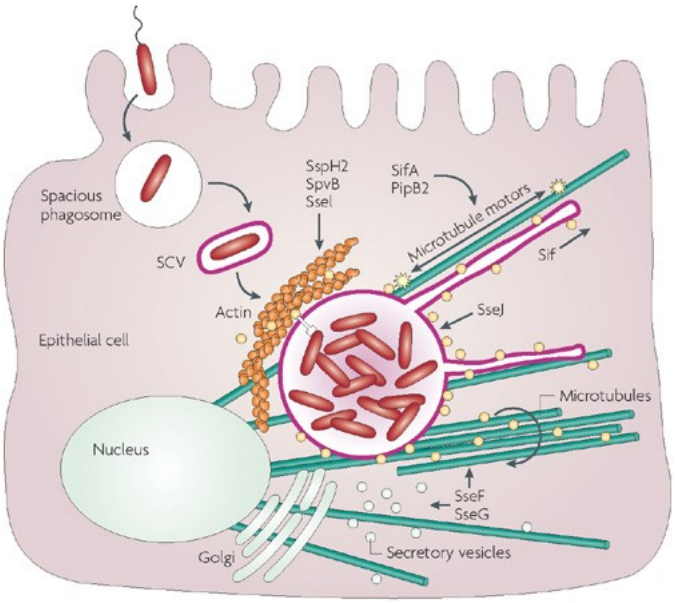

Figure I.4: Modulation of the SCV and involved SPI2 effectors.
The SPI2 encoded T3SS delivers several effector proteins across the SCV membrane into the host cell cytosol where they fulfil different functions to enable intracellular replication.
(Haraga *et al.*, 2008)

activity of the plus-end microtubule motor kinesin via this protein. This process is supposed to prevent uncontrolled elongation of Sifs which is partly induced by the action of another SPI-2 effector, PipB2, which has been shown to redistribute endosomal vesicles to the cell periphery in overexpression experiments (Knodler *et al.*, 2005b). Henry et al. (2006) identified PipB2 as a linker for kinesin to the SCV membrane, thus having a function oppositional to SifA. This was also speculated for the effector SseJ since the deletion of the respective gene was able to rescue the inhibitory effects on Sif formation in a Δ*sifA* background (Ruiz-Albert *et al.*, 2002) and cells infected with a *ssej* mutant strain exhibit increased numbers of Sifs (Birmingham *et al.*, 2005). SseJ is an effector protein sharing similarity to the family of GDSL lipases (Akoh *et al.*, 2004) and deacylase and cholesterol acyltransferase activity has been described for this protein (Ohlson *et al.*, 2005, Nawabi *et al.*, 2008, Lossi *et al.*, 2008). Therefore it was speculated that SseJ contributes to the lipid modification of the vacuolar membrane which might enable Sif curvatures or the generation of membrane microdomains involved in vesicle docking. So far the roles of the effector proteins SseF and SseG have not been clarified completely, since they have been allocated to endosome aggregation, microtubule bundling, recruitment of exocytic vesicles, and intracellular positioning of the SCV (Guy *et al.*, 2000, Kuhle *et al.*, 2004, Kuhle *et al.*, 2006, Salcedo *et al.*, 2003). Taken together it becomes clear that intracellular *Salmonella* heavily modify the SCV in order to promote survival and replication. Through a concerted action of several translocated effector proteins with so far only incompletely understood functions, *Salmonella* builds up membranous Sifs which may have different functions, for example recruitment and fusion of endocytic and/or exocytic vesicles for nutrient supply and

modification of the SCV membrane to form microdomains involved in docking of vesicles or as platforms to influence host cell signaling. Moreover, a stable vacuolar boundary is important for *Salmonella* to avoid the harmful cytosolic environment of the host cell, especially the one of phagocytes which efficiently kills pathogens.

I.2.2.3 Impact on host cell signaling

Infections with *Salmonella* Typhimurium elicit pronounced enteric inflammation reactions accompanied by diarrhoea. The molecular mechanisms underlying this are not fully understood yet, but they are doubtlessly multi-factor events with both pathogen and host properties contributing. Additionally, signaling events connected to inflammation observed in tissue culture cell models may not reflect the *in-vivo* situation which is examined in animal models of enteritis.
The SPI-1 effector dependent stimulation of Rac1 and Cdc42 also activates mitogen activated protein kinases (MAPK) that leads to nuclear responses of the host cell, such as the activation of the transcription factors c-Jun (Hobbie *et al.*, 1997, Chen *et al.*, 1996a) and nuclear factor kappa B (NFκB) as determined by IL-8 secretion of epithelial cells (Eckmann *et al.*, 1993, Hobert *et al.*, 2002). Also other SPI-1 effector proteins have been identified to induce inflammatory reactions in different infection models (Jones *et al.*, 1998, Chang *et al.*, 2007). In a polarized epithelial cell culture model SopB, SopE and SipA dependent disruption of tight junctions was reported (Boyle *et al.*, 2006). Additionally, bacterial flagellin, the main component of flagella, recognized by host cell toll-like-receptor 5 (TLR5) can induce inflammatory responses (Tallant *et al.*, 2004). *In-vivo*, secretion of IL-8 leads to the attraction of polymorphonuclear leukocytes (PMN) and inflammation whereas SopB and SopA mediated tight junction disruption causes ion effluxes and diarrhoea.
Infections with *Salmonella* Typhimurium often result in profound gastro-intestinal disorders, at least partly due to the induction of inflammatory responses described. In order to turn back potentially harmful host responses and to avoid rapid clearance from the gut owing to massive diarrhoea, *Salmonella* Typhimurium has evolved strategies to downmodulate pro-inflammatory signaling cascades. A major aspect is the inhibition of NFκB dependent gene expression. SspH1 is an effector protein which has been described to interact with the host cell kinase PKN1 (Haraga *et al.*, 2003, Haraga *et al.*, 2006), a kinase involved in the NFκB and JNK (c-Jun N-terminal kinase) signaling pathway (Kato *et al.*, 2008) and this is proposed to inhibit NFκB activity, although the authors failed to conclusively proof this. NFκB inhibition was also shown for the secreted effector SseL (Le Negrate *et al.*, 2008). Additionally, SpvC, a factor encoded on a virulence plasmid present in some *Salmonella* serovars (Jones *et al.*, 1982), has been reported to inhibit the MAPKs ERK (extracellular signal-regulated kinase) and JNK. This is achieved via its phosphothreonine lyase activity, an enzymatic property similar to that seen for the *Shigella* effector protein OspF (Mazurkiewicz *et al.*, 2008, Li *et al.*, 2007). JNK is also targeted to downmodulate host immune responses by another effector, AvrA, translocated via the SPI-1 T3SS (Jones *et al.*, 2008). In contrast to the *Yersinia* effector YopJ which was reported to inhibit different MAPKs (Orth *et al.*, 1999), AvrA seems to specifically block JNK signaling.
Thus, taking into account the numerous effector proteins that were described as being able to downregulate pro-inflammatory pathways it emerges that *Salmonella* Typhimurium aspires to control the innate immune response of the host in order to prevent excessive tissue inflammation. This might help the bacteria to colonize the gut epithelium for prolonged times.

I.2.2.4 *Salmonella* and cell death

Apoptosis, one form of programmed cell death, is a complex, tightly regulated process of self-elimination which is essential for normal development, tissue homeostasis and also for repelling infections. It was first described by Kerr et al. (1972) and since then ever increasing knowledge of different apoptosis pathways and their regulation has been accumulated. Apoptosis, as a controlled, non-inflammatory cell death, can be distinguished from necrosis, which leads to the burst of cells and the release of highly inflammatory cytosolic contents into the tissue, although this strict classification has been weakened and several mixed-classes of cell death have been defined (Kroemer *et al.*, 2009). In order to combat intracellular infections, apoptosis constitutes a major strategy to prevent spread of infection. Therefore, the inhibition of host cell apoptosis is crucial for several intracellular pathogens in order to endure the replication niche. On the other hand, induction of apoptosis at the right time of the infection cycle might promote the systemic dissemination and thereby exhibits an attractive route for many pathogens.
The interactions of intracellular *Salmonella* with the host cell's death machinery had long been poorly understood. However, recent studies more and more reveal the complex signaling underlying this process. Initially, *Salmonella* induced apoptotic cell death was described for the macrophage-like cell lines J774A.1 (Chen *et al.*, 1996b) and RAW264.7 (Monack *et al.*, 1996). In the study with J774 cells, the majority of infected macrophages showed the characteristic apoptotic morphology very early during infection. It could be demonstrated that this process was dependent on active invasion since stationary phase bacterial cultures displayed only minor cytotoxic activity. Later, it could be shown that the rapid macrophage killing is dependent on the bacterial protein SipB which is a component of the SPI1-T3SS and that SipB binds to Caspase-1 which causes release of pro-inflammatory IL-1β and IL-18 (Hersh *et al.*, 1999, Monack *et al.*, 2001). Due to the fact that this form of cell death displays characteristics of both apoptosis and necrosis, it has recently been termed pyroptosis (Fink *et al.*, 2007). Most recently, the inflammasome protein Ipaf was identified to play an important role in *Salmonella*-induced pyroptosis (Fink *et al.*, 2008). Although the impact of SipB on host cell death has been emphasized by several other reports, the precise cellular mechanism is still under discussion since it was also described to induce mitochondria-dependent autophagy (Hernandez *et al.*, 2003). Moreover, SipB independent killing during the course of infection has been described (Santos *et al.*, 2001). Additionally, the route of entry into macrophages seems to be important for the cytotoxic effects (Forsberg *et al.*, 2003), which might resemble different stages of the *in-vivo* infection, namely the disseminating infection with actively invading bacteria, accompanied by clinical symptoms, and the silent, persistent stage of mainly phagocytosed bacteria.
Remarkably little is known about apoptosis pathways in *Salmonella* infected epithelial cells. Lundberg et al. (1999) reported that different epithelial cell lines infected with *Salmonella* Typhimurium did not undergo cell death at an early time point as compared to macrophages. Since most epithelial cell lines are derived from carcinoma tissues they often do not go into apoptosis easily, thus, this result has to be assessed carefully. Apoptosis of the colon cancer cell line HT-29 was shown after longer infection with *Salmonella* (Kim *et al.*, 1998), although a significant proportion of the cells also showed features of necrosis. Recently, the *Salmonella* effector SopB, translocated via the SPI1-T3SS, was shown to protect epithelial cells from apoptosis by activating the pro-survival kinase PKB/Akt1 (Knodler *et al.*, 2005a). Owing to the few reports a concluding determination whether *Salmonella* induces or inhibits epithelial apoptosis can not be made. Most likely this depends on the stage of

infection, the tissue type or host responses and *Salmonella* is potentially capable of controlling both directions.

I.2.3 Summary

Salmonella Typhimurium is a Gram negative, facultative intracellular pathogen which has the capacity to infect a wide range of host species and has become an object of intensive scientific studies with regard to pathogen-host cell interactions. It induces its uptake into non-phagocytic cells by the delivery of effector proteins via a sophisticated T3SS. After uptake, the bacteria reside in a phagosome-like compartment which undergoes maturation resembling the endocytic pathway to a certain extent. Throughout the whole infection cycle the bacteria remain inside the vacuolar compartment, termed the *Salmonella*-containing vacuole, which is actively remodelled by the pathogen and where replication is taking place. A second T3SS is expressed intracellularly and a plethora of effector proteins is delivered across the vacuolar membrane into the host cell's cytosol. Although the precise function of the majority of these effector proteins is unknown it is tempting to speculate that they serve to interact with host cell factors in order to control their functions during the establishment of the intracellular replication niche. Thus, *Salmonella* is interacting at several stages of the infection with its host cell in order to facilitate entry, to replicate inside a modified phagosome, and to manipulate host cell signaling pathways to prevent degradation. The whole spectrum of these interactions is still far away from being deciphered.

I.3 Goals of this study

Intracellular pathogens are in close contact to their host cells and rely on their cellular machinery to assure a successful infection. During the evolution of host-pathogen interactions, a complex network has developed with both the host and the pathogen contributing. The identification of host cell functions which are essential for these interactions is crucial for the understanding of the mechanisms underlying pathogenicity and moreover serves to gain deeper insights into important host cell pathways.
The aim of this work was to elucidate host cell factors that affect the intracellular growth of the Gram negative pathogenic bacterium *Salmonella* Typhimurium. For this purpose, a large scale high-throughput RNAi screen should be established and performed using a commercial human kinome-wide siRNA library. Kinases display central regulators of a plethora of cellular processes and are therefore likely targeted by intracellular pathogens to subvert host cell functions. In order to screen a large set of siRNAs a high-throughput system had to be established to automate critical steps such as the transfection of the cells or the plate measurement. Therefore, a flow cytometry based screening assay should be developed using a bacterial reporter strain to monitor *Salmonella* intracellular replication and metabolic activity upon host cell gene knock down. The set-up of a semi-automatic screening assay was intended to be achieved with the help of the flow cytometry device FACS Calibur. The primary data from the screening experiments should be validated with additional siRNA sequences to omit false positive candidate genes from further analysis. The final goal was to functionally characterize host cell genes for their role in *Salmonella* Typhimurium infection.

II Materials and methods

II.1 Chemicals

All chemicals were purchased from Roth (Karlsruhe), Sigma-Aldrich (Steinheim) or Merck (Darmstadt) if not stated otherwise.

II.2 Buffers, solutions, and media

10x PCN buffer

0.8 M	MOPS-KOH (pH 7.4)
0.04 M	tricine
0.5 M	NaCl
2.76 mM	K_2SO_4

PCN medium

1 x	PCN buffer
0.01 mM	$FeSO_4$
15 mM	NH_4Cl
0.5 µM	$CaCl_2$
0.4 % or 0.2 %	glucose or arabinose [w/v]
10 mM	$MgSO_4$
1.25 mM	potassium phosphate buffer pH7.4
0.01 %	casein [w/v]

10x TBS

200 mM	Tris base
1.4 M	NaCl

adjusted to pH 7.4

1x TBS-T

0.1 % [v/v] Tween 20 in 1x TBS

10x SDS running buffer

247 mM	Tris base
1.9 M	glycin
35 mM	sodiumdodecyl sulphate (SDS)

TBE

890 mM	Tris base
890 mM	boric acid
20 mM	EDTA-NA_2

adjusted to pH 7.4

Transfer buffer

25 mM	Tris-HCl pH 8.5
190 mM	glycine
10%	methanol [v/v]
0.1%	SDS [w/v]

RIPA buffer

20 mM	Tris-HCl, pH 7.5
150 mM	NaCl
0.5%	NP-40 [v/v]
0.5%	Triton X-100 [v/v]

Stripping buffer

68 mM	Tris-HCl, pH 7.5
2%	SDS [w/v]
0.8%	β-mercaptoethanol [v/v]

LB medium

10 g	Bacto tryptone (BD, Franklin Lakes, NJ, USA)
5 g	Bacto yeast extract (BD, Franklin Lakes, NJ, USA)
5 g	NaCl

ad 1 L with ddH_2O
adjusted to pH 7.4

for plates 1.5% (w/v) agar was added

LB high salt medium

LB medium with 17.5 g/L NaCl (i.e. 0.3 M)

4% paraformaldehyde (PFA)

for 1 L

solve 40 g PFA in 600 mL ddH_2O and heat at 60-70°C
add conc. NaOH dropwise until solution becomes clear
add 100 mL 10x PBS and add ddH_2O ad 1L
adjust pH 7.4 with HCl and sterilize the solution by filtering through 0.22 µm filters
store aliquots at -20°C

10x PBS

1.36 M	NaCl
27 mM	KCl
14 mM	KH_2PO_4
81 mM	$Na_2HPO_4 \times 2\ H_2O$

adjusted to pH 7.4

antibiotics

antibiotic	supplier	stock concentration	working concentration
ampicillin	Sigma	100 mg/mL	100 µg/mL
kanamycin	Fluka	50 mg/mL	50 µg/mL
gentamicin	Sigma	10 mg/mL	100 or 20 µg/mL

10x PCR buffer

100 mM	Tris
500 mM	KCl

adjusted to pH 8.3

5x DNA loading dye

50 %	glycerol (85%) [v/v]
0.5 x	TBE
0.2%	SDS [w/v]
dash	bromophenol blue

store at 4°C

2x Lämmli buffer

100 mM	Tris-HCl, pH 6.8
4%	SDS [w/v]
20%	glycerol [v/v]
1.5%	β-mercaptoethanol [v/v]
dash	bromophenol blue

in ddH_2O

II.3 Technical equipment

For this work, facilities equipped with state-of-the-art laboratory devices were used.

II.4 Plasmids

The following plasmids were used in this study. They were maintained in *E. coli* DH5α -80°C glycerol stocks or as midi prep samples at -20°C.

Table II.1: Plasmids used in this study

plasmid	description	source	strain collection Nº
pACYC177	cloning vector / AmpR / KanR	Chang and Cohen, 1978 / in-house	H2678
pBAD18	arabinose inducible expression vector / AmpR	Guzman et al., 1995 / in-house	H3125
pFPV25.1	constitutive expression of GFPmut3 / AmpR	Valdivia and Falkow, 1996 / kindly provided by M.	H3892

pFPVmCherry	constitutive expression of mCherry / AmpR	Hensel, Erlangen kindly provided by O. Steele-Mortimer	H3893
pRSET-B mCherry	T7 promoter driven expression of mCherry / template for mCherry PCR / AmpR	Shaner et al. 2004, kindly provided by Tsien Labs, USA	H3894
pOR25	constitutive expression of GFPmut3 / KanR	this study	H3895
pOR26	arabinose inducible expression of mCherry / AmpR	this study	H3812

II.5 Oligonucleotides, small inhibitory RNAs (siRNAs), and antibodies

All oligonucleotides ("primers") used in this study were synthesized by Invitrogen (Karlsruhe).

Table II.2: Oligonucleotides used in this study

oligonucleotide	sequence (5'→ 3')	function
FP_new-F	GCTCTAGATTTAAGAAGGAG ATATACATATGGTGAGCAAG GGCGAGGAG	5' PCR primer for mCherry amplification (5' XbaI restriction site)
FP_new-R	CTCTCAAGCTTATTACTTGTA CAGCTCGTCCA	3' PCR primer for mCherry amplification (3' HindIII restriction site)
pACYC BamHI 5'	GGAAGGTGATGTCATTCTGG	5' sequencing primer for pOR25 quality check
pACYC BamHI 3'	GGCAATACTGAGCTGATGAG	3' sequencing primer for pOR25 quality check
pBAD18 5' MCS	AGATTAGCGGATCCTACCTG	5' sequencing primer for pOR26 quality check
pBAD18 3' MCS	CACTTCTGAGTTCGGCATGG	3' sequencing primer for pOR26 quality check

All siRNA oligonucleotides were synthesized by Qiagen (Hilden), except the Rab7A sequences which were synthesized by Dharmacon (Lafayette, CO, USA). After testing the Rab7A sequences, the Rab7A_2 siRNA was synthesized by Qiagen according to the sequence information provided by Dharmacon.

Table II.3: Small inhibitory RNA (siRNA) oligonucleotides used in this study

siRNA	target gene	siRNA target sequence	remarks
Allstars	none	not available (property of Qiagen)	neutral control
PLK1	polo-like kinase 1 (Drosophila)	CCGGATCAAGAAGAATGAATA	toxic control
Rab7A_1	RAB7A, member RAS oncogene family	AACTAGATAGCTGGAGAGATG	inhibitory control
Rab7A_2	RAB7A, member RAS oncogene family	AAGTACAAAGCCACAATAGGA	inhibitory control
Rab7A_3	RAB7A, member RAS oncogene family	AAAAACGGAGGTGGAGCTGTA	inhibitory control
Rab7A_4	RAB7A, member RAS oncogene family	AACGAATTTCCTGAACCTATC	inhibitory control
MKK7_10	mitogen-activated protein kinase kinase 7	CCCTTAGACGCTTGAGAATAA	
MKK7_13	mitogen-activated protein kinase kinase 7	CTGCGCTGAGAAGCTCAAGAA	
PLA2_1	phospholipase A2, group IVA	AACAAGGAGTTTCTAAGTAAA	
PLA2_2	phospholipase A2, group IVA	TCCCATGACAACTGGATTTAA	

Primary antibodies for immunoblotting were diluted in TBS-T buffer containing 3% [w/v] bovine serum albumine (BSA), fraction V, and stored at -20°C for multiple uses. Primary antibodies for immunofluorescence were diluted antibody-specific in 0.1 % [w/v] BSA/PBS for single use. Secondary antibodies for immunoblotting were diluted 1:2000 (anti-rabbit) or 1:3000 (anti-mouse) in 1x TBS-T, 5% [w/v] dry milk powder. Secondary antibodies for immunofluorescence were diluted 1:150 in 0.1 % [w/v] BSA/PBS.

Table II.4: Antibodies used in this study

antibody	supplier and cat. Nº	species	application
β-actin	Sigma, A5441	monoclonal mouse	immunoblotting

Rab7A	Sigma, R8779	monoclonal mouse	immunoblotting
MKK7	Cell Signaling, 4172	polyclonal rabbit	immunoblotting
cPLA2	Cell Signaling, 2832	polyclonal rabbit	immunoblotting
P-cPLA2 (Ser505)	Cell Signaling, 2831	polyclonal rabbit	immunoblotting
LAMP-1	BD Biosciences, 555798	monoclonal mouse	immunofluorescence
bacterial Hsp60	Alexis, ALX-804-071	monoclonal mouse	immunoblotting
anti-mouse	GE Healthcare, NXA931	sheep	secondary Ab immunoblotting
anti-rabbit	GE Healthcare, NA934	donkey	secondary Ab immunoblotting

II.6 Cell biological methods

II.6.1 Cell lines and cultivation

Cell lines used in this study are described in table II.5. The cells were routinely maintained in RPMI 1640 (Gibco/Invitrogen, Karlsruhe), supplemented with 10% heat-inactivated fetal calf serum, L-glutamine and 25 mM HEPES buffer (i.e. **RPMI full medium**) at 37°C with 5% CO_2 in a humidified temperature-stable cell culture incubator. For longer maintenance, medium was replaced every two to three days and the cells were passaged if appropriate using trypsin detachment.

Table II.5: Mammalian tissue culture cell lines used in this study

cell line	origin	source or reference
HeLa	cervical	DSMZ Nº ACC57, obtained from ATCC CCL-2
HT-29	colonic	DSMZ Nº ACC299
HEp-2	HeLa contaminant	ATCC CCL-23
Hec1b	endometric	HTB-113
HepG2	hepatic	DSMZ Nº ACC180

II.6.2 Bacterial strains

The *Salmonella enterica* subsp. enterica serovar Typhimurium (*Salmonella* Typhimurium) wildtype strain 12023 was utilized for infection experiments. Expression of different fluorescent proteins was facilitated by plasmid transformation (see table II.1). Cloning experiments were performed with the *Escherichia coli* laboratory strain DH5α.

Table II.6: Bacterial strains used in this study

strain	genotype	source or reference	strain collection Nº
S. Typhimurium 12023	wildtype	NCTC 12023 (ATCC 14028)	X102
E. coli DH5α	F^-, ϕ80d*lacZ*ΔM15, Δ(*lacZYA-argF*)U169, *deoR*, *recA*1, *endA*1, *hsdR*17(rk^-, mk^+), *phoA*, *supE*44, λ^-, *thi*-1, *gyrA*96, *relA*1	in-house	E248

II.6.3 Preparation of bacterial glycerol stocks

For long-term storage of bacteria, glycerol stocks were prepared by mixing 600 µL of an overnight LB culture of the strain with 300 µL of sterile glycerol in cryotubes. The stocks were stored at – 80°C.

II.6.4 Preparation and transformation of electro-competent bacteria

In order to transform bacteria with DNA, electro-competent bacteria were prepared freshly before use. An overnight LB culture was diluted 1:100 in fresh, pre-warmed medium and grown until OD_{600} of 0.5. The bacterial culture was cooled down on ice for 30 min and all subsequent steps were performed at 4°C. The bacteria were pelleted and washed three times in a small volume of pre-chilled ddH_2O to achieve a thick, dense solution of bacteria. 50 µL of electro-competent cells were mixed with the DNA and transferred to a pre-chilled Eppendorf tube. The mixture was incubated on ice for 30 min and then transferred to a pre-chilled electroporation cuvette (peqlab, Erlangen). Electroporation was performed under conditions indicated below (see table II.7) in a Gene Pulser electroporator (BioRad, Hercules, CA, USA). 1 mL of warm (37°C) LB medium was added to the cuvette, the mixture was transferred to an Eppendorf tube and incubated at 37 °C, 200 rpm for 60 min to allow recovery of the bacteria and expression of resistance genes. Bacteria were plated at different concentrations on selective agar plates to screen for positive clones.

Table II.7: Electroporation conditions

species	voltage [kV]	resistance [Ohm]	capacity (µF]
Salmonella Typhimurium 12023	2.5	600	25
Escherichia coli DH5α	1.6	200	25

II.6.5 Bacterial infection of mammalian cell lines

The infection of mammalian cells with *Salmonella* Typhimurium was performed based on the infection protocol described by Steele-Mortimer et al. (1999) with minor changes.
Two days before infection a bacterial culture was streaked from the frozen stock on a selective LB agar plate. The next day, an overnight bacterial culture was prepared by inoculating 5 mL of selective LB high-salt medium with one colony from the agar plate. The overnight culture was incubated at 37°C and 200 rpm for 16-20 hours and then diluted 1:33 in fresh, pre-warmed (37°C) selective LB hig-salt medium for a further incubation of 3,5 h. A part of the culture was transferred to 1.5 mL Eppendorf tubes and pelleted in an Eppendorf table top centrifuge at 20,000 x g for 1 min. The pellet was washed once with PBS (RT) and resuspended in RPMI full medium (37°C). In order to infect the cells with the aspired MOI, the bacterial culture was diluted according to the following assumption:

OD_{600} of 1 ≈ 1.5×10^9 cfu/mL

Additionally, the volume of infection solution of the respective plate format was taken into account (see table II.8). To infect cells with the bacterial infection solution, the cell culture medium was aspirated and a plate format specific volume of infection solution was added to the wells. Plates were centrifuged in a Heraeus multifuge 3 S-R (DJB Labcare, Newport Pagnell, UK) at 700 rpm and RT for 5 min to ensure a synchronized infection and incubated at 37 °C with 5% CO_2 in a humidified cell culture incubator to allow invasion. The cells were washed twice with PBS (RT) 60 min p.i. and remaining extracellular bacteria were killed by addition of killing medium (RPMI full medium with 100 µg/mL gentamicin) for 60 min. For the remaining infection period, the antibiotic concentration was lowered to 20 µg/mL.
For arabinose-induced expression of mCherry, cells were washed twice with PBS (RT) and induction-medium was added to the samples (RPMI full medium + 20 µg/mL gentamicin + 0.2% [w/v] L-arabinose) for the desired period of time.

Table II.8: Cell plate formats and volume of infection solution

cell plate format (well)	volume of infection solution [µL]	type of pipette used
96	50	automatic 8 channel
24	500	manual
12	1000	manual
6	1000	manual

II.6.6 Gentamicin protection assay

For the enumeration of intracellular bacterial replication, the gentamicin protection assay (gentamicin assay) was performed. Cells were infected as described and extracellular bacteria were killed with gentamicin. At the desired time-points, cells were washed twice with PBS (RT) and then lysed by adding 0.5% [v/v] triton X-100 in PBS to the wells. The lysates were transferred to 1.5 mL Eppendorf tubes. Serial dilutions of the lysates were prepared by diluting 1:10 in PBS and 100 µL of the appropriate dilution were plated on agar plates (with antibiotics, if needed). The plates were incubated at 37°C until bacterial colonies were visible and the colonies were counted to calculate intracellular bacteria. The replication rate was determined by forming the ratio of two different time points.

II.6.7 Measurement of cPLA2 enzymatic activity

In order to detect the enzymatic activity of cPLA2 in HeLa cells a specific substrate (PED6, Molecular Probes) was used which is taken up by the cells and is cleaved predominantly by activated cPLA2. Thereby turns into a fluorescent compound that can be monitored with the FACS Calibur. HeLa cells were either infected as described or left uninfected. At the respective time-point cells were washed and PED6 (5 µM) was added in complete medium to the cells for 60 min. Cells were washed thoroughly with PBS, trypsinized and resuspended in PBS for FACS analysis. Excitation = 488 nm; Emission = 530 nm (FL-1).

II.6.8 Transfection of mammalian cells with small inhibitory RNA (siRNA)

The RNA interference technique was applied to specifically inhibit the translation of eukaryotic genes. Different experimental procedures were used for 12 well format transfections for single knock-down experiments or for 96 well format large scale RNAi experiments (screening).

II.6.8.1 Transfection in 12 well format

Cells were trypsinized, counted in a Neubauer chamber and seeded at a density of 1 x 10^5 cells/well the day before transfection. For each siRNA to transfect a mixture was prepared and the supernatant was aspirated from the wells. 600 µL of fresh, pre-warmed (37°C) RPMI full medium was added before the dropwise apposition of the transfection mixture. The cells were incubated at 37°C with 5% CO_2 in a humidified cell culture incubator and split the next day as necessary. Three days post transfection the cells were employed for the respective experiments.

siRNA transfection mixture

	96 µL serum-free RPMI
+	4 µL siRNA (20 µM stock)
	mix
+	6 µL Hiperfect
	incubate at RT for 15-20 min, apply on cells

II.6.8.2 Transfection in 96 well format

96 well format transfections for large scale experiments were either performed automatically with the help of a pipetting robot or manually for smaller amounts of plates. Optimized transfection protocols using Hiperfect as transfection reagent were employed.

II.6.8.2.1 Automatic transfection

One day before transfection cells were seeded with a density of 2.5 x 10^3 cells/well using the automatic 8-channel pipette (Biohit, Rosbach v. d. Höhe). A Qiagen pipetting robot (Biorobot 8000) was used for automatic

transfection of 96 well plates under semi-sterile working conditions. The respective program that controlled the pipetting steps of the robot was written and functionally tested by the RNAi group of Nikolaus Machuy and further adjusted to fulfil the specific needs. With the program "Doppelter 2.1.1 für Salmonellen", the transfection of two cell plates with two different transfection plates per run was achieved. Prior to every run, the transfection reagent was prepared freshly (Hiperfect 1:20 in RPMI medium without FCS), pipette tips as well as the cell culture media were refilled and fresh aliquots of control siRNAs (Allstars, PLK and Rab7A; 1:100 in RPMI without FCS) were used. Cells were incubated at 37°C with 5% CO_2 in a humidified cell culture incubator. 24 h post transfection the medium was replaced by fresh, pre-warmed (37°C) RPMI full medium and the cells were incubated for two more days to allow gene knock down.

II.6.8.2.2 Manual transfection

Cells were seeded as described above and the transfection complexes were mixed in sterile deep-well plates (Cole-Parmer, Vernon Hills, IL, USA) according to the table below using a manual 12 channel pipette, an automatic 12 channel pipette and an automatic 8 channel pipette (Biohit, Rosbach v. d. Höhe).

Table II.9: Manual transfection protocol

component	volume per well [µL]
RPMI Ø FCS	30
Hiperfect (1:40 in RPMI Ø FCS)	30
siRNA (1:100 in RPMI Ø FCS)	15
mix incubate at RT for 10 min	
RPMI full medium	150
aspirate 90 µL medium from the cells add 20 µL RPMI full medium to the cells add 75 µL of transfection complex/well	

Following transfection, cells were incubated and treated as described above (see II.6.7.2.1).

II.6.9 Construction of stable shRNA transduced cell lines

The gene silencing mediated by siRNA molecules is a transient one. In order to achieve a permanent gene knock down, lentiviral encoded small hairpin (sh) RNA expression vectors were constructed and these were integrated into the target cell's genome. This ensures a constitutive expression of shRNA molecules and thereby a permanent gene knock down. By using a GFP reporter gene on the lentiviral plasmid, the transfection efficiency could be determined. Respective shRNA sequences (designed with the help of the RNAi designer from Invitrogen, Karlsruhe: https://rnaidesigner.invitrogen.com/rnaiexpress) were cloned into the vector pLVTHM and virus particles were produced by transfecting 293T cells with 20 µg of vector in combination with the packaging vectors psPAX2 (15 µg) and pMD2G (6 µg) using calcium phosphate transfection (DNA in 0.5 M $CaCl_2$ added 1:1 to 2xHBS; DNA-calciumphosphate precipitates are then added to the cells). 48 h post transfection, the filtered virus particles in the supernatant were transferred to HeLa cells with the help of polybrene (final concentration 1 mg/mL). The next day, the medium was replaced by fresh medium and five days later the knock down efficiency was tested by immunoblotting.

Table II.10: Sequences of shRNA constructs used in this study

shRNA	target gene	sequence	strain collection Nº of HeLa cell line	remarks
Luciferase	firefly luciferase	AACTTACGCTGAGTACTTCGA	HeLa05 Luci	neutral control
MKK7.1	mitogen-activated protein kinase kinase 7	GCATTGAGATTGACCAGAAGC	HeLa05 OR01	
PLA2.1	phospholipase A2, group IVA	GGAGATTACGTTAATGGATGC	HeLa05 OR02	

II.7 Molecular biological methods

II.7.1 Preparation of plasmid DNA

Plasmid DNA was used for transformation of bacteria or as template for cloning experiments. For isolation of plasmid DNA from bacteria a mini or midi prep kit from Qiagen (Hilden) was used according to the manufacturer's instructions. The DNA concentration was measured spectrometrically using a Nanodrop ND-1000 device (peqlab, Erlangen).

II.7.2 Polymerase chain reaction (PCR)

PCR was utilized for 1) the amplification of specific DNA fragments with explicit 5´and 3´restriction sites for cloning and 2) for amplification of DNA fragments for analytical purposes (e.g. colony PCR).
In table II.10 the composition of the reaction mixture as well as the standard protocol for PCR is depicted. For larger PCR approaches a master mix was prepared and distributed to the PCR reaction tubes (ABgene, Hamburg). 100-500 ng of purified DNA was used routinely, for colony PCR, some bacterial material was resuspended in 100 µL ASC-H_2O and 1 µL of this mixture was employed for PCR. All reactions were performed in a GeneAmp thermocycler (Applied Biosystems, Carlsbad, CA, USA). Pfx50 DNA polymerase (Invitrogen, Karlsruhe) and "in-house" Taq DNA polymerase were applied for cloning PCR applications and simple analytical purposes, respectively. The PCR products were further analyzed by gel electrophoresis (see II.7.3).

Table II.11: PCR reaction mixture and PCR protocol

standard reaction mixture (30 µL)		standard PCR protocol	
component	volume [µL]	condition	time
10 x reaction buffer	3	1. 95°C	5 min
dNTP's (10 mM each)	0.6	2. 95°C	30 sec
5' primer	0.6	3. 55°C	30-60 sec
3' primer	0.6	4. 68°C or 72°C	dependent on fragment size
DNA template	different	5. repeat steps 2-4 20-30 times	
100 mM $MgCl_2$ (if not part of reaction buffer)	0.9	6. 68°C or 72°C	5 min
enzyme	1		
H_2O	ad 30 µL		

II.7.3 Quantitative Real Time-PCR (RT-PCR)

RT-PCR was used to quantify the amount of specific mRNA populations, e.g. after siRNA or shRNA mediated knock down experiments. For this, total RNA was isolated using the RNeasy RNA purification kit (Qiagen, Hilden). The reverse transcription of mRNA and the subsequent RT-PCR were performed in a ABI Prism 7900 HT system (Applied Biosystems, Carlsbad, CA, USA) using the QuantiTect SYBR Green Kit (Qiagen, Hilden).

II.7.4 Gel electrophoresis

For the preparative analysis of DNA fragments or the excision of specific DNA fragments after restriction reactions, gel electrophoresis was performed. Here, DNA fragments are separated inside an agarose gel according to their migration speed along an electrical field.
Separation and detection of DNA fragments was performed in gels with 0.4-1.2 % [w/v] of agarose in 0.5x TBE and 1 µg/mL ethidiumbromide. The samples were mixed with DNA loading buffer, loaded into the pockets of the gel and separated using 80-140 V for the aspired time. To visualize the DNA, the gel was inspected with a Gene Genius device (Syngene, Cambridge, UK) detecting the fluorescence of the DNA-intercalating dye ethidiumbromide. Fragment sizes were calculated by employing DNA standards (DNA ladder 1kb or 500 bp,

Fermentas, St. Leon-Rot). For excision of fragments from a gel a sharp, clean scalpel was used and the DNA was eluted from the agarose using a gel extraction kit (Qiagen, Hilden).

II.7.5 Endonuclease reaction

In order to open plasmid DNA, to cut out DNA fragments from plasmids or to prepare PCR products for ligation reactions different restriction enzymes (all from NEB, Ipswich, MA, USA) were used. DNA was purified before restriction enzyme reactions using a PCR purification kit (Qiagen, Hilden) and multiple restriction reactions were performed sequentially with purification steps. If appropriate, BSA (NEB, Ipswich, MA, USA) was added to the digestion reaction. All experiments were performed in PCR tubes for two hours in a 37 °C incubator and the reaction products were purified again or separated with gel electrophoresis.

II.7.6 Filling of DNA overhangs

To fill up DNA overhangs produced by enzymatic restriction T4 DNA polymerase (NEB, Ipswich, MA, USA) according to the manufacturer's advice was used. The reaction was incubated in a waterbath at 30°C for 60 min. The enzyme was heat-inactivated at 65°C for 10 min and the DNA was purified using a PCR purification kit (Qiagen, Hilden).

II.7.7 Dephosphorylation of DNA

For dephosphorylation of DNA, Antarctic Phosphatase (NEB, Ipswich, MA, USA) was added to the purified DNA according to the manufacturer's advice and incubated at 37°C for 60 min. The enzyme was heat-inactivated at 65 °C for 10 min and purified using a PCR purification kit (Qiagen, Hilden).

II.7.8 Ligation

Ligations of DNA fragments were carried out with the help of the Rapid DNA Ligation Kit (Roche, Hague Road, IN, USA). For each mixture 10 µL of pre-aliquoted ligation buffer containing ATP was used. A molecular ratio fragment:plasmid of 3:1 was employed and the ligation reaction was incubated for 15-30 min at RT, transferred on ice and then purified using the PCR purification kit (Qiagen, Hilden).

II.8 Biochemical methods

II.8.1 Sodium dodecyl sulphate polyacrylamide gel electrophoresis (SDS-PAGE)

Protein samples were separated according to their migration speed using the SDS PAGE. Samples were resuspended in 1x Laemmli buffer and boiled at 95 °C for 10 min for denaturation of proteins. Acrylamide concentrations from 10-15% were used and the samples were first loaded on a stacking gel before separation over a running gel to ensure similar running conditions. Voltages applied were 60 V and 140 V for stacking and running gel, respectively. A pre-stained protein marker (Fermentas, St. Leon-Rot) was loaded on every gel to inspect SDS PAGE progression and to estimate the size of the desired protein band.

II.8.2. Immunoblotting

To detect specific antigens in a protein sample, the SDS PAGE separated proteins were blotted onto a Polyscreen PVDF membrane (Perkin-Elmer, Waltham, MA, USA). This was done using the semi-dry method and

a semi-dry blotting chamber (Biometra, Göttingen) with 1 mA of current per cm^2 of membrane for 60 min. The membrane was activated prior to use with 100% methanol and washed once in transfer buffer. After protein transfer the membrane was washed once with 1x TBS-T and blocked with 5% dry milk powder in 1x TBS-T at RT for 60 min followed by washing three times for 5 min with 1x TBS-T. In order to visualize specific protein bands, the membrane was incubated with the respective primary antibody, in an antibody specific dilution in 3% BSA/TBS-T, at 4 °C overnight with shaking. The membrane was washed 60 min with TBS-T and then the secondary antibody, coupled to HRP, was added 1:2000-3000 in 5% milk powder/ 1xTBS-T for 60 min at RT. The membrane was washed thoroughly and the antibody signals were detected by applying HRP substrate solution (GE Helathcare, Little Chalfont, UK) to the membrane and exposition to X-ray films (GE Healthcare, Little Chalfont, UK). For sequential detection of different proteins on the same membrane, the PVDF membrane was stripped in stripping buffer (50 °C, 20 min), washed once with isopropanol and thoroughly with distilled H_2O. Subsequently, the membrane was blocked again and treated as described above.

II.8.3 Immunoprecipitation (IP)

For the identification of protein-protein complexes immunoprecipitation was performed. Cells were seeded in 10 cm dishes (Corning, Lowell, MA, USA) to gain approx. 70 % confluency and the respective experiment was conducted. Afterwards, the dishes were put on ice and all subsequent steps were performed on ice and with pre-cooled (4°C) centrifuges. Cells were washed once with cold PBS and then 2 mL of cold PBS + PhosStop (Roche) (broad-range phosphatase inhibitor cocktail; one pellet in 10 mL) was added to the dish. Cells were gently scraped with a rubber policeman and the cell suspension was transferred to 2 mL Eppendorf tubes. The cells were pelleted at 1800 rpm, 4°C for 5 min and the supernatant was discarded. Cells were resuspended in 500 µL RIPA buffer + PhosStop (one pellet in 10 mL), incubated for 5 min on ice and then passaged ten times thorugh a pre-cooled 0,25 mm needle to break up the cells. From this suspension 40 µL was removed and mixed with 40 µL 2x Lämmli buffer to yield the input control. The remaining lysate was centrifuged at 10,000 rpm for 10 min to pellet cell debris and the supernatant was transferred to new 1,5 mL Eppendorf tubes. The lysate was pre-incubated with 20 µL Dynabeads Protein G beads (Invitrogen, Karlsruhe; washed two times with PBS before use) for 30 min on a rotator in the cold room and then the antibody for pull-down was added 1:50. The lysates were incubated on a rotator overnight at 4°C. For recovery of protein complexes 100 µL Dynabeads Protein G beads were added and the lysates were incubated on a rotator at 4°C for 2 h. The samples were then washed two times with cold RIPA buffer by using the Dynal MPC -E concentrator (Invitrogen, Karlsruhe) for pelleting the beads. Afterwards the samples were washed two times with PBS and then 40 µL 2x Lämmli buffer was added and the samples were heated at 95°C for 10 min. The supernatant was transferred to new tubes and the beades were resuspended in 30 µL 2x Lämmli buffer and heated again and the supernatant was added to the previous one. Samples were stored at -20°C until SDS-PAGE and Immunoblotting was performed.
In order to avoid masking of proteins with an approximate molecular weight of around 50 kDa by the predominant denatured heavy chains of the IP antibody, a light-chain specific antibody was used for the immunoblots. A second, HRP-coupled antibody was then employed to detect the light-chain specific antibody.

II.9 Microscopical methods

II.9.1 Immunofluorescence staining

Immunofluorescence staining for confocal microscopy was performed in 24 well format on 12 mm acetone-washed, autoclaved coverslips. Cells were seeded with the desired density and treated as appropriate (e.g. infected with Salmonella Typhimurium).
The cells were fixed by adding 2% paraformaldehyde/PBS and incubating at 37°C for 10 min and then washed three times with PBS. For intracellular staining the cells were permeabilized with triton X-100 (0.2 % [v/v] in PBS at RT for 15 min). Following permeabilization the cells were washed extensively with PBS (RT) and treated as described in table II.12. All staining steps were performed at RT. The incubation with primary or secondary antibody was performed in a humidified chamber to prevent drying of the samples.

Table II.12: Immunofluorescence staining procedure

staining step	component	time

blocking	1% [w/v] BSA/PBS	30 min
primary antibody	antibody 1:50-1:200 in 0.1% BSA/PBS	60 min
washing	five times with PBS	
blocking	1% [w/v] BSA/PBS	15 min
secondary antibody	1:300 in 0.1% BSA/PBS	45 min
washing	five times with PBS	
washing	once with ddH_2O	

The coverslips were mounted on glass-slides with mowiol and subjected to microscopic analysis.

II.9.2 Confocal microscopy

A Leica TCS SP-1 (Wetzlar) was employed for confocal microscopy analysis. The samples were first inspected manually with the 63x objective, then images were acquired using the software Leica LCS. Images were further processed with the software Adobe Photoshop, e.g. to overlay different fluorescence channels.

II.10 Fluorescence activated cell sorting (FACS), Flow Cytometry

During flow cytometric measurements a continuous stream of sample fluid, hydro-dynamically focused by a sheath fluid, passes a laser. Particles inside the sample scatter the laser light in a characteristic manner. Additionally, fluorescent compounds within the particle (such as fluorescent dyes) are excited and emit light of a specific wavelength. Both the scattered light and the emitted light are picked up by detectors, eventually are amplified for dim fluorescence, and thereby the measured particle can be analyzed multiparametrically (see supplementary figure S.4). This gives information about several physical and chemical properties on a single cell level. Historically, flow cytometry was used to phenotypically characterize eukaryotic cells, mainly human blood cells, but it is now also established for the measurement of bacteria.
For all flow cytometry experiments a FACS Calibur (BD, BD, Franklin Lakes, NJ, USA), equipped with a HTS loader device (BD, BD, Franklin Lakes, NJ, USA) for high-throughput applications was employed. The software controlled needle unit of the HTS supply is able to remove a specific sample volume from 96 well or 384 well plates and to apply it to the FACS device for parametric analysis. The software CellQuest Pro V5.2.1 or Plate Manager V1.0.1 (both: BD, BD, Franklin Lakes, NJ, USA) was used for single tube experiments or 96 well plate measurements, respectively. Before conducting 96 well plate experiments single tube measurements were performed to produce the required template and setting files.

II.10.1 Single tube experiments

Samples (e.g. infected cells) were prepared as described elsewhere and then processed for flow cytometry. Cells were trypsinized, resuspended in PBS and fixed with 2% [w/v] PFA, bacterial solutions were fixed 1:1,000 – 1:10,000 in 2% [w/v] PFA and measured directly. It was observed that cells that were FACS-measured directly in the fixative solution displayed differing auto-fluorescence when compared to non-fixed cells. Additionally, the fluorescence of infected cells could not be analyzed adequately, most likely because the PFA altered the properties of the respective fluorescent proteins. Therefore, the fixative had to be removed to obtain proper FACS results which was carried out by transferring the cell samples to 1.5 mL Eppendorf tubes and pelleting them in an Eppendorf tabletop centrifuge at 520 x g at RT for 4 min. The supernatant was discarded and the cell pellet was resuspended in 400 µL PBS, transferred to FACS tubes and subjected to FACS analysis.

II.10.2 High-throughput experiments

For 96 well plate FACS analysis the samples were prepared as described elsewhere. Prior to flow cytometry measurements, the cells were trypsinized inside the wells with 30 µL/well trypsin (RT) and incubated at 37°C

for 5 min until cells detached. The cells were resuspended with 70 µL PBS (RT) and fixed with 2% [w/v] PFA (RT) at 37°C for 10 min. To remove the fixative the plates were centrifuged in a Heraeus multifuge 3 S-R (DJB Labcare, Newport Pagnell, UK) centrifuge at 1200 rpm and RT for 5 min to sediment cells and the supernatant was aspirated carefully from the wells. The cells were resuspended in 100 µL/ well PBS and analyzed by FACS. Before high-throughput FACS acquisition, the system was primed 2-3 times.

II.10.3 General FACS settings and data analysis

The fluorescence channels FL-1 and FL-3 were used to detect GFP or mCherry fluorescence, respectively. Both fluorescence signals were compensated against all other channels by performing single fluorescence experiments. Mammalian cells or bacteria were identified according to their light scattering properties using a forward scatter (FSC) and side scatter (SSC) dot plot. Autofluorescence of eukaryotic cells in the GFP channel was calculated by analysing non-infected cells and was used to define the population of infected cells.
During 96 well plate measurements 40 µL of each well was analysed to allow well-to-well comparison of cell concentrations. The raw data was further analysed with the software FlowJo 7.2.1 (Treestar, Ashland, OR, USA) or FCS Express (DeNovo software, Los Angeles, CA, USA) for high-throughput data and single tube experiment data, respectively. Processed high-throughput data was applied to prefabricated Excel forms for initial statistical analysis.

II.11 Statistical analysis and bioinformatics

The FACS high-throughput raw data was analyzed with regard to the parameters described in table II.13 using the software FlowJo 7.2.1 (Treestar, Ashland, OR, USA). The data was applied to Excel analysis, the analytical parameter were normalized to the Allstars mean values and the mean inhibition of test siRNAs was calculated in relation to the control siRNAs Allstars (neutral) and Rab7A (inhibitory) using the following equation:

$$\frac{\text{Mean GFP value of Allstars controls} - \text{GFP value of test sample}}{\text{Mean GFP value of Allstars control} - \text{Mean GFP value of Rab7A\_2 controls}}$$

The toxic control siRNA PLK was used to inspect the knock down efficiency.

Table II.13: FACS parameters used for statistical analysis

analytical parameter	derived from FACS data
number of cells	number of cells in cell gate (FSC/SSC)
percentage of infected cells	ratio of eGFP-positive cells (FL-1)
eGFP fluorescence of infected cells	median eGFP fluorescence of eGFP-positive cells (FL-1)
percentage of mCherry positive cells	ratio of mCherry-positive cells (FL-3)
mCherry fluorescence of infected cells	median mCherry fluorescence of mCherry-positive cells (FL-3)

Further analysis involved the calculation of mean and standard deviation values from different experiments and the verification of statistical significance using Student's two-tailed t-test.
In general, only siRNAs that fulfilled the following criteria were regarded as possible "hits":

1.) non-toxic (cell count ≥ 0.4)
2.) impact on GFP fluorescence (mean inhibition ≥ 0.5 for inhibitory and ≤ -0.5 for activating siRNAs
3.) statistical significance (p-value ≤ 0.05)

III Results

III.1 Assay development

The interaction between a pathogen and its host cell is a fascinating and highly complex subject that is intensively studied in many different fields of scientific research. A plethora of pathogen-host models is investigated with the aim to unravel important molecular pathways that underlie the elaborate interactions of pathogens and their host cells. Host signaling pathways that are activated in response to the infection or manipulated by the pathogen just like the virulence factors involved in pathogenesis are of strong interest to basic research. Transferring the increasing knowledge of these interactions to the applied sciences might allow developing new strategies to combat infections and control infectious diseases.
With the advent of the RNA interference technique to specifically knock down the expression of eukaryotic genes, it became possible to examine the importance of certain host cell proteins for the establishment of a successful infection on a large scale. Recently, several RNAi based screens have been performed with diverse infection models of intracellular pathogens: *Listeria* (Agaisse *et al.*, 2005), *Chlamydia* (Derre *et al.*, 2007, Elwell *et al.*, 2008) or *Plasmodium* (Prudencio *et al.*, 2008). Without exception, all of these screens were conducted using microscopy as the principal read-out technique.
In this work, a FACS based assay was developed to evaluate the impact of RNAi mediated host cell gene knock down on intracellular growth of *Salmonella* Typhimurium. A *Salmonella* strain was constructed carrying two reporter plasmids which made it possible to monitor bacterial replication and metabolic fitness in one experimental run. Each reporter plasmid was responsible for the expression of a different fluorescent protein that could be detected and distinguished using FACS. This reporter strain satisfied the need and the wish to generate data of high content to cover as many parameters of the infection process as possible. After the construction and validation of the reporter strain, described in III.1.1 and III.1.2, respectively, the high-throughput FACS assay was set up and different conditions (e.g. cell seeding or infection parameters) were tested to ascertain the optimal experimental design (see III.1.3). Pre-screening experiments were performed to test the functionality of the assay and its applicability for large scale experiments (see III.1.4 and III.1.5) before the actual screening of large siRNA libraries was accomplished (see III.2).

III.1.1 Construction of a *Salmonella* Typhimurium reporter strain

Two reporter plasmids were constructed and electroporated into the *Salmonella* Typhimurium wildtype strain 12023 to obtain the sensor strain for monitoring both intracellular bacterial replication and fitness (see figure III.1). This sensor strain was thought to enable the acquisition of very detailed data regarding the impact of host cell gene knock down on the infection process of *Salmonella* in one experimental run.
The plasmid pOR25 drives the constitutive expression of the green fluorescent protein (GFP) from the bacterial promoter **Φ**rpsM. GFP can be easily excited with the FACS laser line of 488 nm and is detected at 530 nm (fluorescence channel FL-1). The vector pACYC177 (Chang *et al.*, 1978) was used as the back bone for cloning pOR25. It harbours two antibiotic resistance genes: *bla* for ampicillin resistance and *kan* for kanamycin resistance. Since it was intended to apply a second reporter construct also carrying an ampicillin resistance gene,

the *bla* gene of pACYC177 had to be interrupted to ensure an equal propagation of both plasmids inside *Salmonella* under selective conditions. For this, the plasmid pACYC177 was

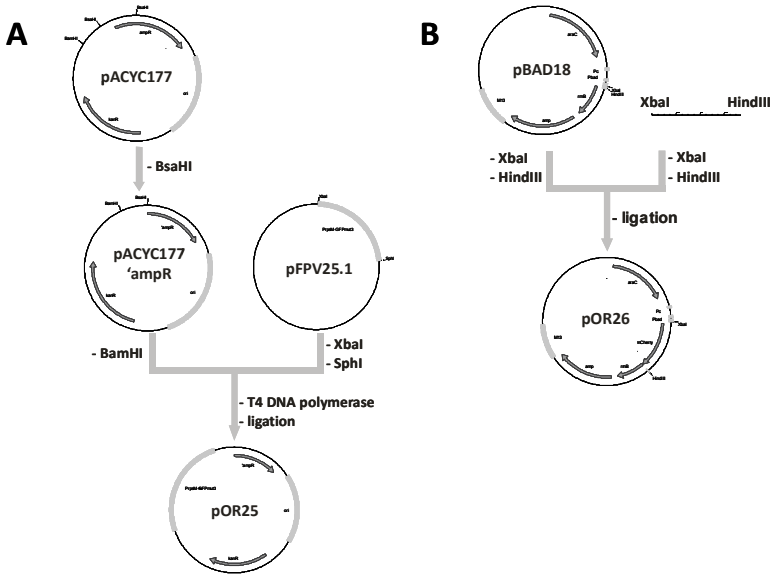

Figure III.1: Schematic diagrams of the cloning strategies for pOR25 and pOR26.
The cloning schemes for the construction of the reporter plasmids pOR25 and pOR26 are shown in [A] and [B], respectively. See text for details.

digested with the enzyme BsaHI to cut the vector 5' of the *bla* gene and inside the gene. Subsequently, the plasmid was re-ligated, electroporated into *E. coli* DH5α, and tested on ampicillin and kanamycin agar plates. No growth on ampicillin plates could be observed indicating that the disruption of the *bla* gene was successful. In order to clone the **ϕ**rpsM-GFP fusion into the modified pACYC177 vector (pACYC177 'ampR), the respective fragment was digested from the plasmid pFPV25.1 (Valdivia *et al.*, 1996) using the enzymes XbaI and SphI and was treated with T4 DNA polymerase to produce blunt ends. The pACYC177 'ampR vector was digested with BamHI, was T4 DNA polymerase-treated and then de-phosphorylated. The rpsM-GFP fragment was ligated into the modified vector pACYC177 to gain the reporter plasmid pOR25 (see figure III.1).
The second reporter plasmid, pOR26, was constructed using the vector pBAD18 (Guzman *et al.*, 1995) which constitutes an arabinose inducible expression system. It has been widely used in heterologous protein expression (Ghigo *et al.*, 2000, Low *et al.*, 2006) and also for the controlled expression of GFP, luciferase, and lysis gene E in a *Salmonella* infection model (Loessner *et al.*, 2007). A DNA fragment of mCherry, flanked by a 5' XbaI and a 3' HindIII restriction site was synthesized from the plasmid pRSET mCherry (Shaner *et al.*, 2004) by PCR with primers FP_new-F and FP_new-R and digested with the enzymes XbaI and HindIII to produce cohesive DNA ends. The vector pBAD18 was digested with XbaI/HindIII, de-phosphorylated and the PCR fragment was ligated to produce the plasmid pOR26 (see figure III.1).

Both plasmids were propagated in *E. coli* DH5α and sequenced with primers flanking the ligated insert. The DNA sequencing was performed by SMB DNA Sequencing Service Martin Meixner (Berlin) and showed a correct DNA sequence for both constructs.
The plasmids were electroporated sequentially into the *Salmonella* Typhimurium 12023 wild type strain and the resulting strain 12023 pOR25/26 was grown on ampicillin/kanamycin selective agar plates to ensure propagation of both plasmids.

III.1.2 Validation of the reporter strain

III.1.2.1 The viability of the reporter strain is not altered

In order to test the viability of the double-transformed strain 12023 pOR25/26, the growth in LB medium was compared to the growth of the wild type 12023 strain. Both strains were grown overnight at 37°C, 200 rpm. They were diluted 1:100 in fresh medium and the OD_{600} was measured at different time points. Figure III.2 depicts the growth curves of both the wild type strain and the strain 12023 pOR25/26. It becomes obvious that there was no significant difference between both strains. This indicates that the viability of the reporter strain was not impaired by the propagation of the two plasmids (see figure III.1).

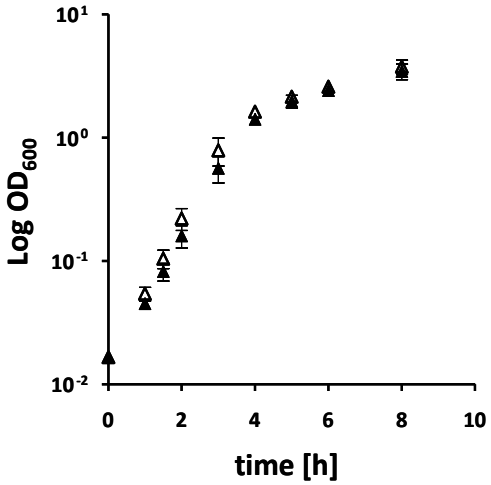

Figure III.2: The reporter strain is not impaired in growth.
The *Salmonella* Typhimurium 12023 wildtype strain and the reporter strain 12023 pOR25/26 were cultivated overnight in LB medium. At the indicated time points after subcultivation, samples were taken and the OD_{600} was measured to control bacterial growth. The plot shows the data of three independent experiments as means with standard deviations for the wildtype strain (open triangles) and the reporter strain (filled triangles).

III.1.2.2 Expression of both fluorescent proteins can be detected and discerned by FACS

III.1.2.2.1 FACS analysis of the reporter strain in-vitro

The functionality of the plasmids pOR25 and pOR26 was first tested *in-vitro*. The strain 12023 pOR25/26 was grown in defined PCN culture medium overnight with glucose and then subcultured 1:50 in fresh PCN medium with glucose for 2h. Since the availability of glucose completely represses the arabinose expression system (Guzman *et al.*, 1995), the bacteria were pelleted, washed two times with ddH_2O and resuspended in PCN medium without glucose, supplemented with 0.2 % [w/v] arabinose to induce the expression of mCherry.

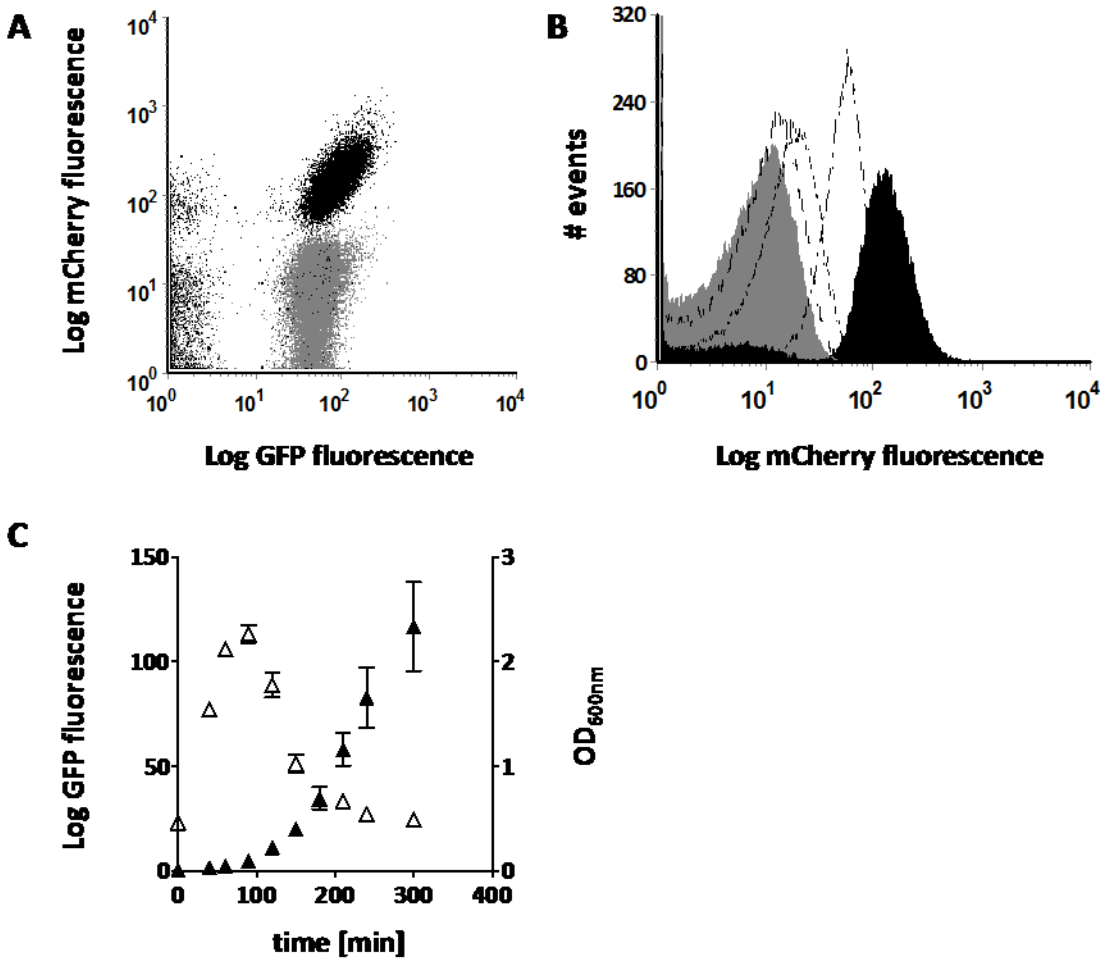

Figure III.3: The expression of both fluorescent proteins can be monitored using FACS.
In order to test the functionality of the reporter strain the fluorescence of GFP and mCherry was monitored using flow cytometry. Bacterial cultures of 12023 pOR25/26 were grown in PCN medium with glucose overnight, subcultured 1:50 in fresh medium for 2 hours and then washed with dH_2O. Pellets were resuspended in PCN medium without glucose, supplemented with 0.2 % [w/v] L-arabinose and grown for the indicated time. Samples were fixed with 2% PFA and then measured with a FACS Calibur. The spectral overlap of GFP and mCherry was compensated during measurements.
[A] Non-induced (grey) and induced (black) cultures were analyzed for their fluorescent characteristics, showing clearly distinguishable populations. [B] The mCherry fluorescence intensity increases with induction time, indicated by the shift of the histograms. Time points were 0 (grey filled), 15 (dashed), 30 (dotted), 60 (dash-dotted) and 120 (black filled) minutes, respectively. [C] The triplicate data of one representative experiment with means and standard deviations for GFP fluorescence (open triangles) and OD_{600} (filled triangles) is shown.

Samples were taken at different time points and analyzed by FACS as described in II.10.1. Figure III.3.A illustrates the respective dot plot for GFP and mCherry fluorescence with spectral compensation. A clearly distinguishable population showing GFP as well as mCherry fluorescence originated 2 h post induction whereas the non-induced bacterial culture only exhibited GFP fluorescence. In figure III.3.B, the mCherry fluorescence at different time points after arabinose addition is depicted. It becomes obvious that a significant shift in fluorescence intensity occurred 2 h post induction that could be easily discerned from the background fluorescence (figure III.3.B; grey shaded curve).
Figure III.3.C displays the GFP fluorescence as well as the OD_{600} of the bacteria over time after subcultivation in glucose-free PCN medium. Characteristic curves showing a growth phase dependent GFP expression driven by the ribosomal protein promoter **Φ**rpsM can be seen.

III.1.2.2.2 FACS analysis of the reporter strain in cell culture infections

In order to test the reporter plasmids *in-vivo* and, moreover, to find the adequate cell line for the performance of the high-throughput screen, several human tissue culture lines were infected with the reporter strain for FACS analysis. 14 h p.i. the samples were treated with induction medium for 2 h, were processed as described in II.10.1 and were analyzed for GFP and mCherry fluorescence. Samples were taken at 2 h p.i. and 16 h p.i. for the analysis of the initial bacterial invasion and the long-term infection process, respectively.
Figure III.4 reveals that the infection efficiency strongly varied among the different cell lines investigated. Using the dot plot view (figure III.4.A) it is possible to discern and quantify different cell populations: 1.) non-infected cells in quadrant three (Q3), 2.) infected cells displaying only GFP-expressing bacteria (Q4) and 3.) infected cells showing both GFP and mCherry fluorescence (Q2). The visual inspection of the dot plots further displays remarkable differences in the infection efficiency of the different human cell lines with *Salmonella* under the conditions used. For instance, GFP intensity as well as the infection rate was much lower in infected HT-29 cells than in infected HeLa cells.
The quantification of important infection parameters within the different cell lines is depicted in figure III.4.B. Samples were analyzed 16 hours p.i. for replication (upper and middle panel) and 2 hours p.i. for invasion (lower panel). The analysis implied the rate of cells showing the correspondent fluorescence signal and the intensity of GFP or mCherry fluorescence. Distinct differences between the cell lines could be observed with regard to the initial bacterial invasion rate, the replication efficiency in these cells or the ability of the bacteria to express the mCherry protein. The invasion rate was comparable among all cell lines tested except HepG2 cells which showed a significantly lower bacterial invasion (see figure III.4.B, lower panel). The amount of GFP fluorescence was equal in HeLa and Hec1b cells but lower in the other cell lines used, indicating that fewer bacteria per cell had entered. 16 h p.i. the percentage of infected cells was in the same range as 2 h p.i. for HeLa, Hec1b, HepG2, and HEp-2 cells but had dropped dramatically for HT-29 cells (see figure III.4.B, upper panel). Additionally, the bacteria in HT-29 and HepG2 cells only showed a weak mCherry induction after overnight infection (see figure III.4.B, middle panel), indicating that the bacterial metabolic activity was weak under these conditions. For HEp-2 cells two distinct populations of infected cells could be observed (see figure III.4.A), one showing a GFP/mCherry fluorescence pattern similar to HeLa cells and one that displayed lower mCherry expression levels which resulted in relatively lower values for mCherry intensity in

the quantification. This suggested that HEp-2 displays a heterogeneous cell line with regard to *Salmonella* infection and was therefore not considered to be used within the screen.
Thus, based on the results gained from infection experiments with different human cell lines, the HeLa cell line proved to be an adequate tool to investigate intracellular replication and fitness of *Salmonella* Typhimurium and it was therefore used for all subsequent experiments if not stated otherwise.

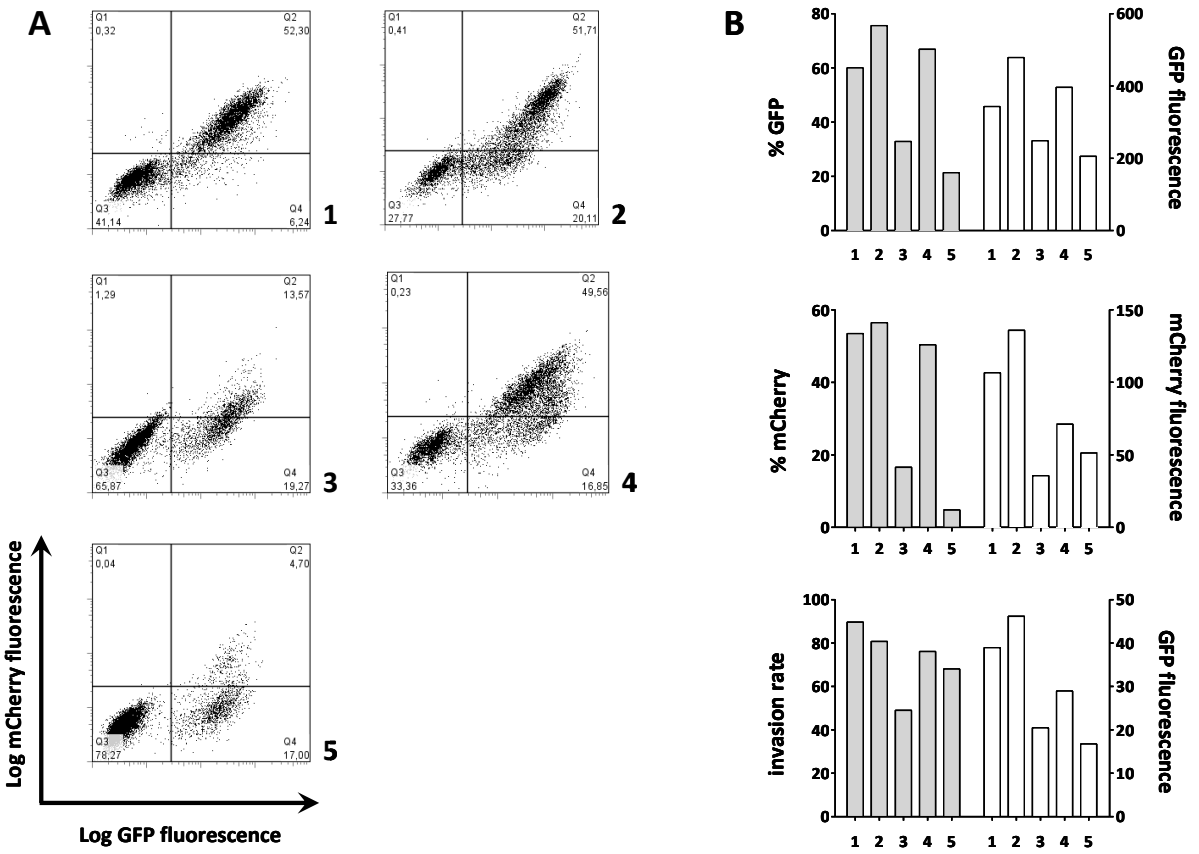

Figure III.4: FACS analysis of different cell lines infected with the reporter strain.
Using the reporter strain in a FACS assay, fundamental infection parameters can be quantified showing significant differences between the cell lines tested. Human cell lines (1: HeLa, 2: Hec1b, 3: HepG2, 4: HEp-2 and 5: HT-29) were seeded in 24 well plates, infected with a MOI of 200 and processed for FACS analysis as described in II.10. Dot plots were generated and then further analyzed for quantification using FlowJo 7.2.1.
[A] Two-parametric dot plots of infected human cell lines with the log GFP fluorescence intensity on the x-axis and the log mCherry fluorescence intensity on the y-axis. [B] Quantification of different infection parameters as indicated. Upper and middle panel: 16 hours p.i. Lower panel: 2 hours p.i.

III.1.2.2.3 Microscopic analysis of the reporter strain in cell culture infection

For microscopic analysis of the reporter strain, HeLa cells were seeded on coverslips, infected with the reporter strain and treated with induction medium to induce mCherry expression or were left untreated.
Figure III.5 depicts the confocal microscopic analysis for sequentially aquired GFP and mCherry fluorescence as well as the image overlay. In the non-induced sample only GFP

fluorescence is detectable, whereas in arabinose stimulated cells most of the bacteria show GFP as well as mCherry fluorescence, as reflected by the overlay image. This is a further proof that the reporter constructs are working reliably and that *Salmonella* bacteria inside their host cell can be induced to express the mCherry protein by the external addition of arabinose.

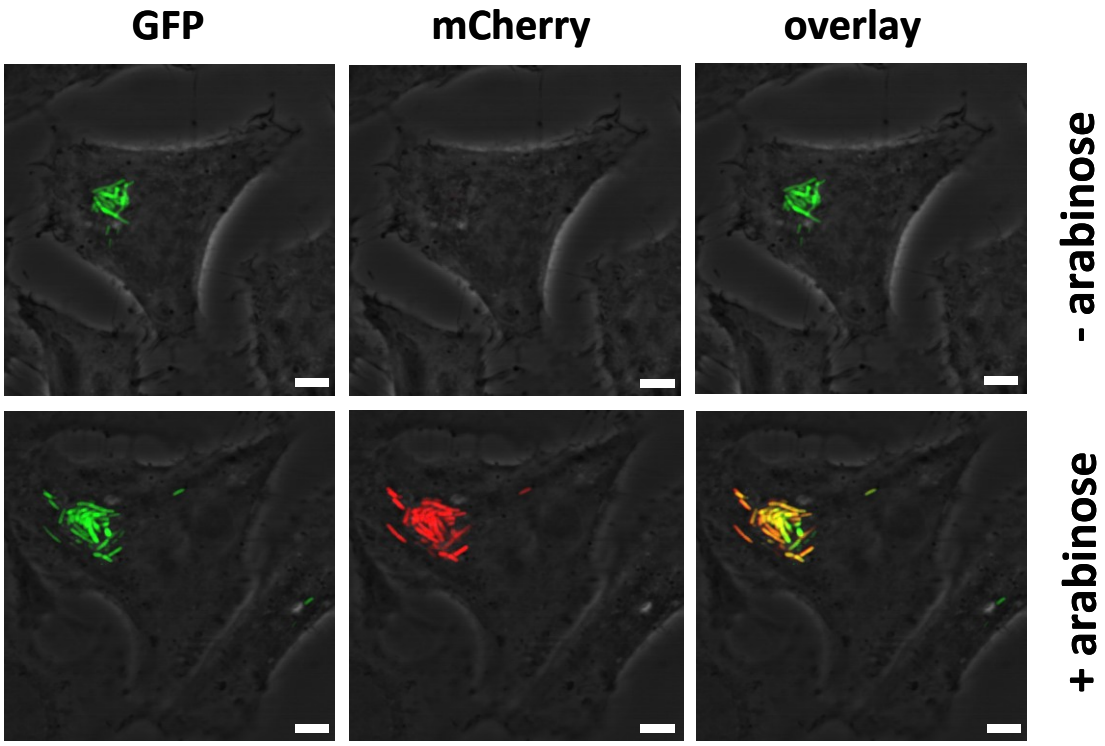

Figure III.5: Intracellular replicating *Salmonella* can be induced to express mCherry.
HeLa cells were seeded on coverslips and infected with the reporter strain as described in II. 14 h p.i., samples were either treated with induction medium for 2 hours or left untreated and were processed for confocal analysis. Images are shown for the GFP fluorescence (left images), the mCherry fluorescence (middle images), and the overlay of both channels (right images). In the upper panel and the lower panel representative intracellular bacteria are shown for non-treated and treated cells, respectively. Scale bar = 2 µm

III.1.3 Development of a high-throughput FACS application

After having evaluated the sensor strain intensively *in-vitro* and *in-vivo*, the assay was transferred to a large scale application to perform high-throughput screening experiments in a 96 well plate format. As mentioned above, it was chosen to use the human epithelial cell line HeLa for the experiments for the following reasons: 1. the cell line is the predominantly used epithelial cell infection model in *Salmonella* research, 2. it gave the best results with respect to the infection parameters measured in the FACS analysis (see III.1.2.2.2 and figure III.4) and 3. there had already been good expertise in successfully transfecting HeLa cells with siRNAs inside the department. For the establishment of the high-throughput assay several details had to be evaluated, such as the overall robustness of the FACS measurements performed with the HTS supply and the proper infection conditions.

III.1.3.1 Stability of measurements

The FACS Calibur HTS supply is equipped with a mobile needle that removes a specified sample volume from a 96 well or 384 well plate and injects it into the flow system which transports the sample to the flow chamber for parametric analysis (see figure S.4 in the supplements).
Since the processing of one 96 well plate with this supply takes about 30 min to 1 h (in normal working mode and dependent on sample volume and sample speed), it was necessary to assure a stable measurement of sample over the time and for the whole plate.
To test the technical variation of measurements over time, HeLa cells fixed with 2 % [w/v] PFA were pipetted into a 96 well plate at a density of $4x10^4$ cells/well and were measured with the help of the HTS supply and the conditions specified below. Only the inner 60 wells were acquired since in the planned RNAi experiments the outer wells would be omitted due to already observed irregular growth behaviours of cells in the outer wells. During the whole time of acquisition, the amount of cells remained stable as in all 60 wells an equal number of cells could be detected (figure III.6). Thus, the high-throughput FACS analysis ensures a high technical reproducibility under the conditions used.

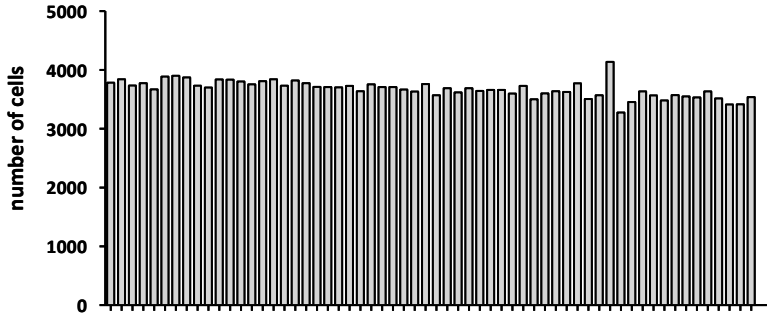

Figure III.6: The HTS FACS aquisition is stable over time.
In order to evaluate the variability of the FACS HTS measurement over time, PFA-fixed cells were pipetted at equal density into the wells of a 96 well plate. Afterwards the inner 60 wells of the plate were measured with identical conditions: 40 µL/well at a speed of 2 µL/sec. Each bar represents a well and the wells are depicted in the order of measurement. The number of acquired cells is presented on the y-axis.

III.1.3.2 Infection conditions and assay accuracy

III.1.3.2.1 Determination of appropriate infection conditions

After having secured that the general technical variation of the measurements was in a range that could be tolerated, the adequate infection conditions had to be determined. In order to evaluate the proper infection dose to avoid cell toxicity, a multiplicity of infection (MOI) titration experiment was performed. The impact of different MOIs on cell survival and infection parameters in a 96 well plate format HeLa cell infection, analyzed by high-throughput FACS acquisition, is shown in figure III.7. The amount of measured cells normalized to non-infected cells exhibited a MOI dependent decrease, indicating

a tremendous cell toxicity of 84% for HeLa cells infected with a MOI of 200 compared to a relatively low toxicity caused by MOIs of 10 and 20 (figure III.7.A).
The infection efficiency (i.e. the percentage of GFP-positive cells that were detected) was also MOI dependent displaying an infection rate of about 80 % for MOI 200 and about 40 % for cells infected with a MOI of 10 (figure III.7.B). For the median GFP fluorescence intensity of infected cells no MOI dependence could be observed. For all MOI conditions employed, a similar value of GFP fluorescence intensity per cell was measured (figure III.7.C).
These results suggested the use of MOI 20 for the infection of HeLa cells with *Salmonella* Typhimurium as the cell toxicity was negligible and at the same time the infection parameters proved to be adequate.

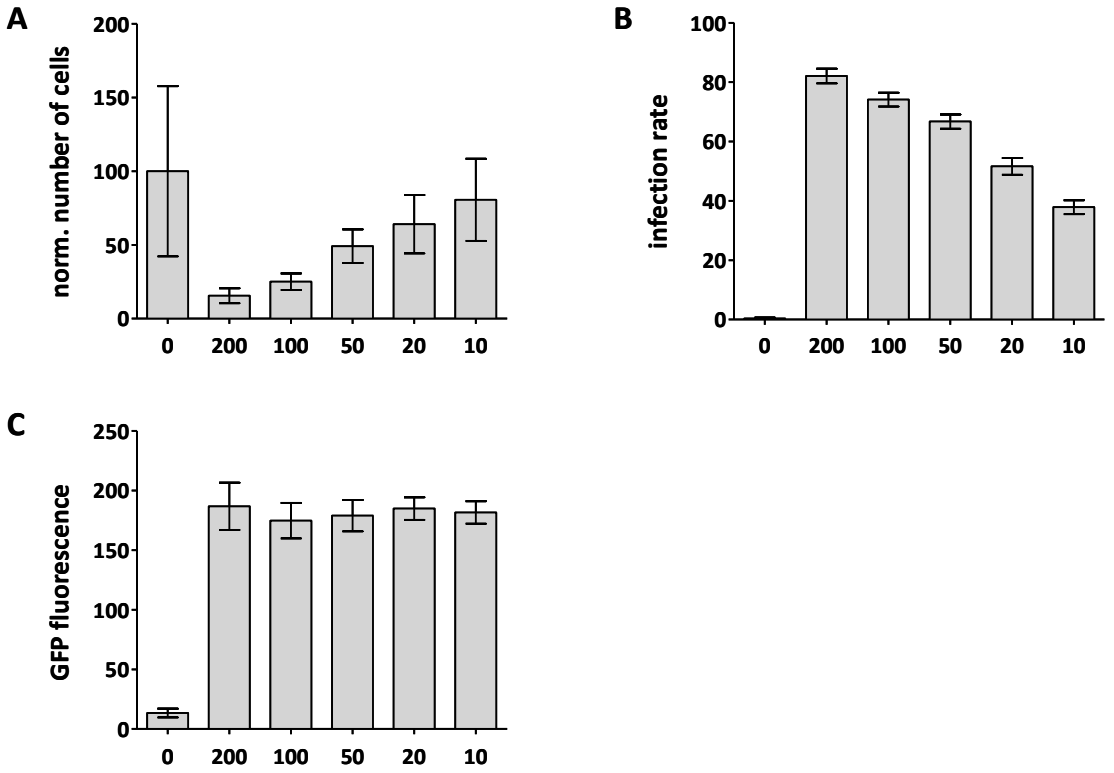

Figure III.7: MOI titration for evaluating the appropriate infection conditions.
HeLa cells were seeded in 96 well format, infected and processed for FACS analysis 16 h p.i. Ten wells for each MOI were analyzed. The data of one representative experiment with means and standard deviations is shown. [A] Number of detected cell particles, normalized to non-infected cells (MOI 0). [B] Percentage of infected cells (i.e. infection rate). [C] Median GFP fluorescence of infected cells.

III.1.3.2.2 Accuracy of the FACS assay

The toxicity of certain siRNAs might lead to variable cell numbers in the wells. The impact of lower or higher cell numbers on the infection was tested in a 96 well format experiment by seeding different cell numbers and infecting at MOI of 20 (see figure III.8). The respective amount of bacteria to reach MOI 20 was adjusted with respect to the samples with $1x10^4$

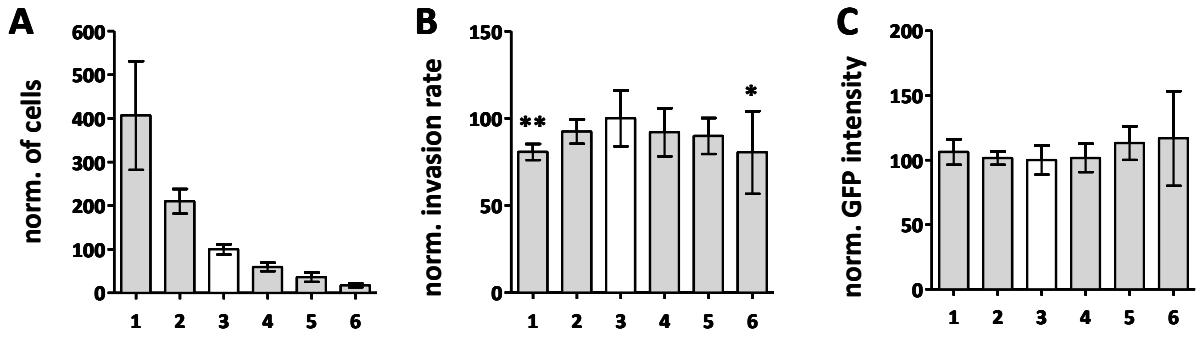

Figure III.8: *Salmonella* reporter strain infections run stable with varying cell densities.
To test the impact of differing cell numbers on the infection parameters, HeLa cells were seeded in 96 well format at a density of 1: $4x10^4$, 2: $2x10^4$, 3: $1x10^4$, 4: $5x10^3$, 5: $2.5x10^3$ and 6: $1.25x10^3$. Cells were infected the next day with a MOI of 20 as adjusted for the cell density of samples with $1x10^4$ cells seeded. 16 h p.i. cells were processed for FACS analysis and ten wells for each condition were measured. The data of one experiment with triplicates, normalized to $1x10^4$ cells seeded (white bar), with means and standard deviations is shown for [A] number of cells detected, [B] invasion rate and [C] median GFP fluorescence of infected cells. P-values *<0.05 and **<0.01 with $1x10^4$ cells as reference.

cells seeded. The FACS analysis showed that the detected cell numbers within a constant volume of 40 µL decreased with diminishing seeding quantities (figure III.8.A). Concerning the invasion rate of the bacteria, a significant difference to the reference value (white bar in figure III.8) could only be detected for extreme high or low cell numbers ($4x10^4$ and $1.25x10^3$), whereas in the range from $2.5x10^3$ to $2x10^4$ cells, the invasion rate was

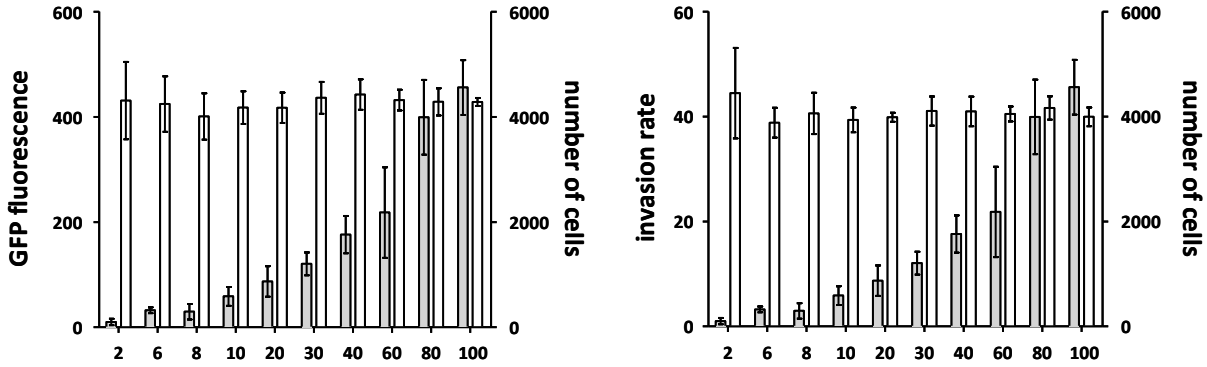

Figure III.9: FACS assay shows high accuracy of measurements over a wide range of particle numbers.
Different volumes of infected cells were loaded from each well and analyzed by flow cytometry. The volume in µL that was analyzed is displayed on the x-axis. The y-axis shows GFP fluorescence [A] or invasion rate [B]on the left and the number of detected cells on the right.

comparable (figure III.8.B). No significant difference could be observed with respect to the GFP fluorescence intensity (figure III.8.C). Thus, the infection with the reporter strain runs similar over a certain range of host cell densities providing certain stability against eventual differences in cell numbers due to toxic siRNAs. Next, it was of interest to figure out whether the detected cell number had an influence on the statistical robustness of measurements. In order to determine the range of cell numbers that gave comparable analysis data, an

accuracy assay experiment was performed. An equal number of HeLa cells was seeded into the wells of a 96 well plate, infected the next day as described (II.6.5) and the plate was processed for flow cytometry. For FACS acquisition, different volumes were taken out of different wells by the HTS supply and analyzed. The quantification of the FACS data is depicted in figure III.9. As expected, the number of detected cell particles increased with rising volumes measured. However, the values for the rate of infected cells and for the GFP fluorescence were comparable within the whole range of analyzed volumes. This shows that even with very low cell numbers, which might occur during the screen as a consequence of toxic siRNAs, a statistical robustness is assured using the FACS technique.

III.1.4 Functionality test: small antibiotic screen

In order to demonstrate that inhibition of bacterial replication inside epithelial cells can be monitored with the bichromatic FASC assay, a small antibiotic screen in 96 well plate format

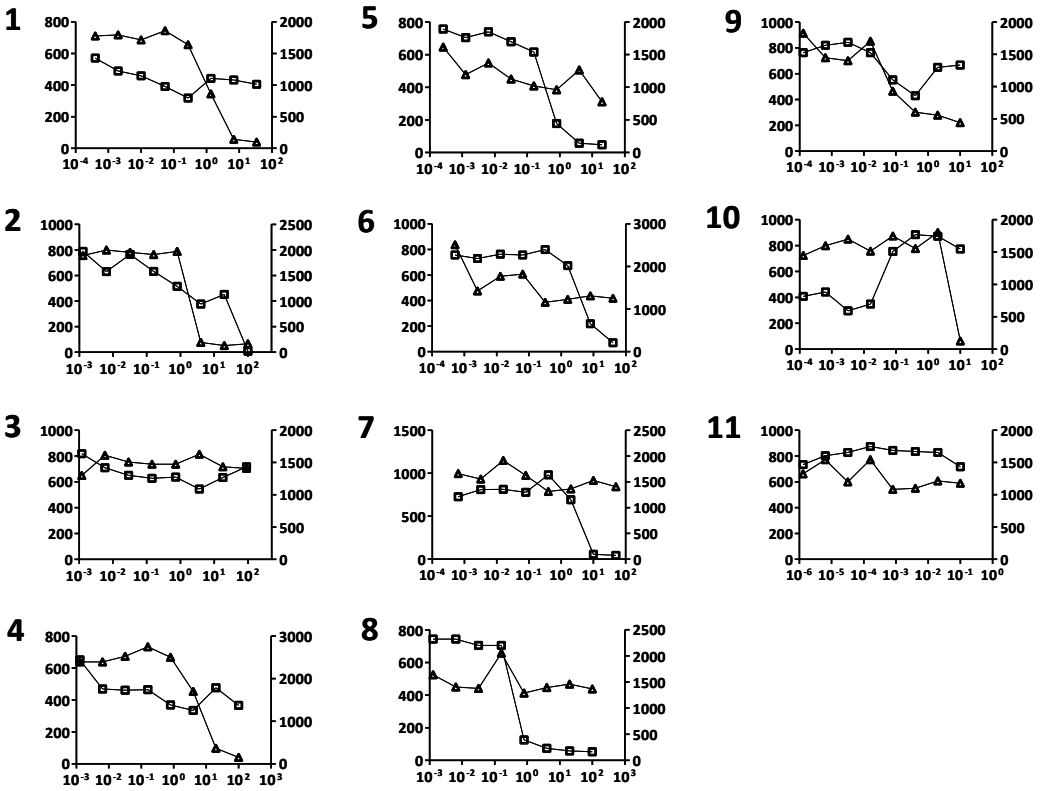

Figure III.10: Small antibiotic screen as a functionality test.
The applicability of the reporter strain FACS assay was finally validated in 96 well format testing several antibiotics in different concentrations for their impact on bacterial replication and host cell toxicity. HeLa cells were infected with the reporter strain and 1 hour p.i. the medium was aspirated and 100 µL/well RPMI full medium, supplemented with 20 µg/mL gentamicin and the indicated concentration of drug was added for the rest of the infection. 14 hours p.i. the medium was aspirated, mCherry expression was induced and 2 hours later the samples were processed for FACS analysis. The plots shows the number of cells detected (right y-axis and open squares) and median GFP fluorescence of infected cells (left y-axis and open triangles) one of experiment. Applied concentrations are displayed on the x-axis. Drugs used were: 1 chloramphenicol, 2 irgasan, 3 streptomycin, 4 erythromycin, 5 tetracyclin, 6 cefixim, 7 rifampicin, 8 trimethoprim, 9 brefeldin A, 10 H-89 and 11 DMSO (as control). Concentration units are as follows: µg/mL (1-9), µM (10), % [v/v] (11).

was performed. Various antibiotics and chemical inhibitors were applied at different concentrations on cells infected with the reporter strain 1 hour post infection for the rest of the infection process and the plate was processed for FACS acquisition.
Figure III.10 shows the impact of different antibiotics on host cell survival and GFP fluorescence of the bacteria. For most of the inhibitors that were used in this small screen a decrease in GFP intensity was observed at higher concentrations. In the case of Irgasan, a phenol compound widely used as disinfectant and preservative, the cell toxicity was also very pronounced at the highest concentration of 100 µg/mL.

III.1.5 Rab7A as the siRNA control for conducting the RNAi screens

After intensive functional evaluation of the bichromatic FACS assay, the set-up of the RNAi screen had to be further approached. Most importantly, it was necessary to find and establish siRNAs that could operate as control siRNAs throughout the whole screen. The siRNA controls are of great importance as they allow for monitoring the transfection efficiency itself and as they serve as markers for the statistical analysis of the siRNAs to test. The following siRNA controls had to be concerned: 1. a neutral control to assess the overall impact of the siRNA transfection process on the host cell as well as on the infection, 2. a toxic siRNA that kills the host cells in a reliable way to directly control the transfection efficiency, and 3. a siRNA that leads to a host cell gene knock down which stably inhibits the bacterial infection process leading to a decrease of fluorescence.
A commercially available scrambled siRNA sequence named Allstars (Qiagen, Hilden) served as the neutral control. This sequence should not lead to a specific gene knock down and, moreover, was designed by the company in a way to cause only minimal off-target effects. A siRNA against the host cell protein PLK1, the polo-like kinase 1 which is involved in mitosis, was used as a toxic control due to already existing profound experiences with this sequence in our laboratory. Upon transfection with this sequence, the majority of cells was killed within three days.
In order to find a control siRNA which would reliably inhibit *Salmonella* replication, the respective literature was screened. Some reports describe a role for Rab7 in the infection process of *Salmonella*. For instance, Meresse et al. (1999) showed that Rab7 is involved in the biogenesis of the *Salmonella* containing vacuole (SCV) by mediating the acquisition of lysosomal glycoproteins (lgp) which are evident on mature vacuoles. In another publication a role of Rab7 for the formation of *Salmonella* induced filaments (Sifs), which is essential for the replication, was reported (Brumell *et al.*, 2001b). Thus, Rab7 seems to play an important role in the accurate maturation of the SCV and thereby ensures the successful bacterial replication inside the vacuole. Based on these observations it was decided to test the impact of Rab7 gene knock down on *Salmonella* intracellular growth by flow cytometry (III.1.5.1), by confocal microscopy (III.1.5.2), and with a gentamicin protection assay (III.1.5.3) to evaluate its employment as the inhibitory siRNA control. For this, Dharmacon Rab7A smart pool siRNAs were purchased and initially tested with the FACS assay.

III.1.5.1 FACS based evaluation of Rab7A knock down on infection

To test the impact of the Dharmacon smart pool mediated Rab7A gene knock down on *Salmonella* intracellular growth, Hela cells were transfected with the respective siRNA in 96 well format, infected three days post transfection, and analyzed by FACS.

As illustrated in figure III.11.A, the mean GFP fluorescence of infected Rab7A knock down cells was reduced to about 50% compared to Allstars control treated cells. This indicates a strong replication defect in the absence of Rab7A. The dot plot analysis of Rab7A treated cells showed a significant shift of the infected cell population compared to Allstars treated cells (figure III.11.C). Additionally, the mCherry signal dropped into the range of the non-infected background intensity, implicating that the bacteria responded only very weakly to the arabinose trigger. This indicates that the Rab7A knock down caused to a strong inhibition of bacterial replication and metabolic activity and, thus, exhibits an excellent control to monitor the inhibition of *Salmonella* infection during the screening conductance.

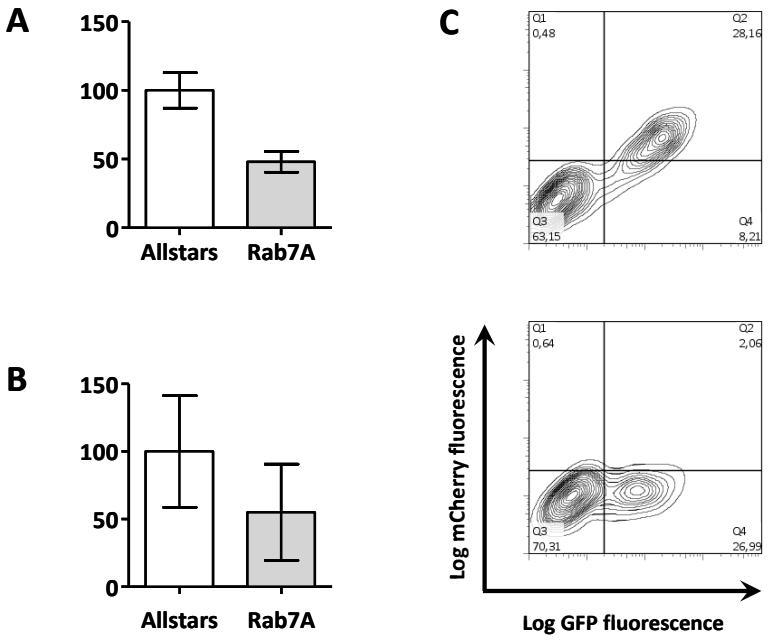

Figure III.11: Impact of Dharmacon smart pool mediated Rab7A knock down on *Salmonella* infection of HeLa cells.
HeLa cells were seeded in 96 well format and transfected with Allstars control siRNA or the Dharmacon Rab7A smart pool siRNAs. Three days later cells were infected with MOI 20 and processed for FACS analysis. Six wells were measured for each condition and the data from one representative experiment with means and standard deviations is shown. [A] Median GFP fluorescence of infected cells normalized to Allstars. [B] Mean number of cells detected, normalized to Allstars. [C] FACS two-parametric dot plots for Allstars (upper plot) and Rab7A (lower plot) treated samples.

However, it has to be noted that the transfection with the smart pool had significant cytotoxic effects as the normalized cell number decreased to about 50% (figure III.11.B). It was therefore resolved to test all four siRNAs that are combined in the smart pool separately. Although the knock down was comparably efficient for all sequences and the smart pool on protein level (figure III.12.C; lower band in Rab7A panel), their influence on cell survival differed significantly (figure III.12.A). Whereas the siRNA sequences 1 and 3 as well as the pool had a negative impact on the number of detected cell particles (16, 18, and 27%, respectively, compared to Allstars), the inhibition of bacterial replication (i.e. the GFP expression) was comparable for all Rab7A siRNAs tested (77.9 ± 15.6 for sequence 1, 65.4 ±

7.4 for sequence 2, 61 ± 14.9 for sequence 3, 78.4 ± 5.8 for sequence 4 and 62.4 ± 10.2 for the pool; Mean ± SD, n=6). Based on these results it was decided to use the Dharmacon Rab7A siRNA sequence 2 because it had a good knock down efficiency, showed no host cell toxicity, and was effective in inhibiting bacterial replication. The FACS analysis of Allstars and Rab7A_2 treated cells is depicted in figure III.12.D (Allstars: left; Rab7A_2: right) demonstrating a strong inhibition of both GFP and mCherry fluorescence after Rab7A_2 transfection.

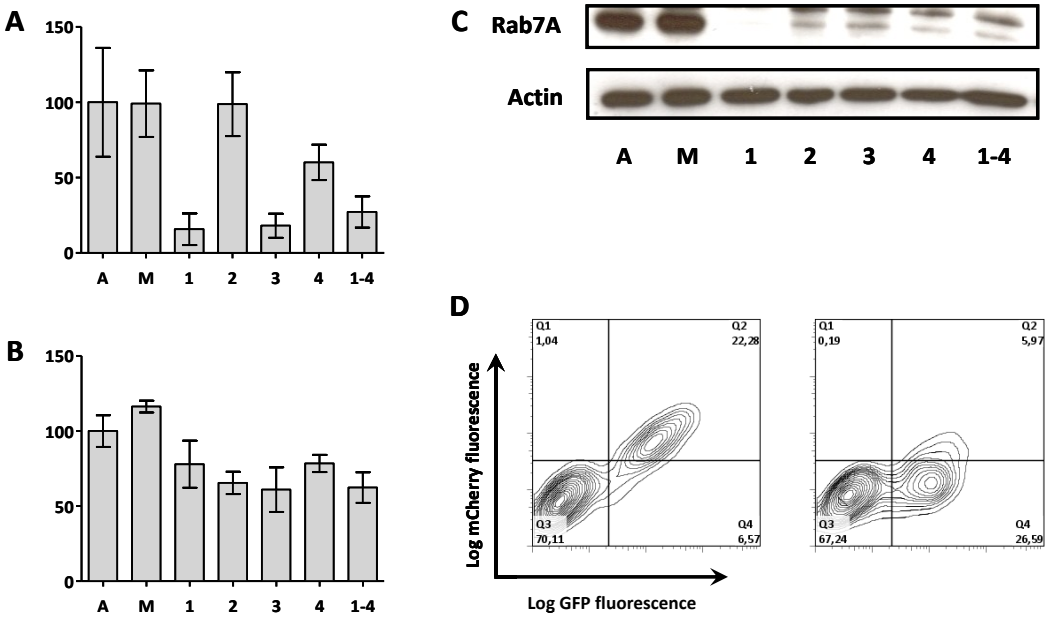

Figure III.12: Individual Rab7A siRNAs differ in their biological properties.
The siRNAs sequences that were part of the Dharmacon Rab7A smart pool were purchased separately and tested for their knock down efficiency and their influence on host cell survival and Salmonella infection. HeLa cells were seeded in 96 well format and transfected with the individual siRNAs and the pool. Three days later the cells were infected with MOI 20 and processed for FACS. The mean cell number [A] and median GFP fluorescence [B] of one representative experiment with means and standard deviations is depicted (n=6). [C] Western blot analysis of cell samples three days post transfection with the respective siRNA. [D] Representative two-parametric dot plots for Allstars (left) and Rab7A_2 (right) treated cells.
A: Allstars M: mock Nº: different Rab7A sequences 1-4: Rab7A siRNA pool

III.1.5.2 Microscopic evaluation of Rab7A knock down on infection

In order to further phenotypically characterize the impact of Rab7A knock down on the bacterial infection process, Rab7A_2 transfected cells were analyzed using a confocal microscope. HeLa cells were seeded and infected as described in II.6.5 and processed for confocal microscopy analysis. The GFP and the mCherry fluorescence channel were aquired sequentially and the editing of the confocal images was performed with Adobe Photoshop.
As can be seen in figure III.13, the knock down of Rab7A caused a dramatic inhibition of the bacterial infection process. No mCherry expression could be detected in the representative infected cell and the GFP-positive vesicle-like structures differed significantly from the usual appearance of the *Salmonella* containing vacuole as shown in the Allstars control images,

namely, significantly less bacteria and a more scattered distribution of the small vesicles. These observations suggest that the absence of Rab7A in the host cell provoked incomplete fusion events between different bacteria-containing phagosomal structures. This would be in accordance to the publications cited above.

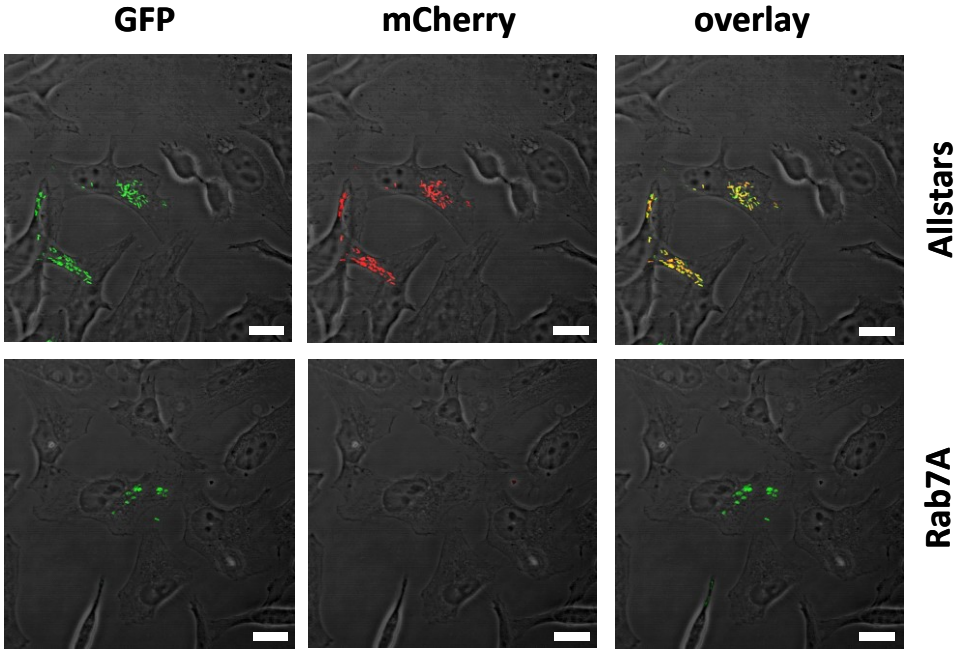

Figure III.13: Confocal analysis of Rab7A knock down cells displays inhibition of bacterial replication and metabolic activitiy.
HeLa cells were seeded on coverslips in 24 well format and transfected either with the Allstars siRNA or the Rab7A siRNA. Three days post transfection the cells were infected and treated with induction medium for two hours. The fluorescence channels for GFP and mCherry were acquired sequentially to avoid spectral overlap and images were edited using Adobe Photoshop. Representative images of Allstars (upper panel) and Rab7A (lower panel) treated cells and the fluorescence channels for GFP (left) and mCherry (middle) as well as the overlay of both channels (right) are depicted. Scale bar = 10 µm.

III.1.5.3 Quantification of bacterial replication

The quantification of bacterial replication in Rab7A_2 treated cells compared to Allstars transfected control cells was carried out with the help of the gentamicin protection assay (see II.6.6). Allstars or Rab7A_2 transfected cells were infected and 2 h p.i. and 16 h p.i. samples were lysed, serial diluted and plated on selective agar plates for counting colony forming units (cfu). The replication rate was calculated by the ratio of cfu at 16 h p.i. and cfu at 2 h p.i.
Figure III.14 presents the bacterial replication rates for Allstars or Rab7A_2 treated cells. It could be observed that the replication rate of *Salmonella* inside Rab7A_2 transfected cells is significantly lower than in Allstars control cells (30 ± 7.9 for Allstars and 12.8 ± 2.4 for Rab7A_2; Mean ± SD, n=3). This finding again allocates that the knock down of Rab7A inhibited bacterial replication inside HeLa cells.

In summary, the data gained with the FACS assay, confocal microscopy, and gentamicin protection assay demonstrate that the depletion of Rab7A has a significant adverse biological effect on the *Salmonella* infection process. The stability of FACS measurements made after Rab7A knock down using the sequence Rab7A_2 additionally legitimates the employment of this siRNA as the inhibitory control for the screening experiments.

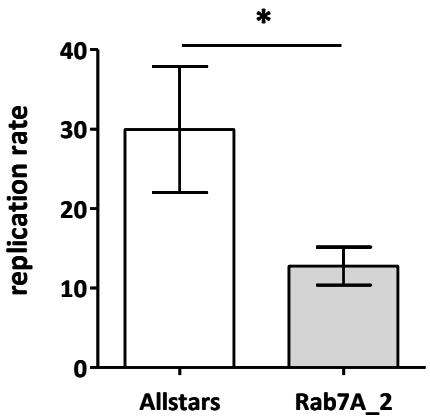

Figure III.14: Gentamicin protection assay demonstrates a significant bacterial replication defect in Rab7A knock down cells.
In order to calculate the bacterial replication rate, a gentamicin protection assay was performed. Transfected HeLa cells were infected and at 2 hours p.i. and 16 h p.i. infected cells were lysed with triton, the lysates were serial diluted and plated on selective agar plates to count bacterial colonies. The replication rate was calculated by the ratio of recovered bacteria at 16 h p.i. and 2 h p.i. The data shows a representative experiment with means and standard deviations (n=3) for Allstars treated and Rab7A_2 treated cells. P-value <0.05.

III.2 Large scale RNAi screening and statistical analysis

III.2.1 Primary screen

Two siRNA libraries were employed for large scale RNAi screening experiments using the high-throughput bi-chromatic FACS assay, namely, 1. the SOS library, containing varied siRNA sequences used in our laboratory, and 2. the validated kinase library (SKV). The composition and the properties of the libraries are summarized in table III.1.
Both libraries were already distributed into the 48 inner wells of 96 well plates, solved in RPMI medium without FCS with a concentration of 200 nM and stored at -80°C. These plates are from now on called the transfection plates. Each plate could be used for two transfection experiments using the pipetting robot. The automatic transfections were carried out as described in II.6.8.2.1 using the plate scheme depicted in figure S.1.
The SOS library was screened first with testing every transfection plate at least three times, followed by the SKV screen. The acquired raw data from the siRNA libraries was further processed with the respective software (see II.11) and analyzed statistically.

Table III.1: siRNA library composition and properties

library	Nº of genes	Nº of siRNAs per gene	Nº of plates	composition	source
SOS	480	1	10	non-related	in-house
SKV	588	2	26	kinase genes	Qiagen

Initially, it was important to validate the quality and robustness of the screening data. In a first analysis step, the mean inhibition values for Rab7A of all plates and runs were calculated and plotted to control the stability of the down-regulating control siRNA throughout the whole screening procedure (see figure III.15). As holds true for both libraries, the GFP fluorescence in the Rab7A samples normalized to Allstars was comparable within the whole amount of plates and runs with a total mean of about 0.68 and 0.65 for the SKV and the SOS library, respectively. Based on these results, the inhibition data of the siRNAs to test that was calculated on the basis of the Allstars and Rab7A values could be considered as reliable and was therefore analyzed further.

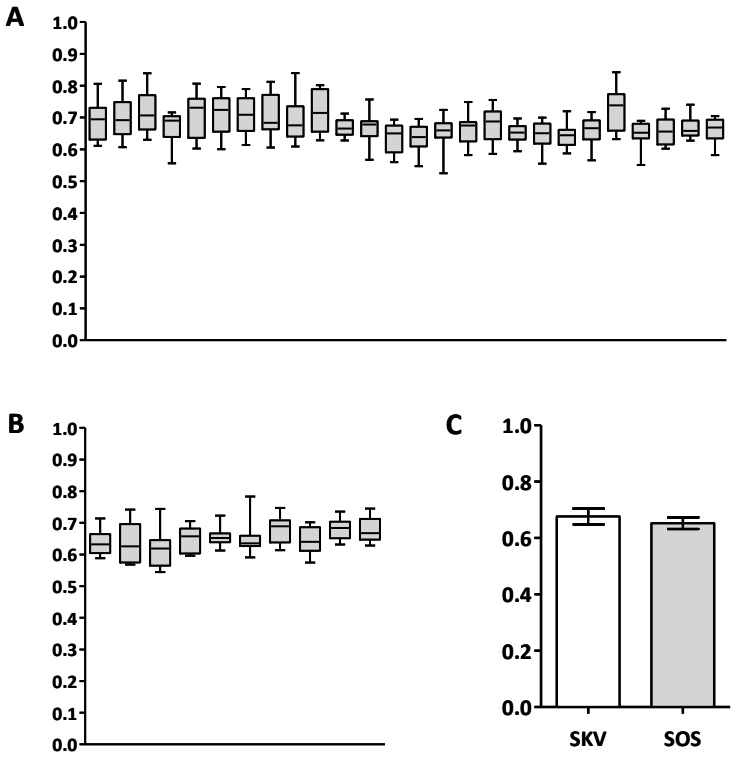

Figure III.15: Statistical robustness of the Rab7A siRNA control.
The reliability and quality of the screening data was validated in a first step by analyzing the stability of the Rab7A inhibitory control for all plates screened. The median values of all Rab7A replicates for each plate were used to calculate the respective decrease in GFP intensity normalized to Allstars. The box-plots show the median (line in box), the upper an lower quartile (box), the 2.5% percentile (lower whisker) and the 97.5% percentile (upper whisker). Plates are shown in their order for the SKV library [A] and the SOS library [B]. The means and standard deviations for the medians of all plates are shown in [C].

To obtain an overview of the distribution of critical screening parameters, the entire data sets for the SKV and the SOS library were further analyzed for mean plate inhibition and cell toxicity as well as inhibition on the single siRNA level. The respective diagrams are shown in

figure III.16. In order to guarantee an unbiased plate allocation of the transfection plates, the mean inhibition of the collectivity of siRNAs in one plate should be in the range of zero. This, indeed, was the case for both library plates as indicated by the box plot characteristics

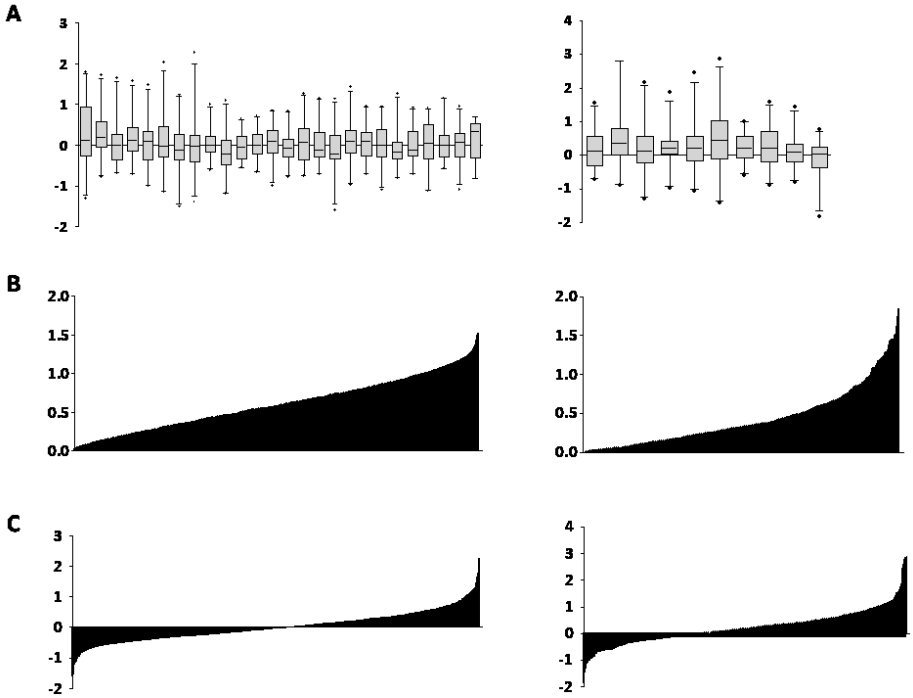

Figure III.16: Analysis of whole screening data.
The entire screening data set that was acquired for the SKV library (left side) and the SOS library (right side) was statistically validated. [A] Mean inhibition of all test siRNAs for each plate reveals no phenotypic bias (mean values approximately zero) in neither the SKV or the SOS library produced by the allocation of the plates. Plates are shown in their order. [B] Overall cell toxicity of every sample siRNA sequence, normalized to Allstars, in quantitative order. [C] Mean inhibition values for every siRNA sequence in quantitative order.

(figure III.16.A). Thus, the quality of the plates with regard to the unbiased distribution of the test siRNAs was proven. The cell number of each siRNA sequence, normalized to Allstars, revealed a difference in cell toxicity between the SKV and the SOS library (figure III.16.B). Whereas the overall toxicity of siRNAs of the SKV library was relatively moderate, a higher number of siRNA sequences of the SOS library showed significant cell toxicity. This is also demonstrated by the quantification diagram (figure III.17.A). Additionally, the mean inhibition values of the individual siRNAs of the SOS library showed a slight bias to a down-regulating phenotype (figure III.16.C). This becomes also obvious from the quantification shown in figure III.17.B. The observed bias is probably founded in the more pronounced toxicity of the SOS siRNAs leading to inadequate infection conditions.
The relatively high number of toxic siRNAs in both libraries made it necessary to carefully check the tested siRNAs for their impact on cell number before evaluating their importance for the bacterial infection process, namely the GFP and mCherry fluorescence. Therefore, a three step selection procedure was performed as described in II.11. First, the normalized cell counts were examined and all siRNAs that showed a significant cell loss (cell counts < 0.4) were excluded from further analysis. Next, the mean inhibition was queried to specify siRNAs as up-regulating (≤ -0.5) or down-regulating (≥ 0.5). As the last criterion, the

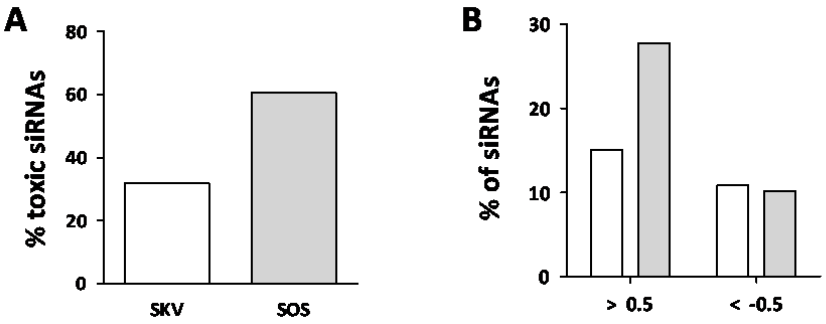

Figure III.17: Higher toxicity and a biased phenotype in the SOS library.
The entire screening data from the SKV and the SOS library was quantified with regard to the cell toxicity [A] and the impact on *Salmonella* growth [B]. > 0.5: relevant inhibition of *Salmonella* replication; < -0.5: relevant up-regulation of *Salmonella* replication.
white bars: SKV library grey bars: SOS library

statistical significance for the mean inhibition with Allstars as reference was calculated using the Student's t-test and a value of < 0.05 was defined as implying significant differences. This procedure is allegorized in figure III.18 which shows "volcano plots" for the data from the SKV and the SOS library. In this two dimensional graphical analysis method the statistical significance of the inhibition values (p-value) was plotted against the values for the mean inhibition. Characteristic volcano shaped distribution patterns occurred and simplified the selection of promising siRNAs for further validation. Only siRNAs located in the shaded areas, i.e. siRNAs that fulfilled the criteria for significance (p-value < 0.05) and inhibition (≤ -0.5 or ≥ 0.5, see above), were considered as being relevant. They were finally evaluated with respect to their cell toxicity. A complete list with the toxicity and phenotypic results for all siRNA sequences from the SKV library can be found in the supplement (see table S.1). The solid analysis with regard to the criteria mentioned above gave a list of candidate genes that

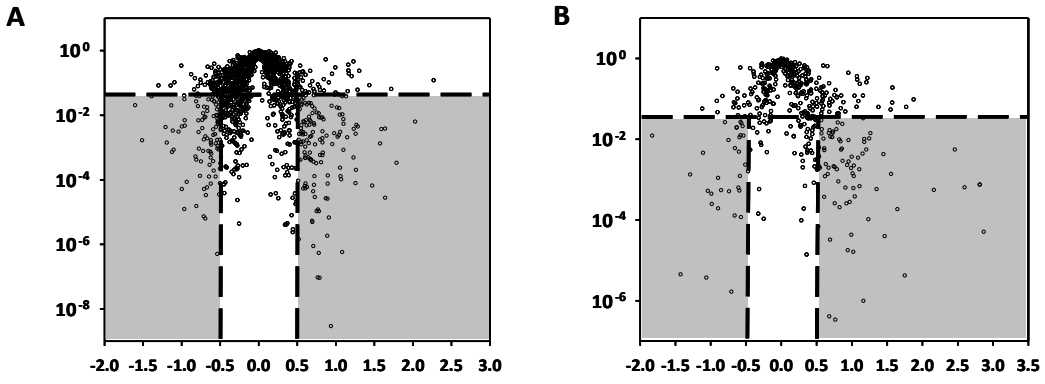

Figure III.18: Volcano plots of SKV and SOS data.
The mean data of all siRNA sequences for mean inhibition (x-axis) and p-value (y-axis) was plotted as is shown for the SKV library [A] and the SOS library [B]. Samples that fulfill the criteria for mean inhibition and significance are located in the grey shaded areas. They were further analyzed by applying the cell count threshold to serve as validation candidates.

were considered as possible screening hits. Due to technical restrictions only a limited number of siRNAs could be integrated into the validation process with the main focus on SKV siRNA targets. The 48 chosen candidate genes of the SKV library with their mean inhibition and p values are listed in figure III.19 and in the supplementary table S.3. 20 of these showed a down-regulating phenotype, whereas 28 caused an upregulation of the infection. It has to be mentioned that for all of the candidate genes that were chosen for the subsequent validation only one out of two siRNAs from the SKV library showed the effect. Although, the library was validated for knock down efficiency, this result might have resulted from inadequate knock down rates.

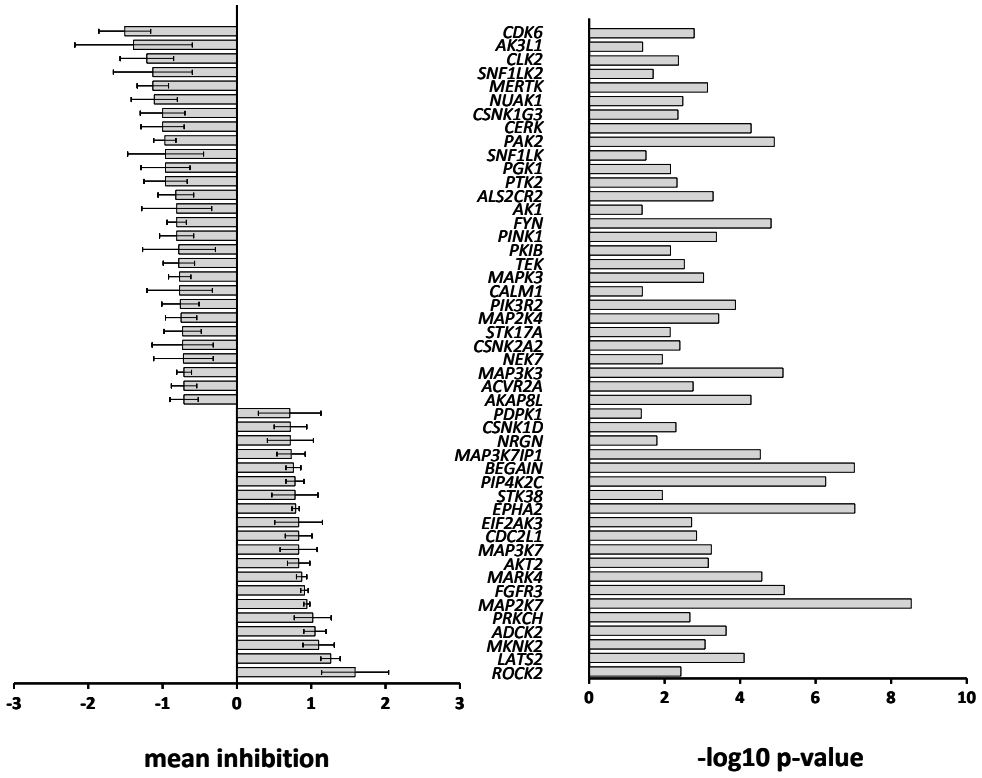

Figure III.19: Selected candidate genes of the primary SKV screen.
After statistical analysis of the data from the primary SKV screen, 48 candidate genes were chosen for validation. Their impact on Salmonella growth is illustrated on the left, the mean values of at least three independent experiments with SD for each candidate. The statistical signifance of the mean inhibition of all candidates with Allstars as reference is shown on the right.

This first selection of siRNA sequences that caused a decrease in GFP fluorescence was further analyzed implying the second fluorescence read-out. For this, the ratio of the mCherry fluorescence and the GFP fluorescence was calculated to test for shifts in the fluorescence intensity (figure III.20.A). The Allstars treated sample was used as a neutral control and as the reference for calculating the statistical significance. Cells depleted of Rab7A displayed a significantly lower ratio, normalized to Allstars (69 ± 5, mean and SD, n= 4, p-value < 0.001). This was also the case for MKNK2 and EIF2AK3 (84 ± 10 and 72 ± 19, p-values < 0.05,), MAP2K7, AKT2, MAP3K7, CDC2L1 and MAP3K7IP1 (75 ± 10, 81 ± 8, 64 ± 17, 79 ± 10 and 63 ± 15, p-values < 0.01) and BEGAIN (66 ± 11, p-value < 0.001).
The difference in the mCherry/GFP ratio gave a first indication that the bacterial metabolic activity could have been impaired after siRNA mediated knock down of the respective genes

since the ratio normally shows a linear course and a lower value would be a sign of differentially distributed cell populations (see figure III.4; dot plots with different cell lines and figure III.12; dot plot of Rab7A depleted cells). To further evaluate this, the quadrants two and four containing GFP/mCherry and GFP-only cells (harboring presumably metabolic inactive bacteria), respectively, were determined and the ratio of the according percentages was calculated. In figure III.20, the diagrams for the ratio normalized to Allstars (figure II.20.B) as well as the respective dot plots (figure II.20.C) are depicted. Rab7A knock down

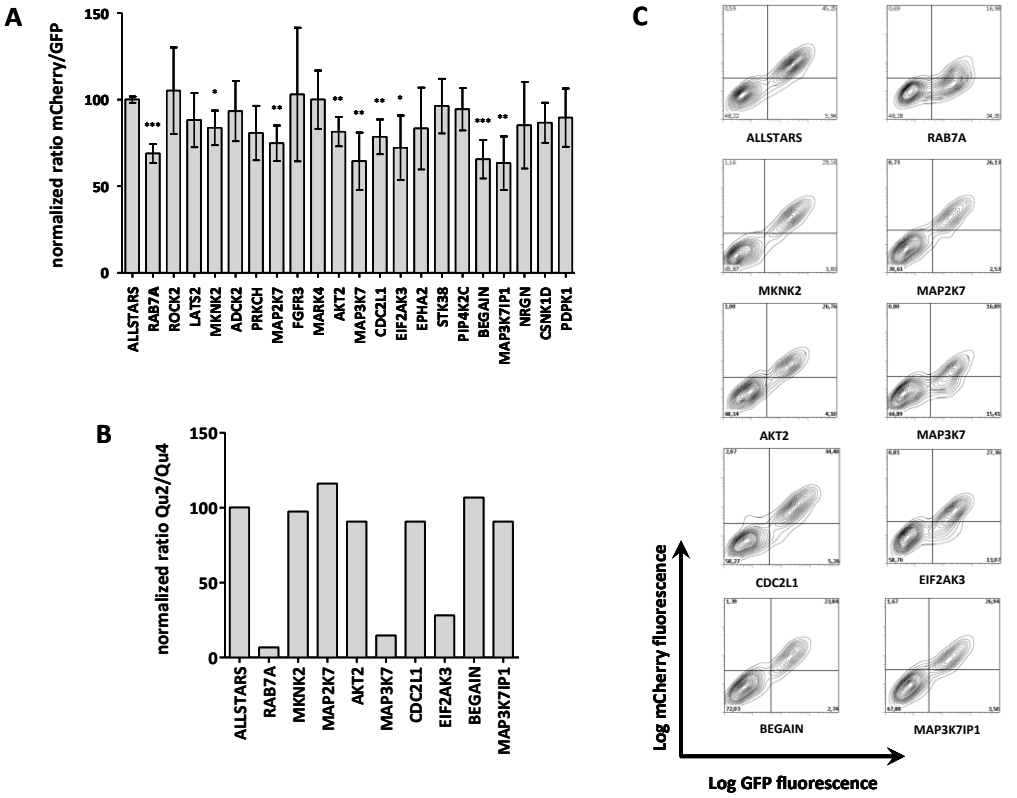

Figure III.20: Bichromatic FACS read-out allows further phenotypically validation of primary hits.

All primary hits that showed a down-regulation of infection were further evaluated using the different fluorescence properties of both fluorescence reporters. [A] Ratio of mCherry and GFP fluorescence of infected cells with the respective siRNAs. The value of Allstars treated cells was taken as reference for the calculation of the statistical significance. Values below the Allstars reference indicate proportionally lower mCherry fluorescence. The data shown are means from at least three independent experiments with SD. P-values are <0.05, <0.01, and <0.001, respectively. [B] The ratio of particles detected in quadrants two (GFP and mCherry) and four (GFP only) for targets that were identified as being significant in [A], normalized to Allstars. [C] Respective dot plots for the targets from [B] with GFP and mCherry fluorescence on the x-axis and y-axis, respectively.

cells displayed a much lower ratio, indicating only small numbers of GFP/mCherry positive cells which was in accordance to the microscopic analysis and bacterial quantification described in III.1.5.2 and III.1.5.3, respectively. A similar phenotype could be seen for MAP3K7IP1 and EIF2AK3, whereas the other samples showed no significant differences to the Allstars control value. The mathematically derived rating could be underlined by the

corresponding dot plots. For Rab7A, MAP3K7IP1 and EIF2AK3 a strong shift of the infected population could be observed (see figure III.20.C)

III.2.2 Validation of screening results

The primary screen resulted in 48 possible hits for the SKV library. In order to increase the reliability of the acquired phenotypes the primary hits had to be further validated. This was achieved by ordering siRNA oligonucleotides targeting the genes of interest with sequences different from those already examined within the screen. Due to technical reasons, the validation was focused on the kinase library (SKV). All genes that were part of the validation process are listed in table S.2 (supplement). For each gene, four individual siRNA sequences were ordered from Qiagen according to their availability. They were delivered in 96 well plates and resuspended to gain the transfection plates for the SKV validation. The transfection and infection experiments were performed manually as described in II.6.8.2.2 and the statistical analysis was carried out similarly to the one described before.
Table III.2 shows the results of the validation experiments for those siRNAs that showed a phenotype in the validation experiments. The mean inhibition values of the primary screen are included, to allow direct comparison of the results for the different siRNAs. For the validation data the strongest inhibition value is given along with the number of siRNA sequences that yielded the respective phenotype.

Table III.2: Validated kinases constituting possible candidates for functional characterization

siRNA target	function	Gene ID	% inhibition		phenotype	
			screen	validation	screen	validation
CSNK1D	casein kinase	1453	0.72	- 0.52 (1/4)	down	up
EIF2AK3	translation initiation factor kinase 3	9451	0.83	- 1.25 (2/4)	down	up
ACVR2	activin receptor	92	- 0.71	- 0.52 (2/4)	up	up
CERK	ceramide kinase	64781	- 1.0	- 0.3 (1/4)	up	(up)
AK1	adenylate kinase		- 0.81	- 0.57 (2/4)	up	up
SNF1LK2	salt-inducible kinase 2	23235	- 1.13	- 0.67 (2/4)	up	up
MAPK3	mitogen-activated kinase 3	5595	- 0.77	- 0.47 (2/4)	up	(up)
PGK1	phosphoglycerate kinase 1	5230	- 0.96	- 0.65 (4/4)	up	up
MAP2K7	mitgen-activated kinase kinase 7	5609	0.94	0.71 (3/4)	down	down
MAP3K7IP1	TAK1-binding protein 1	10454	0.73	- 0.73 (2/4)	down	up
CSNK1G3	casein kinase	1456	- 1.0	0.89 (2/4)	up	down
NEK7	NIMA-related kinase 7	140609	- 0.72	- 0.45 (2/4)	up	(up)
MERTK	c-mer proto-oncogene	10461	- 1.13	- 0.72 (2/4)	up	up
MKNK2	MAPK interacting kinase 2	2872	1.10	- 0.65 (3/4)	down	up
MAP3K7	TGF activated kinase	6885	0.83	- 0.41 (3/4)	down	(up)

III.3 Functional characterization to reveal the role of the mitogen-activated protein kinase kinase 7 (MKK7) during *Salmonella* infection of epithelial cells

After the validation of the primary screening data with additional independent siRNA sequences, a set of host cell genes that play a role during *Salmonella* growth in HeLa cells was compiled (see table III.2). A major challenge was then to decide on the factor that would be integrated into follow-up experiments to derive functional data. First, the comparison between primary screening data and validation results was taken into account, especially the phenotype of *Salmonella* growth (up/down). Interestingly, for a lot of targets oppositional phenotypes were observed (see table III.2) which characterized these targets as less interesting for further studies. Additionally, the robustness of the validation, i.e. the number of siRNA sequences showing the same trend of phenotype, was considered. Finally, it was surveyed whether helpful scientific publications regarding a host cell factor and Salmonella infection had already been published. Therefore, the considerations of possible follow-up targets led to the decision to functionally characterize the mitogen-activated protein kinase kinase 7 (MAP2K7 or MKK7) during *Salmonella* infection for the following reasons:

1. The knock down of MKK7 resulted in the inhibition of *Salmonella* growth both in the primary screen and the validation (same phenotype),
2. Within the validation, three out of four siRNA sequences showed the same phenotypic trend, and
3. MAP kinases are known to play a role during *Salmonella* invasion and replication.k

Several MAPKs have been reported to be activated by *Salmonella*, mainly in the context of pro-inflammatory host responses (see Introduction part for details). Therefore, they play a significant role in infections with this pathogen. MKK7 is involved in mediating the response to pro-inflammatory cytokines such as TNFα and other environmental stress stimuli, predominantly by activating the effector MAPK c-jun N-terminal kinase (JNK)(Tournier *et al.*, 1997). One important pathway of cellular stress is the release of the second messenger arachidonic acid (AA) from cell membrane phospholipids, catalyzed by the ubiquitously expressed enzyme cytosolic phospholipase A2 alpha (cPLA2) (Chakraborti, 2003) which can also be phosphorylated by MAPKs (Lin *et al.*, 1993, Borsch-Haubold *et al.*, 1998, Hefner *et al.*, 2000). AA then stimulates the synthesis of prostaglandins. Interestingly, Galan and colleagues demonstrated that an inhibitor of cPLA2 is able to decrease the invasion rate of *Salmonella* Typhimurium into cultured epithelial cells, arguing that cPLA2 activity is involved in this process (Pace *et al.*, 1993). They also observed an increase in intracellular calcium, which stimulates the localization of cPLA2 from the cytosol to membranes and thereby leads to its activation. In the same report phosphorylation of the MAPK Erk was shown upon *Salmonella* attachment and invasion resembling signaling through the epidermal growth factor receptor (EGFR). Taken together one could speculate that cPLA2 is activated through the MAPK pathway and active cPLA2 is necessary for *Salmonella* invasion and probably also subsequent replication which could be demonstrated for the intracellular bacterium *Chlamydia trachomatis* (Su *et al.*, 2004). In this context, the knock down of MKK7 might lead to a decrease of cPLA2 activity. This could cause an inhibition of bacterial invasion and/or replication. Therefore the role of MKK7 and cPLA2 in *Salmonella* infection was further characterized.

III.3.1 MKK7 knock down reduces *Salmonella* intracellular growth

MKK7 was identified within the kinome screen as being important for *Salmonella* intracellular growth. Infected HeLa cells showed less GFP fluorescence after MKK7 knock down compared to Allstars treated cells. A representative FACS histogram is depicted in figure III.21.A. The grey shaded curve and the black line resembles Allstars treated cells and MKK7 treated cells, respectively. A shift in GFP fluorescence could be observed for MKK7 treated cells resulting in approximately 30 % reduction of GFP intensity (figure III.21.B). In order to evaluate the FACS derived inhibitory phenotype for MKK7 knock down, gentamicin protection assays were performed as described in II.6.6. This allowed quantification of intracellular bacterial replication in Mock, Allstars and MKK7 treated HeLa cells. As a confirmation for the FACS results, the gentamicin protection assay using siRNA-treated HeLa

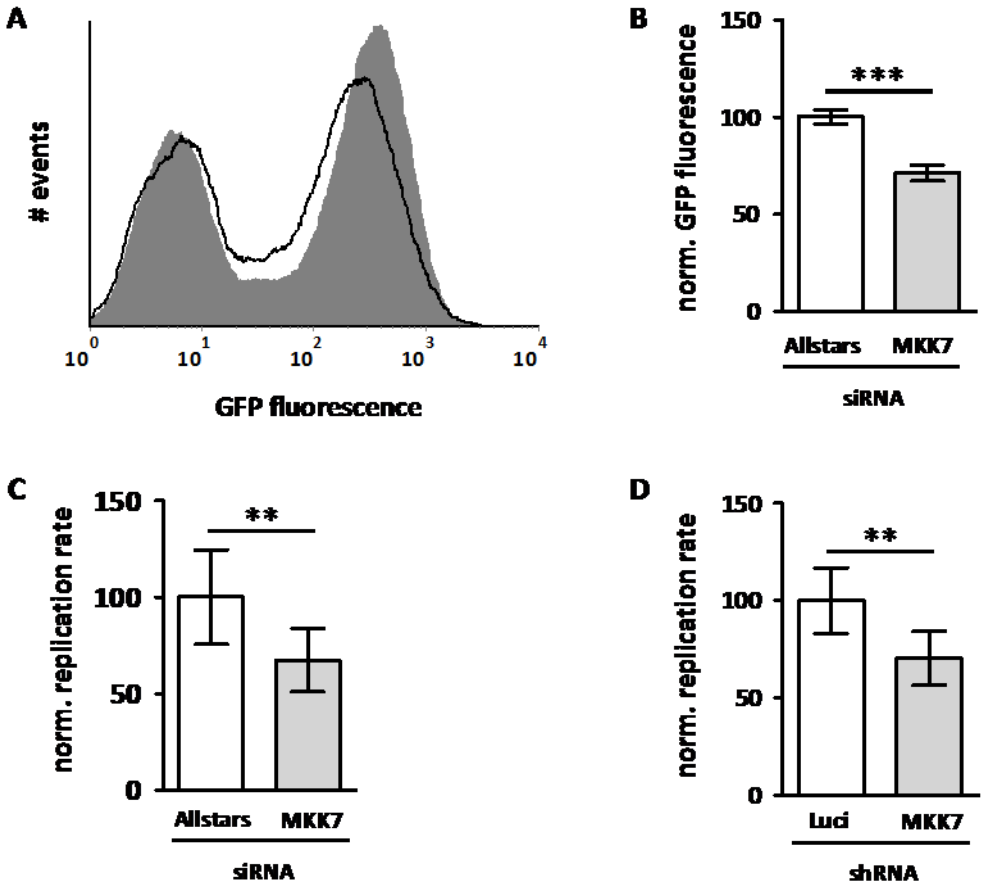

Figure III.21: MKK7 knock down inhibits *Salmonella* intracellular growth.
The impact of MKK7 kd on *Salmonella* intracellular growth was evaluated with the FACS assay and with gentamicin protection assays. [A] A representative FACS histogram showing the GFP fluorescence of Allstars transfected cells (grey shaded curve) and MKK7 transfected cells (black line). [B] Quantification of the GFP fluorescence from infected cells after Allstars or MKK7 transfection as mean with SD from triplicates. [C] Gentamicin assay of Allstars treated cells (white) or MKK7 treated cells (grey) showing the replication rate normalized to Allstars as the mean with SD from three individual experiments. [D] Gentamicin assay of Luciferase (white) or MKK7 (grey) shRNA transfected cells showing the replication rate normalized to Allstars as mean with SD from two individual experiments.

cells revealed a significant decrease of replicating bacteria in MKK7-depleted host cells (figure III.21.C). This was further validated with a shRNA-mediated MKK7 stable knock down HeLa cell line (figure III.21.D).
Taken together, these experimental data verified that the depletion of MKK7 inhibits *Salmonella* intracellular replication.

III.3.2 cPLA2 is activated in *Salmonella* infected cells

MAPK have been reported to be involved in the activation of cPLA2, a molecule that was described to be involved in *Salmonella* invasion. In order to find out whether the knock down of the MAPK MKK7 had an influence on cPLA2 activation directly or indirectly and thereby caused an inhibition of bacterial infection, initially, a possible activation of cPLA2 during *Salmonella* infection was investigated.

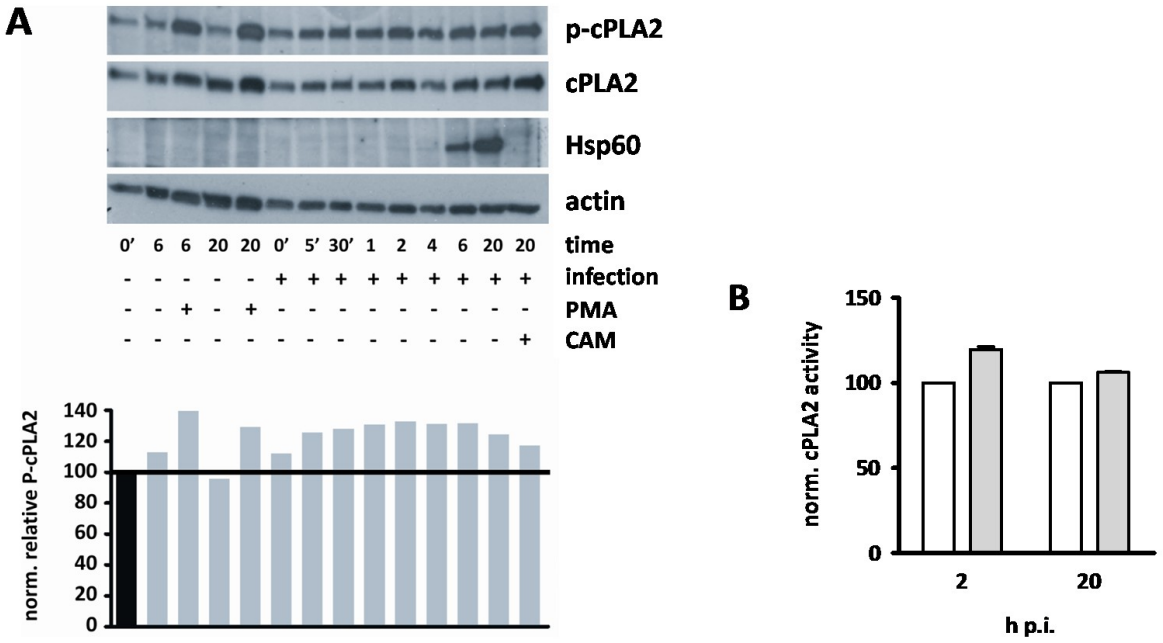

Figure III.22: cPLA2 is phosphorylated and activated upon *Salmonella* infection.
[A] Infected or non-infected HeLa cells were prepared for immunoblotting at different time-points. Cell lysates were probed for Ser505 phosphorylated cPLA2 (p-cPLA2), total cPLA2, bacterial Hsp60 and actin as loading control. [upper part] Immunoblots showing the respective samples. [lower part] Quantification of the relative amount of phosphorylated cPLA2 in the respective samples, normalized to the non-infected control at 0 min (black bar). PMA: phorbol-12-myristate-13-acetate; CAM: chloramphenicol [B] The enzymatic activity of cPLA2 was quantified in non-infected (white bar) and infected (grey bar) cells at the respective time-points using a specific fluorescent dye and FACS analysis.

HeLa cells were seeded in 24 well plate format and were either infected with a MOI of 50 or left uninfected. Uninfected cells were either left untreated or stimulated with 100 nM phorbol-12-myristate-13-acetate (PMA), a non-specific inducer of several pro-inflammatory pathways serving as a positive control. One infected sample was treated with 10 µg/mL chloramphenicol (CAM) 2 h p.i. to prevent bacterial replication. Cells were lysed with 1x Lämmli buffer at different time-points and the cell lysates were tested for cPLA2 phosphorylation by SDS-PAGE and immunoblotting using an antibody specific for

phosphorylated cPLA2. Additionally, bacterial Hsp60 was detected to monitor bacterial replication and total cPLA2 and actin detection were used to assess relative cPLA2 phosphorylation or equal sample loading, respectively. For quantification of the relative amount of phosphorylated cPLA2, immunoblots were processed with ImageJ (http://rsbweb.nih.gov/ij/index.html). First, all actin signals were normalized to the intensity of the non-infected sample from time-point zero. Then, total cPLA2 was normalized to this value and finally the intensity of phosphorylated cPLA2 was set into relation to total cPLA2. Additionally, cPLA2 enzymatic activity was monitored in non-infected and infected cells at different time-points using a specific substrate and resulting fluorescence was measured with a FACS Calibur.

Figure III.22.A reveals that cPLA2 became phosphorylated very early in infection. Already five minutes p.i. a significantly stronger band of expected size compared to the non-infected background level could be observed which could also be quantified using ImageJ (III.22.A, lower part). The phosphorylation of cPLA2 remained equal during the infection time tested with a slight decrease 20 hours p.i. (see quantification in figure III.22). The chloramphenicol-treated sample showed less phosphorylation which, nevertheless, was stronger than in the control sample. This observation was further verified with the quantification of cPLA2 enzymatic activity (figure III.22.B). Here, a higher activity was measured for infected cells 2 h p.i. compared to non-infected which was in comparison to the phosphorylation levels detected. This activity was less at 20 h p.i. but still higher than in control cells, indicating a sustained enzymatic activity of cPLA2 in infected cells. The demonstrated phosphorylation and induction of enzymatic activity by *Salmonella* Typhimuirum might be a hint for the requirement of cPLA2 enzymatic activity for the efficient replication of the pathogen.

III.3.3 cPLA2 is necessary for *Salmonella* intracellular replication

The infection time course revealed an activation of PLA2 during *Salmonella* infection (figure III.22), indicating that cPLA2 might be important for *Salmonella* growth in epithelial cells. To test this, the expression of cPLA2 was silenced using specific siRNAs (PLA2_1 and PLA2_2 as a

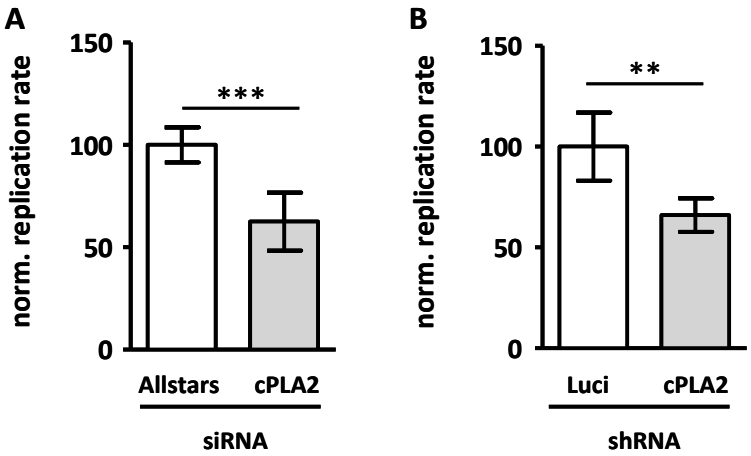

Figure III.23: cPLA is necessary for *Salmonella* intracellular replication.
The intracellular replication rate was quantified with the help of the gentamicin assay for siRNA-treated cells [A] or shRNA treated cells [B]. Intracellular replication was normalized to the controls Allstars [A] or Luciferase [B]. Mean data from two experiments with SD is shown. P-values: **<0.01; ***<0.001.

pool) or by constructing a stable cPLA2 knock down cell line and gentamicin protection assays were performed as described in II.6.6. The results of these experiments are presented in figure III.23. It becomes obvious that the knock down of cPLA2 reduced the intracellular replication of bacteria to about sixty percent of the control level.

III.3.4 MKK7 knock down provokes reduced cPLA2 protein levels

In contrast to the results described above, Galan and colleagues reported on the requirement of cPLA2 for the *Salmonella* invasion process (Pace *et al.*, 1993). In their study, the authors argued that MAPKs are likely to be involved in this process. However, the role of MKK7 in cPLA2 activation was not evaluated. To do so in this work, cPLA2 phosphorylation during infection in the absence of MKK7 was ascertained.
HeLa cells were seeded in 12 well plates and 24 hours later they were either mock transfected or transfected with Allstars siRNA or MKK7 siRNAs. Three days post transfection cells were infected with *Salmonella* Typhimurium 12023 wt with a MOI of 50. 2 h p.i. cells were lysed and tested for cPLA2 phosphorylation by SDS-PAGE and immunoblotting using a

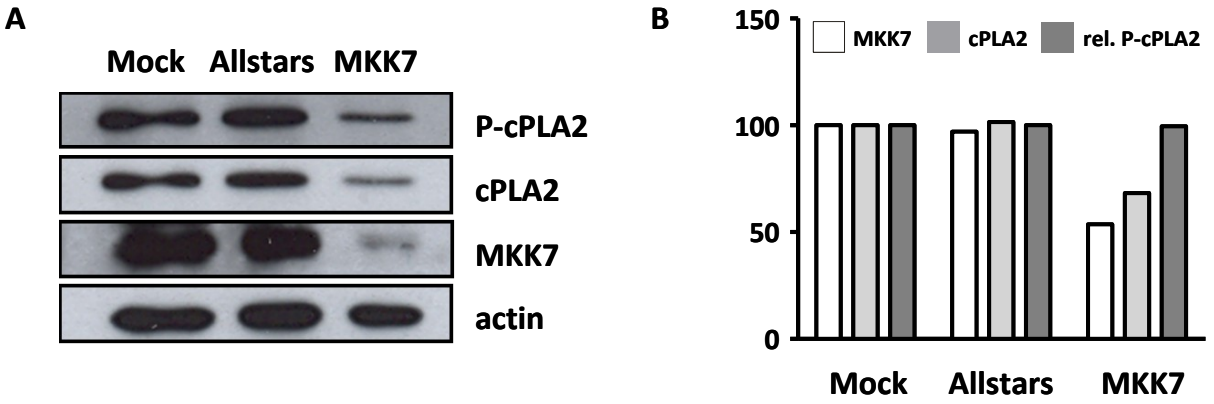

Figure III.24: MKK7 knock down provokes reduced cPLA2 protein levels.
HeLa cells were either mock transfected or transfected with Allstars siRNA or a pool of two siRNAs targeting MKK7. Three days post transfection cells were infected and 2 h p.i. cells were lysed and subjected to SDS-PAGE and immunoblotting. [A] Immunoblot showing respective lysates analyzed for phospho-cPLA2 (first row), total cPLA2 (second row), MKK7 (third row), and actin as loading control (fourth row). [B] Quantification of the immunoblot displayed in [A]. Shown are the values for MKK7 (white bar), cPLA2 (light grey bar), and the ratio of phosphorylated to total cPLA2 (dark grey bar), normalized to mock transfected cells.

phosphorylation-specific antibody. Total cPLA2 and MKK7 levels were detected with respective antibodies and actin detection was used to assess equal sample loading. The knock down of MKK7 using a pool of two siRNAs was successful demonstrated by a significantly weaker band of expected size (see third row for MKK7 siRNA in figure III.24.A and white bar in III.24.B). In the MKK7 knock down sample also the levels of phosphorylated cPLA2 (first row) as well as total cPLA2 (second row) were considerably lower than in control transfected cells (Allstars and Mock), indicating that the knock down of MKK7 caused changes in the protein level of cPLA2 during infection. Although the total levels of cPLA2 were considerably lower in MKK7 depleted cells, the relative phosphorylation level of cPLA2 (i.e. ratio of phosphorylated to total cPLA2) was the same under all conditions applied (see

dark grey bar in III.24.B). Therefore, a MKK7 dependent control of cPLA2 levels seems likely which could account for the observed downregulation of *Salmonella* infection upon MKK7 knock down.

III.3.5 MKK7 and cPLA2 do not form a stable protein complex

Both MKK7 and cPLA2 are involved in the intracellular replication of *Salmonella* in epithelial cells which was demonstrated by siRNA or shRNA mediated knock down experiments. Additionally, it was observed that upon MKK7 depletion the protein levels of cPLA2 decline which could explain the inhibitory phenotype of MKK7 knock down. Although to date, there are no reports on a physical interaction between MKK7 and cPLA2 it could be possible that MKK7 forms a complex with cPLA2, thereby stabilizing this protein. Similar observations have been reported for inhibitor of apoptosis protein (IAP) complexes (Rajalingam *et al.*, 2006).

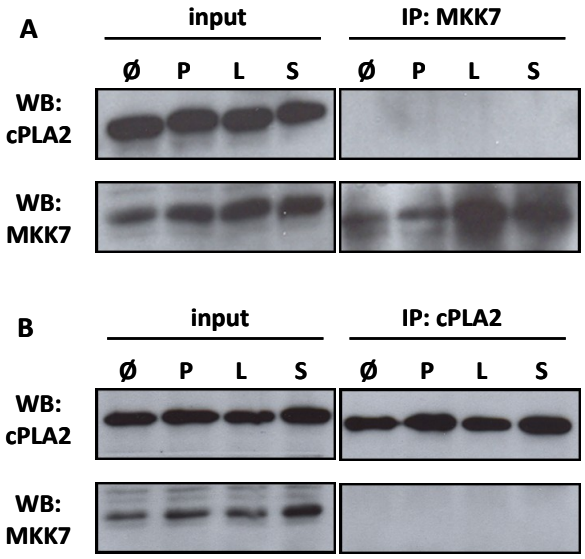

Figure III.25: MKK7 and cPLA2 do not form a stable complex.
HeLa cells were seeded in 10 cm dishes and 24 h later treated for 2 h as follows: Ø, no treatment; P, 100 nM PMA; L, 10 ng/µL *E. coli* LPS; S, *Salmonella* Typhimurium 12023 wt (MOI 50). Samples were prepared for Co-IP as described in II.8.3 and proteins were detected using specific antibodies. [A] Input and IP samples from a Co-IP using a MKK7 antibody that were analyzed for cPLA2 (upper panel) and MKK7 (lower panel). [B] Input and IP samples from a Co-IP using a cPLA2 antibody that were analyzed for cPLA2 (upper panel) and MKK7 (lower panel).

In order to find out whether MKK7 and cPLA2 form a stable complex, co-immunoprecipitation (Co-IP) experiments were performed as described in II.8.3. $2.4x10^6$ HeLa cells were seeded in 10 cm dishes. The next day the cells were differentially treated as described in the legend of figure III.25 and 2 hours later they were processed for Co-IP using either an antibody against MKK7 or against cPLA2 for pull-down. Pre-clear lysates as input control and immunoprecipitated lysates were applied to SDS-PAGE and immunoblotting to detect MKK7 and cPLA2. In order to avoid masking of the MKK7 signal by the denatured heavy chain of the IP antibody, a light chain specific secondary antibody was used (see II.8.3). The Co-IP studies revealed that there is no direct interaction of the MAP kinase and PLA2 (figure III.25). Within all input samples (left part) distinct bands for cPLA2 and MKK7

could be observed. However, after pull down of MKK7 no cPLA2 signal was detected (figure III.25.A, upper panel in right part) and vice versa (figure III.25.B, lower panel in right part), indicating that under the conditions used cPLA2 could not be co-immunoprecipitated with MKK7. This suggests that MKK7 and cPLA2 do not form a stable complex.

III.3.6 MKK7 regulates the expression of cPLA2

Given the fact that the Co-IP for MKK7 and cPLA was negative, a control of cPLA on protein level exerted by MKK7 seemed unlikely. In order to test whether MKK7 regulates the expression of cPLA2, HeLa cells were either transfected with Allstars control siRNA or with different siRNAs targeting MKK7 or cPLA2 and the relative cPLA2 mRNA amounts were detected by quantitative RT-PCR (figure III.26). Indeed, following MKK7 knockdown with two different siRNA sequences, the mRNA levels of cPLA2 also decreased significantly (figure III.26). This implicates that MKK7 is involved in the transcriptional regulation of cPLA2.

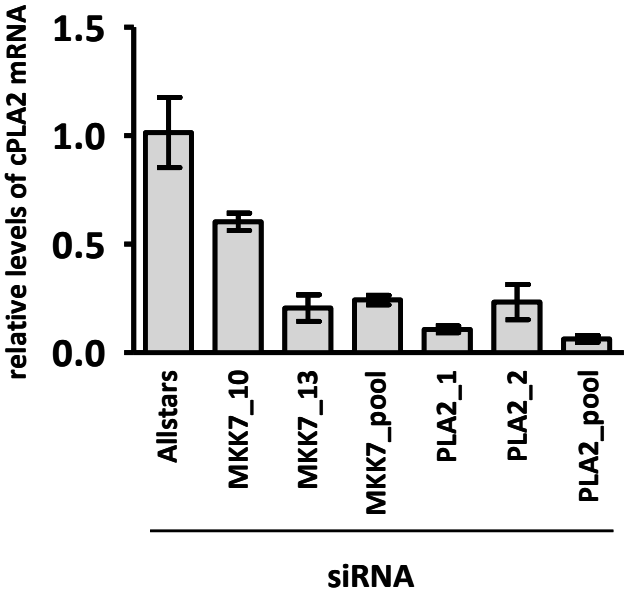

Figure III.26: MKK7 regulates cPLA2 expression.
HeLa cells were transfected with Allstars control siRNA or with different siRNA sequences targeting MKK7 and cPLA2. Three days post transfection cells were lysed and RNA was isolated. The relative cPLA2 mRNA amount was detected using RT-PCR.

III.3.7 cPLA2 knock down leads to an increased formation of filiform Sifs

In order to further functionally characterize the impact of cPLA2 knock down on intracellular bacteria, HeLa cells were either transfected with Allstars or cPLA2 siRNAs, infected with *Salmonella* Typhimurium constantly expressing the mCherry protein and 16 h p.i. the samples were stained for the lysosomal marker protein LAMP-1. This lysosomal marker helps to visualize the strcuture and form of the *Salmonella* induced filaments (Sifs) which are an indication for the accomodation of S*almonella* Typhimurium inside epithelial cells. Figure III.27.A displays exemplary confocal images of Allstars or cPLA2 transfected cells. Bacteria

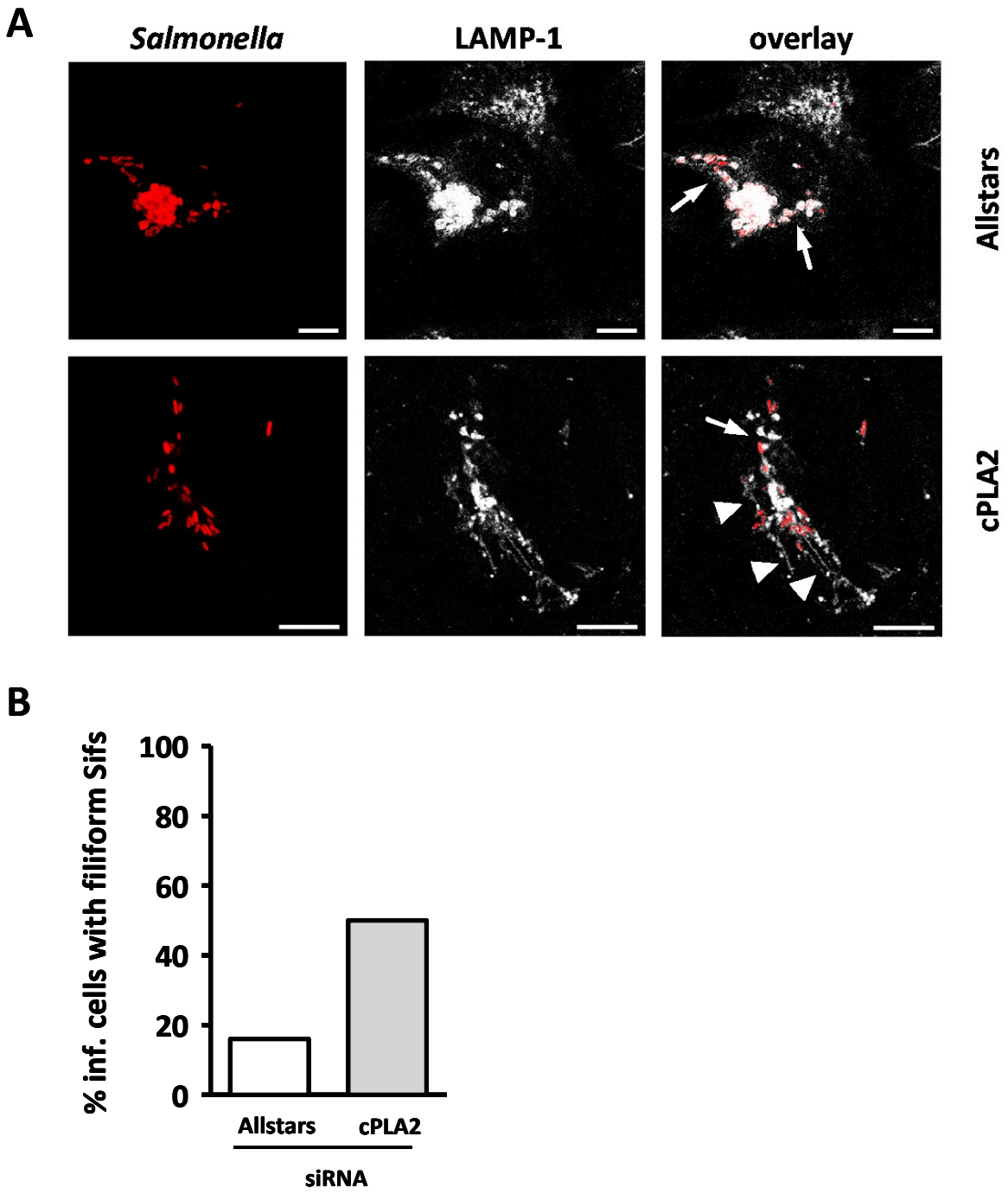

Figure III.27: Knock down of cPLA2 induces the formation of filiform Sifs.
HeLa cells were treated either with Allstars or cPLA2 siRNAs and infected with *Salmonella* Typhimurium, constitutively expressing the mCherry protein (red colour in [A]). 16 h p.i. samples were stained for LAMP-1 (grey colour in [A]) and images were acquired using a confocal microscope. [A] Exemplary images of infected cells treated with Allstars (upper panel) or cPLA2 (lower panel) siRNAs. Thick, mature Sifs are indicated by arrows, filiform Sifs by arrowheads. Scale bar: 10 µm. [B] Quantification of infected cells showing the filiform Sif structure. Data shown is from one experiment and at least twenty infected cells were analyzed.

are false colour stained in red and LAMP-1 is false colour stained in grey. Interestingly, it was observed that in a significant proportion of infected cPLA2 kd cells, Sifs appeared very thin and filamentous (see arrowheads in figure III.27.A) as compared to the more robust and

thick structure of Sifs in Allstars transfected cells (see arrows in figure III.27.A). The initial observation was quantified by counting at least twenty infected cells for both conditions. Stacks of three confocal planes were merged and the percentage of infected cells showing filiform Sifs was calculated (see figure III.27.B). In cPLA2 depleted cells, about 50 % of infected cells show filiform Sifs, compared to 16 % of infected cells in Allstars-treated samples. This indicates that cPLA2 plays a role in the formation of regular Sifs, probably by its enzymatic activity which enables the lipid modification of Sif membranes.

IV Discussion

Intracellular pathogens rely on cellular functions of their host cells to establish a niche suitable for growth and replication. Key aspects of successfully concluding an infection are the invasion of the host cell, intracellular accommodation and replication, and subsequent release from infected cells to initiate a new infectious cycle. During all of these stages, components of the host cell machinery must be exploited to arrange conditions favourable for the pathogen. In this context it is conceivable that different pathogens use common host cell pathways but also distinct ones which reflect specific needs and evolutionary adaptations. The study of molecular pathways used by intracellular pathogens contains the capacity to gain a deeper insight into basic cellular processes of the host cell. *Salmonella* Typhimurium constitutes an ideal model organism to study bacterial interactions with host cells. It is a Gram negative facultative intracellular bacterium which induces its uptake into a variety of different eukaryotic cell types by the delivery of effector proteins via a type three secretion system (T3SS). It can be cultivated on solid agar plates as well as in liquid medium and it is readily accessible to genetic manipulations, making it comparatively easy to deploy under normal laboratory conditions. Since *Salmonella* are also very relevant pathogens for humans and livestock, research on the intracellular lifestyle of this organism shall contribute to further development of antimicrobial therapies. Intensive genetic studies on the bacterial side have identified a number of important virulence factors, which mostly became obvious using *Salmonella* Typhimurium mutants in cell culture or mouse infections. This led to a comparatively good knowledge of bacterial factors and their regulation that play a role in *Salmonella* interplay with host cells. On the other side, only a few host cell factors have been identified so far that are targeted by *Salmonella* to establish a successful infection. This was mainly due to the lack of techniques to routinely generate cell lines exhibiting a specific genetic deletion. Therefore, scientific research was mainly restricted to cells isolated from knock out mice or to overexpression of dominant-negative forms of proteins of interest. With the discovery of the RNAi pathway in eukaryotes, a powerful tool to study eukaryotic gene function emerged which also showed to be auxiliary in disclosing pathogen-host cell interactions on a molecular level. Despite drawbacks of the RNAi technique, the possibility to evaluate the impact of a specific host cell gene knock down on the course of infection will certainly contribute significantly to the understanding of the many ways pathogens have evolved to exploit host cell processes.

In this work, a technical system was set up to precisely monitor the intracellular growth of *Salmonella* Typhimurium inside eukaryotic host cells. This was achieved by using the green fluorescent protein (GFP) together with a derivative of the *Discosoma* sp. Red fluorescent protein (DsRed), named mCherry, as reporter genes for bacterial replication and metabolic activity. The principal readout system for this assay was flow cytometry but it also proofed to be applicable to microscopy. With this robust assay RNAi screens were performed employing two different siRNA libraries and the impact of host cell gene knock down on *Salmonella* intracellular growth was verified. The screening was followed by statistical analysis and intensive validation to distil host cell factors that are involved in *Salmonella* Typhimurium infection of the human epithelial cell line HeLa.

The *Salmonella* Typhimurium reporter strain was generated by constructing two plasmids that were introduced into the wild type strain 12023. The first plasmid, pOR25, expresses the GFP variant GFP*mut3* (Cormack *et al.*, 1996) under a constitutively active promoter,

ΦrpsM. This reporter allows to monitor the bacterial replication both *in-vitro* and *in-vivo*. The FACS analysis of single bacteria *in-vitro* showed a characteristic GFP fluorescence intensity curve over time. This was set in correlation to the growth phase at the respective time-point (see figure III.3.C). Since the promoter **Φ***rpsM* drives the expression of a gene encoding a ribosomal protein which is especially necessary in rapidly dividing bacteria with high protein turnover, the GFP intensity of single bacteria increases when the bacteria are in the logarithmic growth phase. When entering the late-logarithmic and later the stationary phase, the activity of the *rpsM* promoter declines and the GFP intensity decreases due to dilution during cell divisions. However, this scenario can be seen only under ideal growth conditions, especially in a nutrient rich environment. The conditions of the nutrient poor *Salmonella* containing vacuole (SCV) inside the host cell do not allow a dilution of GFP molecules among dividing bacteria when the **Φ***rpsM* activity is reduced, resulting in less GFP intensity, since the replication rates *in-vitro* and *in-vivo* are not comparable. Rather, the relatively long half-life of the GFP molecule, which was estimated to be more than 24 h (Andersen *et al.*, 1998), leads to an accumulation of GFP inside the bacteria and therefore the GFP fluorescence intensity will increase in relation to the number of bacteria inside the vacuole (Thone *et al.*, 2007). This allows for monitoring intracellular bacterial replication using the GFP intensity as a general fluorescence reporter. Nevertheless, when not following the growth of intracellular bacteria in a time-course experiment but rather only determining one time-point, as during the performance of a high-throughput screen, the stability of the GFP*mut3* molecule brings about the problem to distinguish between slowly replicating bacteria and those that are unable to replicate at a certain time-point of the infectious cycle. Both bacterial populations will probably display a comparable GFP intensity but with dramatically different underlying phenotypes. Thus, in order to query the vitality of intracellular bacteria shortly before performing the FACS analysis, an inducible reporter system was developed, the plasmid pOR26. Here, the fluorescent protein mCherry is expressed under the control of the promoter **Φ**araBAD which is induced by arabinose (Guzman *et al.*, 1995). Since the bacteria have to be in a metabolic active state to react to the arabinose trigger, the mCherry fluorescence intensity can serve as an additional indicator for the impact of host cell gene depletion on the fitness of intracellular bacteria. In FACS and confocal microscopy experiments within this work, it could be demonstrated that the external addition of arabinose was able to stimulate intracellular *Salmonella* to express the mCherry protein (see figure III.4 and III.5). Interestingly, these experiments also showed that the compound arabinose was taken up into the SCV, indicating that a respective sugar transporter could be located at the SCV membrane. Additionally, because the presence of glucose totally represses the **Φ**araBAD (Guzman *et al.*, 1995), the induction of mCherry expression from the plasmid pOR26 suggests that the SCV environment is avoid of glucose. In summary, the combination of two functionally distinct bacterial reporter systems in one *Salmonella* reporter strain made it possible to monitor both bacterial replication and metabolic activity in one experimental run. The applicability of the reporter strain could be demonstrated conclusively in HeLa cells that had been depleted of Rab7A by siRNA transfection. The GFP intensity of infected cells after Rab7A siRNA treatment was about 30 % lower than in Allstars treated control cells at 16 h p.i. (see figure III.12.B). This indicated a moderate replication inhibition upon Rab7A depletion. However, the induction of mCherry after arabinose addition nearly completely failed in Rab7A treated cells as can be seen in figure III.12.D, suggesting that the majority of intracellular bacteria resided in a metabolic inactive state, most likely because the Rab7A knock down had a significantly deleterious effect on *Salmonella* survival. Alternatively, it is possible that the transport of arabinose to

the SCV was inhibited in the absence of the small GTPase Rab7A which is a central regulator of endosomal vesicle trafficking. This possibility can be excluded when taking into account the results from the gentamicin protection assay (see figure III.14). The quantification of bacterial replication using this method further demonstrated that the intracellular replication of *Salmonella* Typhimurium is significantly inhibited upon Rab7A knock down. This phenotype could be persuasively verified using the bichromatic reporter strain 12023 pOR25/26, making it an adequate tool for the global RNAi analysis approach.

In order to perform high-throughput RNAi screenings the *Salmonella* reporter strain assay had to be established in an appropriate experimental format. It was chosen to use the 96 well plate format which allows to conduct the screens with a considerable low amount of plates and in an acceptable time frame. The robustness of the 96 well plate assay had to be assured since it was crucial to generate primary data of high quality to minimize the amount of false positive or false negative host cell targets. In this context, especially the reliability of the semi-automatic FACS acquisition using the FACS Calibur with HTS supply was verified intensively. To do so, an adequate human tissue culture cell line had to be found. The FACS analysis of different cell lines that had been infected with the *Salmonella* Typhimurium reporter strain revealed remarkable differences with respect to the permissiveness to the bacterial infection. Although different epithelial cell lines are exerted for *in-vivo Salmonella* infection experiments, an integrated comparison with respect to invasion efficiency and replication capacity has not been reported yet. Therefore, the results from the respective studies conducted in this work should be able to give recommendations for the proper cell culture model for *Salmonella* infection. Hec1b is a cancer cell line derived from an endometrial adenocarcinoma (Kuramoto *et al.*, 1972). So far, no reports have been published concerning *Salmonella* infections with the cell line Hec1b. Also for HepG2, a liver carcinoma cell line (Aden *et al.*, 1979), no reports for the permissiveness to *Salmonella* infections are available. On the other hand, the colon cancer cell line HT-29 has been used casually as a model for polarized epithelial cells in *Salmonella* infection (Raffatellu *et al.*, 2005, Mellor *et al.*, 2009) and the cervix adenocarcinoma cell line HeLa is the standard epithelial cell culture model for *Salmonella* infections. Although these cell lines are all from the epithelial lineage they differed significantly in their permissiveness to *Salmonella* infection which became obvious from the visual analysis and the respective quantification of FACS experiments (see figure III.4). The initial invasion rate (i.e. the percentage of infected cells) was comparable for all cell lines except for HepG2, although the amount of entered bacteria was dramatically different, as could be shown with the GFP fluorescence. Since HepG2 cells tend to grow in colonies, thereby building up clumps of cells, if not seeded on plastic coated with extracellular matrix components, the access to these cells might have been aggravated, explaining the lower invasion rates. Additionally, the responsiveness to *Salmonella* triggered uptake mechanisms might have been variable in the different cell lines, explaining the varying amount of bacteria that entered the cells at an early time-point. With respect to bacterial replication, the observed differences between the cell lines were even more dramatic. The number of infected cells as well as the fluorescence intensities for both GFP and mCherry was significantly lower in HT-29 cells than in any other cell line tested. As the ability of the reporter strain to grow in these cells was very weak, HT-29 cells proofed to be an unsuitable cell line for further experiments. The same was true for HepG2 cells, where only weak infection parameters could be observed. The cell lines Hec1b and HEp-2 instead showed to be very permissive to *Salmonella* infections, because the invasion and replication parameters were comparable to those of HeLa cells. Nevertheless, the dot plot analysis of the mCherry fluorescence showed that two populations of infected cells had emerged, one

showing a good response to the arabinose trigger and another one that exhibited lower mCherry fluorescence intensities. This could argue for a heterogeneous infection process in these cells, probably also for an inherent heterogeneity among the cell lines, which also made these cell lines no proper infection models for the screening experiments. Therefore, the cell line HeLa was chosen for the subsequent experimental work, as it showed to be the best cell line for infections with the reporter strain.

Suitable infection conditions in the 96 well plate format using the HeLa cell line were determined employing different multiplicities of infection (MOI), i.e. the number of bacteria per host cell. It became obvious that high numbers of bacteria, while producing very good infection rates also provoked significantly high cell toxicity, most likely by triggering apoptotic and/or necrotic pathways of the host cell. A MOI of 20 was chosen for the screening experiments since the cell toxicity was tolerable and the invasion rate was about 50 %. Due to the fact that only every second host cell was infected, it had to be assured that the siRNA transfection prior to infection yielded a very high transfection rate to rule out the possibility that a considerable amount of non-transfected cells could be infected. This might lead to unstable phenotypes during the screen and probably also to more false-negative results. Therefore, the transfection conditions were adjusted to gain a very high transfection rate, which was estimated to be nearly 100 %, using the Qiagen Biorobot 8000 and a small amount of cells (approximately 3000) in 96 well format plates (Nikolaus Machuy, personal communication). The toxic siRNA control targeting the human polo-like kinase 1 (PLK1) served as a direct transfection control and the threshold was set to < 5 % cells detected compared to Allstars treated cells. This threshold was achieved in every experimental run, demonstrating adequate and reliable transfection conditions. Interestingly, the median GFP fluorescence intensity of infected cells was independent of the MOI that was applied for infection (see figure III.7.C). This was an unexpected finding as the number of infected cells was significantly dependent on the amount of bacteria used. The equal GFP intensity might have different reasons: The initial amount of bacteria that was taken up by the cells could be identical for every MOI, which would suggest that only a limited number of cellular “invasion platforms” do exist, resulting in an equal number of entering bacteria. However, the observed differing GFP intensities at early time-points for cells infected with varying MOIs would argue against this. Another possibility is that for every *Salmonella*-infected cell a critical number of intracellular bacteria is acceptable, a phenomenon likely to be controlled by the bacteria through a quorum-sensing like process, to prevent killing of the cell. This would then lead to an equal mean GFP fluorescence of infected cells with different MOIs.

Before performing the high-throughput RNAi screening experiments, a small inhibitor screen was conducted. Several antibiotics as well as inhibitors of host cell pathways were applied and the FACS assay was used in 96 well plate format to evaluate their impact on *Salmonella* replication. For most of the antibiotics and for some of the inhibitors a decrease in GFP as well as mCherry fluorescence could be observed with rising concentrations. Another important aspect of the assay is its capability to give information on cell toxicity, reflected by the number of detected cells. Therefore, this assay is also useful in screening experiments with small compound libraries to identify new compounds with antibacterial properties. These compounds could either directly target bacterial metabolism or indirectly inhibit bacterial growth by influencing important host cell pathways. The impact on host cell survival could also be evaluated which would give a first hint on the tolerance of new compounds.

After having evaluated the proper infection conditions and the overall stability of the assay, the RNAi screening was performed. Two siRNA libraries were employed, the SOS library and

the SKV library. The SOS library consisted of ten 96 well plates and the plates were allocated "in-house" with siRNAs of different biological functions, resulting in an only moderately functionally biased library. The SKV library was a commercially available library (Qiagen, Hilden;http://www1.qiagen.com/products/genesilencing/librarysirna/sirnasets/humanvalidatedkinase.aspx) covering the whole human kinome. The genes targeted by this library had been derived from experimental data or from theoretical predictions based on sequence similarities to known kinases. The SKV library was declared to be knock down proven, thus, the knock down efficiciency of all siRNAs of this set had been checked on mRNA levels by the company, although this was performed in different cell lines and no complete list of the results is available. Additionally, for every gene target two siRNA sequences were distributed on different plates to enable an easier pre-selection of "hits".

Kinases are central regulators of many cellular processes, such as cell division, apoptosis, cell development, or signaling and are therefore attractive targets for pathogens to reprogram the host cell. Hence, the main focus of the screening, the data analysis, the validation, and the follow-up work was put on the kinome-wide library. The accumulated primary data from both libraries was carefully analyzed statistically to be able to decide on candidates for validation. The comparison of the results from both libraries gave interesting indications for the quality of the libraries. First, the overall toxicity of all siRNA sequences from both libraries was evaluated. For this, data for the number of detected cells from at least triplicate values was normalized to Allstars and plotted in quantitative order (see figure III.16.B). It was observed that the SOS library had a significantly higher toxicity compared to the SKV library. Here, about 60 % of all test siRNAs resulted in a considerable cell loss (i.e. cell count < 0.4 compared to Allstars). In contrast, the SKV library contained only about 30 % of toxic siRNAs. Thus, in the case of the SOS library two thirds of all siRNAs were already excluded from further analysis because of their toxicity. This probably also removed potentially interesting host cell genes and therefore the quality of the SOS library could be reviewed as inadequate, at least under the conditions applied in this setting. The higher amount of toxic siRNAs in the SOS library compared to the SKV library could be founded in the fact that the siRNAs of the SOS set were designed a couple of years before the SKV sequences and at that time the experimental knowledge of the best possible siRNA sequence design to avoid toxicity and off-target effects was less than today. Additionally, the SOS library contains a lot of apoptosis related target genes or target genes involved in transcription and translation which are likely to have a dramatic negative survival effect when depleted. Nevertheless, the SOS screening had its relevance as a proof-of-principle screen to test all experimental steps of the assay under high-throughput conditions, even though the usefulness with respect to the identification of critical host cell factors has to be assessed as marginal.

Within the primary screen of the SKV more than 70 target sequences resulted in a phenotypic shift that was regarded as significant. Due to technical limitations, only 48 of them (the strongest candidates) were selected for further validation. Interestingly, for all of these candidates only one out of the two sequences yielded the phenotype, whereas the other either showed a significant cytotoxicity or generated no phenotypic change. Such a result was not expected since the supplier of the library had claimed that all siRNA sequences were knock down validated and therefore a phenotype, if specific to the gene knock down, was anticipated for both siRNAs. The rationale behind this result could be that the observed phenotypes were not specific to the gene knock down but were rather based on unspecific effects of the respective siRNA treatments (e.g. off-target effects), and therefore, most likely, would not be strong enough to remain during the validation rounds. Furthermore, the knock down efficiency of the siRNA sequences could have had a high

variation, although validated sequences were proposed for the library. Most likely, an interplay of both matters was responsible for the outcome of the primary SKV screening data. The primary, unvalidated SKV hit list contained kinases of several different functions, making it hard to speculate whether distinct host cell pathways were enriched (see figure III.19). Interestingly, the number of targets that resulted in an upregulation of the infection exceeded the inhibitory siRNAs. If one assumes an equal statistical detection accuracy for both phenotypes (up and down), this implies that the majority of host cell kinases rather have an inhibitory function towards *Salmonella* intracellular replication than a stimulatory one. Although enriched kinase pathways were not obvious among the primary SKV data, three targets that resulted in a down-regulation of the infection could be identified that are located in one functional pathway, namely MAP3K7, MAP3K7IP1, and MAP2K7. All of them are involved in the cellular response to pro-inflammatory cytokines and environmental stresses and lead to the activation of the effector kinase c-Jun N-terminal kinase (JNK) (Wang *et al.*, 2001, Tournier *et al.*, 1999). Although JNK itself did not emerge as a primary hit, these results could point to a role of the JNK pathway during *Salmonella* infection. JNK exists in three forms, JNK1, JNK2, and the neuronal-specific JNK3 (Bode *et al.*, 2007). JNK1 and JNK2 have distinct as well as overlapping functions and therefore, it might be possible that the function of one JNK isoform was substituted by another JNK species after the respective knock down. A closer look with regard to JNK1 revealed that both sequences caused no significant change of the infection phenotype. This would argue against a role of JNK1 itself but, nevertheless, JNK1 was considered to be an interesting candidate for later follow-up studies for which other siRNA sequences should be tested.

Surprisingly, the primary SKV candidate list did not contain any of the kinases or kinase related genes that were identified within a kinome-wide screen performed by Kuijl et al. (2007), published during the accomplishment of this work. This was probably due to different infection models since in the publication the breast cancer cell line MCF-7 and the *Salmonella* Typhimurium strain SL1344 were used. It was described that the histidine auxotroph strain SL1344 has a cell division defect in cell culture infections (Henry *et al.*, 2005) and therefore it might not be a suitable strain for these experiments. The pro-survival serine/threonine kinase Akt1 (Song *et al.*, 2005), also known as PKB was identified by Kuijl et al. as a central regulator of *Salmonella* replication inside epithelial cells. It was described that Akt1 is transiently phosphorylated at an early infection time and thereby inhibits apoptosis of infected epithelial cells (Knodler *et al.*, 2005a). It has to be noted, that the primary data that was provided by Kuijl and colleagues was not very well structured. Additionally, only the data from one out of three experimental runs can be inspected, and thereby it is difficult to comprehend why Akt1 was considered an important target for *Salmonella* infection because the inhibitory effect of Akt1 knockdown was only in a moderate range as compiled from the primary data list. In addition, it was reported that the data from the siRNA screening experiments could be confirmed with shRNA constructs targeting the human kinome. However, there was hardly any phenotypic change using any of these constructs, as provided within the supplementary information. Within the screen of my work, both sequences targeting Akt1 did not lead to a relevant phenotypic alteration of the infection. Moreover, one of the sequences caused significant cytotoxicity. This seems very plausible keeping in mind that Akt1 is a crucial anti-apoptotic factor and, indeed, the activity of Akt1 is increased in many forms of cancer (Altomare *et al.*, 2005). In order to verify the candidates presented by Kuijl et al., four siRNA sequences against all of the 14 published targets were purchased and tested with the FACS assay again (see table S.3). Using four different sequences for every target, there was no significant overlap between both data sets. Summing up, the

work of Kuijl et al. did not appear very convincing and thereby a comparison with the data generated within my kinome screen seemed to be very difficult.
48 candidate genes were nominated for further validation, among them 20 down-regulating targets and 28 which caused an increasing infection phenotype upon knock down. For each gene target four separate siRNA sequences were ordered and tested in 96 well plate format. During the validation 32 possible hits could not be confirmed (i.e. 75%) which was in accordance to experiences of others, showing that commonly only about 20% of primary hit candidates can be verified with solid validation experiments (Nikolaus Machuy, personal communication). The complete list of the remaining 16 targets together with their validation results can be seen in table III.2. Surprisingly, most of the factors showed an opposing phenotype in the primary screen and the validation round, which suggested that either the primary data or the data derived from the validation experiments was based on non-specific, but reproducible knock down effects. Only four of the validation targets (PGK1, MAP2K7, MKNK2, and MAP3K7) gave comparable results with more than two out of four siRNA sequences, which classified these factors as more interesting than the others. PGK1 showed the same phenotype in the primary screen and the validation during which all sequences gave comparable results. However, since PGK1 is a kinase involved in sugar breakdown it was suggested that this factor fulfils a housekeeping gene function and would therefore have an indirect influence on *Salmonella* growth. Hence, PGK1 was excluded from further analysis. MKNK2 and MAP3K7 showed opposing phenotypes in the primary screen and the validation and were therefore also not considered for follow-up experiments, leaving, at this stage, MAP2K7 as the most interesting factor. The depletion of MAP2K7 had an inhibitory impact on *Salmonella* intracellular replication in both the primary screen and the validation. Within the validation, three out of four siRNA sequences showed the same phenotype. Therefore, the role of MAP2K7 (also named MKK7) during *Salmonella* Typhimurium infection of epithelial cells was further investigated.
MKK7 belongs to the group of mitogen-activated protein kinases (MAPK) which are central regulators of diverse cellular processes like apoptosis, growth, differentiation, or inflammation. MAPKs transmit extracellular signals, e.g. from growth factors or apoptotic stimuli, in the form of a signaling cascades into the cell and shape a cellular response either by directly activating other regulatory proteins or by inducing specific transcriptional activities (Zhang *et al.*, 2007). MKK7 is mainly involved in the cellular response to pro-inflammatory cytokines and other environmental stresses. MKK7 can be activated by different upstream kinases, LZK (Ikeda *et al.*, 2001), MAP3K1 (Wu *et al.*, 1997), MAP3K4 (Abell *et al.*, 2007), DLK (Merritt *et al.*, 1999), and TAK1 (Hammaker *et al.*, 2007). Extracellular signals leading to MKK7 activation are mainly the pro-inflammatory cytokines IL-1 and TNF-α, transmitted via DLK and TAK1. Additionally, signals from growth factor receptors, forwarded via the Ras-Rac protein signaling pathway, are able to stimulate MKK7 (Foltz *et al.*, 1998). Once in an active state, MKK7 specifically induces JNK activity whereas the functionally related MAPK MKK4 is able to stimulate both JNK and p38, leading to a diversity of physiological outcomes that still have to be deciphered (Wang *et al.*, 2007). JNK, also named stress-activated protein kinase 1 (SAPK1) is able to activate several transcription factors. Among these are c-JUN, a component of the activator protein-1 (AP-1) complex which binds to specific promoter sites leading to transcription of several genes (Shaulian *et al.*, 2002) and ATF-2, a transcription factor binding both to AP-1 and cAMP response element promoter elements (Gupta *et al.*, 1995). In summary, JNK activation mainly leads to pro-inflammatory and apoptotic cell responses, but dependent on cell type and way of activation it is also important for cell differentiation and growth.

Salmonella Typhimurium activates JNK in infected cells which leads to the expression of the chemokine IL-8 (Hobbie *et al.*, 1997). It was reported that JNK together with the extracellular-regulated kinase (ERK), another member of the MAPK group, can stimulate the expression of cytosolic phospholipase A_2 α (cPLA2) (Van Putten *et al.*, 2001). Moreover, MAPKs are able to phosphorylate cPLA2, thereby enhancing its activity (Lin *et al.*, 1993, Borsch-Haubold *et al.*, 1998, Hefner *et al.*, 2000). PLA2 catalyzes the release of arachidonic acid (AA) from host cell membrane phospholipids which serves as an important second messenger for cellular stress pathways (Chakraborti, 2003). Interestingly, it was reported that the activation of cPLA2 is necessary for *Salmonella* invasion into epithelial cells (Pace *et al.*, 1993). This indicates that the activation of the MKK7-JNK-cPLA2 pathway might be involved in bacterial invasion. For another intracellular pathogen, *Chlamydia trachomatis,* it could be shown that the activity of cPLA2 is important for intracellular growth by providing free fatty acids metabolized by the intracellular bacteria (Su *et al.*, 2004). Intriguingly, *Salmonella* Typhimurium encodes an effector protein, SseJ, which is secreted into the host cell harbouring an enzymatic activity similar to cPLA2 (Lossi *et al.*, 2008) and a *sseJ* mutant is slightly attenuated in a mouse infection model (Ohlson *et al.*, 2005), implying that the deacylase activity is important for intracellular survival, probably by modulating the SCV membrane or by delivering fatty acids to the bacteria. Therefore, the role of cPLA2 and its possible regulation via the MKK7-JNK pathway during *Salmonella* infection was investigated in more detail in this work.

The inhibitory effect of MKK7 depletion on *Salmonella* replication was studied in more detail using both siRNA and shRNA mediated silencing strategies. With both knock down methods decreased replication rates could be observed, demonstrating that MKK7 is involved in the intracellular growth of *Salmonella* (figure III.21). The relatively mild level of about 40 % inhibition was maybe due to a subordinated importance of MKK7 for *Salmonella* growth. Most likely, the pronounced redundancy among kinases, and especially members of the MAP kinase pathways, could account for this. For example, MKK4 is also able to phosphorylate JNK (Lin *et al.*, 1995); thereby it could substitute MKK7 to some extent in MKK7 depleted cells. Interestingly, the mCherry expression of bacteria in MKK7 depleted cells was in a normal range, indicating that MKK7, unlike Rab7, does not play an essential role during *Salmonella* infection but rather contributes, among other factors, to bacterial replication.

The activation of cPLA2 during *Salmonella* infection of HeLa cells was determined by measuring the phosphorylation of cPLA2 and the enzymatic activity using a specific substrate. A very early phosphorylation of cPLA2 upon infection with *Salmonella* was observed. This phosphorylation was sustained over the whole infection period, indicating that cPLA2 was constantly active (figure III.22). Interestingly, this was also the case in the chloramphenicol treated sample, although on a lower level, which suggests that the cPLA2 activity was induced in a robust way during the first two hours of infection. This could have been mediated by a secreted bacterial factor which either targets cPLA2 itself, thereby keeping it in an activate state or by inhibiting a host cell factor which de-phosphorylates cPLA2. The chloramphenicol experiment also shows that bacterial replication is probably not absolutely necessary for the cPLA2 activation, again arguing for an early event. The early and sustained activation implies that the enzymatic activity of cPLA2 is necessary for the intracellular lifestyle of *Salmonella*. This assumption was further supported by the results from gentamicin protection assays in cPLA2 depleted cells. Here, a significant reduction of intracellular replication could be observed compared to infected control cells (figure III.23). When investigating the impact of MKK7 depletion on cPLA2 phosphorylation, it was

observed that total protein levels of cPLA2 but not the relative phosphorylation levels were reduced (figure III.24). This suggests that MKK7 is not a kinase for cPLA2 but does play a role in controlling cPLA2 protein turnover. A possible underlying mechanism could have been that MKK7 directly or indirectly influenced the protein stability of cPLA2, probably through a protein complex formation after stimulation. In this case, the depletion of MKK7 would de-stabilize cPLA2 and therefore target it for degradation pathways. A similar process has been described for inhibitor of apoptosis protein (IAP)-complexes (Rajalingam *et al.*, 2006). Alternatively, MKK7 could control cPLA2 levels at the transcriptional level by regulating the JNK-dependent expression of the cPLA2 gene (Van Putten *et al.*, 2001). A non-specific RNAi mediated degradation of cPLA2 mRNA after transfection with MKK7 siRNA seems unlikely since the effect was observed with two distinct MKK7 sequences. Moreover, sequence alignments revealed that there are only marginal matches of the MKK7 siRNA sequences inside the cPLA2 mRNA. Nevertheless, off-target mediated cPLA2 degradation cannot be ruled out totally. In order to test whether MKK7 and cPLA2 form a complex, co-immunoprecipitation experiments were performed using antibodies against both MKK7 and cPLA2 for pull-down. When the lysates were probed for cPLA2 and MKK7, no stable complex formation could be identified after infection with *Salmonella* (see figure III.25). The fact that an interaction could not be induced with either PMA or LPS, two distinct pro-inflammatory stimuli, argues against a possible MKK7 mediated stabilization of cPLA2 upon environmental stresses. Therefore, it was tested whether MKK7 controls cPLA2 at the level of transcription. HeLa cells were treated with different siRNAs against MKK7 or cPLA2 and three days later the relative amount of cPLA2 mRNA was quantified by RT-PCR. Interestingly, the MKK7-treated samples displayed lower cPLA2 mRNA levels (figure III.26). This was the case for both MKK7 sequences and the MKK7 sequence pool, making off-target effects of the MKK7 siRNAs unlikely. This result indicates that the knock down of MKK7 down-regulates the expression of cPLA2 (likely due to weaker JNK signaling activity), implying that the inhibitory impact of MKK7 depletion on *Salmonella* growth is rather an indirect than a direct one: The knock down of MKK7 negatively regulates the basal cPLA2 protein levels in the cells which negatively influences the bacterial intracellular growth.

The functional role of cPLA2 for *Salmonella* intracellular growth was ascertained further by comparing the structure and appearance of *Salmonella*-induced filaments (Sifs) in Allstars and cPLA2 siRNA treated cells. Sifs are formed along microtubules and are enriched in the lysosomal marker protein LAMP-1 (Garcia-del Portillo *et al.*, 1993, Brumell *et al.*, 2002). It has been reported that the formation of Sifs at early time-points of infection is a highly dynamic process with Sifs branching, extending, or contracting. At later time-points of infection Sifs seem to stabilize and form a regular network displaying a less dynamic behaviour which certainly indicates a form of final maturation step (Rajashekar *et al.*, 2008, Drecktrah *et al.*, 2008). Therefore, the structure of Sifs might give an indication about the successful accommodation of *Salmonella* inside its host cell. Interestingly, a large proportion of cPLA2 depleted cells infected with *Salmonella* Typhimurium showed needle-like, filiform Sif structures which could be immature, non-stable Sif elongations. These structures were only marginally seen in Allstars-treated cells. Here, robust Sifs with a thicker appearance dominated (figure III.27). This observation suggests that cPLA2 is involved in the correct maturation of Sifs. As mentioned earlier, *Salmonella* encodes an effector protein (SseJ) with similar function to cPLA2, and maybe these two proteins complement one another in their enzymatic properties to allow different lipid modifications of the Sif membrane which are crucial for the structural maturation of Sifs. Although it was not successful to immunostain

cPLA2 using two different antibodies, it could be possible that cPLA2 is recruited to the SCV membrane and to Sifs.
In summary, in this work it could be established that MKK7 controls cPLA2 at the transcriptional level and that cPLA2 is involved in *Salmonella* intracellular growth. This is likely mediated by its enzymatic activity towards membrane phospholipids which contributes to the correct formation of mature Sifs, a prerequisite of successful *Salmonella* replication.

Outlook

Within a kinome RNAi screen, the MAPK MKK7 was identified as an important factor in the replication of *Salmonella* Typhimurium inside human epithelial cells. The depletion of MKK7 from cells led not only to a reduction of bacterial replication but, moreover, to a significant decrease in cPLA2 mRNA levels and thereby to reduced protein levels. This pointed to a role of cPLA2 during *Salmonella* infection which, indeed, could be demonstrated with cPLA2 depleted cells. The precise role of cPLA2 during *Salmonella* infection could not be clarified but initial observations made during this work point to a role of cPLA2 in Sif formation. Hence, a cPLA2 mediated modification of the SCV and Sifs could be important for the integrity of the membrane or the elongation of Sifs and should be further investigated. In this context, the localisation cPLA2 in *Salmonella* infected HeLa cells would be of great interest and therefore ectopically expressed fluorescence-tagged cPLA2 would be useful. Additional studies with *Salmonella* mutant strains which are depleted of SseJ, an effector protein that possesses functions similar to that of cPLA2, might give further important insights into the process of Sif formation during *Salmonella* infection.
Also, the signaling pathways leading to a downregulation of cPLA2 expression upon MKK7 knock down have to be analyzed in more detail. It seems likely that cellular homeostasis pathways are altered upon MKK7 depletion. For example, the response to growth factors mediated by the Rac1-MEKK4/12-MKK7-JNK pathway could be affected. To evaluate this, specific knock down experiments should be helpful.
Since the bichromatic FACS assay proved to be a powerful tool for quantifying intracellular replication and metabolic fitness of *Salmonella* Typhimurium in different human cell lines, it is valuable for further investigations of cellular factors, such as small GTPases. Many of them (Rab proteins) are involved in endosomal trafficking processes which have been described to be important for *Salmonella* infection (Kuhle *et al.*, 2006, Drecktrah *et al.*, 2007). In order to gain a complete picture of essential host cell factors for *Salmonella* infection, a screening approach using a human whole genome siRNA library would be the best strategy. However, this brings about new experimental challenges. The large amount of siRNAs makes it necessary to work with a 384 well plate format which premises totally automated working processes. Additionally, the amount of data acquired during genome-wide screens dramatically exceeds the data sets of limited RNAi libraries. Therefore, a reliable way of automated analysis would have to be installed. Thus, whole-genome wide screens have to be established very robustly as there is nearly no possibility to manually evaluate the primary screening results.
It would also be very interesting to compare different intracellular pathogens with regard to the specific infection pathways that have evolved. In principal, a similar FACS assay should be feasible for other bacteria suppositional that plasmid-based reporter systems are accepted in respective pathogens.

Apart from the employment for RNAi screens, the assay established in this work can also be used for high-throughput compound screens to identify new antibacterial drugs. This has been performed on a small scale but should also be practicable on a larger dimension.

V REFERENCES

Abell, A.N., Granger, D.A. and Johnson, G.L. (2007). MEKK4 stimulation of p38 and JNK activity is negatively regulated by GSK3beta. *J Biol Chem* **282,** 30476-30484.

Aden, D.P., Fogel, A., Plotkin, S., Damjanov, I. and Knowles, B.B. (1979). Controlled synthesis of HBsAg in a differentiated human liver carcinoma-derived cell line. *Nature* **282,** 615-616.

Agaisse, H., Burrack, L.S., Philips, J.A., Rubin, E.J., Perrimon, N. and Higgins, D.E. (2005). Genome-wide RNAi screen for host factors required for intracellular bacterial infection. *Science* **309,** 1248-1251.

Akeda, Y. and Galan, J.E. (2005). Chaperone release and unfolding of substrates in type III secretion. *Nature* **437,** 911-915.

Akoh, C.C., Lee, G.C., Liaw, Y.C., Huang, T.H. and Shaw, J.F. (2004). GDSL family of serine esterases/lipases. *Prog Lipid Res* **43,** 534-552.

Althouse, C., Patterson, S., Fedorka-Cray, P. and Isaacson, R.E. (2003). Type 1 fimbriae of Salmonella enterica serovar Typhimurium bind to enterocytes and contribute to colonization of swine in vivo. *Infect Immun* **71,** 6446-6452.

Altomare, D.A. and Testa, J.R. (2005). Perturbations of the AKT signaling pathway in human cancer. *Oncogene* **24,** 7455-7464.

Andersen, J.B., Sternberg, C., Poulsen, L.K., Bjorn, S.P., Givskov, M. and Molin, S. (1998). New unstable variants of green fluorescent protein for studies of transient gene expression in bacteria. *Appl Environ Microbiol* **64,** 2240-2246.

Bajaj, V., Hwang, C. and Lee, C.A. (1995). hilA is a novel ompR/toxR family member that activates the expression of Salmonella typhimurium invasion genes. *Mol Microbiol* **18,** 715-727.

Bajaj, V., Lucas, R.L., Hwang, C. and Lee, C.A. (1996). Co-ordinate regulation of Salmonella typhimurium invasion genes by environmental and regulatory factors is mediated by control of hilA expression. *Mol Microbiol* **22,** 703-714.

Bakowski, M.A., Braun, V. and Brumell, J.H. (2008). Salmonella-containing vacuoles: directing traffic and nesting to grow. *Traffic* **9,** 2022-2031.

Bernstein, E., Caudy, A.A., Hammond, S.M. and Hannon, G.J. (2001). Role for a bidentate ribonuclease in the initiation step of RNA interference. *Nature* **409,** 363-366.

Beuzon, C.R., Meresse, S., Unsworth, K.E., Ruiz-Albert, J., Garvis, S., Waterman, S.R*., et al.* (2000). Salmonella maintains the integrity of its intracellular vacuole through the action of SifA. *EMBO J* **19,** 3235-3249.

Birmingham, C.L., Jiang, X., Ohlson, M.B., Miller, S.I. and Brumell, J.H. (2005). Salmonella-induced filament formation is a dynamic phenotype induced by rapidly replicating Salmonella enterica serovar typhimurium in epithelial cells. *Infect Immun* **73,** 1204-1208.

Boddicker, J.D., Ledeboer, N.A., Jagnow, J., Jones, B.D. and Clegg, S. (2002). Differential binding to and biofilm formation on, HEp-2 cells by Salmonella enterica serovar Typhimurium is dependent upon allelic variation in the fimH gene of the fim gene cluster. *Mol Microbiol* **45,** 1255-1265.

Bode, A.M. and Dong, Z. (2007). The functional contrariety of JNK. *Mol Carcinog* **46,** 591-598.

Borsch-Haubold, A.G., Bartoli, F., Asselin, J., Dudler, T., Kramer, R.M., Apitz-Castro, R*., et al.* (1998). Identification of the phosphorylation sites of cytosolic phospholipase A2 in agonist-stimulated human platelets and HeLa cells. *J Biol Chem* **273,** 4449-4458.

Boucrot, E., Beuzon, C.R., Holden, D.W., Gorvel, J.P. and Meresse, S. (2003). Salmonella typhimurium SifA effector protein requires its membrane-anchoring C-terminal hexapeptide for its biological function. *J Biol Chem* **278,** 14196-14202.

Boucrot, E., Henry, T., Borg, J.P., Gorvel, J.P. and Meresse, S. (2005). The intracellular fate of Salmonella depends on the recruitment of kinesin. *Science* **308,** 1174-1178.

Boyle, E.C., Brown, N.F. and Finlay, B.B. (2006). Salmonella enterica serovar Typhimurium effectors SopB, SopE, SopE2 and SipA disrupt tight junction structure and function. *Cell Microbiol* **8,** 1946-1957.

Bronstein, P.A., Miao, E.A. and Miller, S.I. (2000). InvB is a type III secretion chaperone specific for SspA. *J Bacteriol* **182,** 6638-6644.

Brumell, J.H., Goosney, D.L. and Finlay, B.B. (2002). SifA, a type III secreted effector of Salmonella typhimurium, directs Salmonella-induced filament (Sif) formation along microtubules. *Traffic* **3,** 407-415.

Brumell, J.H., Rosenberger, C.M., Gotto, G.T., Marcus, S.L. and Finlay, B.B. (2001a). SifA permits survival and replication of Salmonella typhimurium in murine macrophages. *Cell Microbiol* **3,** 75-84.

Brumell, J.H., Tang, P., Mills, S.D. and Finlay, B.B. (2001b). Characterization of Salmonella-induced filaments (Sifs) reveals a delayed interaction between Salmonella-containing vacuoles and late endocytic compartments. *Traffic* **2,** 643-653.

Brummelkamp, T.R., Bernards, R. and Agami, R. (2002). Stable suppression of tumorigenicity by virus-mediated RNA interference. *Cancer Cell* **2,** 243-247.

Cantalupo, G., Alifano, P., Roberti, V., Bruni, C.B. and Bucci, C. (2001). Rab-interacting lysosomal protein (RILP): the Rab7 effector required for transport to lysosomes. *EMBO J* **20,** 683-693.

Carlson, S.A., Omary, M.B. and Jones, B.D. (2002). Identification of cytokeratins as accessory mediators of Salmonella entry into eukaryotic cells. *Life Sci* **70,** 1415-1426.

Cerutti, L., Mian, N. and Bateman, A. (2000). Domains in gene silencing and cell differentiation proteins: the novel PAZ domain and redefinition of the Piwi domain. *Trends Biochem Sci* **25,** 481-482.

Chakraborti, S. (2003). Phospholipase A(2) isoforms: a perspective. *Cell Signal* **15,** 637-665.

Chamnongpol, S., Cromie, M. and Groisman, E.A. (2003). Mg2+ sensing by the Mg2+ sensor PhoQ of Salmonella enterica. *J Mol Biol* **325,** 795-807.

Chang, A.C. and Cohen, S.N. (1978). Construction and characterization of amplifiable multicopy DNA cloning vehicles derived from the P15A cryptic miniplasmid. *J Bacteriol* **134,** 1141-1156.

Chang, J., Myeni, S.K., Lin, T.L., Wu, C.C., Staiger, C.J. and Zhou, D. (2007). SipC multimerization promotes actin nucleation and contributes to Salmonella-induced inflammation. *Mol Microbiol* **66,** 1548-1556.

Chen, L.M., Hobbie, S. and Galan, J.E. (1996a). Requirement of CDC42 for Salmonella-induced cytoskeletal and nuclear responses. *Science* **274,** 2115-2118.

Chen, L.M., Kaniga, K. and Galan, J.E. (1996b). Salmonella spp. are cytotoxic for cultured macrophages. *Mol Microbiol* **21,** 1101-1115.

Collazo, C.M. and Galan, J.E. (1997). The invasion-associated type III system of Salmonella typhimurium directs the translocation of Sip proteins into the host cell. *Mol Microbiol* **24,** 747-756.

Cormack, B.P., Valdivia, R.H. and Falkow, S. (1996). FACS-optimized mutants of the green fluorescent protein (GFP). *Gene* **173,** 33-38.

Criss, A.K. and Casanova, J.E. (2003). Coordinate regulation of Salmonella enterica serovar Typhimurium invasion of epithelial cells by the Arp2/3 complex and Rho GTPases. *Infect Immun* **71,** 2885-2891.

Derre, I., Pypaert, M., Dautry-Varsat, A. and Agaisse, H. (2007). RNAi screen in Drosophila cells reveals the involvement of the Tom complex in Chlamydia infection. *PLoS Pathog* **3,** 1446-1458.

Drecktrah, D., Knodler, L.A., Howe, D. and Steele-Mortimer, O. (2007). Salmonella trafficking is defined by continuous dynamic interactions with the endolysosomal system. *Traffic* **8,** 212-225.

Drecktrah, D., Levine-Wilkinson, S., Dam, T., Winfree, S., Knodler, L.A., Schroer, T.A. and Steele-Mortimer, O. (2008). Dynamic behavior of Salmonella-induced membrane tubules in epithelial cells. *Traffic* **9,** 2117-2129.

Eckmann, L., Kagnoff, M.F. and Fierer, J. (1993). Epithelial cells secrete the chemokine interleukin-8 in response to bacterial entry. *Infect Immun* **61,** 4569-4574.

Eichelberg, K., Ginocchio, C.C. and Galan, J.E. (1994). Molecular and functional characterization of the Salmonella typhimurium invasion genes invB and invC: homology of InvC to the F0F1 ATPase family of proteins. *J Bacteriol* **176,** 4501-4510.

Elbashir, S.M., Harborth, J., Lendeckel, W., Yalcin, A., Weber, K. and Tuschl, T. (2001a). Duplexes of 21-nucleotide RNAs mediate RNA interference in cultured mammalian cells. *Nature* **411,** 494-498.

Elbashir, S.M., Lendeckel, W. and Tuschl, T. (2001b). RNA interference is mediated by 21- and 22-nucleotide RNAs. *Genes Dev* **15,** 188-200.

Elwell, C.A., Ceesay, A., Kim, J.H., Kalman, D. and Engel, J.N. (2008). RNA interference screen identifies Abl kinase and PDGFR signaling in Chlamydia trachomatis entry. *PLoS Pathog* **4,** e1000021.

Fink, S.L., Bergsbaken, T. and Cookson, B.T. (2008). Anthrax lethal toxin and Salmonella elicit the common cell death pathway of caspase-1-dependent pyroptosis via distinct mechanisms. *Proc Natl Acad Sci U S A* **105,** 4312-4317.

Fink, S.L. and Cookson, B.T. (2007). Pyroptosis and host cell death responses during Salmonella infection. *Cell Microbiol* **9,** 2562-2570.

Finlay, B.B. and Falkow, S. (1988). Comparison of the invasion strategies used by Salmonella cholerae-suis, Shigella flexneri and Yersinia enterocolitica to enter cultured animal cells: endosome acidification is not required for bacterial invasion or intracellular replication. *Biochimie* **70,** 1089-1099.

Finlay, B.B., Heffron, F. and Falkow, S. (1989). Epithelial cell surfaces induce Salmonella proteins required for bacterial adherence and invasion. *Science* **243,** 940-943.

Fire, A., Xu, S., Montgomery, M.K., Kostas, S.A., Driver, S.E. and Mello, C.C. (1998). Potent and specific genetic interference by double-stranded RNA in Caenorhabditis elegans. *Nature* **391,** 806-811.

Foltz, I.N., Gerl, R.E., Wieler, J.S., Luckach, M., Salmon, R.A. and Schrader, J.W. (1998). Human mitogen-activated protein kinase kinase 7 (MKK7) is a highly conserved c-Jun N-terminal kinase/stress-activated protein kinase (JNK/SAPK) activated by environmental stresses and physiological stimuli. *J Biol Chem* **273,** 9344-9351.

Forsberg, M., Blomgran, R., Lerm, M., Sarndahl, E., Sebti, S.M., Hamilton, A.*, et al.* (2003). Differential effects of invasion by and phagocytosis of Salmonella typhimurium on apoptosis in human macrophages: potential role of Rho-GTPases and Akt. *J Leukoc Biol* **74,** 620-629.

Fu, Y. and Galan, J.E. (1999). A salmonella protein antagonizes Rac-1 and Cdc42 to mediate host-cell recovery after bacterial invasion. *Nature* **401,** 293-297.

Galan, J.E. and Curtiss, R., 3rd (1989). Virulence and vaccine potential of phoP mutants of Salmonella typhimurium. *Microb Pathog* **6,** 433-443.

Garcia-del Portillo, F. and Finlay, B.B. (1995). Targeting of Salmonella typhimurium to vesicles containing lysosomal membrane glycoproteins bypasses compartments with mannose 6-phosphate receptors. *J Cell Biol* **129,** 81-97.

Garcia-del Portillo, F., Foster, J.W., Maguire, M.E. and Finlay, B.B. (1992). Characterization of the micro-environment of Salmonella typhimurium-containing vacuoles within MDCK epithelial cells. *Mol Microbiol* **6,** 3289-3297.

Garcia-del Portillo, F., Zwick, M.B., Leung, K.Y. and Finlay, B.B. (1993). Salmonella induces the formation of filamentous structures containing lysosomal membrane glycoproteins in epithelial cells. *Proc Natl Acad Sci U S A* **90,** 10544-10548.

Garcia Vescovi, E., Soncini, F.C. and Groisman, E.A. (1996). Mg2+ as an extracellular signal: environmental regulation of Salmonella virulence. *Cell* **84,** 165-174.

Ghigo, J.M. and Beckwith, J. (2000). Cell division in Escherichia coli: role of FtsL domains in septal localization, function, and oligomerization. *J Bacteriol* **182,** 116-129.

Gil, J. and Esteban, M. (2000). Induction of apoptosis by the dsRNA-dependent protein kinase (PKR): mechanism of action. *Apoptosis* **5,** 107-114.

Groisman, E.A. (2001). The pleiotropic two-component regulatory system PhoP-PhoQ. *J Bacteriol* **183,** 1835-1842.

Gupta, S., Campbell, D., Derijard, B. and Davis, R.J. (1995). Transcription factor ATF2 regulation by the JNK signal transduction pathway. *Science* **267,** 389-393.

Guy, R.L., Gonias, L.A. and Stein, M.A. (2000). Aggregation of host endosomes by Salmonella requires SPI2 translocation of SseFG and involves SpvR and the fms-aroE intragenic region. *Mol Microbiol* **37,** 1417-1435.

Guzman, L.M., Belin, D., Carson, M.J. and Beckwith, J. (1995). Tight regulation, modulation, and high-level expression by vectors containing the arabinose PBAD promoter. *J Bacteriol* **177,** 4121-4130.

Hammaker, D.R., Boyle, D.L., Inoue, T. and Firestein, G.S. (2007). Regulation of the JNK pathway by TGF-beta activated kinase 1 in rheumatoid arthritis synoviocytes. *Arthritis Res Ther* **9,** R57.

Hammond, S.M., Boettcher, S., Caudy, A.A., Kobayashi, R. and Hannon, G.J. (2001). Argonaute2, a link between genetic and biochemical analyses of RNAi. *Science* **293,** 1146-1150.

Hao, L., Sakurai, A., Watanabe, T., Sorensen, E., Nidom, C.A., Newton, M.A*., et al.* (2008). Drosophila RNAi screen identifies host genes important for influenza virus replication. *Nature* **454,** 890-893.

Haraga, A. and Miller, S.I. (2003). A Salmonella enterica serovar typhimurium translocated leucine-rich repeat effector protein inhibits NF-kappa B-dependent gene expression. *Infect Immun* **71,** 4052-4058.

Haraga, A. and Miller, S.I. (2006). A Salmonella type III secretion effector interacts with the mammalian serine/threonine protein kinase PKN1. *Cell Microbiol* **8,** 837-846.

Haraga, A., Ohlson, M.B. and Miller, S.I. (2008). Salmonellae interplay with host cells. *Nat Rev Microbiol* **6,** 53-66.

Hardt, W.D., Chen, L.M., Schuebel, K.E., Bustelo, X.R. and Galan, J.E. (1998). S. typhimurium encodes an activator of Rho GTPases that induces membrane ruffling and nuclear responses in host cells. *Cell* **93,** 815-826.

Hashim, S., Mukherjee, K., Raje, M., Basu, S.K. and Mukhopadhyay, A. (2000). Live Salmonella modulate expression of Rab proteins to persist in a specialized compartment and escape transport to lysosomes. *J Biol Chem* **275,** 16281-16288.

Hautefort, I., Thompson, A., Eriksson-Ygberg, S., Parker, M.L., Lucchini, S., Danino, V.*, et al.* (2008). During infection of epithelial cells Salmonella enterica serovar Typhimurium undergoes a time-dependent transcriptional adaptation that results in simultaneous expression of three type 3 secretion systems. *Cell Microbiol* **10,** 958-984.

Hayward, R.D., Cain, R.J., McGhie, E.J., Phillips, N., Garner, M.J. and Koronakis, V. (2005). Cholesterol binding by the bacterial type III translocon is essential for virulence effector delivery into mammalian cells. *Mol Microbiol* **56,** 590-603.

Hayward, R.D. and Koronakis, V. (1999). Direct nucleation and bundling of actin by the SipC protein of invasive Salmonella. *EMBO J* **18,** 4926-4934.

Hefner, Y., Borsch-Haubold, A.G., Murakami, M., Wilde, J.I., Pasquet, S., Schieltz, D.*, et al.* (2000). Serine 727 phosphorylation and activation of cytosolic phospholipase A2 by MNK1-related protein kinases. *J Biol Chem* **275,** 37542-37551.

Henry, T., Couillault, C., Rockenfeller, P., Boucrot, E., Dumont, A., Schroeder, N.*, et al.* (2006). The Salmonella effector protein PipB2 is a linker for kinesin-1. *Proc Natl Acad Sci U S A* **103,** 13497-13502.

Henry, T., Garcia-Del Portillo, F. and Gorvel, J.P. (2005). Identification of Salmonella functions critical for bacterial cell division within eukaryotic cells. *Mol Microbiol* **56,** 252-267.

Hernandez, L.D., Pypaert, M., Flavell, R.A. and Galan, J.E. (2003). A Salmonella protein causes macrophage cell death by inducing autophagy. *J Cell Biol* **163,** 1123-1131.

Hersh, D., Monack, D.M., Smith, M.R., Ghori, N., Falkow, S. and Zychlinsky, A. (1999). The Salmonella invasin SipB induces macrophage apoptosis by binding to caspase-1. *Proc Natl Acad Sci U S A* **96,** 2396-2401.

Himber, C., Dunoyer, P., Moissiard, G., Ritzenthaler, C. and Voinnet, O. (2003). Transitivity-dependent and -independent cell-to-cell movement of RNA silencing. *EMBO J* **22,** 4523-4533.

Hobbie, S., Chen, L.M., Davis, R.J. and Galan, J.E. (1997). Involvement of mitogen-activated protein kinase pathways in the nuclear responses and cytokine production induced by Salmonella typhimurium in cultured intestinal epithelial cells. *J Immunol* **159,** 5550-5559.

Hobert, M.E., Sands, K.A., Mrsny, R.J. and Madara, J.L. (2002). Cdc42 and Rac1 regulate late events in Salmonella typhimurium-induced interleukin-8 secretion from polarized epithelial cells. *J Biol Chem* **277,** 51025-51032.

Hutvagner, G. and Zamore, P.D. (2002). A microRNA in a multiple-turnover RNAi enzyme complex. *Science* **297,** 2056-2060.

Ikeda, A., Masaki, M., Kozutsumi, Y., Oka, S. and Kawasaki, T. (2001). Identification and characterization of functional domains in a mixed lineage kinase LZK. *FEBS Lett* **488,** 190-195.

Jones, G.W., Rabert, D.K., Svinarich, D.M. and Whitfield, H.J. (1982). Association of adhesive, invasive, and virulent phenotypes of Salmonella typhimurium with autonomous 60-megadalton plasmids. *Infect Immun* **38,** 476-486.

Jones, M.A., Wood, M.W., Mullan, P.B., Watson, P.R., Wallis, T.S. and Galyov, E.E. (1998). Secreted effector proteins of Salmonella dublin act in concert to induce enteritis. *Infect Immun* **66,** 5799-5804.

Jones, R.M., Wu, H., Wentworth, C., Luo, L., Collier-Hyams, L. and Neish, A.S. (2008). Salmonella AvrA Coordinates Suppression of Host Immune and Apoptotic Defenses via JNK Pathway Blockade. *Cell Host Microbe* **3,** 233-244.

Jordens, I., Fernandez-Borja, M., Marsman, M., Dusseljee, S., Janssen, L., Calafat, J.*, et al.* (2001). The Rab7 effector protein RILP controls lysosomal transport by inducing the recruitment of dynein-dynactin motors. *Curr Biol* **11,** 1680-1685.

Kamath, R.S., Fraser, A.G., Dong, Y., Poulin, G., Durbin, R., Gotta, M.*, et al.* (2003). Systematic functional analysis of the Caenorhabditis elegans genome using RNAi. *Nature* **421,** 231-237.

Kato, T., Jr., Gotoh, Y., Hoffmann, A. and Ono, Y. (2008). Negative regulation of constitutive NF-kappaB and JNK signaling by PKN1-mediated phosphorylation of TRAF1. *Genes Cells* **13,** 509-520.

Kerr, J.F., Wyllie, A.H. and Currie, A.R. (1972). Apoptosis: a basic biological phenomenon with wide-ranging implications in tissue kinetics. *Br J Cancer* **26,** 239-257.

Kiger, A.A., Baum, B., Jones, S., Jones, M.R., Coulson, A., Echeverri, C. and Perrimon, N. (2003). A functional genomic analysis of cell morphology using RNA interference. *J Biol* **2,** 27.

Kim, J.M., Eckmann, L., Savidge, T.C., Lowe, D.C., Witthoft, T. and Kagnoff, M.F. (1998). Apoptosis of human intestinal epithelial cells after bacterial invasion. *J Clin Invest* **102,** 1815-1823.

Kittler, R., Pelletier, L., Heninger, A.K., Slabicki, M., Theis, M., Miroslaw, L*., et al.* (2007). Genome-scale RNAi profiling of cell division in human tissue culture cells. *Nat Cell Biol* **9,** 1401-1412.

Knodler, L.A., Finlay, B.B. and Steele-Mortimer, O. (2005a). The Salmonella effector protein SopB protects epithelial cells from apoptosis by sustained activation of Akt. *J Biol Chem* **280,** 9058-9064.

Knodler, L.A. and Steele-Mortimer, O. (2005b). The Salmonella effector PipB2 affects late endosome/lysosome distribution to mediate Sif extension. *Mol Biol Cell* **16,** 4108-4123.

Krishnan, M.N., Ng, A., Sukumaran, B., Gilfoy, F.D., Uchil, P.D., Sultana, H*., et al.* (2008). RNA interference screen for human genes associated with West Nile virus infection. *Nature* **455,** 242-245.

Kroemer, G., Galluzzi, L., Vandenabeele, P., Abrams, J., Alnemri, E.S., Baehrecke, E.H*., et al.* (2009). Classification of cell death: recommendations of the Nomenclature Committee on Cell Death 2009. *Cell Death Differ* **16,** 3-11.

Kubori, T. and Galan, J.E. (2003). Temporal regulation of salmonella virulence effector function by proteasome-dependent protein degradation. *Cell* **115,** 333-342.

Kubori, T., Matsushima, Y., Nakamura, D., Uralil, J., Lara-Tejero, M., Sukhan, A*., et al.* (1998). Supramolecular structure of the Salmonella typhimurium type III protein secretion system. *Science* **280,** 602-605.

Kuhle, V., Abrahams, G.L. and Hensel, M. (2006). Intracellular Salmonella enterica redirect exocytic transport processes in a Salmonella pathogenicity island 2-dependent manner. *Traffic* **7,** 716-730.

Kuhle, V., Jackel, D. and Hensel, M. (2004). Effector proteins encoded by Salmonella pathogenicity island 2 interfere with the microtubule cytoskeleton after translocation into host cells. *Traffic* **5,** 356-370.

Kuijl, C., Savage, N.D., Marsman, M., Tuin, A.W., Janssen, L., Egan, D.A.*, et al.* (2007). Intracellular bacterial growth is controlled by a kinase network around PKB/AKT1. *Nature* **450,** 725-730.

Kuramoto, H., Tamura, S. and Notake, Y. (1972). Establishment of a cell line of human endometrial adenocarcinoma in vitro. *Am J Obstet Gynecol* **114,** 1012-1019.

Le Negrate, G., Faustin, B., Welsh, K., Loeffler, M., Krajewska, M., Hasegawa, P.*, et al.* (2008). Salmonella secreted factor L deubiquitinase of Salmonella typhimurium inhibits NF-kappaB, suppresses IkappaBalpha ubiquitination and modulates innate immune responses. *J Immunol* **180,** 5045-5056.

Lee, C.A., Jones, B.D. and Falkow, S. (1992). Identification of a Salmonella typhimurium invasion locus by selection for hyperinvasive mutants. *Proc Natl Acad Sci U S A* **89,** 1847-1851.

Lee, Y.S., Nakahara, K., Pham, J.W., Kim, K., He, Z., Sontheimer, E.J. and Carthew, R.W. (2004). Distinct roles for Drosophila Dicer-1 and Dicer-2 in the siRNA/miRNA silencing pathways. *Cell* **117,** 69-81.

Li, H., Xu, H., Zhou, Y., Zhang, J., Long, C., Li, S.*, et al.* (2007). The phosphothreonine lyase activity of a bacterial type III effector family. *Science* **315,** 1000-1003.

Lilic, M., Galkin, V.E., Orlova, A., VanLoock, M.S., Egelman, E.H. and Stebbins, C.E. (2003). Salmonella SipA polymerizes actin by stapling filaments with nonglobular protein arms. *Science* **301,** 1918-1921.

Lin, A., Minden, A., Martinetto, H., Claret, F.X., Lange-Carter, C., Mercurio, F.*, et al.* (1995). Identification of a dual specificity kinase that activates the Jun kinases and p38-Mpk2. *Science* **268,** 286-290.

Lin, L.L., Wartmann, M., Lin, A.Y., Knopf, J.L., Seth, A. and Davis, R.J. (1993). cPLA2 is phosphorylated and activated by MAP kinase. *Cell* **72,** 269-278.

Liu, Q., Rand, T.A., Kalidas, S., Du, F., Kim, H.E., Smith, D.P. and Wang, X. (2003). R2D2, a bridge between the initiation and effector steps of the Drosophila RNAi pathway. *Science* **301,** 1921-1925.

Loessner, H., Endmann, A., Leschner, S., Westphal, K., Rohde, M., Miloud, T.*, et al.* (2007). Remote control of tumour-targeted Salmonella enterica serovar Typhimurium by the use of L-arabinose as inducer of bacterial gene expression in vivo. *Cell Microbiol* **9,** 1529-1537.

Lossi, N.S., Rolhion, N., Magee, A.I., Boyle, C. and Holden, D.W. (2008). The Salmonella SPI-2 effector SseJ exhibits eukaryotic activator-dependent phospholipase A and glycerophospholipid : cholesterol acyltransferase activity. *Microbiology* **154,** 2680-2688.

Low, A.S., Dziva, F., Torres, A.G., Martinez, J.L., Rosser, T., Naylor, S.*, et al.* (2006). Cloning, expression, and characterization of fimbrial operon F9 from enterohemorrhagic Escherichia coli O157:H7. *Infect Immun* **74,** 2233-2244.

Lundberg, U., Vinatzer, U., Berdnik, D., von Gabain, A. and Baccarini, M. (1999). Growth phase-regulated induction of Salmonella-induced macrophage apoptosis correlates with transient expression of SPI-1 genes. *J Bacteriol* **181,** 3433-3437.

Ma, J.B., Ye, K. and Patel, D.J. (2004). Structural basis for overhang-specific small interfering RNA recognition by the PAZ domain. *Nature* **429,** 318-322.

Manche, L., Green, S.R., Schmedt, C. and Mathews, M.B. (1992). Interactions between double-stranded RNA regulators and the protein kinase DAI. *Mol Cell Biol* **12,** 5238-5248.

Marlovits, T.C., Kubori, T., Sukhan, A., Thomas, D.R., Galan, J.E. and Unger, V.M. (2004). Structural insights into the assembly of the type III secretion needle complex. *Science* **306,** 1040-1042.

Martin-Orozco, N., Touret, N., Zaharik, M.L., Park, E., Kopelman, R., Miller, S.*, et al.* (2006). Visualization of vacuolar acidification-induced transcription of genes of pathogens inside macrophages. *Mol Biol Cell* **17,** 498-510.

Martinez, J., Patkaniowska, A., Urlaub, H., Luhrmann, R. and Tuschl, T. (2002). Single-stranded antisense siRNAs guide target RNA cleavage in RNAi. *Cell* **110,** 563-574.

Mazurkiewicz, P., Thomas, J., Thompson, J.A., Liu, M., Arbibe, L., Sansonetti, P. and Holden, D.W. (2008). SpvC is a Salmonella effector with phosphothreonine lyase activity on host mitogen-activated protein kinases. *Mol Microbiol* **67,** 1371-1383.

McCaffrey, A.P., Nakai, H., Pandey, K., Huang, Z., Salazar, F.H., Xu, H.*, et al.* (2003). Inhibition of hepatitis B virus in mice by RNA interference. *Nat Biotechnol* **21,** 639-644.

McGhie, E.J., Hayward, R.D. and Koronakis, V. (2001). Cooperation between actin-binding proteins of invasive Salmonella: SipA potentiates SipC nucleation and bundling of actin. *EMBO J* **20,** 2131-2139.

Meister, G., Landthaler, M., Patkaniowska, A., Dorsett, Y., Teng, G. and Tuschl, T. (2004). Human Argonaute2 mediates RNA cleavage targeted by miRNAs and siRNAs. *Mol Cell* **15,** 185-197.

Mellor, G.E., Goulter, R.M., Chia, T.W. and Dykes, G.A. (2009). Comparative analysis of attachment of Shiga-toxigenic Escherichia coli and Salmonella strains to cultured HT-29 and Caco-2 cell lines. *Appl Environ Microbiol* **75,** 1796-1799.

Meresse, S., Steele-Mortimer, O., Finlay, B.B. and Gorvel, J.P. (1999). The rab7 GTPase controls the maturation of Salmonella typhimurium-containing vacuoles in HeLa cells. *EMBO J* **18,** 4394-4403.

Merritt, S.E., Mata, M., Nihalani, D., Zhu, C., Hu, X. and Holzman, L.B. (1999). The mixed lineage kinase DLK utilizes MKK7 and not MKK4 as substrate. *J Biol Chem* **274,** 10195-10202.

Metzlaff, M., O'Dell, M., Cluster, P.D. and Flavell, R.B. (1997). RNA-mediated RNA degradation and chalcone synthase A silencing in petunia. *Cell* **88,** 845-854.

Miao, E.A. and Miller, S.I. (2000). A conserved amino acid sequence directing intracellular type III secretion by Salmonella typhimurium. *Proc Natl Acad Sci U S A* **97,** 7539-7544.

Miller, S.I., Kukral, A.M. and Mekalanos, J.J. (1989). A two-component regulatory system (phoP phoQ) controls Salmonella typhimurium virulence. *Proc Natl Acad Sci U S A* **86,** 5054-5058.

Mills, I.G., Jones, A.T. and Clague, M.J. (1998). Involvement of the endosomal autoantigen EEA1 in homotypic fusion of early endosomes. *Curr Biol* **8,** 881-884.

Monack, D.M., Detweiler, C.S. and Falkow, S. (2001). Salmonella pathogenicity island 2-dependent macrophage death is mediated in part by the host cysteine protease caspase-1. *Cell Microbiol* **3,** 825-837.

Monack, D.M., Raupach, B., Hromockyj, A.E. and Falkow, S. (1996). Salmonella typhimurium invasion induces apoptosis in infected macrophages. *Proc Natl Acad Sci U S A* **93,** 9833-9838.

Napoli, C., Lemieux, C. and Jorgensen, R. (1990). Introduction of a Chimeric Chalcone Synthase Gene into Petunia Results in Reversible Co-Suppression of Homologous Genes in trans. *Plant Cell* **2,** 279-289.

Nawabi, P., Catron, D.M. and Haldar, K. (2008). Esterification of cholesterol by a type III secretion effector during intracellular Salmonella infection. *Mol Microbiol* **68,** 173-185.

Nykanen, A., Haley, B. and Zamore, P.D. (2001). ATP requirements and small interfering RNA structure in the RNA interference pathway. *Cell* **107,** 309-321.

Oates, A.C., Bruce, A.E. and Ho, R.K. (2000). Too much interference: injection of double-stranded RNA has nonspecific effects in the zebrafish embryo. *Dev Biol* **224,** 20-28.

Ohlson, M.B., Fluhr, K., Birmingham, C.L., Brumell, J.H. and Miller, S.I. (2005). SseJ deacylase activity by Salmonella enterica serovar Typhimurium promotes virulence in mice. *Infect Immun* **73,** 6249-6259.

Orban, T.I. and Izaurralde, E. (2005). Decay of mRNAs targeted by RISC requires XRN1, the Ski complex, and the exosome. *RNA* **11,** 459-469.

Orth, K., Palmer, L.E., Bao, Z.Q., Stewart, S., Rudolph, A.E., Bliska, J.B. and Dixon, J.E. (1999). Inhibition of the mitogen-activated protein kinase kinase superfamily by a Yersinia effector. *Science* **285,** 1920-1923.

Pace, J., Hayman, M.J. and Galan, J.E. (1993). Signal transduction and invasion of epithelial cells by S. typhimurium. *Cell* **72,** 505-514.

Palauqui, J.C., Elmayan, T., Pollien, J.M. and Vaucheret, H. (1997). Systemic acquired silencing: transgene-specific post-transcriptional silencing is transmitted by grafting from silenced stocks to non-silenced scions. *EMBO J* **16,** 4738-4745.

Park, W.S., Hayafune, M., Miyano-Kurosaki, N. and Takaku, H. (2003). Specific HIV-1 env gene silencing by small interfering RNAs in human peripheral blood mononuclear cells. *Gene Ther* **10,** 2046-2050.

Patel, J.C. and Galan, J.E. (2006). Differential activation and function of Rho GTPases during Salmonella-host cell interactions. *J Cell Biol* **175,** 453-463.

Philips, J.A., Rubin, E.J. and Perrimon, N. (2005). Drosophila RNAi screen reveals CD36 family member required for mycobacterial infection. *Science* **309,** 1251-1253.

Pier, G.B., Grout, M., Zaidi, T., Meluleni, G., Mueschenborn, S.S., Banting, G.*, et al.* (1998). Salmonella typhi uses CFTR to enter intestinal epithelial cells. *Nature* **393,** 79-82.

Provost, P., Dishart, D., Doucet, J., Frendewey, D., Samuelsson, B. and Radmark, O. (2002). Ribonuclease activity and RNA binding of recombinant human Dicer. *EMBO J* **21,** 5864-5874.

Prudencio, M., Rodrigues, C.D., Hannus, M., Martin, C., Real, E., Goncalves, L.A.*, et al.* (2008). Kinome-wide RNAi screen implicates at least 5 host hepatocyte kinases in Plasmodium sporozoite infection. *PLoS Pathog* **4,** e1000201.

Raffatellu, M., Wilson, R.P., Chessa, D., Andrews-Polymenis, H., Tran, Q.T., Lawhon, S.*, et al.* (2005). SipA, SopA, SopB, SopD, and SopE2 contribute to Salmonella enterica serotype typhimurium invasion of epithelial cells. *Infect Immun* **73,** 146-154.

Rajalingam, K., Sharma, M., Paland, N., Hurwitz, R., Thieck, O., Oswald, M.*, et al.* (2006). IAP-IAP complexes required for apoptosis resistance of C. trachomatis-infected cells. *PLoS Pathog* **2,** e114.

Rajashekar, R., Liebl, D., Seitz, A. and Hensel, M. (2008). Dynamic remodeling of the endosomal system during formation of Salmonella-induced filaments by intracellular Salmonella enterica. *Traffic* **9,** 2100-2116.

Randall, G., Panis, M., Cooper, J.D., Tellinghuisen, T.L., Sukhodolets, K.E., Pfeffer, S.*, et al.* (2007). Cellular cofactors affecting hepatitis C virus infection and replication. *Proc Natl Acad Sci U S A* **104,** 12884-12889.

Rathman, M., Sjaastad, M.D. and Falkow, S. (1996). Acidification of phagosomes containing Salmonella typhimurium in murine macrophages. *Infect Immun* **64,** 2765-2773.

Reinicke, A.T., Hutchinson, J.L., Magee, A.I., Mastroeni, P., Trowsdale, J. and Kelly, A.P. (2005). A Salmonella typhimurium effector protein SifA is modified by host cell prenylation and S-acylation machinery. *J Biol Chem* **280,** 14620-14627.

Rink, J., Ghigo, E., Kalaidzidis, Y. and Zerial, M. (2005). Rab conversion as a mechanism of progression from early to late endosomes. *Cell* **122,** 735-749.

Romano, N. and Macino, G. (1992). Quelling: transient inactivation of gene expression in Neurospora crassa by transformation with homologous sequences. *Mol Microbiol* **6,** 3343-3353.

Ruiz-Albert, J., Yu, X.J., Beuzon, C.R., Blakey, A.N., Galyov, E.E. and Holden, D.W. (2002). Complementary activities of SseJ and SifA regulate dynamics of the Salmonella typhimurium vacuolar membrane. *Mol Microbiol* **44,** 645-661.

Salcedo, S.P. and Holden, D.W. (2003). SseG, a virulence protein that targets Salmonella to the Golgi network. *EMBO J* **22,** 5003-5014.

Santos, R.L., Tsolis, R.M., Baumler, A.J., Smith, R., 3rd and Adams, L.G. (2001). Salmonella enterica serovar typhimurium induces cell death in bovine monocyte-derived macrophages by early sipB-dependent and delayed sipB-independent mechanisms. *Infect Immun* **69,** 2293-2301.

Scherer, C.A., Cooper, E. and Miller, S.I. (2000). The Salmonella type III secretion translocon protein SspC is inserted into the epithelial cell plasma membrane upon infection. *Mol Microbiol* **37,** 1133-1145.

Schwarz, D.S., Hutvagner, G., Du, T., Xu, Z., Aronin, N. and Zamore, P.D. (2003). Asymmetry in the assembly of the RNAi enzyme complex. *Cell* **115,** 199-208.

Scott, C.C., Cuellar-Mata, P., Matsuo, T., Davidson, H.W. and Grinstein, S. (2002). Role of 3-phosphoinositides in the maturation of Salmonella-containing vacuoles within host cells. *J Biol Chem* **277,** 12770-12776.

Shabalina, S.A. and Koonin, E.V. (2008). Origins and evolution of eukaryotic RNA interference. *Trends Ecol Evol* **23,** 578-587.

Shaner, N.C., Campbell, R.E., Steinbach, P.A., Giepmans, B.N., Palmer, A.E. and Tsien, R.Y. (2004). Improved monomeric red, orange and yellow fluorescent proteins derived from Discosoma sp. red fluorescent protein. *Nat Biotechnol* **22,** 1567-1572.

Shaulian, E. and Karin, M. (2002). AP-1 as a regulator of cell life and death. *Nat Cell Biol* **4,** E131-136.

Shea, J.E., Hensel, M., Gleeson, C. and Holden, D.W. (1996). Identification of a virulence locus encoding a second type III secretion system in Salmonella typhimurium. *Proc Natl Acad Sci U S A* **93,** 2593-2597.

Shi, J., Scita, G. and Casanova, J.E. (2005). WAVE2 signaling mediates invasion of polarized epithelial cells by Salmonella typhimurium. *J Biol Chem* **280,** 29849-29855.

Smith, A.C., Cirulis, J.T., Casanova, J.E., Scidmore, M.A. and Brumell, J.H. (2005). Interaction of the Salmonella-containing vacuole with the endocytic recycling system. *J Biol Chem* **280,** 24634-24641.

Song, G., Ouyang, G. and Bao, S. (2005). The activation of Akt/PKB signaling pathway and cell survival. *J Cell Mol Med* **9,** 59-71.

Song, J.J., Liu, J., Tolia, N.H., Schneiderman, J., Smith, S.K., Martienssen, R.A*., et al.* (2003). The crystal structure of the Argonaute2 PAZ domain reveals an RNA binding motif in RNAi effector complexes. *Nat Struct Biol* **10,** 1026-1032.

Song, J.J., Smith, S.K., Hannon, G.J. and Joshua-Tor, L. (2004). Crystal structure of Argonaute and its implications for RISC slicer activity. *Science* **305,** 1434-1437.

Steele-Mortimer, O., Meresse, S., Gorvel, J.P., Toh, B.H. and Finlay, B.B. (1999). Biogenesis of Salmonella typhimurium-containing vacuoles in epithelial cells involves interactions with the early endocytic pathway. *Cell Microbiol* **1,** 33-49.

Stein, M.A., Leung, K.Y., Zwick, M., Garcia-del Portillo, F. and Finlay, B.B. (1996). Identification of a Salmonella virulence gene required for formation of filamentous structures containing lysosomal membrane glycoproteins within epithelial cells. *Mol Microbiol* **20,** 151-164.

Stender, S., Friebel, A., Linder, S., Rohde, M., Mirold, S. and Hardt, W.D. (2000). Identification of SopE2 from Salmonella typhimurium, a conserved guanine nucleotide exchange factor for Cdc42 of the host cell. *Mol Microbiol* **36,** 1206-1221.

Su, H., McClarty, G., Dong, F., Hatch, G.M., Pan, Z.K. and Zhong, G. (2004). Activation of Raf/MEK/ERK/cPLA2 signaling pathway is essential for chlamydial acquisition of host glycerophospholipids. *J Biol Chem* **279,** 9409-9416.

Tahbaz, N., Kolb, F.A., Zhang, H., Jaronczyk, K., Filipowicz, W. and Hobman, T.C. (2004). Characterization of the interactions between mammalian PAZ PIWI domain proteins and Dicer. *EMBO Rep* **5,** 189-194.

Tallant, T., Deb, A., Kar, N., Lupica, J., de Veer, M.J. and DiDonato, J.A. (2004). Flagellin acting via TLR5 is the major activator of key signaling pathways leading to NF-kappa B and proinflammatory gene program activation in intestinal epithelial cells. *BMC Microbiol* **4,** 33.

Terebiznik, M.R., Vieira, O.V., Marcus, S.L., Slade, A., Yip, C.M., Trimble, W.S*., et al.* (2002). Elimination of host cell PtdIns(4,5)P(2) by bacterial SigD promotes membrane fission during invasion by Salmonella. *Nat Cell Biol* **4,** 766-773.

Thone, F., Schwanhausser, B., Becker, D., Ballmaier, M. and Bumann, D. (2007). FACS-isolation of Salmonella-infected cells with defined bacterial load from mouse spleen. *J Microbiol Methods* **71,** 220-224.

Timmons, L. and Fire, A. (1998). Specific interference by ingested dsRNA. *Nature* **395,** 854.

Tindall, B.J., Grimont, P.A., Garrity, G.M. and Euzeby, J.P. (2005). Nomenclature and taxonomy of the genus Salmonella. *Int J Syst Evol Microbiol* **55,** 521-524.

Tournier, C., Whitmarsh, A.J., Cavanagh, J., Barrett, T. and Davis, R.J. (1997). Mitogen-activated protein kinase kinase 7 is an activator of the c-Jun NH2-terminal kinase. *Proc Natl Acad Sci U S A* **94,** 7337-7342.

Tournier, C., Whitmarsh, A.J., Cavanagh, J., Barrett, T. and Davis, R.J. (1999). The MKK7 gene encodes a group of c-Jun NH2-terminal kinase kinases. *Mol Cell Biol* **19,** 1569-1581.

Tucker, S.C. and Galan, J.E. (2000). Complex function for SicA, a Salmonella enterica serovar typhimurium type III secretion-associated chaperone. *J Bacteriol* **182,** 2262-2268.

Tuschl, T., Zamore, P.D., Lehmann, R., Bartel, D.P. and Sharp, P.A. (1999). Targeted mRNA degradation by double-stranded RNA in vitro. *Genes Dev* **13,** 3191-3197.

Unsworth, K.E., Way, M., McNiven, M., Machesky, L. and Holden, D.W. (2004). Analysis of the mechanisms of Salmonella-induced actin assembly during invasion of host cells and intracellular replication. *Cell Microbiol* **6,** 1041-1055.

Valdivia, R.H. and Falkow, S. (1996). Bacterial genetics by flow cytometry: rapid isolation of Salmonella typhimurium acid-inducible promoters by differential fluorescence induction. *Mol Microbiol* **22,** 367-378.

Van Putten, V., Refaat, Z., Dessev, C., Blaine, S., Wick, M., Butterfield, L.*, et al.* (2001). Induction of cytosolic phospholipase A2 by oncogenic Ras is mediated through the JNK and ERK pathways in rat epithelial cells. *J Biol Chem* **276,** 1226-1232.

Vigne, S., Duraffour, S., Andrei, G., Snoeck, R., Garin, D. and Crance, J.M. (2009). Inhibition of vaccinia virus replication by two siRNAs targeting B1R and G7L genes and their synergistic combination with cidofovir. *Antimicrob Agents Chemother*.

Wang, C., Deng, L., Hong, M., Akkaraju, G.R., Inoue, J. and Chen, Z.J. (2001). TAK1 is a ubiquitin-dependent kinase of MKK and IKK. *Nature* **412,** 346-351.

Wang, X., Destrument, A. and Tournier, C. (2007). Physiological roles of MKK4 and MKK7: insights from animal models. *Biochim Biophys Acta* **1773,** 1349-1357.

Wu, Z., Wu, J., Jacinto, E. and Karin, M. (1997). Molecular cloning and characterization of human JNKK2, a novel Jun NH2-terminal kinase-specific kinase. *Mol Cell Biol* **17,** 7407-7416.

Xie, Z., Johansen, L.K., Gustafson, A.M., Kasschau, K.D., Lellis, A.D., Zilberman, D.*, et al.* (2004). Genetic and functional diversification of small RNA pathways in plants. *PLoS Biol* **2,** E104.

Yang, D., Buchholz, F., Huang, Z., Goga, A., Chen, C.Y., Brodsky, F.M. and Bishop, J.M. (2002). Short RNA duplexes produced by hydrolysis with Escherichia coli RNase III mediate effective RNA interference in mammalian cells. *Proc Natl Acad Sci U S A* **99,** 9942-9947.

Zamore, P.D., Tuschl, T., Sharp, P.A. and Bartel, D.P. (2000). RNAi: double-stranded RNA directs the ATP-dependent cleavage of mRNA at 21 to 23 nucleotide intervals. *Cell* **101,** 25-33.

Zhang, H., Kolb, F.A., Brondani, V., Billy, E. and Filipowicz, W. (2002). Human Dicer preferentially cleaves dsRNAs at their termini without a requirement for ATP. *EMBO J* **21,** 5875-5885.

Zhang, Y. and Dong, C. (2007). Regulatory mechanisms of mitogen-activated kinase signaling. *Cell Mol Life Sci* **64,** 2771-2789.

Zhou, D., Mooseker, M.S. and Galan, J.E. (1999). Role of the S. typhimurium actin-binding protein SipA in bacterial internalization. *Science* **283,** 2092-2095.

Zhou, K., He, H., Wu, Y. and Duan, M. (2008). RNA interference of avian influenza virus H5N1 by inhibiting viral mRNA with siRNA expression plasmids. *J Biotechnol* **135,** 140-144.

VI Acknowledgement

Prof. Dr. Thomas Meyer for the great opportunity to perform the experimental work for my doctoral thesis in an excellently equipped laboratory within a very good scientific environment and his permanent and supportive interest in my project

Dr. Nikolaus Machuy for helping me with all RNA interference issues and for structural suggestions during the assay development

Dr. Dagmar Heuer for good scientific discussions and some ideas for follow-up experiments; unfortunately time was limited

Current and former members of the lab 2.47 and the office 2.38, especially Bianca, Manuel, Malvika, Jura, Manuela, Andi and Munir for endless chats (about science and life) and a lot of fun

Jörg and Anja for technical assistance

All other colleagues of the department

Björn and Kalle for Mini Bar, West Germany, Cake, Privatclub evenings; always a good way of recreation

My parents, who most likely don't have a clue of what I was doing the last years inside this building but certainly have their share in paving the way

Most of all, I want to express my greatest thankfulness to Linda. Her love, faith, patience, **(comma!)** and scientific expertise are of inestimable value for everything that was and everything still to come. You are the lady in my life!

VII SUPPLEMENTARY INFORMATION

VII.1 Curriculum vitae

VII.2 Publications

Riede, O., Heuer, D., Machuy, N., Meyer, T.F. „Kinome-wide RNAi screen identifies MKK7 dependent regulation of *Salmonella* replication by controlling cPLA2 levels" (in preparation)

VII.3 Talks and posters

2009 **1st Joint Congress of the Swiss and German Societies of Cell Biology, Konstanz.**
"Global analysis of host cell functions affecting *Salmonella* intracellular growth." (Poster)

2008 **Symposium „Fachgruppe Mikrobielle Pathogenität", Bad Urach.**
„Global analysis of host cell factors essential for intracellular growth of *Salmonella* Typhimurium." (Oral presentation)

2007 **Fourth Annual EIMID Meeting, Norton Park, UK.**
"Bichromatic flow cytometry high-throughput assay for quantifying bacterial intracellular survival." (Poster)

VII.4 Supplementary data

Figure S.1: 96 well plate scheme

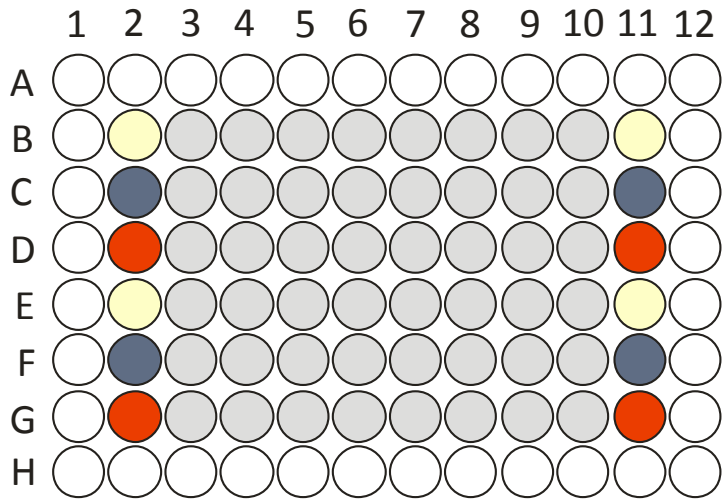

Figure S.1: 96 well plate scheme for automatic transfections.
The scheme shows the general allocation of 96 well plates for the automatic siRNA transfections. The outer wells (white) were left untreated due to observed unsual cell growth behaviour but filled with medium as well. The controls were pipetted into the outer columns (B2-G2 and B11-G11) of the 60 analysis wells and the siRNAs to test were transferred into the 48 wells coloured in grey (B3-G10) according to the order they were allocated in the transfection plates. Controls were: Allstars (yellow), PLK1 (blue) and Rab7A_2 (red).

Table S.1: Complete list of kinase library screening results in quantitative order

Target gene	Gene ID	plate	pos.	sequence name	siRNA sequence	Mean cells	SD cells	phenotype	Mean inh.	SD inh.	phenotype	Sign. inh.
AK1	203	SKV_08	E07	Hs_AK1_5	CCGGGATGCCATGGTGGCCAA	0,47	0,41	OK	2,27	2,00	DOWN	0,121098
PSKH1	5681	SKV_06	D07	Hs_PSKH1_5	CCCGATTAGGGTCGAGTGTCA	0,08	0,05	TOXIC	2,03	0,67	DOWN	0,006342
ADRBK1	156	SKV_01	B03	Hs_ADRBK1_1	CCGGGAGATCTTCGACTCATA	0,15	0,05	TOXIC	1,79	0,27	DOWN	0,000336
GRK4	2868	SKV_02	F08	Hs_GRK4_5	CAGGATGTTACTCACCAAGAA	0,05	0,05	TOXIC	1,72	1,18	DOWN	0,065402
ATM	472	SKV_03	G06	Hs_ATM_9	TTGGCTTATACGCGCAGTGTA	0,27	0,08	TOXIC	1,64	0,13	DOWN	0,000028
AKT2	208	SKV_01	B06	Hs_AKT2_7	ACGGGCTAAAGTGACCATGAA	0,15	0,08	TOXIC	1,64	0,47	DOWN	0,003877
ROCK2	9475	SKV_01	G03	Hs_ROCK2_6	ATGCACTTGTATAAAGCCATA	0,45	0,21	OK	1,59	0,45	DOWN	0,003730
PDK4	5166	SKV_04	B03	Hs_PDK4_6	CAGATGCTATCATCTACTTAA	0,08	0,03	TOXIC	1,57	0,34	DOWN	0,001343
TSSK1B	83942	SKV_05	D07	Hs_STK22D_4	CCAGCTTTCCTTGGCCATCAA	0,17	0,02	TOXIC	1,47	0,15	DOWN	0,000067
TNIK	23043	SKV_18	G09	Hs_TNIK_5	AAGGACCATATTGATAGAACA	0,42	0,55	OK	1,44	1,39	DOWN	0,085831
DMPK	1760	SKV_01	B07	Hs_DMPK_5	AACCAGAACTTCGCCAGTCAA	0,09	0,12	TOXIC	1,30	1,63	DOWN	0,237810
RPS6KA6	27330	SKV_02	B07	Hs_RPS6KA6_5	CAGCGGTATACTGCTGAACAA	0,08	0,05	TOXIC	1,29	0,39	DOWN	0,004491
PRKAB1	5564	SKV_01	C05	Hs_PRKAB1_5	CACGTCTAGAAGTCACATGAA	0,10	0,11	TOXIC	1,28	0,86	DOWN	0,061159
GRK4	2868	SKV_01	B08	Hs_GRK4_6	CCGGGTGTTTCAAAGACATCA	0,26	0,23	TOXIC	1,27	0,39	DOWN	0,005045
FLT4	2324	SKV_21	D07	Hs_FLT4_9	CACGCTCTTGGTCAACAGGAA	0,15	0,09	TOXIC	1,26	0,32	DOWN	0,000204
PIK3CD	5293	SKV_15	E10	Hs_PIK3CD_5	CCGGTCACGCATGAAGGCAAA	0,14	0,08	TOXIC	1,26	0,66	DOWN	0,002669
LATS2	26524	SKV_03	F05	Hs_LATS2_8	AAGGATGTCCTGAACCGGAAT	0,61	0,06	OK	1,26	0,13	DOWN	0,000080
PDPK1	5170	SKV_01	C04	Hs_PDPK1_8	AAGCGGTTAGGCTGTGAGGAA	0,15	0,19	TOXIC	1,23	0,35	DOWN	0,003798
CDK2	1017	SKV_07	E04	Hs_CDK2_8	CAGGTTATATCCAATAGTAGA	0,80	0,69	OK	1,23	2,63	DOWN	0,463503
AKT1	207	SKV_02	F05	Hs_AKT1_8	ACGCTACTTCCTCCTCAAGAA	0,37	0,19	TOXIC	1,23	0,21	DOWN	0,000495
STK32C	282974	SKV_02	C05	Hs_STK32C_5	CCGGGCTTCGTGCCCAACAAA	0,05	0,03	TOXIC	1,21	1,22	DOWN	0,162570
CDC42BPA	8476	SKV_01	F07	Hs_CDC42BPA_6	CAGACTTTCCGTAGCAGCTTA	0,16	0,15	TOXIC	1,17	1,30	DOWN	0,195497
PKN1	5585	SKV_03	B10	Hs_PKN1_6	CCGCAAGGAGCTGAAGCTGAA	0,17	0,27	TOXIC	1,16	1,47	DOWN	0,242949
PRKACA	5566	SKV_01	C07	Hs_PRKACA_5	CAAGGACAACTCAAACTTATA	0,26	0,31	TOXIC	1,16	1,98	DOWN	0,367669
FGFR4	2264	SKV_24	B05	Hs_FGFR4_5	CCGCCTGACCTTCGGACCCTA	0,13	0,03	TOXIC	1,16	0,75	DOWN	0,055711
AKAP3	10566	SKV_16	B06	Hs_AKAP3_6	CCCATTGTAGGTGACCAAGAA	0,05	0,01	TOXIC	1,15	0,57	DOWN	0,002087
GAK	2580	SKV_17	B07	Hs_GAK_6	CCCGTGGTTGTCTGTACAGAA	0,03	0,01	TOXIC	1,13	0,86	DOWN	0,038491
HIPK3	10114	SKV_10	B04	Hs_HIPK3_6	CTCATTCTGGTTGGAGATTAA	0,21	0,11	TOXIC	1,10	0,35	DOWN	0,005471
MKNK2	2872	SKV_06	C04	Hs_MKNK2_15	CAGCCAGGAGTACGCCGTCAA	0,54	0,49	OK	1,10	0,21	DOWN	0,000854
PRKACB	5567	SKV_02	G08	Hs_PRKACB_10	CTGACCAATCAAGTACACTAA	0,19	0,13	TOXIC	1,10	0,38	DOWN	0,007571
PNCK	139728	SKV_07	C03	Hs_PNCK_2	CACGCCCTTTGAGGACTCGAA	0,29	0,12	TOXIC	1,09	0,42	DOWN	0,010639
IKBKG	8517	SKV_15	G05	Hs_IKBKG_5	CTCCTCTAGTTCAGAGACATA	0,06	0,04	TOXIC	1,08	0,97	DOWN	0,038911
TSKS	60385	SKV_16	E05	Hs_TSKS_6	CACCAACGTGTCACTGCTCAA	0,25	0,11	TOXIC	1,08	0,17	DOWN	0,000001
LATS2	26524	SKV_02	B05	Hs_LATS2_7	CTCCGCAAAGGGTACACTCAA	0,13	0,04	TOXIC	1,07	0,12	DOWN	0,000104
CAMK1	8536	SKV_06	D10	Hs_CAMK1_6	CTGCATGACCTGGGCATTGTA	0,35	0,12	TOXIC	1,06	0,13	DOWN	0,000130

Target gene	Gene ID	plate	pos.	sequence name	siRNA sequence	Mean cells	SD cells	phenotype	Mean inh.	SD inh.	phenotype	Sign. inh.
PLK3	1263	SKV_15	C10	Hs_PLK3_5	CAGAAAGACTGTGCACTACAA	0,12	0,05	TOXIC	1,06	0,52	DOWN	0,003056
ADCK2	90956	SKV_04	C10	Hs_ADCK2_5	CCGGAATGTGAAAGCCGTCAA	0,62	0,15	OK	1,05	0,15	DOWN	0,000237
MAPKAPK2	9261	SKV_04	G07	Hs_MAPKAPK2_6	CGCCATCATCGATGACTACAA	0,27	0,08	TOXIC	1,05	0,40	DOWN	0,010413
ALS2CR7	65061	SKV_08	E03	Hs_ALS2CR7_6	CTGGCGTACATCCACCACCAA	0,26	0,18	TOXIC	1,05	0,46	DOWN	0,016700
DGKB	1607	SKV_08	G03	Hs_DGKB_9	CCCGAACTACTTCTCCTGCAA	0,07	0,01	TOXIC	1,04	0,26	DOWN	0,002407
CDK2	1017	SKV_05	G04	Hs_CDK2_7	CACGTACGGAGTTGTGTACAA	0,07	0,03	TOXIC	1,03	0,62	DOWN	0,043652
PRKCH	5583	SKV_01	D08	Hs_PRKCH_5	CGCCGTGTGCTCATCACTGAA	0,54	0,30	OK	1,02	0,25	DOWN	0,002166
ATM	472	SKV_02	C06	Hs_ATM_8	AACCATGAGTCTAGTACTTAA	0,13	0,12	TOXIC	1,01	0,45	DOWN	0,017578
MAST1	22983	SKV_01	G09	Hs_MAST1_6	CAGTATGTTCCGCCGCACCAA	0,17	0,08	TOXIC	1,00	0,63	DOWN	0,050761
KHK	3795	SKV_09	B09	Hs_KHK_6	TAGCCGCACCATCCTATACTA	0,16	0,14	TOXIC	0,99	1,45	DOWN	0,301977
IRAK2	3656	SKV_24	B08	Hs_IRAK2_6	CCAGATCATCCTGAACTGGAA	0,45	0,02	OK	0,98	0,58	DOWN	0,043250
RIOK3	8780	SKV_04	B06	Hs_RIOK3_6	CTGGCTGTATTAGTACAGGAA	0,05	0,02	TOXIC	0,98	0,26	DOWN	0,002798
ULK2	9706	SKV_19	D03	Hs_ULK2_4	TAGGATAATCGGTACAGTTAT	0,19	0,11	TOXIC	0,95	0,34	DOWN	0,001284
SGK2	10110	SKV_01	G06	Hs_SGK2_10	TGGGTACGTGACTATCCCTAA	0,03	0,03	TOXIC	0,95	1,05	DOWN	0,190905
PI4KA	5297	SKV_25	D05	Hs_PIK4CA_10	TCCGGACGCCATCCTCTTCTA	0,30	0,02	TOXIC	0,95	0,43	DOWN	0,019613
MAP2K7	5609	SKV_20	C07	Hs_MAP2K7_13	CTGCGCTGAGAAGCTCAAGAA	0,40	0,06	OK	0,94	0,04	DOWN	0,000000
AATK	9625	SKV_22	B09	Hs_AATK_5	TCCGCTGAGATCAGAAGGCAA	0,07	0,02	TOXIC	0,91	0,75	DOWN	0,104372
FGFR3	2261	SKV_23	B03	Hs_FGFR3_5	ACCCTACGTTACCGTGCTCAA	0,44	0,04	OK	0,91	0,05	DOWN	0,000007
WNK4	65266	SKV_19	F05	Hs_WNK4_10	CTGCCAAGAGTCAACCACTAA	0,16	0,06	TOXIC	0,90	0,18	DOWN	0,000136
PDXK	8566	SKV_18	B09	Hs_PDXK_5	GAGGCTGAACAACATGAATAA	0,21	0,10	TOXIC	0,89	0,19	DOWN	0,000076
PKMYT1	9088	SKV_15	G07	Hs_PKMYT1_3	CTGGGAGGAACTTACCGTCTA	0,25	0,18	TOXIC	0,89	0,21	DOWN	0,000026
TAOK3	51347	SKV_20	F03	Hs_TAOK3_6	CAGCTCCTCCGTCGTGCATAA	0,05	0,02	TOXIC	0,89	0,10	DOWN	0,000002
FES	2242	SKV_21	C09	Hs_FES_5	AAGGCCAAGTTTCTACAGGAA	0,14	0,08	TOXIC	0,88	0,35	DOWN	0,002333
CIT	11113	SKV_01	G07	Hs_CIT_9	ATGGAAGGCACTATTTCTCAA	0,17	0,26	TOXIC	0,87	2,24	DOWN	0,537125
MARK4	57787	SKV_05	D03	Hs_MARK4_5	CCGCATCATGAAGGGCCTAAA	0,57	0,19	OK	0,87	0,07	DOWN	0,000027
CDK9	1025	SKV_05	G10	Hs_CDK9_5	TAGGGACATGAAGGCTGCTAA	0,15	0,10	TOXIC	0,85	0,56	DOWN	0,058206
AKT3	10000	SKV_01	G05	Hs_AKT3_8	CAGCAGGCACGTTAACTCGAA	0,32	0,29	TOXIC	0,85	0,77	DOWN	0,131749
CDK5R2	8941	SKV_13	B07	Hs_CDK5R2_6	CCGCGAGAACCTTCTCCGCAA	0,38	0,21	TOXIC	0,84	0,53	DOWN	0,007465
AKT2	208	SKV_02	F06	Hs_AKT2_8	CAAGCGTGGTGAATACATCAA	0,55	0,28	OK	0,83	0,15	DOWN	0,000699
MAP3K7IP2	23118	SKV_14	E06	Hs_MAP3K7IP2_5	CAGTCAATAGCCAGACCTTAA	0,26	0,03	TOXIC	0,83	0,45	DOWN	0,003179
MAP3K7	6885	SKV_20	D05	Hs_MAP3K7_8	AAGACTTGACTGTAACTGGAA	0,66	0,11	OK	0,83	0,25	DOWN	0,000582
CDC2L1	984	SKV_07	E03	Hs_CDC2L1_9	CACGTCGCTGAGGGAGATCAA	0,40	0,21	OK	0,83	0,18	DOWN	0,001436
EIF2AK3	9451	SKV_17	E09	Hs_EIF2AK3_6	CGGCAGGTCATTAGTAATTAT	0,49	0,17	OK	0,83	0,32	DOWN	0,001943
HIPK1	204851	SKV_08	E04	Hs_HIPK1_9	AGGGAAGCTGTACACCACTAA	0,27	0,15	TOXIC	0,83	0,30	DOWN	0,008615
PTK2	5747	SKV_21	G04	Hs_PTK2_10	CCGGTCGAATGATAAGGTGTA	0,22	0,06	TOXIC	0,81	0,22	DOWN	0,000352
FLT4	2324	SKV_23	B07	Hs_FLT4_8	CACCGTGTGGGCTGAGTTTAA	0,19	0,05	TOXIC	0,80	0,29	DOWN	0,008402
CNKSR1	10256	SKV_17	F05	Hs_CNKSR1_7	CAGGGTGGCGTGTCCCTCCTA	0,12	0,09	TOXIC	0,80	0,30	DOWN	0,001763
CDC2L1	984	SKV_05	G03	Hs_CDC2L1_1	CAAGATCTACATCGTGATGAA	0,06	0,01	TOXIC	0,80	0,53	DOWN	0,061041
ROR2	4920	SKV_23	D08	Hs_ROR2_5	CCGGTTTGGGAAAGTCTACAA	0,28	0,05	TOXIC	0,79	0,14	DOWN	0,000588

Target gene	Gene ID	plate	pos.	sequence name	siRNA sequence	Mean cells	SD cells	phenotype	Mean inh.	SD inh.	phenotype	Sign. inh.
EPHA2	1969	SKV_20	G08	Hs_EPHA2_7	CAGCGCCAAGTAAACAGGGTA	0,42	0,12	OK	0,79	0,05	DOWN	0,000000
AKAP8L	26993	SKV_14	E09	Hs_AKAP8L_7	CCGCGTGGCCGAAGCTGGAAA	0,42	0,48	OK	0,79	0,86	DOWN	0,075065
LIMK1	3984	SKV_24	B09	Hs_LIMK1_6	CTGCCTGGTCCGCGAGAACAA	0,37	0,03	TOXIC	0,78	0,28	DOWN	0,008669
DDR2	4921	SKV_23	D09	Hs_DDR2_2	CCGGTTCATTCCAGTCACCGA	0,28	0,07	TOXIC	0,78	0,05	DOWN	0,000011
STK38	11329	SKV_03	E08	Hs_STK38_5	AACCTTATCGCTCAACATGAA	0,48	0,07	OK	0,78	0,31	DOWN	0,011501
PIP4K2C	79837	SKV_13	F05	Hs_PIP5K2C_6	TTGATGTGTGATAATCTCATA	0,86	0,25	OK	0,78	0,12	DOWN	0,000001
PRKCE	5581	SKV_03	B07	Hs_PRKCE_5	CCCGACCATGGTAGTGTTCAA	0,18	0,18	TOXIC	0,77	0,60	DOWN	0,089533
FYN	2534	SKV_23	B09	Hs_FYN_8	AAGAAGCAGGATGCTGATCTA	0,16	0,07	TOXIC	0,77	0,05	DOWN	0,000012
BEGAIN	57596	SKV_16	E04	Hs_KIAA1446_5	CGGGCGGACCATGTCACCGTA	0,55	0,15	OK	0,76	0,10	DOWN	0,000000
BMPR1B	658	SKV_22	D03	Hs_BMPR1B_5	AACGAATGTAATAAAGACCTA	0,09	0,02	TOXIC	0,75	0,30	DOWN	0,012253
BUB1B	701	SKV_15	B08	Hs_BUB1B_6	CAGATTTAGCACATTTACTAT	0,18	0,11	TOXIC	0,75	0,15	DOWN	0,000011
MAP3K5	4217	SKV_18	D06	Hs_MAP3K5_6	CCGGGAATCTATACTCAATGA	0,19	0,02	TOXIC	0,75	0,20	DOWN	0,000328
FER	2241	SKV_22	G08	Hs_FER_5	CAGATAGATCCTAGTACAGAA	0,16	0,04	TOXIC	0,73	0,16	DOWN	0,001255
MAP3K7IP1	10454	SKV_14	D04	Hs_MAP3K7IP1_7	AACGGCTATGATGGCAACCGA	0,48	0,12	OK	0,73	0,19	DOWN	0,000029
NRGN	4900	SKV_12	C10	Hs_NRGN_6	CACCCAAGCACACTCACTTAA	0,83	0,08	OK	0,72	0,31	DOWN	0,016160
PAK4	10298	SKV_20	E04	Hs_PAK4_3	CAAGGTGTCGCCATCCCTGAA	0,32	0,09	TOXIC	0,72	0,17	DOWN	0,000130
TWF2	11344	SKV_02	D10	Hs_PTK9L_5	AAGACAGAGATCAGTGTGGAA	0,53	0,25	OK	0,72	0,46	DOWN	0,054300
CSNK1D	1453	SKV_07	C06	Hs_CSNK1D_6	CTCCCTGACGATTCCACTGTA	0,62	0,15	OK	0,72	0,22	DOWN	0,005080
WNK1	65125	SKV_19	F04	Hs_WNK1_5	CTAGAGGATCTTGATGCTCAA	0,15	0,08	TOXIC	0,72	0,15	DOWN	0,000070
MAPK14	1432	SKV_09	D05	Hs_MAPK14_7	CTCAGTGATACGTACAGCCAA	0,24	0,08	TOXIC	0,71	0,23	DOWN	0,005684
PDPK1	5170	SKV_02	G04	Hs_PDPK1_9	CACGCCTAACAGGACGTATTA	0,79	0,29	OK	0,71	0,42	DOWN	0,041453
ACVR1B	91	SKV_23	G06	Hs_ACVR1B_6	CCGTTCTTACGTCGCCATAAA	0,26	0,07	TOXIC	0,71	0,11	DOWN	0,000366
CMPK	51727	SKV_25	F07	Hs_UMP-CMPK_6	AAGGCTAATTCTAAACCTGAA	0,23	0,11	TOXIC	0,71	0,49	DOWN	0,065432
AKAP8	10270	SKV_16	B03	Hs_AKAP8_5	CAAGGTTAGCACGCAACAGAA	0,36	0,07	TOXIC	0,71	0,12	DOWN	0,000001
CIB3	117286	SKV_15	B04	Hs_CIB3_3	CTGGAGCAGACGGTGACCAAA	0,17	0,06	TOXIC	0,71	0,20	DOWN	0,000044
ANKK1	255239	SKV_24	G05	Hs_ANKK1_6	GCGGACGGAGTACGCCATCAA	0,38	0,06	TOXIC	0,70	0,19	DOWN	0,003046
DAPK2	23604	SKV_05	B10	Hs_DAPK2_5	CGGAATTTGTTGCTCCAGAAA	0,81	0,16	OK	0,70	0,27	DOWN	0,011613
STK11	6794	SKV_26	C03	Hs_STK11_7	GAGGATGACCTAGCACTGAAA	0,52	0,14	OK	0,70	0,04	DOWN	0,000005
NME3	4832	SKV_09	C05	Hs_NME3_3	CTGCATCGAGGTTGGCAAGAA	0,08	0,04	TOXIC	0,70	0,60	DOWN	0,114606
TYRO3	7301	SKV_22	B06	Hs_TYRO3_6	CGGACTGACCAAATCACCCAA	0,07	0,01	TOXIC	0,70	0,32	DOWN	0,019091
TWF1	5756	SKV_04	B05	Hs_PTK9_5	TCCAAGCAAGTGAAGATGTTA	0,27	0,07	TOXIC	0,69	0,04	DOWN	0,000005
ITPKB	3707	SKV_10	F08	Hs_ITPKB_5	AAGGCCATTCGAACCACTCTA	0,40	0,15	TOXIC	0,68	0,17	DOWN	0,002275
PIK3R1	5295	SKV_15	F04	Hs_PIK3R1_5	CAGCATTAAACCAGACCTTAT	0,27	0,11	TOXIC	0,68	0,26	DOWN	0,000425
HK2	3099	SKV_09	B04	Hs_HK2_5	CCGGCCGTGCTACAATAGGTA	0,59	0,35	OK	0,68	0,11	DOWN	0,000407
PI4KA	5297	SKV_25	E05	Hs_PIK4CA_10	TCCGGACGCCATCCTCTTCTA	0,27	0,05	TOXIC	0,67	0,33	DOWN	0,023665
CAMK2D	817	SKV_04	D06	Hs_CAMK2D_9	CCGCCTGCATAGCATATATTA	0,46	0,16	OK	0,67	0,22	DOWN	0,006517
TNNI3K	51086	SKV_24	F08	Hs_TNNI3K_6	CAGCATTCGGCGTATACCTAA	0,24	0,01	TOXIC	0,67	0,83	DOWN	0,236967
MAPK11	5600	SKV_08	B04	Hs_MAPK11_5	CAGGATGGAGCTGATCCAGTA	0,07	0,03	TOXIC	0,67	0,51	DOWN	0,084484
MAP4K1	11184	SKV_20	E08	Hs_MAP4K1_6	TACGTGGGTGTACTCCATCAA	0,34	0,11	TOXIC	0,67	0,26	DOWN	0,002168

Target gene	Gene ID	plate	pos.	sequence name	siRNA sequence	Mean cells	SD cells	phenotype	Mean inh.	SD inh.	phenotype	Sign. inh.
ADRBK1	156	SKV_02	F03	Hs_ADRBK1_2	CGGCTGGAGGCTCGCAAGAAA	0,23	0,03	TOXIC	0,66	0,23	DOWN	0,007084
SRC	6714	SKV_23	E09	Hs_SRC_6	AAGCAGTGCCTGCCTATGAAA	0,21	0,07	TOXIC	0,66	0,12	DOWN	0,000698
ABL1	25	SKV_19	B09	Hs_ABL1_10	ACGCACGGACATCACCATGAA	0,28	0,14	TOXIC	0,66	0,19	DOWN	0,000452
CHKA	1119	SKV_08	F06	Hs_CHKA_6	CCGGCCCTTACCAAACCTGAT	0,36	0,18	TOXIC	0,66	0,20	DOWN	0,005085
CNKSR3	154043	SKV_16	F05	Hs_MAGI1_6	CGGAGTTGTGTTACTGCTTAA	0,12	0,03	TOXIC	0,65	0,42	DOWN	0,009028
STK19	8859	SKV_04	B07	Hs_STK19_5	CCCGGAGACCTTTGGAGTTAA	0,22	0,12	TOXIC	0,65	0,41	DOWN	0,051278
CDK5R2	8941	SKV_11	D07	Hs_CDK5R2_5	CAGCAAGAAGGTGACACCCAA	0,14	0,09	TOXIC	0,65	0,34	DOWN	0,024181
CAMK1D	57118	SKV_06	G09	Hs_CAMK1D_6	ATGGAGAAGGACCCGAATAAA	0,92	0,40	OK	0,65	0,14	DOWN	0,001368
STYXL1	51657	SKV_16	D07	Hs_DUSP24_5	CAAGATTCAGAAGGACTTGAA	0,31	0,08	TOXIC	0,64	0,26	DOWN	0,000496
LTK	4058	SKV_23	C09	Hs_LTK_6	CCTGCAGATGCTTCTAATAAA	0,91	0,10	OK	0,63	0,06	DOWN	0,000060
CDKL1	8814	SKV_09	G08	Hs_CDKL1_6	TCGGGAAATCCGAATGCTCAA	0,36	0,01	TOXIC	0,63	0,39	DOWN	0,048775
STK36	27148	SKV_25	B08	Hs_STK36_5	ATCCCTGTTTATGTTGATTCA	0,89	0,09	OK	0,62	0,14	DOWN	0,001685
PRKAA1	5562	SKV_06	D06	Hs_PRKAA1_6	TCGGGATCAGTTAGCAACTAT	0,29	0,16	TOXIC	0,62	0,30	DOWN	0,021557
PRKCA	5578	SKV_01	D04	Hs_PRKCA_6	CGCAGTGGAATGAGTCCTTTA	0,17	0,07	TOXIC	0,62	0,19	DOWN	0,004862
PIK3AP1	118788	SKV_12	C03	Hs_PIK3AP1_6	CAGCAGGGTATTTAAGTGCTA	0,24	0,16	TOXIC	0,61	0,21	DOWN	0,007115
ADCK5	203054	SKV_06	B04	Hs_ADCK5_6	CCGCTACTTCCTTATGGCTAA	0,16	0,13	TOXIC	0,61	0,36	DOWN	0,041486
SPEG	10290	SKV_05	B04	Hs_APEG1_6	CAGCTGGAATAACAAGCCCAA	0,10	0,06	TOXIC	0,61	0,65	DOWN	0,179593
MAPK14	1432	SKV_07	F05	Hs_MAPK14_6	CAGAGAACTGCGGTTACTTAA	0,28	0,09	TOXIC	0,61	0,11	DOWN	0,000563
ZC3HC1	51530	SKV_14	F05	Hs_ZC3HC1_5	AGGGAGAATGGTGGAACTGAA	0,13	0,03	TOXIC	0,61	0,24	DOWN	0,000473
MAP2K6	5608	SKV_18	E06	Hs_MAP2K6_6	TAGACCTATGATAAATAACCA	0,49	0,21	OK	0,61	0,13	DOWN	0,000077
MST1R	4486	SKV_21	F05	Hs_MST1R_7	CAGGTCTGCGTAGATGGTGAA	0,38	0,09	TOXIC	0,61	0,25	DOWN	0,002639
SPHK1	8877	SKV_13	B06	Hs_SPHK1_10	TGGGCCCAGCTGCCTATGTAA	0,50	0,12	OK	0,61	0,17	DOWN	0,000055
ITPKC	80271	SKV_12	B07	Hs_ITPKC_5	CAGAAGGAGCCTGTCCCTCAA	0,03	0,01	TOXIC	0,61	0,39	DOWN	0,055555
TSKS	60385	SKV_14	G05	Hs_TSKS_5	AACCAACGTCTTGAAGCAGAA	0,21	0,03	TOXIC	0,60	0,49	DOWN	0,024122
BEGAIN	57596	SKV_14	G04	Hs_KIAA1446_6	CTGCAGCTTCTCTGAACGCTA	0,54	0,11	OK	0,60	0,27	DOWN	0,001061
PDIK1L	149420	SKV_19	G05	Hs_PDIK1L_5	AAGCTAGACTCTACCCTCTAA	0,11	0,03	TOXIC	0,60	0,16	DOWN	0,000485
STK33	65975	SKV_05	D04	Hs_STK33_6	TCCATAAGTGACTGTGCTAAA	0,52	0,17	OK	0,60	0,06	DOWN	0,000065
MAPK12	6300	SKV_08	B09	Hs_MAPK12_5	CTGGACGTATTCACTCCTGAT	0,17	0,06	TOXIC	0,60	0,11	DOWN	0,000714
MKNK2	2872	SKV_26	B03	Hs_MKNK2_8	CAGAACCGTTACTGTGAATGA	0,92	0,10	OK	0,59	0,19	DOWN	0,006178
BCKDK	10295	SKV_02	D08	Hs_BCKDK_5	AACGCCCACCATGATGCTCTA	0,15	0,11	TOXIC	0,58	0,32	DOWN	0,033917
MAP4K3	8491	SKV_18	F07	Hs_MAP4K3_5	GAGGTGGTTCTTTACAGGATA	0,36	0,08	TOXIC	0,58	0,28	DOWN	0,006488
TNK2	10188	SKV_23	F10	Hs_TNK2_6	CGGCAGTCAGATCCTGCATAA	0,08	0,01	TOXIC	0,58	0,16	DOWN	0,003022
GKAP1	80318	SKV_14	G08	Hs_GKAP1_5	AACGCTCAACATGATCTTCCA	0,16	0,03	TOXIC	0,58	0,17	DOWN	0,000054
NRBP1	29959	SKV_17	G07	Hs_NRBP_5	CCGGTTGACTTCTCTGCTAGA	0,46	0,25	OK	0,58	0,19	DOWN	0,001540
PRKCD	5580	SKV_03	B06	Hs_PRKCD_8	CCGCTTCAAGGTTCACAACTA	0,19	0,18	TOXIC	0,58	0,70	DOWN	0,226437
TPK1	27010	SKV_13	C09	Hs_TPK1_6	CAGGTTGTCTGTAGAGAATGA	0,25	0,13	TOXIC	0,57	0,74	DOWN	0,116217
FLT1	2321	SKV_21	D05	Hs_FLT1_5	ACCGCATATGGTATCCCTCAA	0,34	0,08	TOXIC	0,57	0,23	DOWN	0,002563
ILK	3611	SKV_22	D06	Hs_ILK_4	AAGGAAGAGCAGGGACTTCAA	0,14	0,02	TOXIC	0,57	0,34	DOWN	0,044696
MLCK	91807	SKV_07	B10	Hs_LOC91807_6	ACGGAGGACAATGACCTTGCA	0,38	0,21	TOXIC	0,57	0,67	DOWN	0,214480

Target gene	Gene ID	plate	pos.	sequence name	siRNA sequence	Mean cells	SD cells	phenotype	Mean inh.	SD inh.	phenotype	Sign. inh.
PIP4K2A	5305	SKV_11	B04	Hs_PIP5K2A_6	CTGCCCGATGGTCTTCCGTAA	0,40	0,09	TOXIC	0,56	0,41	DOWN	0,059980
PRKACG	5568	SKV_02	G09	Hs_PRKACG_5	AACCAGCTGGATCGCCATCTA	0,11	0,04	TOXIC	0,56	0,67	DOWN	0,220165
DAPK2	23604	SKV_06	F10	Hs_DAPK2_6	CTGGTTAAAGAGACCCGGAAA	0,38	0,25	TOXIC	0,56	0,29	DOWN	0,030273
TSSK2	23617	SKV_06	G03	Hs_STK22B_5	CAAGTTCAATGTGGCTGTCAA	0,24	0,13	TOXIC	0,56	0,27	DOWN	0,022514
TSSK6	83983	SKV_25	D09	Hs_TSSK6_1	GAAGGTGGCCACATCCAAGAA	0,20	0,10	TOXIC	0,56	0,15	DOWN	0,003149
RPS6KB2	6199	SKV_01	F05	Hs_RPS6KB2_6	CGGGCTGAGCGGAACATTCTA	0,31	0,17	TOXIC	0,55	0,15	DOWN	0,002736
ULK1	8408	SKV_15	G03	Hs_ULK1_5	CGCGCGGTACCTCCAGAGCAA	0,20	0,08	TOXIC	0,55	0,32	DOWN	0,004963
IHPK3	117283	SKV_13	F10	Hs_IHPK3_6	CTGAGATACGTTACCCAATTA	0,62	0,33	OK	0,55	0,43	DOWN	0,020463
TEC	7006	SKV_23	F03	Hs_TEC_6	CCGCAGCTAATCAGAATCAGA	0,42	0,04	OK	0,55	0,12	DOWN	0,001493
PTK7	5754	SKV_23	E05	Hs_PTK7_7	CGGGATGATGTCACTGGAGAA	0,20	0,05	TOXIC	0,55	0,12	DOWN	0,001270
ULK1	8408	SKV_17	E03	Hs_ULK1_6	TGCCCTTTGCGTTATATTGTA	1,02	0,30	OK	0,55	0,67	DOWN	0,150703
MAP3K10	4294	SKV_24	C04	Hs_MAP3K10_12	GTCGTCCGTGTCCGACTGCAA	0,25	0,12	TOXIC	0,55	0,32	DOWN	0,041783
NME7	29922	SKV_13	C10	Hs_NME7_6	TTCATGTAGATCACCAGTCAA	0,82	0,31	OK	0,55	0,29	DOWN	0,003964
EPHB3	2049	SKV_22	F09	Hs_EPHB3_10	AGAGGTGTTTGTGGCCATCAA	0,59	0,12	OK	0,54	0,09	DOWN	0,000420
PKN1	5585	SKV_01	D10	Hs_PKN1_5	CAGGACAGTAAGACCAAGATT	0,24	0,24	TOXIC	0,54	0,39	DOWN	0,073844
STK24	8428	SKV_26	B08	Hs_STK24_8	CTCAGTGTTTATCTACAATTA	0,59	0,04	OK	0,54	0,87	DOWN	0,344315
MERTK	10461	SKV_22	C03	Hs_MERTK_8	CACCAGAAACACAGCCTTCAA	0,17	0,01	TOXIC	0,53	0,23	DOWN	0,015345
PIM2	11040	SKV_06	F05	Hs_PIM2_5	CCGGGATTGTCCAATTACTAA	0,70	0,16	OK	0,53	0,38	DOWN	0,075092
ADCK1	57143	SKV_02	E07	Hs_ADCK1_3	TAACAAGTACTTGGACCCTAA	0,12	0,03	TOXIC	0,53	0,62	DOWN	0,211241
STK24	8428	SKV_18	F06	Hs_STK24_5	CCCACCGACGTTGGAAGGAAA	0,33	0,10	TOXIC	0,52	0,21	DOWN	0,002660
CDKN1B	1027	SKV_15	B09	Hs_CDKN1B_5	AAAGCGTTGGATGTAGCATTA	0,52	0,16	OK	0,52	0,25	DOWN	0,001734
IHPK2	51447	SKV_13	D04	Hs_IHPK2_11	TAGGACGGAAACGCCGAGGAA	0,59	0,33	OK	0,52	0,09	DOWN	0,000001
AKAP14	158798	SKV_16	F06	Hs_AKAP14_7	TACGAGGATGAATTGACTCAA	0,55	0,04	OK	0,52	0,19	DOWN	0,000406
EEF2K	29904	SKV_02	E05	Hs_EEF2K_6	CGGGATGGCGCTCTTCTTCTA	0,86	0,21	OK	0,51	0,39	DOWN	0,086015
SLK	9748	SKV_20	E03	Hs_SLK_6	TAGCATCTTGTGATCACCCAA	0,05	0,01	TOXIC	0,51	0,11	DOWN	0,000093
CHEK1	1111	SKV_04	D08	Hs_CHEK1_9	AAGAAAGAGATCTGTATCAAT	0,36	0,21	TOXIC	0,51	0,26	DOWN	0,028296
RYK	6259	SKV_25	F10	Hs_RYK_11	AAGGTGAAGGATATAGCAATA	0,39	0,05	TOXIC	0,51	0,46	DOWN	0,126387
NTRK3	4916	SKV_23	D06	Hs_NTRK3_10	CTGGTTGGAGCGAATCTGCTA	0,21	0,06	TOXIC	0,51	0,19	DOWN	0,010855
RIOK2	55781	SKV_04	C06	Hs_RIOK2_6	CGCGGTTGAAATGGGCATGAA	0,17	0,09	TOXIC	0,50	0,07	DOWN	0,000217
PIP5K1A	8394	SKV_11	C07	Hs_PIP5K1A_5	CAGCCTCTTGATGTCAATCCA	0,55	0,14	OK	0,50	0,25	DOWN	0,102867
EPHB6	2051	SKV_26	B10	Hs_EPHB6_6	CTCCTGGATTACATCTACTTA	0,75	0,11	OK	0,50	0,52	---	0,169948
PIP5K1C	23396	SKV_26	B06	Hs_PIP5K1C_6	CGCGCCCGCCACCGACATCTA	0,47	0,05	OK	0,50	0,55	---	0,193341
MAPK13	5603	SKV_09	F07	Hs_MAPK13_6	CGGGATGAGCCTCATCCGGAA	0,45	0,12	OK	0,50	0,28	---	0,038715
NAGK	55577	SKV_11	G05	Hs_NAGK_5	ACCTGAGTGAAAGCTACTTAA	0,55	0,24	OK	0,50	0,56	---	0,110103
FLT1	2321	SKV_23	B05	Hs_FLT1_6	CACTACAGTATTAGCAAGCAA	0,32	0,05	TOXIC	0,50	0,23	---	0,020123
CAMK1	8536	SKV_04	F10	Hs_CAMK1_5	CAGGTGCTGGATGCTGTGAAA	1,52	0,36	OK	0,50	0,26	---	0,031449
GRK5	2869	SKV_01	B09	Hs_GRK5_5	AGCGTCATAACTAGAACTGAA	0,19	0,09	TOXIC	0,49	0,35	---	0,072246
ACVRL1	94	SKV_22	C08	Hs_ACVRL1_5	CACCGAGTTCGTCAACCACTA	0,68	0,10	OK	0,49	0,17	---	0,007360
MAPK7	5598	SKV_07	G10	Hs_MAPK7_10	TACGAGATCATCGAGACCATA	1,00	0,24	OK	0,49	0,34	---	0,068844

Target gene	Gene ID	plate	pos.	sequence name	siRNA sequence	Mean cells	SD cells	phenotype	Mean inh.	SD inh.	phenotype	Sign. inh.
CAMK1G	57172	SKV_06	G10	Hs_CAMK1G_6	CAGGTCTTGTCGGCAGTGAAA	0,34	0,14	TOXIC	0,49	0,11	---	0,001435
LIMK2	3985	SKV_25	G09	Hs_LIMK2_8	CACGGGCAAAGTGATGGTCAT	0,48	0,11	OK	0,49	0,32	---	0,060337
TNK2	10188	SKV_22	B10	Hs_TNK2_5	ACGCAAGTCGTGGATGAGTAA	0,13	0,02	TOXIC	0,49	0,36	---	0,077935
PDLIM5	10611	SKV_16	B07	Hs_PDLIM5_6	TCCGATGTGCGCCCATTGTAA	0,63	0,13	OK	0,49	0,11	---	0,000021
AURKB	9212	SKV_15	G08	Hs_AURKB_5	AACGCGGCACTTCACAATTGA	0,14	0,10	TOXIC	0,48	0,47	---	0,051425
PHKG2	5261	SKV_06	D04	Hs_PHKG2_6	TACGGGCACTGGGTAAAGAAA	0,28	0,06	TOXIC	0,48	0,29	---	0,045187
TSSK1B	83942	SKV_07	B07	Hs_STK22D_5	TAGAAGCTGATTTAACACCAA	0,36	0,15	TOXIC	0,48	0,26	---	0,032326
UCK1	83549	SKV_12	B08	Hs_UCK1_7	TCCCTCTAGGTCACTGAGAAA	0,73	0,35	OK	0,48	0,03	---	0,000018
MAP3K1	4214	SKV_20	B03	Hs_MAP3K1_10	CACGCATGTCAAATTCTCATA	0,53	0,14	OK	0,48	0,12	---	0,000229
FRAP1	2475	SKV_25	E03	Hs_FRAP1_6	CAGGCCTATGGTCGAGATTTA	0,26	0,10	TOXIC	0,48	0,23	---	0,022971
MAP4K1	11184	SKV_18	G08	Hs_MAP4K1_5	CTGACTAAGAGTCCCAAGAAA	0,15	0,04	TOXIC	0,48	0,38	---	0,047425
MAP3K13	9175	SKV_24	D05	Hs_MAP3K13_5	CAGACTCAATATGCACGGACA	0,65	0,11	OK	0,47	0,40	---	0,109383
STK40	83931	SKV_05	D06	Hs_MGC4796_5	CAGCGCTACCTGCGGAAATAA	0,16	0,03	TOXIC	0,47	0,04	---	0,000038
ADCK4	79934	SKV_04	C08	Hs_ADCK4_6	CCGGGTCCCAGCCGTGGTTAA	0,89	0,20	OK	0,47	0,36	---	0,088909
BRSK2	9024	SKV_06	E05	Hs_STK29_5	CCCGACTGCCAGAGTCTGCTA	0,36	0,29	TOXIC	0,47	0,54	---	0,205525
MOS	4342	SKV_17	B08	Hs_MOS_5	CGCGAACATCTTGATCAGTGA	0,53	0,14	OK	0,47	0,17	---	0,001445
EPHB6	2051	SKV_22	G03	Hs_EPHB6_10	CGGGAAGTCGATCCTGCTTAT	0,27	0,09	TOXIC	0,47	0,45	---	0,143520
PMVK	10654	SKV_11	E04	Hs_PMVK_6	TTGGCTGTGCTTGAAGGCGAA	0,87	0,23	OK	0,47	0,22	---	0,139852
GSK3B	2932	SKV_07	F08	Hs_GSK3B_8	CTGCATTTATCGTTAACCTAA	0,79	0,50	OK	0,46	0,36	---	0,089617
NME2	4831	SKV_10	G04	Hs_NME2_2	ATAGAGCATATTTGCCAATAA	0,30	0,15	TOXIC	0,46	0,30	---	0,056207
MAP4K4	9448	SKV_20	D10	Hs_MAP4K4_5	AGGCAAGATCCTACCCGGAAA	0,56	0,11	OK	0,46	0,28	---	0,018056
MKNK1	8569	SKV_04	G03	Hs_MKNK1_6	TAGATAGTGCTCTGTGCCTAA	0,11	0,03	TOXIC	0,45	0,30	---	0,056487
DAPK3	1613	SKV_06	B10	Hs_DAPK3_8	CCAGTTTGCGATCGTGCGGAA	0,50	0,06	OK	0,44	0,02	---	0,000003
TYRO3	7301	SKV_23	F06	Hs_TYRO3_5	AACGGTGACCTTTAGTGCCAA	0,44	0,08	OK	0,44	0,02	---	0,000002
STK11IP	114790	SKV_15	B03	Hs_STK11IP_8	AAAGTTGTTTCCAACTCATAA	0,24	0,09	TOXIC	0,44	0,12	---	0,000028
MAP4K2	5871	SKV_18	E08	Hs_MAP4K2_5	CTGGCTCTACTGCGTGAACAA	0,08	0,04	TOXIC	0,44	0,36	---	0,048933
EPHA4	2043	SKV_22	F03	Hs_EPHA4_6	CCGCCAGGACATTTCCTATAA	0,13	0,04	TOXIC	0,44	0,22	---	0,026036
PIP5K3	200576	SKV_12	C06	Hs_PIP5K3_9	ACCCAGTAACATAATATTTCA	0,82	0,32	OK	0,44	0,19	---	0,017476
FLT3LG	2323	SKV_13	G08	Hs_FLT3LG_7	CTCCTCCGACTTCGCTGTCAA	0,49	0,46	OK	0,43	0,44	---	0,057300
MAP3K2	10746	SKV_20	E06	Hs_MAP3K2_3	CACAGTAATATGATTGTCCTA	0,57	0,10	OK	0,43	0,11	---	0,000238
AKAP7	9465	SKV_12	E04	Hs_AKAP7_6	CCCGATGACGCTGAACTAGTA	0,64	0,40	OK	0,43	0,26	---	0,047306
NEK11	79858	SKV_19	F07	Hs_NEK11_6	CTGCCTATGCTTGGAGTCATA	0,31	0,11	TOXIC	0,43	0,22	---	0,010046
PIK3CD	5293	SKV_17	C10	Hs_PIK3CD_6	CGCCGTGATCGAGAAAGCCAA	0,84	0,40	OK	0,43	1,12	---	0,474469
ERN1	2081	SKV_15	D06	Hs_ERN1_5	CAGCACGGACGTCAAGTTTGA	0,82	0,18	OK	0,43	0,09	---	0,000008
DYRK4	8798	SKV_09	G07	Hs_DYRK4_6	CTGCATCACGGCGGAGTTGTA	0,74	0,39	OK	0,42	0,15	---	0,008742
ITPKA	3706	SKV_10	F07	Hs_ITPKA_5	CACCAGCGGGCTGATCCTGAA	0,74	0,83	OK	0,42	0,25	---	0,044029
SGK	6446	SKV_01	F06	Hs_SGK_5	CACAGCTGAAATGTACGACAA	0,29	0,22	TOXIC	0,41	0,23	---	0,034420
PIP5K3	200576	SKV_13	G06	Hs_PIP5K3_10	TTGCCGTTACCCAGTAACATA	0,92	0,60	OK	0,41	1,02	---	0,395200
FLT3	2322	SKV_21	D06	Hs_FLT3_7	TACGTTGATTTCAGAGAATAT	0,14	0,06	TOXIC	0,41	0,32	---	0,043007

Target gene	Gene ID	plate	pos.	sequence name	siRNA sequence	Mean cells	SD cells	phenotype	Mean inh.	SD inh.	phenotype	Sign. inh.
SGK2	10110	SKV_03	E06	Hs_SGK2_9	CAGGGCCAATGGGAACATCAA	0,46	0,08	OK	0,40	0,28	---	0,066954
MAP2K6	5608	SKV_20	C06	Hs_MAP2K6_5	AAGGCTTGCATTTCTATTGGA	0,68	0,11	OK	0,40	0,16	---	0,002373
SYK	6850	SKV_23	E10	Hs_SYK_6	TCCGGAATGCATCAACTACTA	0,38	0,15	TOXIC	0,40	0,09	---	0,001242
PIK3R4	30849	SKV_17	G08	Hs_PIK3R4_8	CAAGCAATGCGTGGACTTTAA	0,13	0,08	TOXIC	0,40	0,34	---	0,056424
WNK3	65267	SKV_18	B06	Hs_WNK3_9	AAGATTGGTGATCTAGGATTA	0,37	0,10	TOXIC	0,40	0,17	---	0,003342
ADK	132	SKV_08	E06	Hs_ADK_6	CAAGGGAGAGATGACACTATA	0,69	0,20	OK	0,40	0,17	---	0,015508
PHKG1	5260	SKV_04	F03	Hs_PHKG1_5	CAAGAGCCTGCAAGCACTTAA	0,36	0,15	TOXIC	0,40	0,20	---	0,025296
GUK1	2987	SKV_08	G10	Hs_GUK1_5	CAGGGCTGACATCCTAATAAA	0,84	0,41	OK	0,40	0,58	---	0,299943
LYK5	92335	SKV_19	B07	Hs_LYK5_7	CACCCAGATGCTGCTAGAGAA	0,69	0,25	OK	0,40	0,27	---	0,026923
PKMYT1	9088	SKV_17	E07	Hs_PKMYT1_2	CCGGCCAGAGTCCTTCTTCCA	0,16	0,05	TOXIC	0,40	0,21	---	0,012252
AKAP11	11215	SKV_16	C03	Hs_AKAP11_5	ACCGGTTATCTAAATCTATTA	0,35	0,13	TOXIC	0,40	1,03	---	0,411013
MINK1	50488	SKV_25	E08	Hs_MINK1_1	CACGTACGGGCGCATCATTAA	0,32	0,01	TOXIC	0,39	0,28	---	0,074332
PKLR	5313	SKV_12	F05	Hs_PKLR_15	CACACACAAACCAAGAGCCAA	0,68	0,33	OK	0,39	0,32	---	0,097881
C17orf75	64149	SKV_13	E09	Hs_NJMU-R1_8	AAAGGCCATACAAGACACAAA	0,84	0,35	OK	0,39	0,24	---	0,005784
DGKD	8527	SKV_13	B03	Hs_DGKD_6	CCGCCTCGTGACCAAGTTTAA	0,94	0,26	OK	0,39	0,21	---	0,003377
TK2	7084	SKV_11	C03	Hs_TK2_5	ATGCCAGAAGTGGACTATGTA	0,44	0,41	OK	0,39	0,45	---	0,249618
MAP3K4	4216	SKV_18	D05	Hs_MAP3K4_5	CACCAATCCCTGAAAGATTAA	0,40	0,07	OK	0,39	0,09	---	0,000139
ITPKA	3706	SKV_09	B07	Hs_ITPKA_6	CCGGTCTAACGTCTCACACCA	0,19	0,08	TOXIC	0,39	0,39	---	0,162401
PRKD3	23683	SKV_05	C04	Hs_PRKD3_5	CACGATATGTCAGTACTGCAA	0,53	0,22	OK	0,39	0,16	---	0,013047
STK3	6788	SKV_20	C10	Hs_STK3_6	CGGCGCCTAAGAGTAAACTAA	0,74	0,11	OK	0,39	0,10	---	0,000235
EIF2AK4	440275	SKV_17	G05		CTGCAGGAATTTAGTAACATT	0,40	0,21	OK	0,39	0,41	---	0,108686
PRKCA	5578	SKV_03	B04	Hs_PRKCA_7	TACAAGTTGCTTAACCAAGAA	0,07	0,02	TOXIC	0,38	0,32	---	0,109925
HK1	3098	SKV_10	F03	Hs_HK1_9	CACGATGTAGTCACCTTACTA	0,19	0,16	TOXIC	0,38	0,08	---	0,001306
TPD52L3	89882	SKV_13	F09	Hs_NYD-SP25_9	ATCATATACTTCAGACATCAA	0,99	0,21	OK	0,38	0,27	---	0,013522
NEK9	91754	SKV_18	B10	Hs_NEK9_7	CAGGTGTCATGTGGTGATGAT	0,15	0,09	TOXIC	0,37	0,37	---	0,090274
STK3	6788	SKV_18	E10	Hs_STK3_5	CCGGCGCCTAAGAGTAAACTA	0,67	0,15	OK	0,37	0,05	---	0,000005
SKP2	6502	SKV_12	D05	Hs_SKP2_5	AAGTGATAGTGTCATGCTAAA	0,48	0,22	OK	0,37	0,27	---	0,074403
SGK	6446	SKV_03	D06	Hs_SGK_9	TCGCAGTGTTTCAGTTCTTTA	1,07	0,32	OK	0,37	0,20	---	0,032493
DYRK1A	1859	SKV_07	F06	Hs_DYRK1A_6	TACGGTCGCTGACTACTTGAA	0,79	0,08	OK	0,37	0,05	---	0,000172
FUK	197258	SKV_12	C05	Hs_FUK_6	TGGCTTAGAGTTGTAGACTTA	0,74	0,27	OK	0,37	0,21	---	0,036307
PXK	54899	SKV_18	C09	Hs_PXK_5	CTGGCAGATTGTTAGAAGATA	0,20	0,06	TOXIC	0,37	0,66	---	0,305210
STK31	56164	SKV_18	C10	Hs_STK31_5	CCCAGTGTGGATCACTTGCTA	0,19	0,08	TOXIC	0,37	0,10	---	0,000286
SPHK1	8877	SKV_11	D06	Hs_SPHK1_6	CTGCCTATGTAAGGCCTTCTA	0,44	0,03	OK	0,36	0,06	---	0,297365
PDK2	5164	SKV_03	G09	Hs_PDK2_6	TAGGTCTGTGATGGTCCCTAA	0,36	0,22	TOXIC	0,36	0,40	---	0,196112
CAMKK2	10645	SKV_19	D07	Hs_CAMKK2_7	CTAGCTGATTGTTGTGGTCAA	0,99	0,14	OK	0,36	0,05	---	0,000004
PDK3	5165	SKV_02	C10	Hs_PDK3_7	CTCGTTACTTTGGGTAAAGAA	0,60	0,01	OK	0,36	0,23	---	0,055666
PLK4	10733	SKV_19	D08	Hs_PLK4_7	AAGGACTTGGTCTTACAACTA	0,13	0,11	TOXIC	0,36	0,67	---	0,323814
MATK	4145	SKV_23	D03	Hs_MATK_9	ACGGATTCTAAGGACTCTAAA	0,62	0,04	OK	0,36	0,11	---	0,005495
PRKCDBP	112464	SKV_14	G10	Hs_PRKCDBP_4	CACGCCCTAATAAGGAGCGAA	0,49	0,48	OK	0,35	0,47	---	0,130510

Target gene	Gene ID	plate	pos.	sequence name	siRNA sequence	Mean cells	SD cells	phenotype	Mean inh.	SD inh.	phenotype	Sign. inh.
KSR1	8844	SKV_24	F04	Hs_KSR_10	CTGGAAGTCAGCTGACATTAA	0,47	0,11	OK	0,35	0,13	---	0,008985
ERBB4	2066	SKV_22	G06	Hs_ERBB4_6	TCGGGATTTGGCAGCCCGTAA	0,39	0,05	TOXIC	0,35	0,29	---	0,102120
STK11	6794	SKV_06	D08	Hs_STK11_12	TACAACGAAGAGAAGCAGAAA	0,56	0,59	OK	0,35	0,19	---	0,032654
CLK3	1198	SKV_07	F04	Hs_CLK3_5	CACGAAGATCTCGGTCCAGAA	0,23	0,08	TOXIC	0,35	0,23	---	0,056671
CDK5R1	8851	SKV_13	B05	Hs_CDK5R1_6	TGAGCTGGTTTGACTCATTAA	0,36	0,16	TOXIC	0,35	0,43	---	0,105398
STK19	8859	SKV_02	D07	Hs_STK19_6	CTGTTATTACTCTGTCTTGAA	0,34	0,21	TOXIC	0,35	0,32	---	0,129378
ROR2	4920	SKV_21	F08	Hs_ROR2_6	CTGGTGCTTTACGCAGAATAA	0,09	0,05	TOXIC	0,35	0,24	---	0,033013
CHEK2	11200	SKV_05	B07	Hs_CHEK2_10	AGGACTGTCTTATAAAGATTA	0,70	0,13	OK	0,35	0,34	---	0,156698
STK4	6789	SKV_18	F03	Hs_STK4_6	CACCATTTGCTGTGCGAATTA	0,56	0,06	OK	0,34	0,08	---	0,000138
PAK1	5058	SKV_20	B07	Hs_PAK1_9	TTGAAGAGAACTGCAACTGAA	0,36	0,11	TOXIC	0,34	0,11	---	0,000717
GK	2710	SKV_08	G09	Hs_GK_5	CCACCACTTAAGTGACATAAA	0,48	0,23	OK	0,34	0,34	---	0,156913
VRK3	51231	SKV_05	F04	Hs_VRK3_5	CTCACTCAAACTGGATGCCAA	0,18	0,10	TOXIC	0,34	0,43	---	0,244409
PLK3	1263	SKV_16	G10	Hs_PLK3_6	CTGCATCAAGCAGGTTCACTA	0,29	0,14	TOXIC	0,34	0,07	---	0,000004
SMG1	23049	SKV_02	E03	Hs_SMG1_5	CACCATGGTATTACAGGTTCA	0,19	0,10	TOXIC	0,34	0,17	---	0,024525
WEE1	7465	SKV_25	C05	Hs_WEE1_9	ACAATTACGAATAGAATTGAA	0,35	0,07	TOXIC	0,34	0,74	---	0,467906
PACSIN2	11252	SKV_14	E04	Hs_PACSIN2_5	CACCCTTAATGTCCCGAGCAA	0,07	0,01	TOXIC	0,34	0,71	---	0,314487
IKBKE	9641	SKV_15	G10	Hs_IKBKE_7	CCGCATCATCGAACGGCTAAA	0,24	0,17	TOXIC	0,34	0,17	---	0,002777
MAP2K2	5605	SKV_20	C03	Hs_MAP2K2_6	CCGGCCTGCCATGGCCATCTT	0,13	0,06	TOXIC	0,34	0,36	---	0,108625
SGK3	23678	SKV_02	B04	Hs_SGKL_6	CCACAGCGAGACCCTAGTTAA	0,79	0,21	OK	0,34	0,29	---	0,112316
NME7	29922	SKV_11	E10	Hs_NME7_5	CCCGGCATTTACGCCCTGGAA	0,40	0,24	TOXIC	0,33	0,04	---	0,358990
CNKSR3	154043	SKV_15	B05	Hs_MAGI1_5	CCGGAGTTGTGTTACTGCTTA	0,58	0,15	OK	0,33	0,19	---	0,004524
HUNK	30811	SKV_05	C06	Hs_HUNK_6	TCGGACCAAGATCAAACCAAA	1,12	0,27	OK	0,33	0,26	---	0,090972
PIK3CA	5290	SKV_26	B09	Hs_PIK3CA_8	CTCCGTGAGGCTACATTAATA	0,90	0,29	OK	0,33	0,09	---	0,002953
ALS2CR2	55437	SKV_19	B05	Hs_ALS2CR2_5	CAGGAACACTGGTAACTATAA	0,10	0,07	TOXIC	0,33	0,51	---	0,243742
BMPR2	659	SKV_22	D04	Hs_BMPR2_5	AAGCACCGAAGCGAAACTTAA	0,65	0,15	OK	0,33	0,47	---	0,290367
KSR2	283455	SKV_24	G06	Hs_KSR2_5	CAGGCTTACCGTGGACGCCTA	0,30	0,04	TOXIC	0,33	0,60	---	0,397650
ICK	22858	SKV_10	B05	Hs_ICK_11	AAGGACTATATACATCTAATA	1,03	0,11	OK	0,33	0,17	---	0,028672
NEK6	10783	SKV_19	D10	Hs_NEK6_5	ACCGGAGAGGATCCATGAGAA	0,60	0,29	OK	0,33	0,28	---	0,058839
STK38	11329	SKV_01	G08	Hs_STK38_6	TACGTCGGCCATAAACAGCTA	0,25	0,12	TOXIC	0,33	0,41	---	0,239269
PRKAG1	5571	SKV_02	G10	Hs_PRKAG1_5	CCCTAAGATAATAGCACAACA	0,27	0,15	TOXIC	0,33	0,96	---	0,587656
DYRK3	8444	SKV_09	G05	Hs_DYRK3_10	TCGACAGTACGTGGCCCTAAA	0,34	0,36	TOXIC	0,32	0,05	---	0,000247
MAP2K3	5606	SKV_20	C04	Hs_MAP2K3_5	ACGGATATCCTGCATGTCCAA	0,15	0,03	TOXIC	0,32	0,35	---	0,112698
TNK1	8711	SKV_23	F08	Hs_TNK1_5	AAGGATCTAGTCTGCCCACTA	0,07	0,03	TOXIC	0,32	0,30	---	0,137662
PACSIN3	29763	SKV_16	D03	Hs_PACSIN3_5	AAGGATATGCTGCTCACCTTA	0,70	0,09	OK	0,32	0,17	---	0,002517
NEK8	284086	SKV_19	G06	Hs_NEK8_5	ACGGACAGTTGGGCACCAATA	0,10	0,04	TOXIC	0,32	0,23	---	0,034326
HIPK1	204851	SKV_10	C04	Hs_HIPK1_10	CTGAGCTATGTTTGTAATGCA	0,47	0,30	OK	0,32	0,15	---	0,020629
WNK4	65266	SKV_25	G10	Hs_WNK4_1	CACTAGTGTCTCAGACCAGAA	0,17	0,03	TOXIC	0,31	0,63	---	0,437770
CDKN2C	1031	SKV_16	G05	Hs_CDKN2C_5	CAGGCTTATGAATATATTTAA	0,68	0,21	OK	0,31	0,34	---	0,070261
BCR	613	SKV_02	C08	Hs_BCR_7	ACGGCAGTCCATGACGGTGAA	0,39	0,23	TOXIC	0,31	0,22	---	0,073182

Target gene	Gene ID	plate	pos.	sequence name	siRNA sequence	Mean cells	SD cells	phenotype	Mean inh.	SD inh.	phenotype	Sign. inh.
CKM	1158	SKV_10	D08	Hs_CKM_10	CTCAGTATTTGACGTGTCCAA	0,33	0,13	TOXIC	0,31	0,18	---	0,037679
MAP2K3	5606	SKV_18	E04	Hs_MAP2K3_6	CCGGGCCACCGTGAACTCACA	0,14	0,08	TOXIC	0,31	0,48	---	0,238090
CDKN2D	1032	SKV_15	C06	Hs_CDKN2D_5	ACCCAAGGGCAGAGCATTTAA	0,06	0,02	TOXIC	0,31	0,38	---	0,102497
UHMK1	127933	SKV_19	G03	Hs_UHMK1_9	TAGGTTGTCTTTAAAGATATA	0,42	0,09	OK	0,31	0,16	---	0,009144
FRK	2444	SKV_21	D08	Hs_FRK_6	CTGGGAGTACCTAGAACCCTA	0,44	0,15	OK	0,31	0,38	---	0,150042
RPS6KA2	6196	SKV_03	D03	Hs_RPS6KA2_10	CCGGAGGTCCTGAAGCGTCAA	0,58	0,20	OK	0,31	0,22	---	0,073006
PTK2B	2185	SKV_22	G07	Hs_PTK2B_14	CAGGAGAACTTAAAGCCCAAA	0,50	0,08	OK	0,31	0,20	---	0,052183
PANK4	55229	SKV_13	D08	Hs_PANK4_6	TCGACATAGGCGGGTCGTTAA	1,40	0,36	OK	0,31	0,16	---	0,002669
PIM1	5292	SKV_06	D05	Hs_PIM1_10	TGGGATAGGACTAGCACCATT	0,27	0,14	TOXIC	0,31	0,45	---	0,299947
PIK3R4	30849	SKV_19	E08	Hs_PIK3R4_7	AAGATGTACTTGACTAGTTTA	0,77	0,11	OK	0,31	0,17	---	0,010611
HK1	3098	SKV_09	B03	Hs_HK1_10	CCGTGTCGTATGACCTAGTAA	0,10	0,05	TOXIC	0,31	0,26	---	0,111977
FRK	2444	SKV_23	B08	Hs_FRK_5	CAGGACAGTCAAGGTGATATA	0,67	0,08	OK	0,31	0,11	---	0,007306
WNK3	65267	SKV_19	F06	Hs_WNK3_10	CCGGGTGACGCCAATAAAGAA	0,70	0,15	OK	0,30	0,18	---	0,015858
RIOK1	83732	SKV_04	C09	Hs_RIOK1_6	TACCATGTCCAGAACCAATAA	0,36	0,09	TOXIC	0,30	0,12	---	0,010897
MARK1	4139	SKV_06	C05	Hs_MARK1_11	AAGCTGTGATAAATACTGTAA	0,86	0,53	OK	0,30	0,31	---	0,173759
ADCK1	57143	SKV_04	C07	Hs_ADCK1_5	TACGACGGCTGTCATCAGTTA	0,44	0,25	OK	0,30	0,24	---	0,099242
UHMK1	127933	SKV_18	C03	Hs_UHMK1_8	CAGAAACATCGTGACTTTGTA	0,65	0,15	OK	0,30	0,09	---	0,000643
MAPK9	5601	SKV_08	B05	Hs_MAPK9_7	ATCGTGAACTTGTCCTCTTAA	0,51	0,18	OK	0,30	0,17	---	0,037471
FGFR4	2264	SKV_22	D05	Hs_FGFR4_6	CAGGCTCTTCCGGCAAGTCAA	0,37	0,13	TOXIC	0,30	0,22	---	0,078550
FES	2242	SKV_22	G09	Hs_FES_6	CAGCCTGAGGCTGAGTACCAA	0,31	0,16	TOXIC	0,30	0,40	---	0,267615
PAK3	5063	SKV_18	D09	Hs_PAK3_5	TTCCAGTACTTTGTACAGGAA	0,47	0,15	OK	0,30	0,63	---	0,380224
PMVK	10654	SKV_13	C04	Hs_PMVK_5	CCCAGTGTGGATACTAATAAA	0,74	0,04	OK	0,29	0,15	---	0,003450
GAK	2580	SKV_15	D07	Hs_GAK_5	ACGCGTGTGACATTCAAGAAA	0,17	0,13	TOXIC	0,29	0,20	---	0,012979
MAP3K8	1326	SKV_25	E04	Rn_Map3k8_1	ATCCCTCCTACCTGTACATAA	0,61	0,23	OK	0,29	0,25	---	0,115091
PANK2	80025	SKV_12	B06	Hs_PANK2_5	CAGAGCGACTTTGATCACCAT	0,16	0,07	TOXIC	0,29	0,43	---	0,314499
GSK3A	2931	SKV_09	D07	Hs_GSK3A_12	AAGAAAGACGAGCTTTACCTA	0,93	0,20	OK	0,29	0,13	---	0,018476
STK35	140901	SKV_25	C10	Hs_STK35_6	TGCCGTTGTCGTGTTCTCACA	0,51	0,07	OK	0,28	0,17	---	0,046445
CDK7	1022	SKV_05	G09	Hs_CDK7_5	CCGGATGGCTCTGGACGTGAA	0,66	0,28	OK	0,28	0,26	---	0,129143
ADRBK2	157	SKV_02	F04	Hs_ADRBK2_6	CAAGTGTATGGGATTAACTAA	0,73	0,26	OK	0,28	0,13	---	0,021717
MYLK2	85366	SKV_07	B08	Hs_MYLK2_6	CGGGATCCTCTTCATGCACAA	0,56	0,40	OK	0,28	0,34	---	0,230801
PRKACA	5566	SKV_02	G07	Hs_PRKACA_6	CAGAAGGTGGTGAAACTGAAA	0,60	0,28	OK	0,28	0,36	---	0,254908
MAP3K11	4296	SKV_24	C05	Hs_MAP3K11_5	CCGGAGGAGAAACGTCTTCGA	0,38	0,19	TOXIC	0,27	0,21	---	0,082399
TNIK	23043	SKV_20	E09	Hs_TNIK_6	CTGGAATATAAGCGCAAACAA	0,11	0,07	TOXIC	0,27	0,29	---	0,108627
UGP2	7360	SKV_12	G04	Hs_UGP2_6	CCCAAAGTTAGTTACTCTTAA	0,81	0,30	OK	0,27	0,30	---	0,192587
CDC42BPG	55561	SKV_03	G03	Hs_CDC42BPG_5	CGCCGGTGGCTTTGCACTCTA	0,63	0,40	OK	0,27	0,37	---	0,267818
PI4K2A	55361	SKV_11	G03	Hs_PI4KII_6	CCGCATCGGGCTACCACCAAA	0,42	0,34	OK	0,27	0,14	---	0,512684
NEK3	4752	SKV_15	E03	Hs_NEK3_10	CAGAGATATCAAGTCCAAGAA	0,06	0,03	TOXIC	0,27	0,71	---	0,413839
PIP5K1B	8395	SKV_12	G08	Hs_PIP5K1B_10	CACCAGAATTATCCACAGCAA	0,71	0,20	OK	0,27	0,50	---	0,400181
GKAP1	80318	SKV_16	E08	Hs_GKAP1_6	CATGCTGTTTGTAACGCTCAA	0,40	0,09	OK	0,27	0,13	---	0,002100

Target gene	Gene ID	plate	pos.	sequence name	siRNA sequence	Mean cells	SD cells	phenotype	Mean inh.	SD inh.	phenotype	Sign. inh.
PDLIM5	10611	SKV_14	D07	Hs_PDLIM5_5	CAGCAGGGAAACGAACTCCGA	0,49	0,36	OK	0,27	0,59	---	0,346279
AAK1	22848	SKV_17	G03	Hs_AAK1_5	AACGTGAGTAGCGGTGATGTA	0,29	0,05	TOXIC	0,26	0,45	---	0,281124
PRKAR2A	5576	SKV_11	B07	Hs_PRKAR2A_6	AACTTGAAAGTCAGCACTAAA	0,86	0,06	OK	0,26	0,34	---	0,544527
PRKCQ	5588	SKV_03	C04	Hs_PRKCQ_7	CAGATTTAAAGTCTACAATTA	0,32	0,10	TOXIC	0,26	0,13	---	0,026739
WEE1	7465	SKV_25	B05	Hs_WEE1_8	CAAGACCTGCTAAGAGAATTA	0,09	0,06	TOXIC	0,26	0,84	---	0,622222
CDKN1B	1027	SKV_16	F09	Hs_CDKN1B_6	ACCGACGATTCTTCTACTCAA	0,16	0,09	TOXIC	0,25	0,07	---	0,000027
BCR	613	SKV_03	G08	Hs_BCR_8	CAGCATTCCGCTGACCATCAA	0,14	0,08	TOXIC	0,25	0,44	---	0,375606
MAP3K9	4293	SKV_25	G04	Hs_MAP3K9_6	ACCATAGAGAATGTTCGCCAA	0,99	0,20	OK	0,25	0,14	---	0,036438
ABL1	25	SKV_20	F09	Hs_ABL1_11	CCAGTGGAGATAACACTCTAA	0,53	0,03	OK	0,25	0,18	---	0,035234
ERN2	10595	SKV_17	F06	Hs_ERN2_5	AAGGATGAAACTGGCTTCTAT	0,55	0,13	OK	0,25	0,21	---	0,054550
SKP1A	6500	SKV_25	B04	Hs_SKP1A_9	TCGCAAGACCTTCAATATCAA	0,58	0,11	OK	0,25	0,30	---	0,216041
TSSK2	23617	SKV_05	C03	Hs_STK22B_6	GTCGGCCTTCACGTAAACTAA	0,47	0,28	OK	0,25	0,33	---	0,263675
PINK1	65018	SKV_19	F03	Hs_PINK1_3	CCGGACGCTGTTCCTCGTTAT	0,63	0,28	OK	0,25	0,16	---	0,023272
DYRK1B	9149	SKV_08	D03	Hs_DYRK1B_5	AAGGACGAAAGAACTCAGGAA	0,16	0,06	TOXIC	0,24	0,07	---	0,003166
FN3K	64122	SKV_11	G08	Hs_FN3K_6	CCCAGTGTTCGTCAAAGTCAA	0,58	0,23	OK	0,24	0,04	---	0,599254
NEK8	284086	SKV_18	C06	Hs_NEK8_6	CCAGAAGCTGGTGATCATCAA	0,56	0,13	OK	0,24	0,06	---	0,000204
AK3	50808	SKV_11	F03	Hs_AK3L1_5	CCCGTGGCACTATGTAAATAA	0,24	0,19	TOXIC	0,24	0,24	---	0,612108
LMTK2	22853	SKV_22	C04	Hs_LMTK2_5	CACCTCCGACTTAAATGTGAA	1,05	0,23	OK	0,24	0,04	---	0,000786
PBK	55872	SKV_17	G10	Hs_PBK_5	AAGTGTGGCTTGCGTAAATAA	0,16	0,10	TOXIC	0,24	0,37	---	0,254437
NADK	65220	SKV_13	F03	Hs_FLJ13052_5	AAAGAGCGTCCTTGTCATCAA	0,72	0,46	OK	0,23	0,29	---	0,106305
PCTK3	5129	SKV_07	G04	Hs_PCTK3_6	CAGGTTGGATACGGATGGCAT	0,22	0,15	TOXIC	0,23	0,77	---	0,631319
HUNK	30811	SKV_06	G06	Hs_HUNK_5	CACGGGCAAAGTGCCCTGTAA	0,10	0,11	TOXIC	0,23	0,62	---	0,558040
CAMKK2	10645	SKV_17	F07	Hs_CAMKK2_6	CCGCAAGATCTTCTCTGGGAA	0,78	0,11	OK	0,23	0,16	---	0,029054
CSNK2B	1460	SKV_15	D05	Hs_CSNK2B_5	CAGGTCCCTCACTACCGACAA	0,12	0,08	TOXIC	0,22	0,26	---	0,094388
PRKY	5616	SKV_03	C08	Hs_PRKY_1	CAGCAGTACAGTCCTTCCTAA	0,17	0,13	TOXIC	0,22	0,46	---	0,442375
UCK1	83549	SKV_13	F08	Hs_UCK1_6	AAGGCTGGTTGTGGCCTACAA	0,26	0,15	TOXIC	0,22	0,46	---	0,303777
PRKACG	5568	SKV_01	C09	Hs_PRKACG_6	CTGGATCGCCATCTATGAGAA	0,37	0,21	TOXIC	0,22	0,40	---	0,382641
MAPKAP1	79109	SKV_14	G07	Hs_MAPKAP1_6	CTAGGTATCTCTGGAGACAAA	0,37	0,16	TOXIC	0,22	0,59	---	0,414829
SRPK1	6732	SKV_08	B10	Hs_SRPK1_9	GAGGATCTACATAATGCTAAT	0,60	0,25	OK	0,22	0,38	---	0,365639
ERBB2	2064	SKV_21	C04	Hs_ERBB2_14	AACAAAGAAATCTTAGACGAA	0,61	0,23	OK	0,22	0,04	---	0,000039
MAPK8IP1	9479	SKV_12	E06	Hs_MAPK8IP1_3	CTGGAGGAGTTTGAGGATGAA	0,25	0,34	TOXIC	0,22	2,06	---	0,861951
HCK	3055	SKV_23	B10	Hs_HCK_8	CCGGGATAGCGAGACCACTAA	0,29	0,04	TOXIC	0,22	0,20	---	0,127340
MAPK9	5601	SKV_09	F05	Hs_MAPK9_6	AAAGTCGATTTATGTGTATTA	1,13	0,25	OK	0,22	0,37	---	0,366188
SNF1LK	150094	SKV_07	C04	Hs_SNF1LK_12	ATGCTTTACATCGTCACTGAA	0,71	0,20	OK	0,22	0,13	---	0,039321
MAP3K6	9064	SKV_20	D08	Hs_MAP3K6_5	CACCATCCAAATGCTGTTGAA	0,60	0,33	OK	0,22	0,26	---	0,140575
HIPK2	28996	SKV_10	B07	Hs_HIPK2_6	TCCCGAAGTCTCCATACTAAA	1,06	0,32	OK	0,22	0,04	---	0,000837
IKBKE	9641	SKV_17	E10	Hs_IKBKE_6	ACGGCGGAACAAGGAGATCAT	0,78	0,14	OK	0,21	0,10	---	0,004869
EPHA2	1969	SKV_19	C08	Hs_EPHA2_8	TCGGACAGACATATAGGATAT	0,21	0,07	TOXIC	0,21	0,15	---	0,032355
TPD52L3	89882	SKV_12	B09	Hs_NYD-SP25_10	CACGTTAAATCAAGGAAGGAA	0,12	0,03	TOXIC	0,21	0,47	---	0,480091

Target gene	Gene ID	plate	pos.	sequence name	siRNA sequence	Mean cells	SD cells	phenotype	Mean inh.	SD inh.	phenotype	Sign. inh.
FER	2241	SKV_21	C08	Hs_FER_6	CAGAACAACTTAGTAGGATAA	0,41	0,21	OK	0,21	0,36	---	0,287518
PFKFB2	5208	SKV_09	C07	Hs_PFKFB2_5	CCAGAGCAAGATAGTCTACTA	0,26	0,23	TOXIC	0,21	0,02	---	0,000122
MAP3K4	4216	SKV_20	B05	Hs_MAP3K4_6	CTCAAGCATCGCATAGTTTAA	0,40	0,12	TOXIC	0,21	0,25	---	0,141805
YES1	7525	SKV_22	B07	Hs_YES1_7	GAGGCTCCTGCTTATTTATAA	0,42	0,07	OK	0,21	0,19	---	0,124969
AURKA	6790	SKV_19	G07	Hs_AURKA_4	CAGGGCTGCCATATAACCTGA	0,20	0,06	TOXIC	0,21	0,32	---	0,242519
CSNK1G1	53944	SKV_05	F05	Hs_CSNK1G1_5	ATGGACCATCCTAGTAGGGAA	1,01	0,26	OK	0,21	0,46	---	0,474350
ROR1	4919	SKV_21	F07	Hs_ROR1_5	CCCAGTGAGTAATCTCAGTAA	0,39	0,41	TOXIC	0,20	0,35	---	0,287087
PLK2	10769	SKV_17	F09	Hs_PLK2_7	CACCTTTCAGGTGAATTTCTA	1,00	0,34	OK	0,20	1,00	---	0,698757
MELK	9833	SKV_04	G10	Hs_MELK_6	CTGGATCATGCAAGATTACAA	0,57	0,07	OK	0,20	0,36	---	0,389282
CAMKK1	84254	SKV_19	F08	Hs_CAMKK1_5	AGCGATGAGCAAACTCTATAA	0,44	0,15	OK	0,20	0,29	---	0,217120
PRKAG2	51422	SKV_02	B08	Hs_PRKAG2_5	TTCCAGTGATGTTGAAATTAA	0,60	0,15	OK	0,20	0,09	---	0,020274
PANK3	79646	SKV_12	B04	Hs_PANK3_1	AAGCGAGAATCTGTTAGTAAA	0,74	0,55	OK	0,20	0,29	---	0,298098
PNCK	139728	SKV_25	G03	Hs_PNCK_8	ACACTGGAAGCGAGCCTTCAA	0,33	0,22	TOXIC	0,20	0,19	---	0,145521
MAPK8	5599	SKV_08	B03	Hs_MAPK8_13	GCCCAGTAATATAGTAGTAAA	0,89	0,01	OK	0,20	0,10	---	0,029693
NRGN	4900	SKV_13	G10	Hs_NRGN_11	CTTGCTCTGACCGGAAGAGAA	0,80	0,13	OK	0,20	0,24	---	0,100846
DGKA	1606	SKV_08	F10	Hs_DGKA_5	ATCCATCTTCTCAACATGCAA	0,89	0,28	OK	0,20	0,72	---	0,657778
CSNK1D	1453	SKV_05	E06	Hs_CSNK1D_5	CCGGTCTAGGATCGAAATGTT	0,53	0,12	OK	0,20	0,11	---	0,031686
CDKN2A	1029	SKV_16	G03	Hs_CDKN2A_12	CACGCCCTAAGCGCACATTCA	0,08	0,05	TOXIC	0,20	0,26	---	0,127627
SMG1	23049	SKV_04	C03	Hs_SMG1_7	CAGAATCTGGTTGATAATATA	0,20	0,12	TOXIC	0,20	0,19	---	0,139734
MAPK11	5600	SKV_09	F04	Hs_MAPK11_6	CTGAGCGACGAGCACGTTCAA	0,91	0,27	OK	0,20	0,15	---	0,092501
NRGN	4900	SKV_25	F03	Hs_NRGN_7	AACAATAAAGAGGAATGTCCA	0,39	0,06	TOXIC	0,20	0,22	---	0,202880
MAP4K5	11183	SKV_18	G07	Hs_MAP4K5_5	CTTGCCTATTTGCATACTAAA	0,58	0,73	OK	0,20	0,26	---	0,173139
PRKCZ	5590	SKV_01	E05	Hs_PRKCZ_5	CGGAAGCATGACAGCATTAAA	0,78	0,13	OK	0,19	0,19	---	0,154938
TPK1	27010	SKV_11	E09	Hs_TPK1_5	AACCTGGTGCATCGAAATGTA	0,63	0,15	OK	0,19	0,12	---	0,752444
TGFBR2	7048	SKV_24	C09	Hs_TGFBR2_6	CTCCAATATCCTCGTGAAGAA	0,49	0,07	OK	0,19	0,07	---	0,011080
RPS6KA4	8986	SKV_01	F08	Hs_RPS6KA4_5	CAGGCTGTGCCTTTGACTTTA	0,48	0,10	OK	0,19	0,18	---	0,145973
KDR	3791	SKV_23	C07	Hs_KDR_6	AAGGCTAATACAACTCTTCAA	0,27	0,05	TOXIC	0,19	0,28	---	0,291344
BRSK2	9024	SKV_04	G05	Hs_STK29_6	GCGAGCTACTGTAAACTTTAA	0,16	0,05	TOXIC	0,19	0,28	---	0,314431
CMPK	51727	SKV_13	D05	Hs_CMPK_4	AACATGGTAATTACTAAATTA	0,93	0,23	OK	0,19	0,32	---	0,227903
PDXK	8566	SKV_19	F09	Hs_PDXK_10	ATGGCTGTTATGGCTGAATTA	0,26	0,05	TOXIC	0,19	0,29	---	0,246674
TTBK1	84630	SKV_07	D06	Hs_TTBK1_6	TGGCAGGAACGAGAAGTTTAA	1,06	0,40	OK	0,19	0,29	---	0,323031
RPS6KC1	26750	SKV_03	F06	Hs_RPS6KC1_11	CTGGTGAATTGGAGTCAACAA	0,05	0,02	TOXIC	0,19	0,78	---	0,700959
CAMK4	814	SKV_06	B05	Hs_CAMK4_5	CAGAAGCCTTATGCTCTCAAA	0,55	0,36	OK	0,19	0,10	---	0,034896
PIK3C3	5289	SKV_15	E07	Hs_PIK3C3_5	AACGCGAAAGTGGAAATCGTA	1,03	0,27	OK	0,19	0,12	---	0,010472
MVK	4598	SKV_09	B10	Hs_MVK_6	GCGGTGGGCCTGGTTAAATAA	0,56	0,20	OK	0,18	0,19	---	0,167918
DMPK	1760	SKV_02	F07	Hs_DMPK_2	GAGCCTGAGGGCTAAATTTAA	0,67	0,29	OK	0,18	0,44	---	0,509032
TESK2	10420	SKV_24	D06	Hs_TESK2_5	CCGGGAAGAATCGCTATCTGA	1,22	0,07	OK	0,18	0,28	---	0,327756
PRKCB1	5579	SKV_03	B05	Hs_PRKCB1_6	CCGGATGAAACTGACCGATTT	0,63	0,17	OK	0,18	0,16	---	0,119392
AURKC	6795	SKV_15	F09	Hs_AURKC_5	AAGATGTAAGATGCTAATTAA	0,84	0,13	OK	0,18	0,16	---	0,033773

Target gene	Gene ID	plate	pos.	sequence name	siRNA sequence	Mean cells	SD cells	phenotype	Mean inh.	SD inh.	phenotype	Sign. inh.
MARK2	2011	SKV_04	E03	Hs_MARK2_6	CACCTCTAATTCTTACTCTAA	0,57	0,30	OK	0,18	0,10	---	0,038080
TWF1	5756	SKV_02	D05	Hs_PTK9_6	ACCGGCATCCAAGCAAGTGAA	0,25	0,13	TOXIC	0,18	0,14	---	0,098310
ERN1	2081	SKV_17	B06	Hs_ERN1_6	CAGGACGTGAGCGACAGAATA	0,56	0,17	OK	0,18	0,05	---	0,000307
GRK5	2869	SKV_02	F09	Hs_GRK5_7	CCCGCCAGATCTGAACAGAAA	0,72	0,46	OK	0,18	0,23	---	0,258376
IHPK1	9807	SKV_13	B08	Hs_IHPK1_9	AAGGTGGATGTCCGCATGATT	0,72	0,12	OK	0,17	0,29	---	0,216798
STK38L	23012	SKV_03	E10	Hs_STK38L_6	TACAACCATGATAACCATTAT	0,39	0,06	TOXIC	0,17	0,26	---	0,309120
FN3K	64122	SKV_13	E08	Hs_FN3K_5	CCAGCTGTTTAACTACCTGAA	0,89	0,34	OK	0,17	0,31	---	0,241085
CDK6	1021	SKV_05	G08	Hs_CDK6_5	AAGACTCAAGGTGGTCAGTAA	0,30	0,16	TOXIC	0,17	0,25	---	0,306823
PNKP	11284	SKV_11	E05	Hs_PNKP_7	CTGGAGGATCTTGTACCCAGA	0,67	0,29	OK	0,17	0,23	---	0,829764
CALM2	805	SKV_08	F03	Hs_CALM2_8	GACCTTGTACAGAATGTGTTA	0,60	0,18	OK	0,17	0,38	---	0,482254
TLK2	11011	SKV_25	B07	Hs_TLK2_7	GTCGGATCCTTGAGTGATAAA	0,55	0,09	OK	0,17	0,20	---	0,219322
PRKD2	25865	SKV_05	C05	Hs_PRKD2_5	CACGACCAACAGATACTATAA	0,21	0,04	TOXIC	0,17	0,39	---	0,504214
PIM1	5292	SKV_04	F05	Hs_PIM1_6	CAACATTTACAACTCATTCCA	0,58	0,21	OK	0,17	0,13	---	0,088289
RAF1	5894	SKV_24	C06	Hs_RAF1_7	TGGGAAATAGAAGCCAGTGAA	0,52	0,22	OK	0,17	0,48	---	0,584272
CSK	1445	SKV_19	C06	Hs_CSK_2	CCGGTACAGAATGTATTGCCA	0,23	0,07	TOXIC	0,16	0,18	---	0,119363
NEK1	4750	SKV_15	D09	Hs_NEK1_5	ATGGCTCTCTCTACATAGTAA	0,63	0,28	OK	0,16	0,17	---	0,070203
MVK	4598	SKV_10	F10	Hs_MVK_5	CCGCTTGGCGATGCCAGCCAA	0,25	0,19	TOXIC	0,16	0,43	---	0,548784
MYLK2	85366	SKV_05	D08	Hs_MYLK2_5	AACGCTGTAACCGACGCCTTA	1,19	0,20	OK	0,16	0,13	---	0,102828
MAST4	375449	SKV_19	B08	Hs_LOC375449_5	GAGGAGCTTGACCACATATTA	0,85	0,20	OK	0,16	0,10	---	0,019254
ADCK5	203054	SKV_04	D04	Hs_ADCK5_5	AAGGCCTTTGCTGAGCAGATA	0,09	0,02	TOXIC	0,16	0,44	---	0,568596
DAPK3	1613	SKV_04	D10	Hs_DAPK3_3	CCCAGAGATTGTGAACTATGA	0,29	0,12	TOXIC	0,16	0,26	---	0,361310
PANK1	53354	SKV_11	F06	Hs_PANK1_6	CCGAAGGATATTACAGCCGAA	0,74	0,22	OK	0,15	0,27	---	0,881513
PDGFRA	5156	SKV_23	D10	Hs_PDGFRA_7	CGCAGGAAGCCTACTATTTAA	0,40	0,08	OK	0,15	0,01	---	0,000035
PI4KB	5298	SKV_12	F03	Hs_PIK4CB_6	CGACATGTTCAACTACTATAA	0,29	0,14	TOXIC	0,15	0,24	---	0,320264
ATR	545	SKV_03	G07	Hs_ATR_2	CCGCTAATCTTCTAACATTAA	0,35	0,21	TOXIC	0,15	0,59	---	0,680256
STK25	10494	SKV_18	G05	Hs_STK25_7	CCGGCCGAGTCCACACAGCAA	0,27	0,10	TOXIC	0,15	0,65	---	0,656281
DGKQ	1609	SKV_10	E05	Hs_DGKQ_6	CCGGAAGGTGACGCTCACCAA	0,37	0,18	TOXIC	0,15	0,74	---	0,748356
DBF4	10926	SKV_14	D08	Hs_ASK_9	CAGGTTAAACTAAGAATCCAA	0,62	0,42	OK	0,15	0,35	---	0,380837
MAP3K7IP2	23118	SKV_16	C06	Hs_MAP3K7IP2_6	TGGCTGGGTATCTCAGTTTAA	0,58	0,09	OK	0,15	0,05	---	0,000512
BMPR2	659	SKV_24	B04	Hs_BMPR2_6	CTCGTAAGTATGTAAAGGAAA	0,48	0,12	OK	0,14	0,52	---	0,652501
MAPK4	5596	SKV_07	G08	Hs_MAPK4_5	AAGGATCGTTGATCAGCATTA	0,54	0,25	OK	0,14	0,75	---	0,759242
AXL	558	SKV_20	G03	Hs_AXL_9	CCGGTGTTCTAAGATGTGATA	1,03	0,15	OK	0,14	0,13	---	0,067777
ACVRL1	94	SKV_23	G08	Hs_ACVRL1_11	CTGGGTAGAGGTAGTGTGAGT	0,88	0,01	OK	0,14	0,07	---	0,026726
PGK1	5230	SKV_09	C10	Hs_PGK1_6	GAGGAACGGATCAGATGTCTA	0,36	0,12	TOXIC	0,14	0,56	---	0,689693
AKT3	10000	SKV_03	E05	Hs_AKT3_7	AACTGTTGGCTTTGGATTAAA	0,78	0,12	OK	0,14	0,19	---	0,266807
DAPK1	1612	SKV_06	B09	Hs_DAPK1_6	CGGCTATTACTCTGTGGCCAA	0,56	0,28	OK	0,14	0,33	---	0,514003
LYN	4067	SKV_23	C10	Hs_LYN_12	CCCGGACGACTTGTCTTTCAA	0,93	0,06	OK	0,14	0,17	---	0,230526
ACVRL1	94	SKV_26	B04	Hs_ACVRL1_6	CAGCTTTGAGGACATGAAGAA	0,31	0,09	TOXIC	0,14	0,64	---	0,729137
CKB	1152	SKV_08	F07	Hs_CKB_2	CCAGATTGAAACTCTCTTCAA	0,70	0,25	OK	0,14	0,46	---	0,635524

Target gene	Gene ID	plate	pos.	sequence name	siRNA sequence	Mean cells	SD cells	phenotype	Mean inh.	SD inh.	phenotype	Sign. inh.
FUK	197258	SKV_13	G05	Hs_FUK_5	CCGAAGGGAGTTGATTGGACA	0,87	0,26	OK	0,14	0,56	---	0,595159
AK3L1	205	SKV_10	C09	Hs_AK3_9	CAGGAAGATGTGGTCATTCAT	0,32	0,18	TOXIC	0,14	0,26	---	0,416570
NEK7	140609	SKV_19	G04	Hs_NEK7_5	ACGACCGGATATGGGCTATAA	0,10	0,07	TOXIC	0,13	0,54	---	0,637027
WNK4	65266	SKV_18	B05	Hs_WNK4_5	CAGGAGGAGCCAGCACCATTA	0,21	0,08	TOXIC	0,13	0,16	---	0,138415
PIP4K2B	8396	SKV_11	C09	Hs_PIP5K2B_6	CAAGGACTTGCCAACATTCAA	0,38	0,01	TOXIC	0,13	0,09	---	0,954650
MKNK2	2872	SKV_04	E04	Hs_MKNK2_5	CCGCTTCTACCTGGTGTTTGA	0,95	0,30	OK	0,13	0,16	---	0,227634
STK25	10494	SKV_20	E05	Hs_STK25_5	CACCAAGCTATGGATCATCAT	0,67	0,12	OK	0,13	0,16	---	0,144322
PIK3R3	8503	SKV_17	E04	Hs_PIK3R3_13	CCAAATAACAATATAGAACAA	0,68	0,21	OK	0,13	0,10	---	0,046769
PDK2	5164	SKV_02	C09	Hs_PDK2_5	AAGAACCTTGTTAGACCGAGA	0,58	0,09	OK	0,13	0,04	---	0,005007
PRKCB1	5579	SKV_01	D05	Hs_PRKCB1_5	CAAGAGCTAAGTAGATGTGTA	0,64	0,23	OK	0,13	0,13	---	0,165610
ROCK2	9475	SKV_03	E03	Hs_ROCK2_5	AAGCTACATATGGAGCTTAAA	0,25	0,08	TOXIC	0,13	0,34	---	0,550621
ALPK2	115701	SKV_04	D03	Hs_ALPK2_7	CAGGGATGGGAAAGAAATAAA	0,50	0,26	OK	0,13	0,32	---	0,522830
OSR1	130497	SKV_25	C06	Hs_OXSR1_7	AAAGAGTAAATTGTCCTTAAA	0,71	0,13	OK	0,13	0,34	---	0,554039
SLK	9748	SKV_18	G03	Hs_SLK_5	CCAGATCAGGACCGTGATAAA	0,51	0,26	OK	0,12	0,31	---	0,455171
TESK2	10420	SKV_24	F06	Hs_TESK2_6	CGAGATGAGCCCTATAATGAA	0,55	0,09	OK	0,12	0,17	---	0,283699
VRK2	7444	SKV_05	F03	Hs_VRK2_5	CAGGTTTATCTTGCAGATTAT	0,12	0,08	TOXIC	0,12	0,66	---	0,765294
CDK4	1019	SKV_05	G06	Hs_CDK4_1	CCGAACTGACCGGGAGATCAA	0,96	0,36	OK	0,12	0,42	---	0,650877
ILKAP	80895	SKV_14	G09	Hs_ILKAP_5	TTCGGTGATCTTTGGTCTGAA	0,34	0,58	TOXIC	0,12	0,53	---	0,638279
PIP5K1A	8394	SKV_12	G07	Hs_PIP5K1A_6	CCCTGCCTTGATAATATGTTA	1,16	0,25	OK	0,12	0,11	---	0,148734
PRKAG1	5571	SKV_01	C10	Hs_PRKAG1_6	TTGGCCCTGATTCAACCCTAA	0,45	0,17	OK	0,12	0,62	---	0,763179
RPS6KC1	26750	SKV_02	B06	Hs_RPS6KC1_6	ATCAGTAAATTTCTAAACAGA	0,79	0,38	OK	0,11	0,15	---	0,247555
MST1R	4486	SKV_23	D05	Hs_MST1R_6	TCCCGGTGACACAGACACAAA	0,53	0,06	OK	0,11	0,04	---	0,008089
SKP1A	6500	SKV_25	C04	Hs_SKP1A_10	AAGATGATGAGAACAAAGAAA	0,79	0,10	OK	0,11	0,24	---	0,466794
AK3	50808	SKV_13	D03	Hs_AK3L1_6	CCGTGGCACTATGTAAATAAA	0,72	0,15	OK	0,11	0,23	---	0,331235
CDK3	1018	SKV_05	G05	Hs_CDK3_5	ATGGATATGTTCCAGAAGGTA	0,54	0,29	OK	0,11	0,16	---	0,298444
MAPKBP1	23005	SKV_14	E05	Hs_MAPKBP1_5	CAGGACCGAAATATTCGGATA	0,80	0,09	OK	0,11	0,17	---	0,187492
NAGK	55577	SKV_13	E05	Hs_NAGK_6	CCCGGTCTTGTTCCAGGGCAA	1,02	0,30	OK	0,11	0,21	---	0,282916
MAP3K8	1326	SKV_25	D04	Hs_MAP3K8_7	AAGGATAATAGAGTAGCCTAA	0,23	0,08	TOXIC	0,11	0,40	---	0,667704
PRKDC	5591	SKV_04	B04	Hs_PRKDC_5	CTCGTGTATTACAGAAGGAAA	0,48	0,25	OK	0,11	0,12	---	0,209626
NUAK2	81788	SKV_05	D05	Hs_SNARK_5	GACCATAAGATCCTAGTGAAA	0,74	0,37	OK	0,11	0,26	---	0,527662
PKM2	5315	SKV_12	F06	Hs_PKM2_6	CCCGATCAGTGGAGACGTTGA	1,38	0,50	OK	0,10	0,07	---	0,071791
DYRK4	8798	SKV_08	C07	Hs_DYRK4_5	CTCCATATGAACAAAGTGAAA	1,15	0,17	OK	0,10	0,33	---	0,621259
CKMT1B	1159	SKV_10	D09	Hs_CKMT1_6	CTGGACGTTACTATAGGCTCA	0,20	0,05	TOXIC	0,10	0,16	---	0,344447
FGFR3	2261	SKV_21	D03	Hs_FGFR3_6	CCGATGTTATTAGATGTTACA	0,68	0,33	OK	0,10	1,09	---	0,860242
MAPK10	5602	SKV_09	F06	Hs_MAPK10_6	TCCGAGCACAATAAACTCAAA	1,05	0,20	OK	0,10	0,32	---	0,620960
PICK1	9463	SKV_14	C03	Hs_PRKCABP_5	TCGCCTCACCATCAAGAAGTA	0,13	0,05	TOXIC	0,10	0,43	---	0,618668
PRKAA2	5563	SKV_25	C03	Hs_PRKAA2_7	ATGGAAGGTAGTGAATGCATA	0,72	0,18	OK	0,10	0,12	---	0,235942
STK10	6793	SKV_20	D04	Hs_STK10_6	CAGCTCAAACTGATGAAGAAA	0,27	0,06	TOXIC	0,10	0,30	---	0,534260
AKAP1	8165	SKV_12	D06	Hs_AKAP1_10	CACGCAGAGATGACAGTACAA	0,32	0,16	TOXIC	0,10	0,30	---	0,605110

Target gene	Gene ID	plate	pos.	sequence name	siRNA sequence	Mean cells	SD cells	phenotype	Mean inh.	SD inh.	phenotype	Sign. inh.
AXL	558	SKV_19	C03	Hs_AXL_10	TCCAAGATTCTAGATGATTAA	0,53	0,19	OK	0,10	0,31	---	0,560632
ITPKB	3707	SKV_09	B08	Hs_ITPKB_6	GACGTAAAGATTCTATGAATA	0,84	0,31	OK	0,09	0,16	---	0,366612
AK7	122481	SKV_12	C04	Hs_AK7_6	CAAGATTGTCTTGACCATTTA	0,88	0,31	OK	0,09	0,13	---	0,280571
KSR1	8844	SKV_24	D04	Hs_KSR_9	AAGGGCGAAGCTGGTCCGTTA	1,02	0,16	OK	0,09	0,28	---	0,596891
CDKL2	8999	SKV_09	G10	Hs_CDKL2_6	TTCTACGGACTTTAAATTAAA	1,09	0,15	OK	0,09	0,37	---	0,708464
AKT1	207	SKV_01	B05	Hs_AKT1_11	CACCATGAGCGACGTGGCTAT	0,42	0,28	OK	0,09	0,50	---	0,783905
PDIK1L	149420	SKV_18	C05	Hs_PDIK1L_6	CAGCCAAAGTACGATCTAATA	0,90	0,18	OK	0,09	0,12	---	0,213162
PIK3C2A	5286	SKV_15	E04	Hs_PIK3C2A_5	CAAGATGGTCGAATCAAGGAA	0,58	0,23	OK	0,08	0,27	---	0,506014
RP6-213H19.1	51765	SKV_19	B04	Hs_MST4_5	CCAAACCTACGTCAAGATTAA	0,34	0,09	TOXIC	0,08	0,29	---	0,586738
MAP2K4	6416	SKV_18	E09	Hs_MAP2K4_7	AGGGAGAATGGTGCTGTTTAA	0,49	0,12	OK	0,08	0,28	---	0,575662
C17orf75	64149	SKV_11	G09	Hs_NJMU-R1_9	CAGGCTTGAATTGGACAAGTA	0,62	0,43	OK	0,08	0,34	---	0,869551
PRKAR2B	5577	SKV_11	B08	Hs_PRKAR2B_5	ACGAACATGGATATTGTTGAA	0,80	0,12	OK	0,08	0,22	---	0,867673
BUB1	699	SKV_15	B07	Hs_BUB1_5	CAGCTTGTGATAAAGAGTCAA	0,37	0,10	TOXIC	0,08	0,22	---	0,443854
ILKAP	80895	SKV_16	E09	Hs_ILKAP_8	ATGGAGGAATTCGAGCCTCAA	0,73	0,12	OK	0,08	0,15	---	0,292879
SRPK1	6732	SKV_09	F10	Hs_SRPK1_7	ACGCTTATGGAACGTGATACA	0,28	0,09	TOXIC	0,08	0,23	---	0,600986
PANK2	80025	SKV_13	F06	Hs_PANK2_6	CTGTGTGTGAACTTACTGTAA	1,27	0,37	OK	0,08	0,29	---	0,567167
MAP3K5	4217	SKV_20	B06	Hs_MAP3K5_5	CAGCGAGTAGATAATATCGAA	0,83	0,07	OK	0,08	0,13	---	0,289361
RPS6KL1	83694	SKV_02	C04	Hs_RPS6KL1_5	CGCGATGTTAGTGAGGACTAT	0,74	0,56	OK	0,07	0,35	---	0,732709
UGP2	7360	SKV_11	C04	Hs_UGP2_5	CGAGTTCAAGTCTGTATCAAA	0,86	0,18	OK	0,07	0,16	---	0,842387
TLK2	11011	SKV_25	C07	Hs_TLK2_8	AACGTTAACGTTAGCAGAATA	0,57	0,07	OK	0,07	0,21	---	0,573409
NEK2	4751	SKV_15	D10	Hs_NEK2_6	TTACGAGGATGTTAAACTTAA	0,71	0,22	OK	0,07	0,08	---	0,074268
MAP3K2	10746	SKV_18	G06	Hs_MAP3K2_7	CAGAATGATGTCCGAGTCAAA	0,53	0,26	OK	0,07	0,07	---	0,093104
DYRK1A	1859	SKV_09	D06	Hs_DYRK1A_5	CAAGAATGGGTTGCCATTAAA	0,91	0,06	OK	0,07	0,11	---	0,330905
MAPK1	5594	SKV_09	E06	Hs_MAPK1_13	ATCATGGTAGTCACTAACATA	1,20	0,28	OK	0,07	0,36	---	0,751707
UCKL1	54963	SKV_13	D07	Hs_UCKL1_6	TACAATGAACACGGCACGCAA	0,44	0,19	OK	0,07	0,21	---	0,477356
NEK2	4751	SKV_17	B10	Hs_NEK2_5	TACGAGGATGTTAAACTTAAA	0,80	0,15	OK	0,07	0,34	---	0,704017
CAMK1G	57172	SKV_05	C10	Hs_CAMK1G_5	AACAGGCCGCCTGAAACTCAA	0,36	0,23	TOXIC	0,07	0,29	---	0,709133
BAIAP2L1	55971	SKV_16	D09	Hs_LOC55971_5	CACGGAGAGCACCTACCGGAA	0,45	0,12	OK	0,07	0,28	---	0,616535
NME6	10201	SKV_11	E03	Hs_NME6_5	CAGACTTCTCCTAGACATCTA	0,38	0,20	TOXIC	0,06	0,02	---	0,810638
PLK1	5347	SKV_15	F06	Hs_PLK1_6	CCGGATCAAGAAGAATGAATA	0,01	0,01	TOXIC	0,06	0,28	---	0,626902
IRAK1	3654	SKV_24	B07	Hs_IRAK1_6	TCCCATCGCCATGCAGATCTA	0,45	0,06	OK	0,06	0,16	---	0,556118
RBKS	64080	SKV_13	E07	Hs_RBKS_5	AACACAGTCATCTTACCCTTA	1,27	0,19	OK	0,06	0,17	---	0,453965
CLK3	1198	SKV_09	D04	Hs_CLK3_6	CTGCATTCTCTTTGAGTACTA	0,55	0,05	OK	0,06	0,30	---	0,755227
TGFBR1	7046	SKV_24	C08	Hs_TGFBR1_7	TGGGATTGTACTATACCAGTA	0,49	0,25	OK	0,06	0,27	---	0,737692
IRAK1	3654	SKV_22	D07	Hs_IRAK1_5	CCGGGCAATTCAGTTTCTACA	0,85	0,21	OK	0,06	0,05	---	0,149611
CARKL	23729	SKV_13	C07	Hs_CARKL_6	CAGGTAGTTTATTCAAAGAGA	0,71	0,33	OK	0,05	0,25	---	0,632450
NLK	51701	SKV_08	D09	Hs_NLK_5	TTGGTGTTGTCTGGTCAGTAA	0,51	0,15	OK	0,05	0,33	---	0,793877
CIB2	10518	SKV_14	D05	Hs_CIB2_5	CACCGAAGAGCAGCTAGACAA	0,27	0,06	TOXIC	0,05	0,36	---	0,750457
CHEK1	1111	SKV_06	B08	Hs_CHEK1_13	TTGGAATAACTCACAGGGATA	0,36	0,20	TOXIC	0,05	0,14	---	0,549307

Target gene	Gene ID	plate	pos.	sequence name	siRNA sequence	Mean cells	SD cells	phenotype	Mean inh.	SD inh.	phenotype	Sign. inh.
PRKRA	8575	SKV_11	D04	Hs_PRKRA_6	TAAGTATGATTGATTGTTAAA	1,03	0,31	OK	0,05	0,29	---	0,767225
PRKRIR	5612	SKV_25	G08	Hs_PRKRIR_8	CACATTATTCAGGAACTTAAA	0,72	0,22	OK	0,05	0,19	---	0,665588
RIOK2	55781	SKV_02	E06	Hs_RIOK2_5	AACGCGATTATCATAAACATA	0,70	0,32	OK	0,05	0,19	---	0,679096
BUB1B	701	SKV_16	F08	Hs_BUB1B_5	ACGAGAATACCTAATATGTGA	0,32	0,06	TOXIC	0,05	0,34	---	0,747253
CALM2	805	SKV_10	D03	Hs_CALM2_9	AAGCCCTTCTGCACATCTAAA	0,43	0,14	OK	0,05	0,02	---	0,028848
RPS6KA5	9252	SKV_01	F10	Hs_RPS6KA5_8	AAGCCAGTCATTCGAGATGAA	0,45	0,34	OK	0,05	0,33	---	0,823529
FASTK	10922	SKV_02	D09	Hs_FASTK_8	CAGCAGCAAGGTGGTACAGAA	0,11	0,03	TOXIC	0,04	0,49	---	0,880952
ATR	545	SKV_02	C07	Hs_ATR_11	AAGGACATGTGCATTACCTTA	1,10	0,27	OK	0,04	0,12	---	0,555581
HSPB8	26353	SKV_04	C04	Hs_HSPB8_6	CGCATGGTTTGGTTAATGAAA	0,76	0,36	OK	0,04	0,05	---	0,215934
NUAK1	9891	SKV_05	B03	Hs_ARK5_6	CTTGAGTTGATGATCAATTAA	0,65	0,15	OK	0,04	0,39	---	0,854458
CSNK1A1L	122011	SKV_05	F07	Hs_CSNK1A1L_5	CAGATTATCTTTAGAATTCCA	1,05	0,36	OK	0,04	0,42	---	0,873283
STK40	83931	SKV_07	B06	Hs_MGC4796_6	CCGGATGGTTAAGAAGATGAA	0,31	0,13	TOXIC	0,04	0,53	---	0,899711
PDK1	5163	SKV_01	C03	Hs_PDK1_5	CCCGAACTAGAACTTGAAGAA	0,29	0,23	TOXIC	0,04	0,61	---	0,916904
EEF2K	29904	SKV_04	C05	Hs_EEF2K_5	CAGACACTACATGAACACGAA	0,70	0,17	OK	0,04	0,19	---	0,739110
EPHA5	2044	SKV_22	F04	Hs_EPHA5_6	CCCGGCAGTATGTGTCTGTAA	0,08	0,05	TOXIC	0,04	0,20	---	0,769048
PLK2	10769	SKV_19	D09	Hs_PLK2_5	CAGATTGTGTCTGGACTGAAA	0,31	0,14	TOXIC	0,04	0,21	---	0,733983
MAPK8IP1	9479	SKV_14	C06	Hs_MAPK8IP1_4	TGGCATCAGCTTACAGTGCAA	0,64	0,17	OK	0,04	0,62	---	0,899610
CALM1	801	SKV_10	C10	Hs_CALM1_6	CTGGTTGTATCTTATTAGCAA	0,30	0,04	TOXIC	0,04	0,43	---	0,893700
MAP2K1IP1	8649	SKV_14	B08	Hs_MAP2K1IP1_5	ATGCCCAGGCTTGCAGAATAA	0,41	0,65	OK	0,03	0,39	---	0,850211
MAP2K2	5605	SKV_18	E03	Hs_MAP2K2_5	CAGCATTTGCATGGAACACAT	0,24	0,08	TOXIC	0,03	0,11	---	0,576223
PACSIN3	29763	SKV_14	F03	Hs_PACSIN3_6	CAGAGGACAATCAGCCGGAAA	0,33	0,04	TOXIC	0,03	0,12	---	0,548202
PSKH1	5681	SKV_04	F07	Hs_PSKH1_6	CCGCTCCACACGCTCCAATAA	0,50	0,10	OK	0,03	0,22	---	0,807970
PRKACB	5567	SKV_01	C08	Hs_PRKACB_9	CAGCCTGTGTAGTGTGACAAA	0,27	0,24	TOXIC	0,03	0,55	---	0,926853
CKM	1158	SKV_08	F08	Hs_CKM_5	GACCCTTGAACTCTACAAGAA	1,08	0,45	OK	0,03	0,07	---	0,512635
ANKK1	255239	SKV_24	E05	Hs_ANKK1_5	AGGAGCCGAGATGGAAATTTA	0,84	0,19	OK	0,03	0,35	---	0,888955
MAP2K1	5604	SKV_18	D10	Hs_MAP2K1_8	CTGGATCAAGTCCTGAAGAAA	0,21	0,07	TOXIC	0,03	0,27	---	0,839969
FLT3LG	2323	SKV_12	C08	Hs_FLT3LG_1	AGCCTGGAGCCCAACAACCTA	1,08	0,17	OK	0,03	0,23	---	0,843669
PRKAG3	53632	SKV_03	F09	Hs_PRKAG3_6	CAGATCTATGAGATTGAACAA	0,34	0,15	TOXIC	0,03	0,26	---	0,874382
TIE1	7075	SKV_25	E07	Hs_TIE1_2	CCCAGTGAGAACGTGACGTTA	0,82	0,21	OK	0,02	0,08	---	0,621866
IKBKB	3551	SKV_25	D10	Hs_IKBKB_9	CTGGAGAAGTACAGCGAGCAA	0,35	0,06	TOXIC	0,02	0,45	---	0,932141
CIB3	117286	SKV_16	F04	Hs_CIB3_2	CACGAGCAGCTGGAAGCGTAT	0,03	0,02	TOXIC	0,02	1,51	---	0,974010
LATS1	9113	SKV_01	F09	Hs_LATS1_6	CGCGATCTAGTATATGTTTAA	0,65	0,06	OK	0,02	0,31	---	0,908845
PTK2B	2185	SKV_21	C07	Hs_PTK2B_13	AAGCTGATCGGCATCATTGAA	0,64	0,11	OK	0,02	0,25	---	0,868099
MAPKAPK3	7867	SKV_04	F09	Hs_MAPKAPK3_5	CAGGCTTTCACTGAGAGAGAA	1,02	0,08	OK	0,02	0,09	---	0,731348
RIPK4	54101	SKV_24	E03	Hs_RIPK4_6	CACACGCAGTATGAAGATAAA	0,48	0,11	OK	0,02	0,80	---	0,967816
BCKDK	10295	SKV_04	B08	Hs_BCKDK_13	AACATGAGAAATGTATGCCAA	0,42	0,24	OK	0,02	0,18	---	0,881207
RPS6KA1	6195	SKV_03	C10	Hs_RPS6KA1_9	CCCAACATCATCACTCTGAAA	0,56	0,13	OK	0,02	0,55	---	0,963144
ITPK1	3705	SKV_10	F06	Hs_ITPK1_6	CCGATTAATGTCTGTACGTCA	0,67	0,32	OK	0,01	0,66	---	0,971521
TK1	7083	SKV_12	F10	Hs_TK1_6	TCGGCTCTGCTACTTCAAGAA	0,37	0,13	TOXIC	0,01	0,15	---	0,903353

Target gene	Gene ID	plate	pos.	sequence name	siRNA sequence	Mean cells	SD cells	phenotype	Mean inh.	SD inh.	phenotype	Sign. inh.
CDKL1	8814	SKV_08	C08	Hs_CDKL1_5	CTGGACCGAGTGACTACTATA	0,62	0,08	OK	0,01	0,23	---	0,940318
MKNK1	8569	SKV_06	E03	Hs_MKNK1_5	CCAGCAAAGATGATACCTTAA	0,41	0,31	OK	0,01	0,04	---	0,659311
IRAK2	3656	SKV_22	D08	Hs_IRAK2_5	CAGCAACGTCAAGAGCTCTAA	0,48	0,08	OK	0,01	0,09	---	0,887276
AKAP6	9472	SKV_12	E05	Hs_AKAP6_7	CAGAGATTGCTTTAATTATAA	0,57	0,52	OK	0,01	0,75	---	0,987716
PIM2	11040	SKV_05	B05	Hs_PIM2_6	CGGGATTGTCCAATTACTAAA	0,96	0,09	OK	0,01	0,47	---	0,982669
HSPB8	26353	SKV_02	E04	Hs_HSPB8_5	CCGCATGGTTTGGTTAATGAA	0,63	0,21	OK	0,01	0,43	---	0,984444
ERBB4	2066	SKV_21	C06	Hs_ERBB4_5	CTACGTGTTAGTGGCTCTTAA	0,47	0,12	OK	0,00	0,05	---	0,856597
PAK3	5063	SKV_20	B09	Hs_PAK3_2	CCGCTAAGACTGCAAGCCTTA	0,58	0,08	OK	0,00	0,15	---	0,951984
PRPF4B	8899	SKV_08	C09	Hs_PRPF4B_10	AAGGGTTTGAGTAAATACAAA	0,83	0,15	OK	0,00	0,35	---	0,984702
STK32C	282974	SKV_03	G05	Hs_STK32C_6	TCCGAGAATGACTATCTTCAA	0,41	0,26	OK	0,00	0,32	---	0,984602
RFK	55312	SKV_11	F10	Hs_RFK_8	AAGGTTGATAGTTTATCATAA	0,31	0,12	TOXIC	0,00	0,07	---	0,614924
CSNK1G1	53944	SKV_07	D05	Hs_CSNK1G1_11	CTGAGTATTCTCAGAGGTTAA	0,57	0,07	OK	0,00	0,46	---	0,992025
RAGE	5891	SKV_09	F08	Hs_RAGE_7	CAGGAATACCTCTACTAACAA	0,35	0,21	TOXIC	0,00	0,68	---	0,998854
MYLK	4638	SKV_04	E07	Hs_MYLK_9	AACCTGAAATCCGCTAGCAAA	1,15	0,50	OK	0,00	0,08	---	0,999878
YES1	7525	SKV_23	F07	Hs_YES1_6	CCAGCCTACATTCACTTCTAA	0,40	0,06	OK	0,00	0,44	---	0,996253
PHKB	5257	SKV_04	E10	Hs_PHKB_5	AGGGCTGTTCGTGGTCAGTTA	0,70	0,16	OK	0,00	0,29	---	0,993018
IHPK1	9807	SKV_11	D08	Hs_IHPK1_10	CCGGCAGATGCGGAAATGCGA	0,80	0,17	OK	0,00	0,14	---	0,596082
ROCK1	6093	SKV_01	E09	Hs_ROCK1_9	AACGGTTAGAACAAGAGGTAA	0,53	0,14	OK	0,00	0,28	---	0,980902
ITPKC	80271	SKV_13	F07	Hs_ITPKC_4	GACCATCTTGATACTTATTTA	1,22	0,31	OK	0,00	0,19	---	0,961540
PRPF4B	8899	SKV_09	G09	Hs_PRPF4B_9	AAGCATAAACACAGAAGTAAA	0,78	0,43	OK	-0,01	0,56	---	0,987789
BUB1	699	SKV_16	F07	Hs_BUB1_6	TGGCACTTACATGAAAGTGAA	0,83	0,10	OK	-0,01	0,13	---	0,895955
AKAP12	9590	SKV_12	E08	Hs_AKAP12_5	ACGGATGTAGTGTTGAAAGTA	0,75	0,37	OK	-0,01	0,30	---	0,965534
TK2	7084	SKV_12	G03	Hs_TK2_6	CGGGATCGAATATTAACTCCA	1,19	0,33	OK	-0,01	0,66	---	0,979979
MAPKAP1	79109	SKV_16	E07	Hs_MAPKAP1_5	GACCCTGTTACGAATCAGAAA	0,45	0,17	OK	-0,01	0,27	---	0,934564
IRAK3	11213	SKV_24	D07	Hs_IRAK3_5	CACATTCGAATCGGTATATTA	0,89	0,16	OK	-0,01	0,27	---	0,946979
FGFR2	2263	SKV_23	B04	Hs_FGFR2_12	CCCATCTGACAAGGGAAATTA	0,45	0,06	OK	-0,01	0,27	---	0,947100
PRKAR2A	5576	SKV_12	F07	Hs_PRKAR2A_5	AACGGCATGTCTCTCCAACAA	0,45	0,32	OK	-0,01	0,28	---	0,949374
CNKSR1	10256	SKV_19	D05	Hs_CNKSR1_5	ACCCATGACTTCCAGAGCATA	0,91	0,19	OK	-0,01	0,16	---	0,886526
PRKAG3	53632	SKV_02	B09	Hs_PRKAG3_7	TAGCCTGTTTGAAGCTGTCTA	0,30	0,05	TOXIC	-0,01	0,44	---	0,965028
MAP4K5	11183	SKV_20	E07	Hs_MAP4K5_8	TCCGCTTATTAGGATCAGACA	0,55	0,18	OK	-0,01	0,12	---	0,832387
FASTK	10922	SKV_04	B09	Hs_FASTK_5	AAGGGTTGGAAGCTGCTCTAA	0,23	0,16	TOXIC	-0,01	0,12	---	0,847585
TTBK1	84630	SKV_05	F06	Hs_TTBK1_5	CAGGAACGAGAAGTTTAACTA	0,69	0,13	OK	-0,02	0,05	---	0,581569
CDC2L6	23097	SKV_08	D06	Hs_CDC2L6_5	CACTGTCGTCAGGAAGATATA	0,28	0,09	TOXIC	-0,02	0,49	---	0,957061
EPHA4	2043	SKV_21	B03	Hs_EPHA4_5	CCCGCGAATGAAGTTACCTTA	0,93	0,20	OK	-0,02	0,10	---	0,746286
PRKCQ	5588	SKV_01	E04	Hs_PRKCQ_12	CACAAGAAGTGTATTGATAAA	0,69	0,48	OK	-0,02	0,91	---	0,976140
CASK	8573	SKV_06	E04	Hs_CASK_6	AAGGACGACAGATCTATGTAA	0,63	0,44	OK	-0,02	0,59	---	0,962950
RPS6KL1	83694	SKV_03	G04	Hs_RPS6KL1_6	CTGAATTTGATTGGAAAGGAA	0,48	0,27	OK	-0,02	0,44	---	0,949692
PFKM	5213	SKV_09	C09	Hs_PFKM_6	AAGGACTTTCGGGAACGAGAA	0,55	0,17	OK	-0,02	0,12	---	0,816336
STK33	65975	SKV_07	B04	Hs_STK33_7	GAGCATAGGCGTCGTAATGTA	0,11	0,04	TOXIC	-0,02	0,06	---	0,612523

Target gene	Gene ID	plate	pos.	sequence name	siRNA sequence	Mean cells	SD cells	phenotype	Mean inh.	SD inh.	phenotype	Sign. inh.
MAPK8IP2	23542	SKV_14	E07	Hs_MAPK8IP2_6	CCAGGACTCCCTAAACAACAA	0,44	0,50	OK	-0,02	0,33	---	0,905228
MAPK6	5597	SKV_07	G09	Hs_MAPK6_6	CAGGCTTCCTGTTGAAATAAA	0,47	0,33	OK	-0,02	0,24	---	0,898566
WNK1	65125	SKV_18	B04	Hs_WNK1_6	CTGCGACGACTACGAGATAAA	0,91	0,14	OK	-0,02	0,07	---	0,616762
STK32B	55351	SKV_03	F10	Hs_STK32B_5	CTGGGACGCGGTGTTCAAGAA	0,57	0,06	OK	-0,02	0,33	---	0,920886
MAP3K1	4214	SKV_18	D03	Hs_MAP3K1_11	CTCCGGGTGTTTCAACTAGAA	0,07	0,01	TOXIC	-0,02	0,18	---	0,806537
CSNK1E	1454	SKV_05	E07	Hs_CSNK1E_5	GAGCTTTATCGTGGTTGTTAA	1,17	0,15	OK	-0,02	0,09	---	0,683259
EPHA8	2046	SKV_22	F06	Hs_EPHA8_9	ACGGCCCACCAGGGTATGTAA	0,56	0,12	OK	-0,02	0,22	---	0,858042
CDC2	983	SKV_07	D10	Hs_CDC2_1	TTGACTAACTATGGAAGATTA	0,25	0,09	TOXIC	-0,03	0,13	---	0,758263
PCTK1	5127	SKV_09	D10	Hs_PCTK1_5	CACGCCAACATCGTTACGCTA	0,91	0,06	OK	-0,03	0,20	---	0,834052
NUCKS1	64710	SKV_14	G06	Hs_NUCKS_1	AAGGTGTACCACGGTTGTAAA	0,86	0,18	OK	-0,03	0,19	---	0,764249
EIF2AK4	440275	SKV_19	E05	Hs_EIF2AK4_4	TCCGATAATCTTGCAGTGCAA	0,38	0,09	TOXIC	-0,03	0,46	---	0,910416
STK32B	55351	SKV_02	B10	Hs_STK32B_6	TTGGGCTGAGTTCACGAATTA	0,66	0,15	OK	-0,03	0,30	---	0,883618
SPEG	10290	SKV_06	F04	Hs_APEG1_5	AACACCTATTTCTTAACTCAA	0,96	0,36	OK	-0,03	0,39	---	0,909989
PHKA2	5256	SKV_06	C09	Hs_PHKA2_5	CCGCCTAACAAGGTAGATGAA	0,18	0,12	TOXIC	-0,03	0,27	---	0,864596
DGKG	1608	SKV_08	G04	Hs_DGKG_6	TAGCCACTCACATAAAGTTTA	0,97	0,13	OK	-0,03	0,07	---	0,517642
HGS	9146	SKV_14	B10	Hs_HGS_6	GCACGTCTTTCCAGAATTCAA	0,70	0,39	OK	-0,03	0,65	---	0,914114
LIMK2	3985	SKV_22	D10	Hs_LIMK2_7	ATGAGCTTGCACCATATTTAA	0,85	0,16	OK	-0,03	0,15	---	0,708960
PIP5K1B	8395	SKV_11	C08	Hs_PIP5K1B_5	TACACTCTATTCAAACAGCAA	0,54	0,18	OK	-0,04	0,10	---	0,503958
CDC2L6	23097	SKV_10	B06	Hs_CDC2L6_6	GAGGATTTGTTTGAGTACGAA	0,90	0,13	OK	-0,04	0,32	---	0,840470
TBK1	29110	SKV_19	E06	Hs_TBK1_7	CTGACTTGACACGTTTGTAAA	1,35	0,14	OK	-0,04	0,12	---	0,523937
SNRK	54861	SKV_06	G07	Hs_SNRK_11	CCCTGTAGTGATAAATTACAA	0,96	0,37	OK	-0,04	0,34	---	0,841423
CDKN1A	1026	SKV_08	F05	Hs_CDKN1A_7	CTGGCATTAGAATTATTTAAA	0,99	0,17	OK	-0,04	0,06	---	0,304991
PI4K2B	55300	SKV_13	D09	Hs_PI4K2B_7	CAGAGTACTGGCCTTGTTCAA	0,76	0,14	OK	-0,04	0,29	---	0,741630
MAPK13	5603	SKV_08	B07	Hs_MAPK13_5	CCGGAGTGGCATGAAGCTGTA	0,74	0,15	OK	-0,04	0,19	---	0,699035
TTBK2	146057	SKV_07	D08	Hs_TTBK2_8	AGGCATCACCTCAAGATGAAA	0,78	0,50	OK	-0,04	0,32	---	0,820654
DDR1	780	SKV_20	G05	Hs_DDR1_10	CAGGAATGATTTCCTGAAAGA	0,80	0,26	OK	-0,05	0,23	---	0,698216
CDC42BPB	9578	SKV_03	E04	Hs_CDC42BPB_6	TAGGACCTTAAGAGAATAGTA	0,77	0,26	OK	-0,05	0,25	---	0,758026
PRKCD	5580	SKV_01	D06	Hs_PRKCD_11	CAGCAGCAAGTGCAACATCAA	0,32	0,27	TOXIC	-0,05	0,88	---	0,925170
CDKL5	6792	SKV_09	G04	Hs_CDKL5_6	AAGGCAATAATGCTAATTACA	0,93	0,24	OK	-0,05	0,22	---	0,687012
GIT2	9815	SKV_12	E09	Hs_GIT2_5	CAGCGTTGAGAGTCAAGACAA	0,61	0,30	OK	-0,05	0,16	---	0,579694
PAK4	10298	SKV_18	G04	Hs_PAK4_5	CGAGAATGTGGTGGAGATGTA	0,24	0,20	TOXIC	-0,06	0,39	---	0,779337
IRAK3	11213	SKV_24	F07	Hs_IRAK3_6	CTGGATGTTCGTCATATTGAA	0,69	0,11	OK	-0,06	0,25	---	0,714868
AURKB	9212	SKV_17	E08	Hs_AURKB_6	ACGCGGCACTTCACAATTGAT	0,09	0,01	TOXIC	-0,06	0,51	---	0,826121
CHEK2	11200	SKV_06	F07	Hs_CHEK2_9	ACGCCGTCCTTTGAATAACAA	0,65	0,62	OK	-0,06	0,07	---	0,233793
PDK3	5165	SKV_03	G10	Hs_PDK3_8	CCCGTCTGTATGCTAGATATT	0,40	0,15	OK	-0,06	0,45	---	0,834251
AKAP8	10270	SKV_14	D03	Hs_AKAP8_6	GAGGCCGGTAGTGATCCTCAA	0,30	0,05	TOXIC	-0,06	0,63	---	0,841766
PIK3AP1	118788	SKV_13	G03	Hs_PIK3AP1_7	CACCAAGTATATCGAACCATA	0,93	0,24	OK	-0,06	0,42	---	0,760523
CDK5	1020	SKV_07	E07	Hs_CDK5_10	CCGGGAGATCTGCCTACTCAA	0,06	0,05	TOXIC	-0,06	0,53	---	0,854970
CLK2	1196	SKV_09	D03	Hs_CLK2_6	TCGCCTGGATTGGGATGAGAA	0,54	0,15	OK	-0,06	0,16	---	0,549622

Target gene	Gene ID	plate	pos.	sequence name	siRNA sequence	Mean cells	SD cells	phenotype	Mean inh.	SD inh.	phenotype	Sign. inh.
CAMK2G	818	SKV_06	B07	Hs_CAMK2G_11	CGCCATGAAGCCGATGAGAAA	1,01	0,39	OK	-0,06	0,29	---	0,722499
MARK1	4139	SKV_26	C04	Hs_MARK1_6	TCGATACGTAGCATTGCAGAA	0,51	0,22	OK	-0,06	0,22	---	0,645818
UCK2	7371	SKV_12	G05	Hs_UCK2_5	CCGGATGCCTTTGACAATGAA	0,45	0,34	OK	-0,06	0,11	---	0,366021
PDK4	5166	SKV_02	D03	Hs_PDK4_7	AAGTTCGAAATAGACACCATA	0,33	0,17	TOXIC	-0,06	0,36	---	0,772597
CAMK2N1	55450	SKV_06	G08	Hs_CaMKIINalpha_6	CGGGTTGTTATTGAAGATGAT	0,53	0,17	OK	-0,06	0,48	---	0,826634
MAP4K4	9448	SKV_18	F10	Hs_MAP4K4_6	TCGGAGCTGCACCGAGGGCAA	0,34	0,09	TOXIC	-0,07	0,21	---	0,553082
PRKX	5613	SKV_03	C07	Hs_PRKX_6	TTGGAATACTCTAAGAGAATA	0,75	0,34	OK	-0,07	0,32	---	0,733357
AKAP9	10142	SKV_14	C10	Hs_AKAP9_5	CAGCCTATCAGTGAACATCAA	0,38	0,45	TOXIC	-0,07	0,32	---	0,643050
IHPK2	51447	SKV_11	F04	Hs_IHPK2_6	CTGCTGAGATGCGCAAATTCA	0,58	0,25	OK	-0,07	0,10	---	0,416984
CRKRS	51755	SKV_10	B10	Hs_CRK7_6	ATCGGGATATTAAGTGTTCTA	1,31	0,50	OK	-0,07	0,65	---	0,860750
GIT1	28964	SKV_14	E10	Hs_GIT1_5	CAGCCTTGACTTATCCGAATT	0,83	0,11	OK	-0,07	0,18	---	0,396089
MAP2K7	5609	SKV_18	E07	Hs_MAP2K7_9	CAGGAAGAGACCAAAGTATAA	0,29	0,12	TOXIC	-0,07	0,34	---	0,679989
PAK7	57144	SKV_19	B06	Hs_PAK7_6	ATGGTGTGCACGTTTCATTAA	0,24	0,14	TOXIC	-0,08	0,56	---	0,797417
EPHA5	2044	SKV_21	B04	Hs_EPHA5_5	ACCAGTTGGATCTCCAATGAA	0,97	0,18	OK	-0,08	0,14	---	0,319643
MAPKAPK3	7867	SKV_06	D09	Hs_MAPKAPK3_6	CCAGATAGTAATAAACACCAT	0,53	0,48	OK	-0,08	0,30	---	0,680632
CAMK2G	818	SKV_04	D07	Hs_CAMK2G_7	CTCGGATATGTCGACTTCTGA	0,84	0,24	OK	-0,08	0,15	---	0,416702
MARK1	4139	SKV_04	E05	Hs_MARK1_5	TCCCTCGTTACTGTCCGCATA	1,13	0,67	OK	-0,08	0,28	---	0,657739
IBTK	25998	SKV_19	E04	Hs_IBTK_6	TAGAAGAGTCATTACACCATA	0,42	0,13	OK	-0,08	0,23	---	0,518339
KIDINS220	57498	SKV_14	G03	Hs_KIDINS220_5	CAGGCGAGACTCCTTATAATA	0,83	0,14	OK	-0,08	0,20	---	0,396813
MAP3K13	9175	SKV_24	F05	Hs_MAP3K13_6	GCGAATAATTTATACATGGAA	0,74	0,16	OK	-0,08	0,61	---	0,834478
NRBP1	29959	SKV_19	E07	Hs_NRBP_6	TCGGTGGAGGAGGGAGTCAAA	0,04	0,03	TOXIC	-0,08	0,26	---	0,559784
CDKN2C	1031	SKV_15	C05	Hs_CDKN2C_6	TGCCTCTACTTTATCAATTAA	0,89	0,03	OK	-0,08	0,09	---	0,071612
CKB	1152	SKV_10	D07	Hs_CKB_3	CCGGCCTCACCCAGATTGAAA	0,06	0,05	TOXIC	-0,08	0,18	---	0,460815
PIK3C2G	5288	SKV_15	E06	Hs_PIK3C2G_5	CCAGATCAAGAAATTCGTAAA	1,44	0,15	OK	-0,08	0,15	---	0,233238
MAPK15	225689	SKV_10	C05	Hs_MAPK15_2	TTGCTTGGAGGCTACTCCCAA	0,27	0,23	TOXIC	-0,08	0,29	---	0,635765
PRKD2	25865	SKV_06	G05	Hs_PRKD2_6	TTGGGTGGTTCATTACAGCAA	1,01	0,39	OK	-0,08	0,45	---	0,760332
PIK3CB	5291	SKV_15	E09	Hs_PIK3CB_5	CCCTTCGATAAGATTATTGAA	0,91	0,22	OK	-0,09	0,21	---	0,386126
KSR2	283455	SKV_24	E06	Hs_KSR2_6	AAGGAAATCCATTACTTCAAA	0,89	0,19	OK	-0,09	0,12	---	0,290073
BMX	660	SKV_20	G04	Hs_BMX_5	CCCAATATGACAACGAATCAA	0,45	0,08	OK	-0,09	0,27	---	0,544240
STK24	8428	SKV_20	D06	Hs_STK24_14	TCCATATGTAACCAAATATTA	1,16	0,19	OK	-0,09	0,27	---	0,530322
MAGI3	260425	SKV_13	G07	Hs_MAGI3_2	CCAGGCAAAGTCATTAATAAA	1,00	0,24	OK	-0,09	0,28	---	0,482646
BMPR1A	657	SKV_23	G10	Hs_BMPR1A_6	GCGGCAGACATTAAAGGTACA	0,19	0,06	TOXIC	-0,09	0,40	---	0,711850
PDGFRA	5156	SKV_21	F10	Hs_PDGFRA_6	ACGCAGGAAGCCTACTATTTA	0,73	0,07	OK	-0,09	0,20	---	0,380248
MAPK8IP2	23542	SKV_16	C07	Hs_MAPK8IP2_9	GAGATGATCGATGACAATGAA	0,57	0,12	OK	-0,09	0,04	---	0,001742
EPHA7	2045	SKV_21	B05	Hs_EPHA7_6	CAGGCTGCGAAGGAAGTACTA	0,96	0,19	OK	-0,09	0,12	---	0,177564
NADK	65220	SKV_12	B03	Hs_FLJ13052_6	CCAGGAGAACATGATCGTGTA	0,92	0,16	OK	-0,09	0,05	---	0,038451
PI4KB	5298	SKV_11	B03	Hs_PIK4CB_5	TCGGCTGATAGTGGCATGATT	0,64	0,15	OK	-0,10	0,16	---	0,355949
CSNK1A1	1452	SKV_07	C05	Hs_CSNK1A1_5	AGGGCTAAAGGCTGCAACAAA	0,83	0,38	OK	-0,10	0,41	---	0,701168
CINP	51550	SKV_14	F06	Hs_CINP_5	CGGCTGATTGGCACAATTTAA	0,74	0,23	OK	-0,10	0,32	---	0,513610

Target gene	Gene ID	plate	pos.	sequence name	siRNA sequence	Mean cells	SD cells	phenotype	Mean inh.	SD inh.	phenotype	Sign. inh.
CERK	64781	SKV_11	G10	Hs_CERK_5	ATGGCATTATTTGATCTGAAA	0,91	0,32	OK	-0,10	0,08	---	0,348042
BMX	660	SKV_19	C04	Hs_BMX_6	CGGAACAAAGTTTCCAGTCAA	0,51	0,12	OK	-0,10	0,15	---	0,242049
CDC2L5	8621	SKV_08	C06	Hs_CDC2L5_5	AACGACGTAGTTTCATTGGAA	0,48	0,14	OK	-0,10	0,14	---	0,290255
RYK	6259	SKV_23	E08	Hs_RYK_20	CTGGTCTGCCTTGTACAAGAA	0,18	0,05	TOXIC	-0,10	0,21	---	0,444072
NME6	10201	SKV_13	C03	Hs_NME6_7	CAGGATCTAGCCTTCTATCTA	0,82	0,18	OK	-0,10	0,33	---	0,484937
ITPK1	3705	SKV_09	B06	Hs_ITPK1_5	CACGCCGTCATTGACATCAAT	0,80	0,27	OK	-0,11	0,43	---	0,693605
CAMKK1	84254	SKV_18	B08	Hs_CAMKK1_6	CGGCGTTATCTGGAAAGTGGA	0,65	0,12	OK	-0,11	0,18	---	0,284000
MAP4K2	5871	SKV_20	C08	Hs_MAP4K2_6	TCGGTCAGCCTCAGAATTCCA	0,61	0,10	OK	-0,11	0,10	---	0,069166
MAPK12	6300	SKV_09	F09	Hs_MAPK12_6	TGGAAGCGTGTTACTTACAAA	1,12	0,28	OK	-0,11	0,29	---	0,554144
SRPK2	6733	SKV_09	G03	Hs_SRPK2_8	CAGCTCCTATGAACAATTCAA	0,59	0,37	OK	-0,11	0,17	---	0,319877
PRKCZ	5590	SKV_03	C05	Hs_PRKCZ_6	GACCAAATTTACGCCATGAAA	0,60	0,13	OK	-0,11	0,25	---	0,480459
TYK2	7297	SKV_22	B05	Hs_TYK2_5	CACCATCTGGTAATAAACTCA	0,67	0,11	OK	-0,11	0,22	---	0,425266
ERBB2	2064	SKV_22	G04	Hs_ERBB2_15	CACGTTTGAGTCCATGCCCAA	0,18	0,17	TOXIC	-0,12	1,37	---	0,891169
BMPR1A	657	SKV_22	C10	Hs_BMPR1A_5	CAGCTACGCCGGACAATAGAA	0,51	0,14	OK	-0,12	0,15	---	0,238735
PDK1	5163	SKV_02	G03	Hs_PDK1_6	TCGGGTTTCTATAGGAAACTA	0,70	0,10	OK	-0,12	0,45	---	0,675323
JAK1	3716	SKV_21	E04	Hs_JAK1_5	ACCGGATGAGGTTCTATTTCA	1,15	0,08	OK	-0,12	0,15	---	0,166523
BCKDK	10295	SKV_25	G07	Hs_BCKDK_7	CACAATGGAGAGTCACCTAGA	0,61	0,24	OK	-0,12	0,32	---	0,556388
PRKAG2	51422	SKV_25	F04	Hs_PRKAG2_6	AACATTTAAGCCTTTAGTGAA	0,88	0,14	OK	-0,12	0,08	---	0,056179
PIK3CG	5294	SKV_15	F03	Hs_PIK3CG_6	CACCTTTACTCTATAACTCAA	0,98	0,21	OK	-0,12	0,18	---	0,161518
KIT	3815	SKV_23	C08	Hs_KIT_6	CTCGCACCTTTCCAAAGTTAA	1,15	0,07	OK	-0,12	0,14	---	0,208062
CDKN2B	1030	SKV_15	C04	Hs_CDKN2B_6	GAGAGCAATTGTAACGGTTAA	0,96	0,24	OK	-0,12	0,10	---	0,027783
SH3KBP1	30011	SKV_16	D04	Hs_SH3KBP1_6	TAGCTTATATATGACGGTATA	1,06	0,12	OK	-0,12	0,16	---	0,119814
CAMK4	814	SKV_04	D05	Hs_CAMK4_6	TTGCAAGTTAACACAACGTAA	1,20	0,32	OK	-0,12	0,08	---	0,046734
ACVR1B	91	SKV_22	C06	Hs_ACVR1B_5	CTGTGATTACCTCTCAATCTA	0,73	0,03	OK	-0,13	0,22	---	0,378920
EPHA7	2045	SKV_22	F05	Hs_EPHA7_5	ACCAGTCATGATAGTAATAGA	0,95	0,02	OK	-0,13	0,08	---	0,058216
EPHB1	2047	SKV_21	B07	Hs_EPHB1_5	ATGGCCCTGGATTATCTACTA	0,99	0,10	OK	-0,13	0,10	---	0,044384
PIP5K1C	23396	SKV_13	C06	Hs_PIP5K1C_11	CCCATGATAGAAGTCTGTAAA	1,26	0,34	OK	-0,13	0,28	---	0,323758
PRKAR2B	5577	SKV_12	F08	Hs_PRKAR2B_6	CACGCCATTGGGACTGTCAAA	0,44	0,12	OK	-0,13	0,15	---	0,221562
RIPK2	8767	SKV_24	D03	Hs_RIPK2_7	CAGGGACTTGATCATGAAAGA	1,19	0,32	OK	-0,13	0,21	---	0,359089
TAOK2	9344	SKV_20	D09	Hs_TAOK2_5	GCCCAAGAGCCTCAAATCTAA	0,61	0,07	OK	-0,13	0,24	---	0,328153
CSNK1G2	1455	SKV_07	C08	Hs_CSNK1G2_5	AAGAATCTCTATACAAATGAA	0,86	0,58	OK	-0,13	0,23	---	0,385559
PIP4K2A	5305	SKV_12	F04	Hs_PIP5K2A_5	ATGGAATTAAGTGCCATGAAA	0,70	0,33	OK	-0,13	0,22	---	0,366969
RIPK2	8767	SKV_25	G05	Hs_RIPK2_10	ATGCTCTTCAGCAATAATAAA	0,89	0,26	OK	-0,13	0,41	---	0,605932
CIB2	10518	SKV_16	B05	Hs_CIB2_6	CTGCACCTTCTTCAATAAGAA	0,52	0,05	OK	-0,13	0,21	---	0,191232
GSK3B	2932	SKV_09	D08	Hs_GSK3B_7	AACACTGGTCACGTTTGGAAA	0,99	0,25	OK	-0,13	0,33	---	0,530525
EPHA8	2046	SKV_21	B06	Hs_EPHA8_10	GAGCGTGTGCTTATCCGTTAA	0,99	0,16	OK	-0,13	0,08	---	0,017551
DGKQ	1609	SKV_08	G05	Hs_DGKQ_5	CAGCGACACCAGGTTTGAGAA	0,80	0,34	OK	-0,13	0,07	---	0,031356
PRKAB2	5565	SKV_02	G06	Hs_PRKAB2_6	TCCAATATTAGTTGGAGTTAA	1,18	0,16	OK	-0,13	0,23	---	0,366174
NME5	8382	SKV_11	C06	Hs_NME5_6	ATGATATTAGCTAGACATAAA	0,84	0,20	OK	-0,14	0,39	---	0,275855

Target gene	Gene ID	plate	pos.	sequence name	siRNA sequence	Mean cells	SD cells	phenotype	Mean inh.	SD inh.	phenotype	Sign. inh.
HK2	3099	SKV_10	F04	Hs_HK2_6	CGGCCGTGCTACAATAGGTAA	0,46	0,29	OK	-0,14	0,33	---	0,505349
VRK3	51231	SKV_07	D04	Hs_VRK3_7	CAGACCTTTGTCAATCCACAT	0,14	0,01	TOXIC	-0,14	0,22	---	0,342373
CAMK2D	817	SKV_06	B06	Hs_CAMK2D_10	GTGCGACTTCATGATAGCATA	0,59	0,13	OK	-0,14	0,14	---	0,162016
STK11	6794	SKV_04	F08	Hs_STK11_5	AACGTGAAGAAGGAAATTCAA	1,06	0,17	OK	-0,14	0,08	---	0,034762
NLK	51701	SKV_10	B09	Hs_NLK_10	ATGGTGGAAGATAATGTACTA	0,61	0,28	OK	-0,14	0,25	---	0,377056
ROS1	6098	SKV_23	E07	Hs_ROS1_6	ACCGAGAAGGGTTAAACTATA	0,93	0,10	OK	-0,14	0,16	---	0,193069
CDC2L5	8621	SKV_09	G06	Hs_CDC2L5_6	TCAGAGTATTATCAATATGAA	0,93	0,37	OK	-0,14	0,04	---	0,002890
PKLR	5313	SKV_11	B05	Hs_PKLR_2	GAGGCCTATCTGAGACTATAA	0,49	0,22	OK	-0,14	0,39	---	0,262751
PXK	54899	SKV_19	G09	Hs_PXK_6	TAAGATCCCTACAAAGTTAAA	0,80	0,20	OK	-0,14	0,21	---	0,217379
STK4	6789	SKV_20	D03	Hs_STK4_5	AGGATTCATAGCATCACTATA	0,83	0,17	OK	-0,14	0,10	---	0,033910
ETNK1	55500	SKV_11	G04	Hs_ETNK1_5	CCGTATGTGGTGGATTAGAAA	1,15	0,43	OK	-0,14	0,43	---	0,260456
PIP4K2B	8396	SKV_12	G09	Hs_PIP5K2B_9	CACGATCAATGAGCTGAGCAA	0,71	0,04	OK	-0,14	0,43	---	0,589921
RAGE	5891	SKV_08	B08	Hs_RAGE_8	TTGCACTAATATGTGAACTTA	0,74	0,32	OK	-0,15	0,17	---	0,206205
AURKA	6790	SKV_18	C07	Hs_STK6_5	CACCTTCGGCATCCTAATATT	0,12	0,07	TOXIC	-0,15	0,24	---	0,267705
PANK1	53354	SKV_13	D06	Hs_PANK1_5	AACGCTGGTTAAATTGGTGTA	1,12	0,27	OK	-0,15	0,27	---	0,260981
PBK	55872	SKV_19	E10	Hs_PBK_6	TCAGTAGTTATTAGACTCTAA	0,66	0,13	OK	-0,15	0,31	---	0,375539
KDR	3791	SKV_21	E07	Hs_KDR_5	AACGCTGACATGTACGGTCTA	1,29	0,17	OK	-0,15	0,09	---	0,015812
ABL2	27	SKV_20	F10	Hs_ABL2_9	CAGGTCTATGACCTACTAGAA	0,36	0,17	TOXIC	-0,15	0,11	---	0,032088
CDC42SE2	56990	SKV_16	D10	Hs_CDC42SE2_3	CAGGAGACCTGTTCAGTGGAA	0,33	0,04	TOXIC	-0,15	0,20	---	0,126747
RIPK2	8767	SKV_24	F03	Hs_RIPK2_16	AAGAAAGTTTGCCATATGATA	1,00	0,25	OK	-0,15	0,42	---	0,561157
EPHB4	2050	SKV_21	B10	Hs_EPHB4_6	TCGGACAAACACGGACAGTAT	1,33	0,17	OK	-0,15	0,12	---	0,039751
IRAK4	51135	SKV_24	D09	Hs_IRAK4_6	ATCCTATTAGTCATATATTTA	0,93	0,26	OK	-0,15	0,45	---	0,584450
TK1	7083	SKV_11	B10	Hs_TK1_5	CGGGCCGATGTTCTCAGGAAA	0,23	0,07	TOXIC	-0,16	0,37	---	0,239117
JAK1	3716	SKV_23	C04	Hs_JAK1_6	CACGGATAACATCAGCTTCAT	0,25	0,04	TOXIC	-0,16	0,12	---	0,092281
CKS2	1164	SKV_16	G09	Hs_CKS2_8	TAGGTTACTGTAAGATGTTTA	1,17	0,29	OK	-0,16	0,06	---	0,000290
PCTK3	5129	SKV_09	E04	Hs_PCTK3_11	CAGAGACAGATAATATATTTA	1,08	0,11	OK	-0,16	0,29	---	0,396289
LYK5	92335	SKV_20	F07	Hs_LYK5_5	CTGGTTCTAGTTCTGGTTCTA	0,85	0,28	OK	-0,16	0,15	---	0,074333
PIP4K2C	79837	SKV_12	B05	Hs_PIP5K2C_5	CCGGAGCAGTATGCTAAGCGA	0,61	0,14	OK	-0,16	0,23	---	0,295899
DCLK1	9201	SKV_06	E06	Hs_DCAMKL1_6	CCGGAAGTGATAACACGCAAA	0,67	0,39	OK	-0,16	0,11	---	0,067985
PRKCDBP	112464	SKV_16	E10	Hs_PRKCDBP_6	AAGGAGCGAATCCTACATCCA	0,47	0,13	OK	-0,16	0,11	---	0,011296
ADCK4	79934	SKV_02	E08	Hs_ADCK4_5	CAGATGCTGAGAGTTCTTGAA	0,70	0,23	OK	-0,16	0,08	---	0,021473
NME4	4833	SKV_09	C06	Hs_NME4_5	ACCAACTACCTCCGTCAGCAA	0,48	0,12	OK	-0,16	0,08	---	0,022952
RFK	55312	SKV_13	D10	Hs_RFK_9	TAGGATGGAACCCATATTACA	1,10	0,37	OK	-0,17	0,26	---	0,184375
PKIA	5569	SKV_14	B03	Hs_PKIA_10	TCACTTGATCATATGACGAAA	1,00	0,36	OK	-0,17	0,17	---	0,059923
EPHB2	2048	SKV_21	B08	Hs_EPHB2_10	CCGAGAGGACCTCGTCTACAA	0,98	0,12	OK	-0,17	0,09	---	0,008138
MYLK	4638	SKV_06	C07	Hs_MYLK_10	CAGCATCCATGGCTAATGAAA	0,71	0,71	OK	-0,17	0,33	---	0,424903
JAK2	3717	SKV_21	E05	Hs_JAK2_7	AGCCATCATACGAGATCTTAA	1,09	0,10	OK	-0,17	0,10	---	0,016634
XYLB	9942	SKV_11	D09	Hs_XYLB_5	CTGAAATTATTGGACGTCATA	0,75	0,36	OK	-0,17	0,12	---	0,213813
IKBKAP	8518	SKV_17	E06	Hs_IKBKAP_6	GCGGTTTACTATAGACAAATA	0,79	0,25	OK	-0,17	0,30	---	0,292395

Target gene	Gene ID	plate	pos.	sequence name	siRNA sequence	Mean cells	SD cells	phenotype	Mean inh.	SD inh.	phenotype	Sign. inh.
PRKY	5616	SKV_01	E08	Hs_PRKY_3	TACAGTGAGTTTGTTCTGAAA	0,84	0,14	OK	-0,17	0,33	---	0,410364
CDK9	1025	SKV_07	E10	Hs_CDK9_6	TGGGCACAGTTTGGTCCGTTA	1,19	0,40	OK	-0,18	0,12	---	0,059840
NEK4	6787	SKV_17	D08	Hs_NEK4_8	CTGGGTCTGTGAGCAGTTCAA	1,13	0,11	OK	-0,18	0,19	---	0,109226
CDKL3	51265	SKV_08	D08	Hs_CDKL3_8	CTAAAGCAATTTCATCACGAA	0,74	0,14	OK	-0,18	0,51	---	0,579664
MADD	8567	SKV_14	B07	Hs_MADD_1	CTCAACAAGTTCTATACTAAA	1,13	0,32	OK	-0,18	0,26	---	0,158538
MAPK7	5598	SKV_09	E10	Hs_MAPK7_9	CAGACCCACCTTTCAGCCTTA	0,67	0,27	OK	-0,18	0,37	---	0,447686
MAK	4117	SKV_07	F09	Hs_MAK_5	GCCCGATTCCTTCATGCTATA	0,78	0,33	OK	-0,18	0,38	---	0,454133
PRKAA1	5562	SKV_04	F06	Hs_PRKAA1_5	CCCACGATATTCTGTACACAA	0,79	0,19	OK	-0,18	0,11	---	0,040458
MAGI3	260425	SKV_12	C07	Hs_MAGI-3_6	CTGGATAGTCAGTGGTGTCAA	0,52	0,15	OK	-0,18	0,60	---	0,623140
RPS6KA4	8986	SKV_03	D08	Hs_RPS6KA4_6	CGCCACCTTCATGGCATTCAA	0,46	0,16	OK	-0,18	0,37	---	0,441872
DGUOK	1716	SKV_10	E07	Hs_DGUOK_10	CAGCACGATGGTCCTACACAT	0,39	0,18	TOXIC	-0,19	0,04	---	0,001092
PICK1	9463	SKV_12	E03	Hs_PRKCABP_7	CACCTCGGCGGCCTTTATTTA	1,05	0,30	OK	-0,19	0,08	---	0,018192
RPS6KA5	9252	SKV_03	D10	Hs_RPS6KA5_9	CTGGATCTCTTACGTAATTCA	0,55	0,37	OK	-0,19	0,63	---	0,633147
RBKS	64080	SKV_11	G07	Hs_RBKS_6	CAGGTGGTAATCATTACCTTA	1,16	0,12	OK	-0,19	0,19	---	0,187154
ETNK1	55500	SKV_13	E04	Hs_ETNK1_6	TCCGTATGTGGTGGATTAGAA	1,12	0,14	OK	-0,19	0,34	---	0,247351
TAOK2	9344	SKV_18	F09	Hs_TAOK2_11	AACGGAAACCACCGCTCTTTA	0,77	0,11	OK	-0,19	0,25	---	0,170089
MAP3K6	9064	SKV_18	F08	Hs_MAP3K6_6	TCAGAGGAGCTGAGTAATGAA	0,16	0,12	TOXIC	-0,19	0,42	---	0,399827
PKN2	5586	SKV_01	E03	Hs_PKN2_5	AAAGTATGATATCTACGCAAA	0,60	0,21	OK	-0,19	0,37	---	0,423688
PRKRA	8575	SKV_13	B04	Hs_PRKRA_5	ATGATTGATTGTTAAATTTCA	0,85	0,23	OK	-0,19	0,22	---	0,087456
MATK	4145	SKV_21	F03	Hs_MATK_10	GACGGATTCTAAGGACTCTAA	0,57	0,14	OK	-0,20	0,17	---	0,064707
CSNK2A1	1457	SKV_17	B03	Hs_CSNK2A1_10	CTGGTCGCTTACATCACTTTA	0,80	0,17	OK	-0,20	0,08	---	0,003271
PIK3C2G	5288	SKV_17	C06	Hs_PIK3C2G_6	CCCGTAGAAATGATAACTCCA	1,04	0,28	OK	-0,20	0,15	---	0,041970
MAP3K9	4293	SKV_22	E03	Hs_MAP3K9_5	CAGGAGCTCAGTCGTCCCAAA	0,93	0,22	OK	-0,20	0,10	---	0,022161
STK35	140901	SKV_25	B10	Hs_STK35_7	CAAAGTTAGTTTCCAATACTA	0,58	0,16	OK	-0,20	0,37	---	0,400973
MARK3	4140	SKV_04	E06	Hs_MARK3_7	CACGACGAAATACTTATGTTT	1,49	0,46	OK	-0,20	0,08	---	0,014190
AKAP5	9495	SKV_12	E07	Hs_AKAP5_5	AGGGCTTTCATCAAGAAATTA	1,47	0,44	OK	-0,20	0,11	---	0,031129
JAK3	3718	SKV_21	E06	Hs_JAK3_6	TCCGGGAGGCGCAGACACTTA	1,32	0,16	OK	-0,20	0,18	---	0,062577
AKAP13	11214	SKV_16	B10	Hs_AKAP13_6	CTCGGTGTTTCAGGCACTAAA	0,67	0,15	OK	-0,20	0,15	---	0,016386
EPHA3	2042	SKV_19	C10	Hs_EPHA3_6	TTGGATAGTTTCCTACGTAAA	1,21	0,30	OK	-0,20	0,09	---	0,005020
ACVR2A	92	SKV_23	G07	Hs_ACVR2_4	ACCAATCAAACTGGTGTTGAA	0,96	0,19	OK	-0,21	0,18	---	0,116744
TTK	7272	SKV_15	F10	Hs_TTK_6	CAGCAATACCTTGGATGATTA	0,44	0,18	OK	-0,21	0,08	---	0,000278
AK7	122481	SKV_13	G04	Hs_AK7_7	GACGATCAATATATAATTAGA	1,28	0,25	OK	-0,21	0,25	---	0,098708
ITK	3702	SKV_21	E03	Hs_ITK_5	CAGGACTTTAGTAGAGACTGA	1,20	0,14	OK	-0,21	0,15	---	0,031645
MAST4	375449	SKV_20	F08	Hs_LOC375449_4	ATGAATTGCCACCACATTAAA	0,57	0,08	OK	-0,21	0,16	---	0,035679
ZMYND8	23613	SKV_16	C08	Hs_PRKCBP1_8	CACCATTGAACAGTTATCCTA	0,59	0,13	OK	-0,21	0,15	---	0,014664
KIDINS220	57498	SKV_16	E03	Hs_KIDINS220_6	TCGCAGATGCGCTATTATCTA	0,74	0,14	OK	-0,21	0,18	---	0,029178
ERBB3	2065	SKV_22	G05	Hs_ERBB3_6	CTTCGTCATGTTGAACTATAA	0,41	0,09	OK	-0,21	0,53	---	0,524584
CASK	8573	SKV_04	G04	Hs_CASK_5	AACCAATGGGAATCACTTTAA	0,22	0,02	TOXIC	-0,21	0,26	---	0,225718
MAP3K11	4296	SKV_22	E05	Hs_MAP3K11_6	CCCGACGTCTGGAGGACTCAA	1,20	0,17	OK	-0,21	0,06	---	0,003274

Target gene	Gene ID	plate	pos.	sequence name	siRNA sequence	Mean cells	SD cells	phenotype	Mean inh.	SD inh.	phenotype	Sign. inh.
CAMK2N1	55450	SKV_05	C08	Hs_CaMKIINalpha_5	AGCAAGCGGGTTGTTATTGAA	0,76	0,10	OK	-0,21	0,34	---	0,339517
PRKRIR	5612	SKV_12	F09	Hs_PRKRIR_14	ATGGGAGTATCTGTTGCATTA	1,25	0,59	OK	-0,21	0,23	---	0,183096
DAPK1	1612	SKV_04	D09	Hs_DAPK1_5	AAGCATGTAATGTTAATGTTA	1,14	0,26	OK	-0,21	0,29	---	0,266475
PRKDC	5591	SKV_02	D04	Hs_PRKDC_6	TTCGGCTAACTCGCCAGTTTA	0,66	0,17	OK	-0,21	0,24	---	0,195856
EPHB4	2050	SKV_22	F10	Hs_EPHB4_5	CCCAGCCAATAGCCACTCTAA	0,48	0,04	OK	-0,22	0,16	---	0,083402
PKIG	11142	SKV_14	D09	Hs_PKIG_8	CCACAAGATGTTATTTATTGA	1,02	0,60	OK	-0,22	0,45	---	0,313328
LOC161635	161635	SKV_07	D09	LOC161635	TTGGTCGTGTGAATTATTAAA	1,11	0,20	OK	-0,22	0,40	---	0,401997
EPHB6	2051	SKV_21	C03	Hs_EPHB6_5	AACCGCCAATCTCTAGATCAA	0,61	0,15	OK	-0,22	0,17	---	0,039265
CDKN2B	1030	SKV_16	G04	Hs_CDKN2B_5	CTGCTTACTTATGCCATAGAA	0,64	0,15	OK	-0,22	0,29	---	0,130103
AURKAIP1	54998	SKV_16	D08	Hs_AKIP_6	CTGCTGTGATCCGTAGTAATA	0,33	0,13	TOXIC	-0,22	0,18	---	0,025935
MAP3K7	6885	SKV_18	F05	Hs_MAP3K7_6	CCCGTGTGAACCATCCTAATA	0,56	0,11	OK	-0,22	0,26	---	0,140828
UCK2	7371	SKV_11	C05	Hs_UCK2_6	TCAGTACATTACGTTCGTCAA	0,83	0,07	OK	-0,22	0,08	---	0,144424
PRKG1	5592	SKV_25	E06	Hs_PRKG1_5	GAGGTTCGTTTGAAGATTCTA	0,63	0,06	OK	-0,22	0,04	---	0,000872
CDKL3	51265	SKV_10	B08	Hs_CDKL3_7	AGCTCCCGAATTAGTATTAAA	0,73	0,21	OK	-0,22	0,15	---	0,058690
ADK	132	SKV_10	C06	Hs_ADK_11	AAGAAAGATCATTATTTAATA	1,22	0,08	OK	-0,22	0,31	---	0,276367
SGK3	23678	SKV_03	F04	Hs_SGKL_5	ACCAACTAACTTACATGCTTA	0,67	0,25	OK	-0,23	0,35	---	0,327573
CALM3	808	SKV_10	D04	Hs_CALM3_5	CACCAATTGATTGACTGAGAA	0,76	0,25	OK	-0,23	0,70	---	0,608522
RIPK4	54101	SKV_24	G03	Hs_RIPK4_5	AAGCCTGATGACGAAGTGAAA	0,42	0,06	OK	-0,23	0,51	---	0,482413
ZAK	51776	SKV_24	F10	Hs_ZAK_15	AAGGAATGCATTATTTACATA	0,75	0,10	OK	-0,23	0,06	---	0,002442
TGFBR1	7046	SKV_22	E08	Hs_TGFBR1_6	TCCATTGGTGGAATTCATGAA	1,17	0,20	OK	-0,23	0,06	---	0,002181
GUK1	2987	SKV_10	E10	Hs_GUK1_6	CCCGGCGAGGAGAACGGCAAA	0,81	0,42	OK	-0,23	0,09	---	0,012658
CDK7	1022	SKV_07	E09	Hs_CDK7_6	GAGGCTTTAAGGTAGCTTTAA	0,20	0,13	TOXIC	-0,23	0,32	---	0,277108
PIK3CG	5294	SKV_17	D03	Hs_PIK3CG_5	ATCGAAGTTTGCAGAGACAAA	1,14	0,36	OK	-0,23	0,13	---	0,011150
AKAP3	10566	SKV_14	D06	Hs_AKAP3_5	AGGGATCATGACCTATGCTAA	0,81	0,22	OK	-0,23	0,33	---	0,151064
MARK2	2011	SKV_06	C03	Hs_MARK2_7	CCACCTCTAATTCTTACTCTA	0,89	0,08	OK	-0,24	0,12	---	0,023922
PLK1	5347	SKV_17	D06	Hs_PLK1_7	CGCGGGCAAGATTGTGCCTAA	0,04	0,02	TOXIC	-0,24	0,55	---	0,413402
NEK1	4750	SKV_17	B09	Hs_NEK1_8	AACCAGGAATACTATATCGAA	0,78	0,09	OK	-0,24	0,26	---	0,112877
RAF1	5894	SKV_22	E06	Hs_RAF1_6	CAGATCTTAGTAAGCTATATA	1,24	0,19	OK	-0,24	0,11	---	0,019866
PFKFB3	5209	SKV_10	G08	Hs_PFKFB3_6	CTCCAATATCATGGAAGTTAA	0,75	0,29	OK	-0,24	0,23	---	0,143387
PFKFB2	5208	SKV_10	G07	Hs_PFKFB2_6	CCGTGACAAGCCAACTAACAA	0,30	0,20	TOXIC	-0,24	0,77	---	0,612343
AK5	26289	SKV_13	C08	Hs_AK5_6	CAGCAATTATAAATTAATATA	0,97	0,35	OK	-0,24	0,14	---	0,006077
EIF2AK2	5610	SKV_17	D07	Hs_EIF2AK2_5	ACGGAAAGACTTACGTTATTA	1,11	0,31	OK	-0,24	0,16	---	0,021318
RPS6KA3	6197	SKV_01	F04	Hs_RPS6KA3_6	TCCAAACATTATCACTCTAAA	0,83	0,24	OK	-0,25	0,19	---	0,086321
LTK	4058	SKV_21	E09	Hs_LTK_5	ACAGATCTTTGGAGTGCCTAA	1,28	0,24	OK	-0,25	0,10	---	0,002463
PRKAA2	5563	SKV_25	B03	Hs_PRKAA2_6	CCGAAGTCAGAGCAAACCGTA	0,61	0,14	OK	-0,25	0,42	---	0,372001
XYLB	9942	SKV_13	B09	Hs_XYLB_6	TCAGGACTCCAGCTAAATCAA	0,77	0,21	OK	-0,25	0,26	---	0,067877
CSNK2A1	1457	SKV_15	D03	Hs_CSNK2A1_9	TCCATTGAAGCTGAAATGGTA	0,36	0,11	TOXIC	-0,25	0,32	---	0,122052
HIPK3	10114	SKV_08	D04	Hs_HIPK3_5	CACGTTTGGCCAGGTAGTTAA	0,51	0,20	OK	-0,25	0,65	---	0,543394
EPHB3	2049	SKV_21	B09	Hs_EPHB3_7	TCCCAGATTACACAACCTTCA	0,49	0,17	OK	-0,25	0,23	---	0,074882

Target gene	Gene ID	plate	pos.	sequence name	siRNA sequence	Mean cells	SD cells	phenotype	Mean inh.	SD inh.	phenotype	Sign. inh.
PIK3R2	5296	SKV_17	D05	Hs_PIK3R2_5	CCGCGAGTATGACCAGCTTTA	1,13	0,20	OK	-0,25	0,16	---	0,022621
PLK4	10733	SKV_17	F08	Hs_PLK4_6	CAGACATATAAGTTTAATAAA	0,89	0,14	OK	-0,25	0,08	---	0,000679
MAP3K10	4294	SKV_22	E04	Hs_MAP3K10_5	CAGGATGTTCACTCTATTTAT	1,05	0,16	OK	-0,25	0,01	---	0,000004
CDC2	983	SKV_05	F10	Hs_CDC2_13	TCGGGAAATTTCTCTATTAAA	0,49	0,54	OK	-0,25	0,03	---	0,000120
SNF1LK2	23235	SKV_05	B09	Hs_SNF1LK2_6	CCGAAGGATGTTGGTCCTAGA	0,52	0,26	OK	-0,26	0,17	---	0,056432
RIOK1	83732	SKV_02	E09	Hs_RIOK1_5	GCCCAACAAGATAATATTCTA	1,04	0,27	OK	-0,26	0,30	---	0,214518
CDC42SE2	56990	SKV_14	F10	Hs_CDC42SE2_2	AAGGGAGGTTATGGAGGTGGA	0,37	0,47	TOXIC	-0,26	0,34	---	0,133390
FLT3	2322	SKV_23	B06	Hs_FLT3_6	CCGGCTTGAGTGAATTGTGTA	0,67	0,08	OK	-0,26	0,30	---	0,211551
AK2	204	SKV_08	E08	Hs_AK2_4	ATGGGTGGGAATGATAGGACA	0,63	0,31	OK	-0,26	0,31	---	0,228424
PIK3CA	5290	SKV_17	C08	Hs_PIK3CA_13	AAGCTTTAGAATAATGCGCAA	1,24	0,12	OK	-0,26	0,11	---	0,004044
PIK3CA	5290	SKV_15	E08	Hs_PIK3CA_5	CTGAGTCAGTATAAGTATATA	0,72	0,21	OK	-0,26	0,27	---	0,064427
CMPK	51727	SKV_11	F05	Hs_UMP-CMPK_5	CGCGTATATATCCCTCTAGTA	0,79	0,17	OK	-0,26	0,17	---	0,105340
MAP2K1IP1	8649	SKV_12	D08	Hs_MAP2K1IP1_6	TAGCATATAGATGTAATTTAT	0,90	0,09	OK	-0,26	0,09	---	0,007348
MAP3K3	4215	SKV_20	B04	Hs_MAP3K3_6	CCACGTGTCTGTGCACCACAA	0,23	0,07	TOXIC	-0,26	0,49	---	0,328513
PIK3C2A	5286	SKV_17	C04	Hs_PIK3C2A_6	TACCCACTAATTGCATTGGAA	1,00	0,21	OK	-0,26	0,22	---	0,056999
PIP5K1B	8395	SKV_25	F09	Hs_PIP5K1B_7	AAGGGTTACCTTCCAGTTCAA	0,21	0,09	TOXIC	-0,26	0,28	---	0,186351
PIK3C2B	5287	SKV_17	C05	Hs_PIK3C2B_5	GAGGGAGGAGCTAAACGGTTA	1,11	0,09	OK	-0,26	0,14	---	0,010727
CDC42BPG	55561	SKV_02	C03	Hs_CDC42BPG_6	CTCGCCGCCTACCAACTTCAA	0,14	0,13	TOXIC	-0,26	0,38	---	0,292367
NEK3	4752	SKV_17	C03	Hs_NEK3_9	ACGATAGAGGTGGTTCTGTAA	1,05	0,27	OK	-0,26	0,18	---	0,025151
TWF2	11344	SKV_04	B10	Hs_PTK9L_6	TTGGGATGGTTGAATGCTGTA	0,05	0,05	TOXIC	-0,27	0,92	---	0,641519
MAP2K5	5607	SKV_18	E05	Hs_MAP2K5_12	CAAGACGTATGTTGGAACAAA	0,32	0,12	TOXIC	-0,27	0,45	---	0,276900
ILK	3611	SKV_24	B06	Hs_ILK_5	TAGCCGTAGTGTAATGATTGA	1,00	0,07	OK	-0,27	0,17	---	0,051571
NUAK2	81788	SKV_07	B05	Hs_NUAK2_5	TACCTAATGGTCTCTACCTAA	0,72	0,38	OK	-0,27	0,38	---	0,287947
DCLK1	9201	SKV_04	G06	Hs_DCAMKL1_5	CAGGTTTATAACTTCGACACA	0,63	0,05	OK	-0,27	0,11	---	0,014376
CINP	51550	SKV_16	D06	Hs_CINP_6	GCGGCTGATTGGCACAATTTA	0,46	0,08	OK	-0,27	0,14	---	0,003023
EPHB1	2047	SKV_22	F07	Hs_EPHB1_6	GCGGGATGATGTGACCTACAA	0,33	0,12	TOXIC	-0,27	0,29	---	0,187924
AKAP5	9495	SKV_14	C07	Hs_AKAP5_6	ATCAGGTTGATCTTTAAATAA	0,84	0,16	OK	-0,27	0,33	---	0,104603
MOS	4342	SKV_15	D08	Hs_MOS_6	CTCGGTGTACAAGGCGACTTA	0,70	0,27	OK	-0,27	0,10	---	0,000274
EPHA1	2041	SKV_20	G09	Hs_EPHA1_5	CAGATGGGATCCCGTATCGAA	1,00	0,06	OK	-0,27	0,20	---	0,032253
MARCKS	4082	SKV_12	C09	Hs_MARCKS_6	TTGAGTTTCTTTGTTGAAGAA	0,81	0,42	OK	-0,27	0,27	---	0,151934
RPS6KA1	6195	SKV_01	E10	Hs_RPS6KA1_10	TGCCACGTACTCCGCACTCAA	0,44	0,35	OK	-0,27	0,85	---	0,608429
SKIP	51763	SKV_25	C09	Hs_SKIP_12	CCCGGAGAAATACTTAAGATA	0,74	0,44	OK	-0,27	1,19	---	0,711802
CIT	11113	SKV_03	E07	Hs_CIT_3	CAGGATATACCGTAACACGAA	0,58	0,12	OK	-0,27	0,42	---	0,325601
NME5	8382	SKV_12	G06	Hs_NME5_7	CATGATATTAGCTAGACATAA	0,74	0,15	OK	-0,27	0,20	---	0,076895
ZC3HC1	51530	SKV_16	D05	Hs_ZC3HC1_1	CCGCTTGAGGCTCTCTATGAA	0,29	0,07	TOXIC	-0,27	0,10	---	0,000223
MARK4	57787	SKV_07	B03	Hs_MARK4_6	CTGCAGCCTGTTGCCCAATAA	0,42	0,25	OK	-0,28	0,10	---	0,008953
MAPKAPK2	9261	SKV_06	E07	Hs_MAPKAPK2_5	CTACGAGCAGATCAAGATAAA	0,77	0,45	OK	-0,28	0,02	---	0,000024
FGFR2	2263	SKV_21	D04	Hs_FGFR2_7	CAGCATATGTGTAAAGATTTA	1,00	0,21	OK	-0,28	0,10	---	0,001146
ARAF	369	SKV_22	C09	Hs_ARAF_5	CCGACTCATCAAGGGACGAAA	1,08	0,11	OK	-0,28	0,14	---	0,023989

Target gene	Gene ID	plate	pos.	sequence name	siRNA sequence	Mean cells	SD cells	phenotype	Mean inh.	SD inh.	phenotype	Sign. inh.
ACVR1	90	SKV_22	C05	Hs_ACVR1_6	CTGGTCTGTCTTTGGATAATA	0,40	0,03	OK	-0,28	0,32	---	0,203081
KIAA1804	84451	SKV_24	E04	Hs_KIAA1804_5	ACGGACCATGTCTGATGGAAA	0,71	0,16	OK	-0,28	0,29	---	0,172515
STK39	27347	SKV_18	G10	Hs_STK39_5	TGGAATAGTCTCAGATCTAAA	0,70	0,29	OK	-0,28	0,24	---	0,060305
EPHB2	2048	SKV_22	F08	Hs_EPHB2_9	CACGCTTTCTAGAGGACGATA	0,87	0,10	OK	-0,28	0,06	---	0,001259
PIK3R1	5295	SKV_17	D04	Hs_PIK3R1_6	TAGCTGGTTATGAACTAGTAA	1,14	0,22	OK	-0,28	0,21	---	0,037683
PHKG1	5260	SKV_06	D03	Hs_PHKG1_6	CCGGGAGATCGTCATCCGAGA	0,46	0,36	OK	-0,28	0,41	---	0,294206
TNNI3K	51086	SKV_24	D08	Hs_TNNI3K_7	GGAGCTAATGTCAATATTCAA	0,81	0,09	OK	-0,28	0,08	---	0,002867
CSK	1445	SKV_20	G06	Hs_CSK_3	TACGCGCCTCATTAAACCAAA	1,06	0,29	OK	-0,28	0,31	---	0,116742
PIK3C3	5289	SKV_17	C07	Hs_PIK3C3_6	TCGGTTGGTGCATCTAATGAA	1,01	0,18	OK	-0,29	0,07	---	0,000215
BMPR1B	658	SKV_24	B03	Hs_BMPR1B_6	ACGGATATTGTTTCACGATGA	0,82	0,23	OK	-0,29	0,54	---	0,414692
STK36	27148	SKV_25	C08	Hs_STK36_6	TGCCAGCTCTTTCTTATTCTA	0,70	0,02	OK	-0,29	0,09	---	0,006161
PHKA1	5255	SKV_06	C08	Hs_PHKA1_6	CCCAATCGTCTGTACTATGAA	0,52	0,13	OK	-0,29	0,24	---	0,104087
SH3KBP1	30011	SKV_14	F04	Hs_SH3KBP1_5	CTCTGAGATCTCAATGCGAAA	0,73	0,17	OK	-0,29	0,12	---	0,000707
PKIG	11142	SKV_16	B09	Hs_PKIG_5	GAGCTCCATGTCCCAGATAAA	0,34	0,07	TOXIC	-0,29	0,26	---	0,038684
AKAP7	9465	SKV_14	C04	Hs_AKAP7_5	AACGATGGGTCTGAAGTCCAA	0,63	0,39	OK	-0,29	0,20	---	0,014204
TIE1	7075	SKV_25	D07	Hs_TIE1_5	CTGGAGCAACACAGTAGAAGA	0,72	0,06	OK	-0,29	0,04	---	0,000236
STK31	56164	SKV_19	G10	Hs_STK31_8	AAGGAGATAATTTCAAATACA	0,66	0,27	OK	-0,29	0,36	---	0,158881
PIK3R3	8503	SKV_25	F08	Hs_PIK3R3_7	AAGGGAGGCAATAATAAGTTA	0,86	0,13	OK	-0,29	0,24	---	0,108387
HK3	3101	SKV_10	F05	Hs_HK3_6	CCGGAATGCGATGTCTCCTTA	0,93	0,22	OK	-0,29	0,26	---	0,125084
GIT2	9815	SKV_14	C09	Hs_GIT2_6	CCCGTTGATTATGCAAGGCAA	0,44	0,40	OK	-0,29	0,26	---	0,035895
STK16	8576	SKV_18	C08	Hs_STK16_9	CACATAGTGTTCTGACTCCAA	0,51	0,14	OK	-0,29	0,28	---	0,081442
PFKFB3	5209	SKV_09	C08	Hs_PFKFB3_5	CAGGGACTTGTCGCTGATCAA	0,45	0,13	OK	-0,29	0,18	---	0,048351
SYK	6850	SKV_21	G10	Hs_SYK_5	CCCGCTCTTAAAGATGAGTTA	0,96	0,22	OK	-0,29	0,14	---	0,004940
MAP3K7IP1	10454	SKV_16	B04	Hs_MAP3K7IP1_10	ATGTAGTAAAGAAGTAATAAA	0,80	0,17	OK	-0,29	0,18	---	0,006626
ZMYND8	23613	SKV_14	E08	Hs_PRKCBP1_7	AGCGAACTTGTCATAGATTTA	0,96	0,23	OK	-0,29	0,18	---	0,005911
LIMK1	3984	SKV_22	D09	Hs_LIMK1_7	GAGCATCTAGGAAGTATTAAA	1,20	0,17	OK	-0,29	0,14	---	0,020215
LIMK2	3985	SKV_24	B10	Hs_LIMK2_15	TTGATCAGACTAAATAAATTA	0,83	0,07	OK	-0,30	0,50	---	0,356568
CDKN1A	1026	SKV_10	D05	Hs_CDKN1A_6	CAGTTTGTGTGTCTTAATTAT	0,95	0,09	OK	-0,30	0,34	---	0,205792
PSKH2	85481	SKV_05	D09	Hs_PSKH2_5	AAGGACTTTATAGACAAACTA	0,94	0,15	OK	-0,30	0,31	---	0,174231
EPHA3	2042	SKV_20	G10	Hs_EPHA3_5	TCGGATATGATTGTTTCTCAA	0,99	0,31	OK	-0,30	0,11	---	0,001308
DDR2	4921	SKV_21	F09	Hs_DDR2_3	ACGCACTGTCAGTTACACCAA	0,47	0,06	OK	-0,30	0,08	---	0,000371
PTK7	5754	SKV_21	G05	Hs_PTK7_3	CCGAGAGAAGCCCACTATTAA	0,54	0,09	OK	-0,30	0,26	---	0,061862
TYK2	7297	SKV_23	F05	Hs_TYK2_7	CTGATGCTATATTTCCGCATA	0,83	0,09	OK	-0,30	0,09	---	0,005185
GSK3A	2931	SKV_07	F07	Hs_GSK3A_5	CCGGGTGTAAATAGATTGTTA	1,06	0,32	OK	-0,30	0,31	---	0,163217
EGFR	1956	SKV_20	G07	Hs_EGFR_6	CCCATCCAATTTATCAAGGAA	0,53	0,37	OK	-0,30	0,45	---	0,226283
TGFBR2	7048	SKV_22	E09	Hs_TGFBR2_7	TCGGTTAATAACGACATGATA	1,15	0,13	OK	-0,30	0,07	---	0,001400
MAPK6	5597	SKV_09	E09	Hs_MAPK6_5	CAAGTTCAATTTGAAAGGAAA	0,87	0,20	OK	-0,31	0,13	---	0,015018
FRAP1	2475	SKV_25	D03	Hs_FRAP1_5	ACTCGCTGATCCAAATGACAA	0,56	0,12	OK	-0,31	0,55	---	0,384055
RPS6KA6	27330	SKV_03	F07	Hs_RPS6KA6_6	GGCGAGGTAAATGGTCTTAAA	0,50	0,20	OK	-0,31	0,33	---	0,180906

Target gene	Gene ID	plate	pos.	sequence name	siRNA sequence	Mean cells	SD cells	phenotype	Mean inh.	SD inh.	phenotype	Sign. inh.
MAPK15	225689	SKV_08	E05	Hs_MAPK15_1	CCACTGACTTCCTCCAATAAA	0,90	0,38	OK	-0,31	0,26	---	0,109504
EIF2AK3	9451	SKV_15	G09	Hs_EIF2AK3_5	CACAAACTGTATAACGGTTTA	1,10	0,43	OK	-0,31	0,19	---	0,007674
PCTK2	5128	SKV_07	G03	Hs_PCTK2_5	AGGCTTAATTCTTGCGTATAA	1,10	0,30	OK	-0,31	0,21	---	0,059781
KIAA1804	84451	SKV_24	G04	Hs_KIAA1804_6	CGGGAACTTAACATTCTGATA	1,17	0,25	OK	-0,31	0,21	---	0,056849
CDK5	1020	SKV_05	G07	Hs_CDK5_9	CCCTTTGTGGACTTTATTTAA	0,93	0,38	OK	-0,32	0,08	---	0,002059
SPHK2	56848	SKV_13	E06	Hs_SPHK2_6	CCGAGGGTAGTGCCTGATCAA	0,35	0,20	TOXIC	-0,32	0,29	---	0,041121
ITK	3702	SKV_23	C03	Hs_ITK_6	CTGGTGAGTTAAGTAAGATTA	0,81	0,08	OK	-0,32	0,04	---	0,000208
DTYMK	1841	SKV_10	E08	Hs_DTYMK_6	TCCCGGAAAGATCAACTGAAA	0,81	0,27	OK	-0,32	0,41	---	0,253537
RIPK1	8737	SKV_24	C10	Hs_RIPK1_5	TACCACTAGTCTGACGGATAA	0,70	0,21	OK	-0,32	0,22	---	0,063016
LYN	4067	SKV_21	E10	Hs_LYN_13	CGGGAAATATGGGATGTATAA	1,29	0,18	OK	-0,32	0,13	---	0,003170
DGKZ	8525	SKV_12	G10	Hs_DGKZ_5	CTGGAGCGAGTCAGCGACATA	1,29	0,25	OK	-0,32	0,42	---	0,260026
PIP5K1C	23396	SKV_11	E06	Hs_PIP5K1C_5	CCGCGTCGTGGTCATGAACAA	0,26	0,08	TOXIC	-0,32	0,39	---	0,059910
VRK2	7444	SKV_07	D03	Hs_VRK2_6	AGGGAAGAAGTTACAGATTTA	0,54	0,08	OK	-0,32	0,19	---	0,040973
RPS6KC1	26750	SKV_26	B05	Hs_RPS6KC1_7	CCTGATCTTCTTGTAAATTTA	0,84	0,26	OK	-0,32	0,14	---	0,017940
PAK2	5062	SKV_20	B08	Hs_PAK2_8	CCGCGACCGGATCATACGAAA	0,79	0,07	OK	-0,33	0,08	---	0,000150
JAK2	3717	SKV_23	C05	Hs_JAK2_8	CTGCCTTACGATGACAGAAAT	0,94	0,12	OK	-0,33	0,17	---	0,030922
CKS1B	1163	SKV_16	G08	Hs_CKS1B_5	AAGAAATCTGTTCATGTTAAA	1,13	0,45	OK	-0,33	0,22	---	0,010573
GRK6	2870	SKV_01	B10	Hs_GRK6_9	AAGGATGTTCTGGACATTGAA	0,38	0,39	TOXIC	-0,33	0,80	---	0,512743
ARAF	369	SKV_23	G09	Hs_ARAF_6	CCGGGATGGCATGAGTGTCTA	0,98	0,26	OK	-0,33	0,08	---	0,001555
KHK	3795	SKV_10	F09	Hs_KHK_7	TAGGGTGGGTAAGGCCTTATA	0,66	0,31	OK	-0,33	0,56	---	0,360877
CDKL5	6792	SKV_08	C04	Hs_CDKL5_5	AAGATAGACGCTTCATGTTAA	0,60	0,11	OK	-0,34	0,46	---	0,275570
VRK1	7443	SKV_05	E10	Hs_VRK1_6	CCAGGTGTACTTGGTAGATTA	0,95	0,10	OK	-0,34	0,33	---	0,152004
PRKG2	5593	SKV_03	C06	Hs_PRKG2_6	TTGAGTACTACTAACGTTTAA	0,57	0,14	OK	-0,34	0,24	---	0,073262
EPHA1	2041	SKV_19	C09	Hs_EPHA1_6	TACCTCAGTAATCACAATTAT	0,97	0,12	OK	-0,34	0,17	---	0,006331
AKAP14	158798	SKV_15	B06	Hs_AKAP14_6	CCCATTGTCGTTTCTTATGTA	0,61	0,16	OK	-0,34	0,25	---	0,014785
STK38L	23012	SKV_01	G10	Hs_STK38L_5	AGGGAGATGTACTGTATTATA	0,76	0,17	OK	-0,34	0,23	---	0,062616
NUCKS1	64710	SKV_25	F05	Hs_NUCKS_7	AAGAACCTACTTAAGATAGAA	0,53	0,25	OK	-0,34	0,22	---	0,057214
CDK5R1	8851	SKV_11	D05	Hs_CDK5R1_5	CCGGAAGGCCACGCTGTTTGA	0,56	0,24	OK	-0,34	0,40	---	0,049359
STYXL1	51657	SKV_14	F07	Hs_DUSP24_8	CAGGCTTGTCTGGAAGGAGAA	0,24	0,09	TOXIC	-0,34	0,22	---	0,007615
PNKP	11284	SKV_13	C05	Hs_PNKP_4	CGGGAAGTCCACCTTTCTCAA	0,76	0,10	OK	-0,34	0,22	---	0,009145
FGFR1	2260	SKV_22	G10	Hs_FGFR1_7	CCGGCCTCTATGCTTGCGTAA	1,07	0,10	OK	-0,34	0,25	---	0,076517
MAPK1	5594	SKV_07	G06	Hs_MAPK1_12	AACACTTGTCAAGAAGCGTTA	0,62	0,32	OK	-0,35	0,22	---	0,053894
IHPK3	117283	SKV_12	B10	Hs_IHPK3_5	AAGACTGGTGGACAAGTGTAA	0,27	0,16	TOXIC	-0,35	0,74	---	0,462180
PDGFRB	5159	SKV_23	E03	Hs_PDGFRB_5	CCGAGCAACTTTGATCAACGA	0,67	0,12	OK	-0,35	0,30	---	0,119286
IBTK	25998	SKV_17	G04	Hs_IBTK_5	CAGATTGAGGAGCATGCCATA	0,30	0,18	TOXIC	-0,35	0,34	---	0,088092
RET	5979	SKV_21	G06	Hs_RET_10	TAGGCTGGTTCTCAACCGGAA	1,17	0,18	OK	-0,35	0,34	---	0,085683
HK3	3101	SKV_09	B05	Hs_HK3_5	CACTCAGGTTAGCAATATATA	0,75	0,36	OK	-0,35	0,34	---	0,145950
TESK1	7016	SKV_22	E07	Hs_TESK1_5	CAGGACCGCCCTGACACACAA	1,02	0,22	OK	-0,35	0,08	---	0,001636
GIT1	28964	SKV_16	C10	Hs_GIT1_6	GCCGCTGAGGATGTCCCGAAA	0,50	0,17	OK	-0,35	0,11	---	0,000177

Target gene	Gene ID	plate	pos.	sequence name	siRNA sequence	Mean cells	SD cells	phenotype	Mean inh.	SD inh.	phenotype	Sign. inh.
VRK1	7443	SKV_07	C10	Hs_VRK1_5	CAGGTTATACTCCTTAAGTTA	0,88	0,62	OK	-0,35	0,25	---	0,072639
JAK3	3718	SKV_23	C06	Hs_JAK3_5	CGGGAGATTCAGATCCTCAAA	0,30	0,05	TOXIC	-0,35	0,35	---	0,151693
MINK1	50488	SKV_25	D08	Hs_MINK1_6	CCGGAAGTACAAGAAGCGATT	0,56	0,05	OK	-0,35	0,42	---	0,221181
CARKL	23729	SKV_11	E07	Hs_CARKL_5	ATGAAACATATTGTCTCTTTA	1,09	0,07	OK	-0,36	0,16	---	0,042269
CDK3	1018	SKV_07	E05	Hs_CDK3_6	CAGACTGGATTTGGAGATGGA	0,31	0,25	TOXIC	-0,36	0,18	---	0,025387
PRKAB1	5564	SKV_02	G05	Hs_PRKAB1_6	CTGGCTATGGAACTAAATACA	0,47	0,33	OK	-0,36	0,49	---	0,277178
CAMK1D	57118	SKV_05	C09	Hs_CAMK1D_7	CTGAGAAAGATTAAGCATGAA	0,29	0,25	TOXIC	-0,36	0,10	---	0,003077
DGUOK	1716	SKV_08	G07	Hs_DGUOK_9	CACCTTTGTAAAGAATCTGTA	0,67	0,59	OK	-0,36	0,45	---	0,234327
RYK	6259	SKV_21	G08	Hs_RYK_9	CGGTCTTGATGCAGAACTTTA	0,83	0,14	OK	-0,36	0,32	---	0,065215
AKAP1	8165	SKV_14	B06	Hs_AKAP1_9	AGCGCTGAACTTGATTGGGAA	0,98	0,38	OK	-0,36	0,19	---	0,003243
RIPK1	8737	SKV_22	E10	Hs_RIPK1_6	CCGACATTTCCTGGCATTGAA	1,28	0,26	OK	-0,36	0,19	---	0,030138
MAP3K9	4293	SKV_24	C03	Hs_MAP3K9_3	CACGACCATCTTTCACGAATA	1,10	0,27	OK	-0,36	0,14	---	0,011717
MAST2	23139	SKV_03	F03	Hs_MAST2_5	CAGGAGTGTGCTGTCTGGCAA	0,32	0,13	TOXIC	-0,37	0,15	---	0,012327
TTBK2	146057	SKV_05	F08	Hs_TTBK2_5	CACATTGGTCATGACATGTTA	0,86	0,24	OK	-0,37	0,25	---	0,062057
PKN2	5586	SKV_03	C03	Hs_PKN2_6	CACGTCAAAGTATGATATCTA	0,24	0,19	TOXIC	-0,37	0,41	---	0,193906
GNE	10020	SKV_11	D10	Hs_GNE_9	CTGCTTACTAATGTATTAATA	0,94	0,40	OK	-0,37	0,16	---	0,037741
MAP2K5	5607	SKV_20	C05	Hs_MAP2K5_11	AAGACGTATGTTGGAACAAAT	0,38	0,11	TOXIC	-0,37	0,37	---	0,095201
IKBKB	3551	SKV_25	E10	Hs_MAPKAP1_3	AAGATTAGAACGACTCCGAAA	0,67	0,14	OK	-0,37	0,10	---	0,002800
CKS2	1164	SKV_15	C09	Hs_CKS2_5	CTGTAAGATGTTTAAGATAAA	0,47	0,24	OK	-0,37	0,24	---	0,010216
HGS	9146	SKV_12	D10	Hs_HGS_5	CCGGAACGAGCCCAAGTACAA	0,21	0,10	TOXIC	-0,38	0,83	---	0,474753
NME1	4830	SKV_09	C03	Hs_NME1_10	CCCTGAGGAACTGGTAGATTA	1,02	0,27	OK	-0,38	0,08	---	0,001484
TEC	7006	SKV_22	B03	Hs_TEC_5	CAGTACAAAGTCGCAATCAAA	0,57	0,11	OK	-0,38	0,17	---	0,019313
CSNK1A1	1452	SKV_05	E05	Hs_CSNK1A1_6	CAAGAGTAACATGAAAGGTTT	1,08	0,07	OK	-0,38	0,48	---	0,248314
CHUK	1147	SKV_16	G07	Hs_CHUK_6	TTCCATAAGCTTGGTGACAAA	0,36	0,14	TOXIC	-0,38	0,34	---	0,035202
RP6-213H19.1	51765	SKV_20	F04	Hs_MST4_6	CAGCAAGTCGTTGCTATTAAA	0,69	0,10	OK	-0,38	0,34	---	0,068292
DYRK1B	9149	SKV_10	B03	Hs_DYRK1B_6	CCAGGATTCGAGCAACAAGAA	0,43	0,35	OK	-0,38	0,48	---	0,241272
MAPK8	5599	SKV_09	F03	Hs_MAPK8_12	GTGGAAAGAATTGATATATAA	0,64	0,26	OK	-0,38	0,11	---	0,003444
SRPK2	6733	SKV_08	C03	Hs_SRPK2_7	CAGAAAGTGATTACACATATA	0,94	0,17	OK	-0,38	0,18	---	0,019424
TESK1	7016	SKV_24	C07	Hs_TESK1_6	CTGCGGTACCTGCACTCCAAA	0,52	0,08	OK	-0,39	0,11	---	0,003577
MAST1	22983	SKV_03	E09	Hs_MAST1_5	CAACGAGATCGTGATGATGAA	0,43	0,11	OK	-0,39	0,25	---	0,055972
OSR1	130497	SKV_25	B06	Hs_OXSR1_6	AAGGAGAAAGTGGCAATCAAA	0,46	0,03	OK	-0,39	0,21	---	0,034667
PRKAB2	5565	SKV_01	C06	Hs_PRKAB2_5	ACCCAAAGTACTACTCATTTA	0,41	0,29	OK	-0,39	0,33	---	0,112578
ROS1	6098	SKV_21	G07	Hs_ROS1_5	AAGGTAATTGCTCTAACTTTA	0,71	0,26	OK	-0,39	0,33	---	0,059024
STK17B	9262	SKV_04	G08	Hs_STK17B_8	TGGTTAGACAATGTATATCAA	1,18	0,25	OK	-0,39	0,15	---	0,009869
CDK4	1019	SKV_07	E06	Hs_CDK4_7	AAGGTAATCCGGAGTGAGCAA	0,34	0,12	TOXIC	-0,40	0,45	---	0,200754
CSNK1G1	53944	SKV_26	C05	Hs_CSNK1G1_7	TTGGACCATGTGGGAAATATA	0,56	0,15	OK	-0,40	0,43	---	0,183411
TTK	7272	SKV_17	D10	Hs_TTK_7	TCCGACTTTATGATTATGAAA	1,19	0,12	OK	-0,40	0,22	---	0,011782
CSNK1E	1454	SKV_07	C07	Hs_CSNK1E_6	GTGGTTGTTAATTTGAAGTAA	0,29	0,17	TOXIC	-0,40	0,38	---	0,141434
STK17A	9263	SKV_04	G09	Hs_STK17A_6	TCCATTGTAACCGAAGAGTTA	1,26	0,28	OK	-0,40	0,23	---	0,041031

Target gene	Gene ID	plate	pos.	sequence name	siRNA sequence	Mean cells	SD cells	phenotype	Mean inh.	SD inh.	phenotype	Sign. inh.
PANK3	79646	SKV_13	F04	Hs_PANK3_3	TCCAAAGGTGATAGCACACAA	0,19	0,12	TOXIC	-0,40	0,31	---	0,018612
PCTK2	5128	SKV_09	E03	Hs_PCTK2_6	TAGGCTTAATTCTTGCGTATA	1,06	0,24	OK	-0,40	0,47	---	0,208115
STK10	6793	SKV_18	F04	Hs_STK10_5	CACGGAATTAGAGAACCTGGA	0,11	0,03	TOXIC	-0,41	0,76	---	0,324562
DGKD	8527	SKV_11	D03	Hs_DGKD_5	CAGCAGATTCTCTTCTATGAA	0,58	0,33	OK	-0,41	0,44	---	0,025517
MET	4233	SKV_23	D04	Hs_MET_8	ACCGAGGGAATCATCATGAAA	0,88	0,14	OK	-0,41	0,23	---	0,035936
DTYMK	1841	SKV_08	G08	Hs_DTYMK_5	ATCAGTTGGAATTCTCCTAAA	0,75	0,23	OK	-0,41	0,39	---	0,143014
NME2	4831	SKV_09	C04	Hs_NME2_3	TAGAGCATATTTGCCAATAAA	0,77	0,24	OK	-0,41	0,27	---	0,056727
SKP2	6502	SKV_14	B05	Hs_SKP2_8	ACCCTTCAACTGTTAAAGGAA	0,64	0,48	OK	-0,41	0,40	---	0,052596
DYRK3	8444	SKV_08	C05	Hs_DYRK3_9	AGCCAATAAGCTTAAAGCTAA	0,74	0,06	OK	-0,41	0,20	---	0,021475
PAK1	5058	SKV_18	D07	Hs_PAK1_8	TCCACTGATTGCTGCAGCTAA	0,66	0,17	OK	-0,41	0,11	---	0,000243
AK5	26289	SKV_11	E08	Hs_AK5_3	TAGAGGCATCAAGCAAGTAAA	1,08	0,37	OK	-0,42	0,63	---	0,024138
RIOK3	8780	SKV_02	D06	Hs_RIOK3_5	ATGCGGCAGTTATATCATGAA	0,52	0,31	OK	-0,42	0,20	---	0,024080
RPS6KA2	6196	SKV_01	F03	Hs_RPS6KA2_9	CCGAGTGAGATCGAAGATGGA	0,25	0,16	TOXIC	-0,42	0,34	---	0,101826
PI4K2B	55300	SKV_11	F09	Hs_PI4K2B_6	ATGAACTTTGTGCAAGATTTA	0,97	0,11	OK	-0,42	0,21	---	0,021471
NME3	4832	SKV_10	G05	Hs_NME3_2	ACGCACCTTCCTGGCCGTGAA	0,63	0,64	OK	-0,42	0,17	---	0,011866
SKIP	51763	SKV_25	B09	Hs_SKIP_11	CTGGACAAAGAGAGAATTCAA	0,70	0,13	OK	-0,42	0,13	---	0,004341
PKIB	5570	SKV_12	D04	Hs_PKIB_6	CCGGAATGCCTTACCAGACAT	0,21	0,12	TOXIC	-0,43	0,40	---	0,139222
PIK3CB	5291	SKV_17	C09	Hs_PIK3CB_6	TCGGGAAGCTACCATTTCTTA	1,35	0,24	OK	-0,43	0,25	---	0,014222
PSKH2	85481	SKV_07	B09	Hs_PSKH2_6	GAGGATCAAGTTTACATGGTA	0,77	0,32	OK	-0,43	0,46	---	0,181082
MAK	4117	SKV_09	D09	Hs_MAK_9	AGCGTTCAAATTTATATTCAA	1,03	0,20	OK	-0,43	0,39	---	0,126212
CDKN2D	1032	SKV_16	G06	Hs_CDKN2D_6	ATGAGTTATGAGTTATTCATA	0,88	0,17	OK	-0,43	0,15	---	0,000258
ICK	22858	SKV_08	D05	Hs_ICK_7	AAGGACTATTATATTATATAA	0,65	0,20	OK	-0,43	0,29	---	0,061839
TSSK6	83983	SKV_25	E09	Hs_SSTK_1	ATCGAGGTGTGCAACGGGAAA	0,71	0,19	OK	-0,43	0,28	---	0,057550
GNE	10020	SKV_13	B10	Hs_GNE_8	ATGAAGGTTTCTACAACATAT	0,43	0,15	OK	-0,43	0,28	---	0,008677
AURKAIP1	54998	SKV_14	F08	Hs_AKIP_5	ATCCGTAGTAATAAATTCTCA	0,79	0,41	OK	-0,43	0,13	---	0,000083
CALM3	808	SKV_08	F04	Hs_CALM3_7	CCGCAGAGCTGCGTCACGTAA	0,87	0,08	OK	-0,44	0,21	---	0,022940
TAOK3	51347	SKV_19	B03	Hs_TAOK3_5	CAAACAGTATAAAGCACTCAA	0,13	0,07	TOXIC	-0,44	0,28	---	0,020409
PFTK1	5218	SKV_07	G05	Hs_PFTK1_6	CTGGGTCTTGTCAACATCTAA	0,65	0,07	OK	-0,44	0,24	---	0,034288
BMP2K	55589	SKV_17	G09	Hs_BMP2K_6	TCCGATGTGCATTGAAGCGAA	0,62	0,13	OK	-0,44	0,19	---	0,003291
ERN2	10595	SKV_19	D06	Hs_ERN2_6	CACCTGCATTCTTTACACATA	0,38	0,15	TOXIC	-0,44	0,40	---	0,067264
KIT	3815	SKV_21	E08	Hs_KIT_5	CACGGTTGAATGTAAGGCTTA	0,88	0,06	OK	-0,45	0,07	---	0,000039
KALRN	8997	SKV_06	F06	Hs_TRAD_5	CCCATTGAGTATCAACGGAAA	1,20	0,46	OK	-0,45	0,29	---	0,058256
PRKG1	5592	SKV_25	D06	Hs_PRKG1_6	CCAGTCTTTCTTAGAACTTTA	0,73	0,26	OK	-0,45	0,42	---	0,140993
PRKG2	5593	SKV_01	E06	Hs_PRKG2_5	GACCTACAATTTGATTCTCAA	0,59	0,05	OK	-0,45	0,37	---	0,105472
ADRBK2	157	SKV_01	B04	Hs_ADRBK2_5	AAGATGTTCAGTGTTGGGTAA	0,26	0,18	TOXIC	-0,45	0,12	---	0,002658
PHKB	5257	SKV_06	C10	Hs_PHKB_6	TCGATGGGTCTTTGAATAGAA	0,41	0,22	OK	-0,45	0,28	---	0,049401
CRKRS	51755	SKV_08	D10	Hs_CRK7_5	ACCGGATATCGGGAAGTTCAA	0,57	0,31	OK	-0,45	0,59	---	0,252190
STK11IP	114790	SKV_16	F03	Hs_STK11IP_5	CTCTGCGTTTCTTGAACCTAA	0,24	0,01	TOXIC	-0,46	0,45	---	0,053733
AKAP4	8852	SKV_12	D09	Hs_AKAP4_7	GTCGGTGAACACATTCTCAAA	0,93	0,20	OK	-0,46	0,26	---	0,038707

Target gene	Gene ID	plate	pos.	sequence name	siRNA sequence	Mean cells	SD cells	phenotype	Mean inh.	SD inh.	phenotype	Sign. inh.
CKS1B	1163	SKV_15	C08	Hs_CKS1B_4	AACATCTTTCTGATAACATTA	0,39	0,19	TOXIC	-0,46	0,25	---	0,004619
PIK3R3	8503	SKV_15	G04	Hs_PIK3R3_5	GAGGATATCAATCGAGTACAA	0,12	0,08	TOXIC	-0,46	0,29	---	0,009437
MAPK10	5602	SKV_08	B06	Hs_MAPK10_5	CCGCATGTGTCTGTATTCATA	0,91	0,19	OK	-0,46	0,31	---	0,063939
ZAK	51776	SKV_24	D10	Hs_ZAK_6	CTATGATTACATTAACAGTAA	0,75	0,24	OK	-0,46	0,49	---	0,177406
MADD	8567	SKV_12	D07	Hs_MADD_7	CACACCGTCCACTGAATTCAA	0,68	0,16	OK	-0,46	0,31	---	0,060569
AKAP11	11215	SKV_14	E03	Hs_AKAP11_6	CTGACCGGTTATCTAAATCTA	0,54	0,11	OK	-0,47	0,37	---	0,022933
UCKL1	54963	SKV_11	F07	Hs_UCKL1_5	ACCCAGGACTGTTGAATACAA	0,64	0,33	OK	-0,47	0,29	---	0,012616
TEK	7010	SKV_22	B04	Hs_TEK_5	ACGGGCCAGATTGTAAGCTTA	0,62	0,14	OK	-0,47	0,17	---	0,008370
PANK4	55229	SKV_11	F08	Hs_PANK4_5	CTGGGAGACGTTCATATTGGA	0,75	0,44	OK	-0,47	0,66	---	0,013107
TLK1	9874	SKV_19	D04	Hs_TLK1_5	CAGAGAGTATAGAATACACAA	0,97	0,90	OK	-0,47	0,39	---	0,051177
SNRK	54861	SKV_05	C07	Hs_SNRK_7	CACCACTGAATTGGAACGGAT	0,43	0,04	OK	-0,47	0,27	---	0,040039
NEK9	91754	SKV_19	F10	Hs_NEK9_5	CACGAACCAGTGAAGTCTATA	0,55	0,20	OK	-0,47	0,30	---	0,018908
HCK	3055	SKV_21	D10	Hs_HCK_7	CGGCAGGGAGATACCGTGAAA	0,99	0,17	OK	-0,47	0,16	---	0,001140
DGKB	1607	SKV_10	E03	Hs_DGKB_10	CTCATTCTAGTCCAATGGTAA	0,32	0,09	TOXIC	-0,48	0,44	---	0,132362
AURKC	6795	SKV_17	D09	Hs_AURKC_6	CCGGGTGTACCTGATTCTGGA	1,37	0,34	OK	-0,48	0,30	---	0,019130
PRKRIR	5612	SKV_11	B09	Hs_PRKRIR_5	AAGGTGTATGTAGACCACTTA	0,44	0,07	OK	-0,48	0,28	---	0,011153
CDKN1C	1028	SKV_15	B10	Hs_CDKN1C_5	AAGCTTTAAGAGTCATTTATA	1,06	0,09	OK	-0,48	0,31	---	0,008504
PRKD3	23683	SKV_06	G04	Hs_PRKD3_6	CGGGAGAGTGTTACCATTGAA	0,25	0,11	TOXIC	-0,48	0,31	---	0,052528
MAPK4	5596	SKV_09	E08	Hs_MAPK4_6	CGCCTTAAATCTAATCAGCAA	0,77	0,07	OK	-0,49	0,27	---	0,036823
PCTK1	5127	SKV_07	F10	Hs_PCTK1_7	TCCGCAGAGGATGCCATGAAA	0,99	0,43	OK	-0,49	0,19	---	0,010802
MAPK3	5595	SKV_09	E07	Hs_MAPK3_6	CCCGTCTAATATATAAATATA	1,14	0,23	OK	-0,49	0,46	---	0,137423
AKAP12	9590	SKV_14	C08	Hs_AKAP12_6	CCCGAAATAATCGAACAGATT	0,70	0,35	OK	-0,49	0,17	---	0,000514
PRKAG2	51422	SKV_03	F08	Hs_PRKAG2_14	TCGGTTGGTGGTGGTAAATGA	0,70	0,31	OK	-0,49	0,14	---	0,003475
CDKN2A	1029	SKV_15	C03	Hs_CDKN2A_11	CAGGTGTGCCACATTCGCTAA	0,35	0,07	TOXIC	-0,49	0,16	---	0,000340
RIPK1	8737	SKV_24	G07	Hs_RIPK1_5	TACCACTAGTCTGACGGATAA	1,20	0,02	OK	-0,49	0,15	---	0,004980
AKAP6	9472	SKV_14	C05	Hs_AKAP6_5	CACGTTTGTCACTGCCGTTTA	0,74	0,14	OK	-0,49	0,25	---	0,003686
CDKN1C	1028	SKV_16	F10	Hs_CDKN1C_6	TACACTGGTCCCAAAGTGTAA	0,47	0,10	OK	-0,50	0,19	---	0,000322
NME1	4830	SKV_10	G03	Hs_NME1_9	CAAGTTGGCAGGAACATTATA	0,66	0,05	OK	-0,50	0,66	---	0,262237
MLCK	91807	SKV_05	D10	Hs_LOC91807_7	GACCATGAATTTCATTGTAAA	0,98	0,43	OK	-0,50	0,33	UP	0,060375
IKBKAP	8518	SKV_15	G06	Hs_IKBKAP_5	CAGCGGTTTACTATAGACAAA	0,34	0,15	TOXIC	-0,50	0,34	UP	0,012611
ABL2	27	SKV_19	B10	Hs_ABL2_8	AACCCTGTCCTTAATAACTTA	0,77	0,21	OK	-0,50	0,13	UP	0,000223
CHKA	1119	SKV_10	D06	Hs_CHKA_5	AGCCGGCGATTAGATACTGAA	0,49	0,18	OK	-0,50	0,53	UP	0,177383
FGFR1	2260	SKV_21	C10	Hs_FGFR1_6	CAGAGATTTACCCATCGGGTA	0,73	0,13	OK	-0,50	0,11	UP	0,000078
BAIAP2L1	55971	SKV_14	F09	Hs_LOC55971_6	CTCAACGAGAGTCTTGATGAA	0,58	0,23	OK	-0,50	0,33	UP	0,009750
DDR1	780	SKV_19	C05	Hs_DDR1_9	ACGGTGTGAATCACACATCCA	0,40	0,09	OK	-0,50	0,24	UP	0,005741
BMP2K	55589	SKV_19	E09	Hs_BMP2K_5	AGGCATCACCTGAATATCTTA	0,88	0,14	OK	-0,50	0,19	UP	0,001741
DCK	1633	SKV_10	E06	Hs_DCK_6	TTGGTATAAATTAATTTGTTA	1,46	0,14	OK	-0,51	0,41	UP	0,100737
SPHK1	8877	SKV_25	F06	Hs_SPHK1_7	AAGGATGGGAAAGGTGTGTTT	0,61	0,29	OK	-0,51	0,44	UP	0,113955
TLK1	9874	SKV_17	F04	Hs_TLK1_6	CCGGAGAAGAAACAATCGGAA	0,56	0,09	OK	-0,51	0,38	UP	0,035635

Target gene	Gene ID	plate	pos.	sequence name	siRNA sequence	Mean cells	SD cells	phenotype	Mean inh.	SD inh.	phenotype	Sign. inh.
CHUK	1147	SKV_15	C07	Hs_CHUK_5	CAGGAGAAGTTCGGTTTAGTA	0,60	0,10	OK	-0,51	0,13	UP	0,000035
CDC42BPA	8476	SKV_03	D07	Hs_CDC42BPA_7	CAGATAATAGTCGGAAACAAA	0,31	0,11	TOXIC	-0,51	0,58	UP	0,200737
MET	4233	SKV_21	F04	Hs_MET_9	CGCGCCGTGATGAATATCGAA	0,82	0,08	OK	-0,52	0,17	UP	0,000866
MELK	9833	SKV_06	E10	Hs_MELK_5	CGGGTTGTCTTCCGTCAGATA	0,67	0,30	OK	-0,52	0,29	UP	0,036460
PNCK	139728	SKV_05	E03	Hs_PNCK_5	CTCGAAGATCATGGTCTCTGA	0,79	0,09	OK	-0,52	0,26	UP	0,025342
CSNK1G2	1455	SKV_05	E08	Hs_CSNK1G2_6	TAGGAAAGAATCTCTATACAA	0,41	0,19	OK	-0,52	0,78	UP	0,311743
SPHK2	56848	SKV_11	G06	Hs_SPHK2_5	CAGGATTGCGCTCGCTTTCAT	0,52	0,59	OK	-0,52	0,61	UP	0,006973
RPS6KA3	6197	SKV_03	D04	Hs_RPS6KA3_5	AGCGCTGAGAATGGACAGCAA	0,68	0,27	OK	-0,52	0,24	UP	0,018454
CSNK2B	1460	SKV_17	B05	Hs_CSNK2B_6	GTGGTGGGAATATGAAATAAA	0,57	0,10	OK	-0,53	0,40	UP	0,037773
KALRN	8997	SKV_05	B06	Hs_TRAD_7	CAGGACATCAATCAAGTCTTA	0,46	0,26	OK	-0,53	0,53	UP	0,160826
DGKZ	8525	SKV_11	C10	Hs_DGKZ_7	TCGCGTCAGCATGCACGACTA	0,70	0,37	OK	-0,53	0,27	UP	0,006018
NEK4	6787	SKV_15	F08	Hs_NEK4_7	CTCATCTAGGGTATATACAAA	0,44	0,17	OK	-0,53	0,30	UP	0,005422
PRKCI	5584	SKV_03	B09	Hs_PRKCI_8	ACGCCGCTGGAGAAAGCTTTA	0,49	0,41	OK	-0,53	0,18	UP	0,006269
PRKCI	5584	SKV_01	D09	Hs_PRKCI_10	CAGATTGTTCTTTGTTATAGA	0,77	0,24	OK	-0,54	0,11	UP	0,001139
CKMT1B	1159	SKV_08	F09	Hs_CKMT1_5	ACGGATCTAGATGCCAGTAAA	1,10	0,31	OK	-0,54	0,20	UP	0,010002
DCK	1633	SKV_08	G06	Hs_DCK_5	AAGTTGCAAAGTGGAATTAAA	0,88	0,09	OK	-0,54	0,19	UP	0,007835
PHKA2	5256	SKV_04	E09	Hs_PHKA2_6	CCGGATTCTTAGTCACATATA	0,99	0,28	OK	-0,54	0,11	UP	0,000926
LOC161635	161635	SKV_05	F09	LOC161635	TCCATCGATCTGGAATTTATA	1,12	0,09	OK	-0,54	0,02	UP	0,000001
PIK3C2B	5287	SKV_15	E05	Hs_PIK3C2B_6	CACTGTAGACTTGCTTATCTA	0,86	0,31	OK	-0,54	0,26	UP	0,001733
EGFR	1956	SKV_19	C07	Hs_EGFR_10	TACGAATATTAAACACTTCAA	0,37	0,13	TOXIC	-0,54	0,56	UP	0,102076
RPS6KB2	6199	SKV_03	D05	Hs_RPS6KB2_5	ACCGCAGAGAACCGGAAGAAA	0,15	0,05	TOXIC	-0,54	0,23	UP	0,015234
ADCK2	90956	SKV_02	E10	Hs_ADCK2_6	CAGATTGACCTGCGTTACGAA	0,73	0,22	OK	-0,55	0,37	UP	0,061239
IKBKG	8517	SKV_17	E05	Hs_IKBKG_6	TTCGGAAATGCCTCACATATA	0,95	0,09	OK	-0,55	0,28	UP	0,010163
PKM2	5315	SKV_11	B06	Hs_PKM2_8	AACATCAAGATTATCAGCAAA	0,49	0,17	OK	-0,55	0,34	UP	0,004406
PACSIN2	11252	SKV_16	C04	Hs_PACSIN2_6	GAAGCTTTACATAGAACCTTA	0,77	0,14	OK	-0,56	0,25	UP	0,001348
MARK3	4140	SKV_06	C06	Hs_MARK3_8	CTCGCATTGTGCAGAATTAAA	0,97	0,10	OK	-0,56	0,56	UP	0,158541
STK17B	9262	SKV_06	E08	Hs_STK17B_16	CACGAGATTGCTGTGCTTGAA	0,69	0,42	OK	-0,56	0,46	UP	0,100365
PKIA	5569	SKV_12	D03	Hs_PKIA_9	ATGATTATCATTAGAAGCTAA	0,43	0,18	OK	-0,56	0,69	UP	0,234335
MAP2K1	5604	SKV_20	B10	Hs_MAP2K1_7	CTGGAAGAATTCCTGAACAAA	0,47	0,10	OK	-0,56	0,13	UP	0,000127
PASK	23178	SKV_05	B08	Hs_PASK_6	CGCGCTGACACTGTTTGGTTA	0,86	0,11	OK	-0,56	0,65	UP	0,207344
CSNK1G3	1456	SKV_07	C09	Hs_CSNK1G3_5	CAACATATCTTCGTTATGTAA	0,96	0,06	OK	-0,56	0,34	UP	0,046320
DGKA	1606	SKV_10	D10	Hs_DGKA_6	CACGACCAGTGTGCCATGAAA	0,58	0,14	OK	-0,57	0,43	UP	0,084532
EIF2AK2	5610	SKV_15	F07	Hs_EIF2AK2_6	CGGAAAGACTTACGTTATTAA	0,81	0,28	OK	-0,57	0,28	UP	0,002603
ALPK2	115701	SKV_06	B03	Hs_ALPK2_1	CAGGATTTGCGACCAGGTTTA	0,30	0,18	TOXIC	-0,58	1,05	UP	0,394014
ROCK1	6093	SKV_03	C09	Hs_ROCK1_10	CAAGCTCGAATTACATCTTTA	0,56	0,15	OK	-0,58	0,29	UP	0,026864
IRAK4	51135	SKV_24	F09	Hs_IRAK4_7	TTGCAGGACAGTGGTTATTAA	0,49	0,21	OK	-0,58	0,29	UP	0,027058
PI4K2A	55361	SKV_13	E03	Hs_PI4KII_5	ACGCAAATGTATGAATAACAA	0,52	0,31	OK	-0,58	0,60	UP	0,062083
CDKL2	8999	SKV_08	C10	Hs_CDKL2_5	ATGATGTGTTTAGGTAATCTA	0,85	0,08	OK	-0,58	0,58	UP	0,155480
AKAP4	8852	SKV_14	B09	Hs_AKAP4_8	TACAGTGTCTATGCCGATCAA	0,75	0,36	OK	-0,58	0,20	UP	0,000194

Target gene	Gene ID	plate	pos.	sequence name	siRNA sequence	Mean cells	SD cells	phenotype	Mean inh.	SD inh.	phenotype	Sign. inh.
LATS1	9113	SKV_03	D09	Hs_LATS1_5	CCCATGAATCCTCCTAATCAA	0,82	0,11	OK	-0,58	0,22	UP	0,009435
ACVR1	90	SKV_23	G05	Hs_ACVR1_5	CGGATGGTGAGCAATGGTATA	1,11	0,16	OK	-0,59	0,15	UP	0,002447
DBF4	10926	SKV_16	B08	Hs_ASK_5	CAGTATCAAGTTGTTGATGAT	0,38	0,11	TOXIC	-0,59	0,23	UP	0,000379
NTRK3	4916	SKV_21	F06	Hs_NTRK3_9	CACGGATAACTTTATCTTGTT	0,79	0,14	OK	-0,59	0,26	UP	0,003648
CSNK1A1L	122011	SKV_07	D07	Hs_CSNK1A1L_11	AAGGACTAAAGGCTATGACAA	0,18	0,10	TOXIC	-0,60	0,34	UP	0,037675
GRK6	2870	SKV_02	F10	Hs_GRK6_10	AGGCATGTGGGCGGCACGTAA	0,65	0,15	OK	-0,61	0,32	UP	0,029884
CSNK2A2	1459	SKV_17	B04	Hs_CSNK2A2_6	CTGGGACAACATTCACGGAAA	0,43	0,18	OK	-0,61	0,54	UP	0,066455
PFTK1	5218	SKV_09	E05	Hs_PFTK1_5	AAGGGACACCTTTCACAGCTA	0,74	0,37	OK	-0,61	0,88	UP	0,294492
CDC42BPB	9578	SKV_01	G04	Hs_CDC42BPB_5	CGCCGAGATATTCCATGTATA	0,69	0,14	OK	-0,62	0,13	UP	0,001235
SRC	6714	SKV_21	G09	Hs_SRC_7	CGGCTTGTGGGTGATGTTTGA	0,70	0,11	OK	-0,62	0,19	UP	0,000650
PDGFRB	5159	SKV_21	G03	Hs_PDGFRB_6	CTGCCGAGCAACTTTGATCAA	0,83	0,23	OK	-0,62	0,22	UP	0,001416
STK39	27347	SKV_20	E10	Hs_STK39_6	TTGGAGTATTTGTAACTTCTA	0,38	0,11	TOXIC	-0,62	0,13	UP	0,000076
AKAP13	11214	SKV_14	D10	Hs_AKAP13_5	CCGCCTGTTTGGGTTAACAAA	0,70	0,18	OK	-0,62	0,25	UP	0,000487
PRKAR1A	5573	SKV_03	B03	Hs_PRKAR1A_7	CAGCTAGTGCCAAATAATTGA	0,59	0,09	OK	-0,63	0,53	UP	0,111571
PAK7	57144	SKV_20	F06	Hs_PAK7_5	ATGATCTGGATCCGTATTATA	0,87	0,18	OK	-0,64	0,17	UP	0,000291
LMTK2	22853	SKV_23	G04	Hs_LMTK2_6	CAGATCAGACTAAGTATAGTA	0,64	0,07	OK	-0,65	0,08	UP	0,000126
MARCKS	4082	SKV_13	G09	Hs_MARCKS_5	CTCCTTCAAGAAGAACAAGAA	0,53	0,21	OK	-0,65	0,56	UP	0,031083
MAPKBP1	23005	SKV_16	C05	Hs_MAPKBP1_6	CCCGTTTGTACTGATGTATGA	0,63	0,09	OK	-0,65	0,26	UP	0,000787
GK	2710	SKV_10	E09	Hs_GK_6	CTGAGGGTAGCCCATTTATAA	0,62	0,20	OK	-0,66	0,55	UP	0,104633
AKAP9	10142	SKV_12	E10	Hs_AKAP9_6	CAGCTTCAAAGGGATATACAA	0,48	0,19	OK	-0,66	1,01	UP	0,318892
RET	5979	SKV_23	E06	Hs_RET_9	CCGCTGGTGGACTGTAATAAT	0,97	0,01	OK	-0,67	0,27	UP	0,013540
TNK1	8711	SKV_22	B08	Hs_TNK1_6	ATCGGTCATGATGAACTTGGA	0,30	0,05	TOXIC	-0,67	0,16	UP	0,001928
PASK	23178	SKV_06	F08	Hs_PASK_5	ATCCTGGTTGCTAACGACAAA	0,87	0,09	OK	-0,67	0,30	UP	0,017657
PRKCH	5583	SKV_03	B08	Hs_PRKCH_6	GACCAGATTTGTGGCTTATAA	0,20	0,22	TOXIC	-0,68	0,71	UP	0,170344
NUCKS1	64710	SKV_16	E06	Hs_NUCKS1_5	TCGGGCCCTCCCACTAAGAAA	0,89	0,09	OK	-0,69	0,19	UP	0,000034
STK16	8576	SKV_19	G08	Hs_STK16_2	CAGGAGAATGTGTAACAAGAA	0,41	0,14	OK	-0,69	0,27	UP	0,002231
PHKA1	5255	SKV_04	E08	Hs_PHKA1_5	ATGGGAGTGCTTGGAACTTCA	0,80	0,22	OK	-0,69	0,25	UP	0,008943
NEK11	79858	SKV_18	B07	Hs_NEK11_7	TGAGATAAGCTTATAGATCAA	0,70	0,14	OK	-0,69	0,09	UP	0,000006
PHKG2	5261	SKV_04	F04	Hs_PHKG2_5	CTGCATGCACTGCATATGAAA	0,51	0,19	OK	-0,70	0,25	UP	0,008437
AAK1	22848	SKV_19	E03	Hs_AAK1_6	CCAGGTGGTAAACCTGATGAA	0,14	0,06	TOXIC	-0,71	0,44	UP	0,018416
AKAP8L	26993	SKV_16	C09	Hs_AKAP8L_6	CCTGTGATTATGGATATGGAA	0,72	0,12	OK	-0,71	0,19	UP	0,000052
ACVR2A	92	SKV_22	C07	Hs_ACVR2_1	GAGGTATTAGAGGGTGCTATA	0,44	0,07	OK	-0,71	0,17	UP	0,001778
MAP3K3	4215	SKV_18	D04	Hs_MAP3K3_5	CAGGAATACTCAGATCGGGAA	0,79	0,08	OK	-0,71	0,10	UP	0,000007
NEK7	140609	SKV_18	C04	Hs_NEK7_6	CCGGATATGGGCTATAATACA	0,65	0,13	OK	-0,72	0,40	UP	0,011481
ERBB3	2065	SKV_21	C05	Hs_ERBB3_5	ACCACGGTATCTGGTCATAAA	0,37	0,08	TOXIC	-0,72	0,23	UP	0,000789
CSNK2A2	1459	SKV_15	D04	Hs_CSNK2A2_5	CAGGAGTACAATGTTCGTGTA	0,88	0,30	OK	-0,73	0,41	UP	0,003989
STK17A	9263	SKV_06	E09	Hs_STK17A_5	AACCAGGATATTTAACAGGTA	0,91	0,36	OK	-0,73	0,25	UP	0,007150
MAP2K4	6416	SKV_20	C09	Hs_MAP2K4_8	AGGGTGTATAGTGTTCACAAA	0,96	0,26	OK	-0,75	0,21	UP	0,000372
DGKG	1608	SKV_10	E04	Hs_DGKG_5	ACCGCAAATGTGAATTATCAA	0,84	0,06	OK	-0,75	0,61	UP	0,101038

Target gene	Gene ID	plate	pos.	sequence name	siRNA sequence	Mean cells	SD cells	phenotype	Mean inh.	SD inh.	phenotype	Sign. inh.
HIPK2	28996	SKV_08	D07	Hs_HIPK2_5	AACCAGTACCCTTACATATAA	0,84	0,11	OK	-0,76	0,68	UP	0,125579
PIK3R2	5296	SKV_15	F05	Hs_PIK3R2_6	TTGGTACGTGGGCAAGATCAA	0,58	0,29	OK	-0,76	0,25	UP	0,000133
CALM1	801	SKV_08	E10	Hs_CALM1_5	CGGCAACTTACACACATTGAA	0,82	0,11	OK	-0,77	0,44	UP	0,038799
MAPK3	5595	SKV_07	G07	Hs_MAPK3_7	CTCCCTGACCCGTCTAATATA	0,87	0,38	OK	-0,77	0,15	UP	0,000932
TEK	7010	SKV_23	F04	Hs_TEK_6	TCGGTGCTACTTAACAACTTA	0,85	0,04	OK	-0,78	0,21	UP	0,003004
PKIB	5570	SKV_14	B04	Hs_PKIB_5	CAGCATGTGTATATTAGATAA	0,87	0,35	OK	-0,78	0,49	UP	0,006984
AATK	9625	SKV_23	F09	Hs_AATK_7	CTCCAACGTGTCAGCCAACAA	0,36	0,05	TOXIC	-0,79	0,36	UP	0,019181
MAST2	23139	SKV_02	B03	Hs_MAST2_6	CAGTGAAATAATAATGATGAA	0,40	0,21	TOXIC	-0,79	0,59	UP	0,079700
PINK1	65018	SKV_18	B03	Hs_PINK1_4	GACGCTGTTCCTCGTTATGAA	0,49	0,15	OK	-0,81	0,23	UP	0,000422
FYN	2534	SKV_21	D09	Hs_FYN_5	AAGACATGTGGTGTATATAAA	0,76	0,09	OK	-0,81	0,13	UP	0,000015
TBK1	29110	SKV_17	G06	Hs_TBK1_6	CAGAACGTAGATTAGCTTATA	0,22	0,12	TOXIC	-0,81	0,56	UP	0,026754
AK1	203	SKV_10	C07	Hs_AK1_6	GCGGCTGGAGACCTATTACAA	0,53	0,18	OK	-0,81	0,47	UP	0,039848
ALS2CR2	55437	SKV_20	F05	Hs_ALS2CR2_6	CCAGTGGAACTCACACAGTAA	0,48	0,17	OK	-0,82	0,24	UP	0,000528
PKLR	5313	SKV_26	B07	Hs_PKLR_9	CGGCAGCTGTTTGAGGAGCTA	0,44	0,09	OK	-0,83	0,78	UP	0,140502
NME4	4833	SKV_10	G06	Hs_NME4_6	CAGCACATGGGTGGTACACTA	0,64	0,13	OK	-0,84	0,57	UP	0,063185
PRKX	5613	SKV_01	E07	Hs_PRKX_5	CGGATGGGATTCACTTAAGAA	0,27	0,22	TOXIC	-0,88	0,95	UP	0,186301
NEK6	10783	SKV_17	F10	Hs_NEK6_7	AAGGGATAAAGTGGAAATCAT	0,28	0,06	TOXIC	-0,93	0,20	UP	0,000086
PTK2	5747	SKV_23	E04	Hs_PTK2_5	CACCTGGGTACTGGTATGGAA	0,79	0,03	OK	-0,96	0,29	UP	0,004749
PGK1	5230	SKV_10	G10	Hs_PGK1_5	CACAATTATAGATTAGATCAA	1,08	0,25	OK	-0,96	0,33	UP	0,006993
SNF1LK	150094	SKV_05	E04	Hs_SNF1LK_6	TCCACACATCATAAAGCTTTA	0,57	0,20	OK	-0,96	0,51	UP	0,031523
PAK2	5062	SKV_18	D08	Hs_PAK2_9	CCGGATCATACGAAATCAATT	0,72	0,12	OK	-0,97	0,15	UP	0,000012
PFKM	5213	SKV_10	G09	Hs_PFKM_5	AACAGATCAGTGCCAATATAA	0,23	0,07	TOXIC	-0,97	0,56	UP	0,040689
CERK	64781	SKV_13	E10	Hs_CERK_6	CGGCTTAAACTTTGATCTGTA	1,20	0,38	OK	-1,00	0,29	UP	0,000052
CSNK1G3	1456	SKV_05	E09	Hs_CSNK1G3_6	TACCGCAAACTTGATATGGAA	1,24	0,08	OK	-1,00	0,30	UP	0,004468
PRKCE	5581	SKV_01	D07	Hs_PRKCE_6	CACGGAAACACCCGTACCTTA	0,18	0,17	TOXIC	-1,00	1,62	UP	0,343082
ROR1	4919	SKV_23	D07	Hs_ROR1_6	CCGTACTGCGATGAAACTTCA	0,29	0,11	TOXIC	-1,04	0,28	UP	0,003091
MAP3K10	4294	SKV_25	G06	Hs_MAP3K10_7	CAAGCGCAAGGGCAACTTCAA	0,16	0,05	TOXIC	-1,09	0,90	UP	0,104461
MAP4K3	8491	SKV_20	D07	Hs_MAP4K3_6	TCGAGCTGTTGGATAAAGTAA	0,38	0,11	TOXIC	-1,10	0,36	UP	0,000860
NUAK1	9891	SKV_06	F03	Hs_ARK5_5	TAGGGATTTACTGGCATGGTA	0,48	0,17	OK	-1,11	0,31	UP	0,003348
MERTK	10461	SKV_23	G03	Hs_MERTK_14	CAGATGAATGTTGTTAAGTAA	0,80	0,14	OK	-1,13	0,21	UP	0,000728
SNF1LK2	23235	SKV_06	F09	Hs_SNF1LK2_11	CAGGATTACATCCGTTTATTA	0,97	0,31	OK	-1,13	0,53	UP	0,020271
AK2	204	SKV_10	C08	Hs_AK2_5	CCACATGTAAAGACTTGGTTA	0,85	0,21	OK	-1,14	0,86	UP	0,083260
ALS2CR7	65061	SKV_10	C03	Hs_ALS2CR7_5	CTGGACATAAACTAAGTCTAA	0,13	0,06	TOXIC	-1,19	0,26	UP	0,001423
CLK2	1196	SKV_07	F03	Hs_CLK2_5	CAGCTACAGACGCAACGATTA	0,47	0,14	OK	-1,21	0,36	UP	0,004334
PRKAR1A	5573	SKV_01	D03	Hs_PRKAR1A_8	CTGGACCGACCTAGATTTGAA	0,22	0,10	TOXIC	-1,30	0,98	UP	0,083531
AK3L1	205	SKV_08	E09	Hs_AK3_10	CCTGGTAACAGTGAAATTGAA	0,53	0,18	OK	-1,39	0,79	UP	0,038371
CDK6	1021	SKV_07	E08	Hs_CDK6_6	TCTGAAGTGTTTGACATTTAA	0,93	0,47	OK	-1,51	0,35	UP	0,001673
ULK2	9706	SKV_17	F03	Hs_ULK2_6	CAGCCTGAGATACGTGCCTTA	0,03	0,01	TOXIC	-1,60	1,03	UP	0,020374

pos.: position in plate **inh.: inhibition** **Sign.: significance**

Table S.2: List of SKV targets ordered for validation

A: downregulating siRNAs

Target gene	Gene ID	plate	pos.	sequence name	SKV siRNA sequence	Mean cells	SD cells	phenotype	Mean inh.	SD inh.	phenotype	Sign. inh.
ROCK2	9475	SKV_01	G03	Hs_ROCK2_6	ATGCACTTGTATAAAGCCATA	0,45	0,21	OK	1,59	0,45	DOWN	0,003730
LATS2	26524	SKV_03	F05	Hs_LATS2_8	AAGGATGTCCTGAACCGGAAT	0,61	0,06	OK	1,26	0,13	DOWN	0,000080
MKNK2	2872	SKV_06	C04	Hs_MKNK2_15	CAGCCAGGAGTACGCCGTCAA	0,54	0,49	OK	1,10	0,21	DOWN	0,000854
ADCK2	90956	SKV_04	C10	Hs_ADCK2_5	CCGGAATGTGAAAGCCGTCAA	0,62	0,15	OK	1,05	0,15	DOWN	0,000237
PRKCH	5583	SKV_01	D08	Hs_PRKCH_5	CGCCGTGTGCTCATCACTGAA	0,54	0,30	OK	1,02	0,25	DOWN	0,002166
MAP2K7	5609	SKV_20	C07	Hs_MAP2K7_13	CTGCGCTGAGAAGCTCAAGAA	0,40	0,06	OK	0,94	0,04	DOWN	0,000000
FGFR3	2261	SKV_23	B03	Hs_FGFR3_5	ACCCTACGTTACCGTGCTCAA	0,44	0,04	OK	0,91	0,05	DOWN	0,000007
MARK4	57787	SKV_05	D03	Hs_MARK4_5	CCGCATCATGAAGGGCCTAAA	0,57	0,19	OK	0,87	0,07	DOWN	0,000027
AKT2	208	SKV_02	F06	Hs_AKT2_8	CAAGCGTGGTGAATACATCAA	0,55	0,28	OK	0,83	0,15	DOWN	0,000699
MAP3K7	6885	SKV_20	D05	Hs_MAP3K7_8	AAGACTTGACTGTAACTGGAA	0,66	0,11	OK	0,83	0,25	DOWN	0,000582
CDC2L1	984	SKV_07	E03	Hs_CDC2L1_9	CACGTCGCTGAGGGAGATCAA	0,40	0,21	OK	0,83	0,18	DOWN	0,001436
EIF2AK3	9451	SKV_17	E09	Hs_EIF2AK3_6	CGGCAGGTCATTAGTAATTAT	0,49	0,17	OK	0,83	0,32	DOWN	0,001943
EPHA2	1969	SKV_20	G08	Hs_EPHA2_7	CAGCGCCAAGTAAACAGGGTA	0,42	0,12	OK	0,79	0,05	DOWN	0,000000
STK38	11329	SKV_03	E08	Hs_STK38_5	AACCTTATCGCTCAACATGAA	0,48	0,07	OK	0,78	0,31	DOWN	0,011501
PIP4K2C	79837	SKV_13	F05	Hs_PIP5K2C_6	TTGATGTGTGATAATCTCATA	0,86	0,25	OK	0,78	0,12	DOWN	0,000001
BEGAIN	57596	SKV_16	E04	Hs_KIAA1446_5	CGGGCGGACCATGTCACCGTA	0,55	0,15	OK	0,76	0,10	DOWN	0,000000
MAP3K7IP1	10454	SKV_14	D04	Hs_MAP3K7IP1_7	AACGGCTATGATGGCAACCGA	0,48	0,12	OK	0,73	0,19	DOWN	0,000029
NRGN	4900	SKV_12	C10	Hs_NRGN_6	CACCCAAGCACACTCACTTAA	0,83	0,08	OK	0,72	0,31	DOWN	0,016160
CSNK1D	1453	SKV_07	C06	Hs_CSNK1D_6	CTCCCTGACGATTCCACTGTA	0,62	0,15	OK	0,72	0,22	DOWN	0,005080
PDPK1	5170	SKV_02	G04	Hs_PDPK1_9	CACGCCTAACAGGACGTATTA	0,79	0,29	OK	0,71	0,42	DOWN	0,041453

B: upregulating siRNAs

Target gene	Gene ID	plate	pos.	sequence name	SKV siRNA sequence	Mean cells	SD cells	phenotype	Mean inh.	SD inh.	phenotype	Sign. inh.
CDK6	1021	SKV_07	E08	Hs_CDK6_6	TCTGAAGTGTTTGACATTTAA	0,93	0,47	OK	-1,51	0,35	UP	0,001673
AK3L1	205	SKV_08	E09	Hs_AK3_10	CCTGGTAACAGTGAAATTGAA	0,53	0,18	OK	-1,39	0,79	UP	0,038371
CLK2	1196	SKV_07	F03	Hs_CLK2_5	CAGCTACAGACGCAACGATTA	0,47	0,14	OK	-1,21	0,36	UP	0,004334
SNF1LK2	23235	SKV_06	F09	Hs_SNF1LK2_11	CAGGATTACATCCGTTTATTA	0,97	0,31	OK	-1,13	0,53	UP	0,020271
MERTK	10461	SKV_23	G03	Hs_MERTK_14	CAGATGAATGTTGTTAAGTAA	0,80	0,14	OK	-1,13	0,21	UP	0,000728
NUAK1	9891	SKV_06	F03	Hs_ARK5_5	TAGGGATTTACTGGCATGGTA	0,48	0,17	OK	-1,11	0,31	UP	0,003348
CSNK1G3	1456	SKV_05	E09	Hs_CSNK1G3_6	TACCGCAAACTTGATATGGAA	1,24	0,08	OK	-1,00	0,30	UP	0,004468
CERK	64781	SKV_13	E10	Hs_CERK_6	CGGCTTAAACTTTGATCTGTA	1,20	0,38	OK	-1,00	0,29	UP	0,000052

PAK2	5062	SKV_18	D08	Hs_PAK2_9	CCGGATCATACGAAATCAATT	0,72	0,12	OK	-0,97	0,15	UP	0,000012
SNF1LK	150094	SKV_05	E04	Hs_SNF1LK_6	TCCACACATCATAAAGCTTTA	0,57	0,20	OK	-0,96	0,51	UP	0,031523
PGK1	5230	SKV_10	G10	Hs_PGK1_5	CACAATTATAGATTAGATCAA	1,08	0,25	OK	-0,96	0,33	UP	0,006993
PTK2	5747	SKV_23	E04	Hs_PTK2_5	CACCTGGGTACTGGTATGGAA	0,79	0,03	OK	-0,96	0,29	UP	0,004749
ALS2CR2	55437	SKV_20	F05	Hs_ALS2CR2_6	CCAGTGGAACTCACACAGTAA	0,48	0,17	OK	-0,82	0,24	UP	0,000528
AK1	203	SKV_10	C07	Hs_AK1_6	GCGGCTGGAGACCTATTACAA	0,53	0,18	OK	-0,81	0,47	UP	0,039848
FYN	2534	SKV_21	D09	Hs_FYN_5	AAGACATGTGGTGTATATAAA	0,76	0,09	OK	-0,81	0,13	UP	0,000015
PINK1	65018	SKV_18	B03	Hs_PINK1_4	GACGCTGTTCCTCGTTATGAA	0,49	0,15	OK	-0,81	0,23	UP	0,000422
PKIB	5570	SKV_14	B04	Hs_PKIB_5	CAGCATGTGTATATTAGATAA	0,87	0,35	OK	-0,78	0,49	UP	0,006984
TEK	7010	SKV_23	F04	Hs_TEK_6	TCGGTGCTACTTAACAACTTA	0,85	0,04	OK	-0,78	0,21	UP	0,003004
MAPK3	5595	SKV_07	G07	Hs_MAPK3_7	CTCCCTGACCCGTCTAATATA	0,87	0,38	OK	-0,77	0,15	UP	0,000932
CALM1	801	SKV_08	E10	Hs_CALM1_5	CGGCAACTTACACACATTGAA	0,82	0,11	OK	-0,77	0,44	UP	0,038799
PIK3R2	5296	SKV_15	F05	Hs_PIK3R2_6	TTGGTACGTGGGCAAGATCAA	0,58	0,29	OK	-0,76	0,25	UP	0,000133
MAP2K4	6416	SKV_20	C09	Hs_MAP2K4_8	AGGGTGTATAGTGTTCACAAA	0,96	0,26	OK	-0,75	0,21	UP	0,000372
STK17A	9263	SKV_06	E09	Hs_STK17A_5	AACCAGGATATTTAACAGGTA	0,91	0,36	OK	-0,73	0,25	UP	0,007150
CSNK2A2	1459	SKV_15	D04	Hs_CSNK2A2_5	CAGGAGTACAATGTTCGTGTA	0,88	0,30	OK	-0,73	0,41	UP	0,003989
NEK7	140609	SKV_18	C04	Hs_NEK7_6	CCGGATATGGGCTATAATACA	0,65	0,13	OK	-0,72	0,40	UP	0,011481
MAP3K3	4215	SKV_18	D04	Hs_MAP3K3_5	CAGGAATACTCAGATCGGGAA	0,79	0,08	OK	-0,71	0,10	UP	0,000007
ACVR2A	92	SKV_22	C07	Hs_ACVR2_1	GAGGTATTAGAGGGTGCTATA	0,44	0,07	OK	-0,71	0,17	UP	0,001778
AKAP8L	26993	SKV_16	C09	Hs_AKAP8L_6	CCTGTGATTATGGATATGGAA	0,72	0,12	OK	-0,71	0,19	UP	0,000052

pos.: position in plate **inh.: inhibition** **Sign.: significance**

Table S.3: Comparison of kinase knock down results

target gene	phenotype Kuijl et al., (2007)	phenotype this work
ABL1	down	---
AKT1	down	up (1/4)
CALM3	down	---
CAMK2B	down	---
CINP	down	---
FASTK	down	---
LYN	down	---
MAP3K14	down	down (1/4)
MAPK8IP2	down	down (1/4)
PAK4	down	---
PCTK1	down	up (1/4)
PIK3C2G	down	---
PIK3CA	down	---
PRKD2	down	up (1/4)

Figure S.4: Principle of multi-paramteric flow cytometry

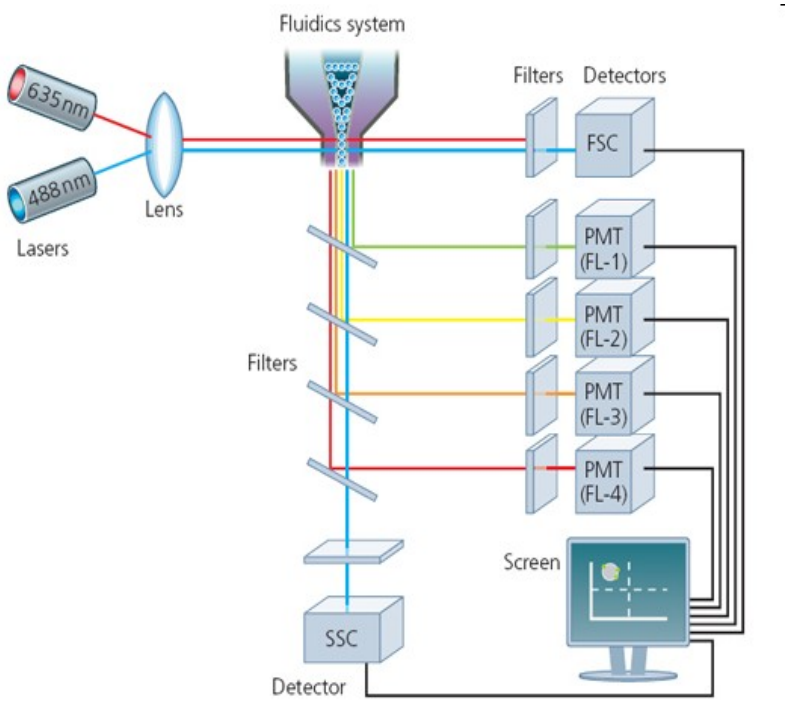

Figure S.4: Principle of multi-parametric flow cytometry.
The schematic illustration shows the principle of multi-parametric flow cytometry as implemented in the FACS Calibur. Particles delivered by the fluidics subsequently pass two laser beams and their characteristic light scattering and light emitting properties can be monitored and amplified by different detectors. The data for every parameter can be saved and analyzed on a single cell level.
(Taken from: http://www.abdserotec.com/support/signal_processing-710.html)

VIII Selbständigkeitserklärung

Hiermit erkläre ich, dass ich die vorliegende Arbeit selbständig und nur unter Verwendung der angegebenen Hilfsmittel angefertigt habe.

Berlin, den

_____

Oliver Riede